

Seeing Through the Tectal Eye: Visual Representations in  
the Primate Superior Colliculus With and Without Eye Movements

Dissertation

zur Erlangung des Grades eines  
Doktors der Naturwissenschaften

der Mathematisch-Naturwissenschaftlichen Fakultät  
und  
der Medizinischen Fakultät  
der Eberhard-Karls-Universität Tübingen

vorgelegt  
von

Chen, Chih-Yang  
aus New Taipei City, Taiwan

April - 2017

Tag der mündlichen Prüfung: 26.10.2017

Dekan der Math.-Nat. Fakultät: Prof. Dr. W. Rosenstiel

Dekan der Medizinischen Fakultät: Prof. Dr. I. B. Autenrieth

1. Berichterstatter: Prof. Dr. Z. M. Hafed

2. Berichterstatter: Prof. Dr. A. Nieder

Prüfungskommission: Prof. Dr. Z. M. Hafed

Prof. Dr. A. Nieder

Prof. Dr. C. Schwarz

Prof. Dr. U. Ilg

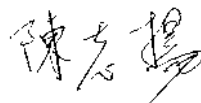
**Declaration:**

I hereby declare that I have produced the work entitled “Seeing Through the Tectal Eye: Visual Representations in the Primate Superior Colliculus With and Without Eye Movements”, submitted for the award of a doctorate, on my own (without external help), have used only the sources and aids indicated and have marked passages included from other works, whether verbatim or in content, as such. I swear upon oath that these statements are true and that I have not concealed anything. I am aware that making a false declaration under oath is punishable by a term of imprisonment of up to three years or by a fine.

Tübingen,

April 30, 2017

Date



.....  
Signature

## **Acknowledgments**

I would like to thank my supervisor, Prof. Ziad Hafed, for all his support during my pursuit of my PhD degree. Ziad has been a really good advisor in giving me feedback about my work. Discussing my work with him is always exciting and stimulating. In the end, we really expanded my thesis beyond the original topic and got extremely nice results. He has also been a nice mentor in guiding me on the path of science. He not only gives me a lot of opportunities to go to international conferences to present our work, but he also gives me advice on presentation skills and also gives me the chance to make connections to the whole world. He is also a good friend of mine, and we always have a lot of fun chatting together. It has been a great pleasure to work with him. I do think that he made me who I am, and I will keep on the good work that I learned from Ziad.

Also, I would like to thank my former and current lab members. I would like to thank our former technician, Christina, and our former post-doc, Alla, who both provided great help in my work and also in my private life. Thanks are also due to our current lab members, Tian, Joachim, Antimo, and Konstantin. It is always fruitful to discuss science with you all, and I really enjoy working with all of you.

Special thanks are also in order for everyone in the Nieder's group. It was a really great time to work side by side with them in the same floor for a great proportion of my time here.

I would like to thank my family and friends for their support, especially my sister and my brother in law. Without them, I would not be working in Germany. They have been a really great help for my life here. I also thank my two little nephews who have dragged me out from daily work and enriched my life.

I appreciate the contribution of all of the animals that I have worked with. As Ziad always says, "Good data comes from happy monkeys, and happy monkeys come from our lab." I hope that I have made you all happy. Thanks to Nano and Pico in particular.

Finally, the two fishes in the lab have enriched all of our time that we spent at work, and they will be always remembered.



## Table of Contents

|   |    |
|---|----|
| I. List of publications appended .....  | 8  |
| II. Summary .....   | 9  |
| III. Synopsis .....   | 11 |
| 1. Introduction.....  | 11 |
| 1.1. Anatomical and physiological organization of the SC .....                | 12 |
| 1.1.1. Anatomy.....   | 12 |
| 1.1.2. Physiology.....  | 15 |
| 1.2. Role of the SC in vision.....  | 20 |
| 1.2.1. Retinal input.....   | 21 |
| 1.2.2. Cortical input .....   | 21 |
| 1.2.3. Visual thalamus connections.....                                       | 23 |
| 1.3. Role of the SC in saccade and microsaccade control .....                 | 24 |
| 1.3.1. Cortical control of saccades .....                                     | 26 |
| 1.3.2. Subcortical control of saccades and microsaccades.....                 | 28 |
| 1.4. The SC and active vision .....   | 31 |
| 1.4.1. Transsaccadic spatial updating, memory, and attentional shifts .....   | 32 |
| 1.4.2. Saccadic suppression .....   | 36 |
| 1.5. Open questions.....  | 38 |
| 2. Main results.....  | 40 |
| 2.1. Visual responses to first order stationary stimuli in the SC.....        | 40 |
| 2.2. Differences between upper and lower visual fields in the SC .....        | 41 |
| 2.3. Neuronal response gain modulations around microsaccades in the SC.....   | 43 |
| 2.4. Spatial frequency dependent microsaccadic suppression in the SC .....    | 44 |
| 2.5. Pre- and post-microsaccadic modulation of ocular drift gain control..... | 46 |
| 3. Discussion.....  | 48 |
| 3.1. The SC as an important neuronal locus for blindsight.....                | 48 |
| 3.2. Updated topography in the SC .....                                       | 49 |

|   |     |
|---|-----|
| 3.3. Covert visual attention and microsaccades .....  | 50  |
| 3.4. Studying visual stability using microsaccades as a tool .....  | 51  |
| 3.5. Postmicrosaccadic enhancement contribution to visual stability.....  | 52  |
| 4. Concluding remark .....  | 54  |
| 5. Abbreviation .....   | 56  |
| 6. Reference .....  | 57  |
| IV. Statement of contributions .....  | 79  |
| V. Appendix: Individual studies .....   | 80  |
| 1. Postmicrosaccadic enhancement of slow eye movements.....   | 80  |
| 2. Neuronal response gain enhancement prior to microsaccades .....  | 93  |
| 3. Sharper, stronger, faster upper visual field representation in primate superior<br>colliculus.....                                     | 115 |
| 4. A neural locus for spatial-frequency specific saccadic suppression in<br>visual-motor neurons of the primate superior colliculus ..... | 143 |
| 5. Spatial vision by macaque midbrain.....  | 161 |
| 6. Orientation and contrast tuning properties and temporal flicker fusion<br>characteristics of primate superior colliculus.....          | 196 |

## **I. List of publications appended**

**Chen, C. -Y.** and Hafed, Z. M. (2013). Postmicrosaccadic enhancement of slow eye movements. *The Journal of Neuroscience*, Vol. 33, No. 12, pp. 5375-5386.

**Chen, C. -Y.**, Ignashchenkova, A., Thier, P., and Hafed, Z. M. (2015). Neuronal response gain enhancement prior to microsaccades. *Current Biology*, Vol. 25, No. 16, pp. 2065-2074.

Hafed, Z. M. and **Chen, C. -Y.** (2016). Sharper, stronger, faster upper visual field representation in primate superior colliculus. *Current Biology*, Vol. 26, No. 13, pp. 1647-1658

**Chen, C. -Y.** and Hafed, Z. M. (2017). A neural locus for spatial-frequency specific saccadic suppression in visual-motor neurons of the primate superior colliculus. *Journal of Neurophysiology*, Vol. 117, No. 4, pp. 1657-1673

**Chen, C. -Y.**, Sonnenberg, L., Weller, S., Witschel, T., and Hafed, Z. M. Spatial vision by macaque midbrain. In Preparation.

**Chen, C. -Y.** and Hafed, Z. M. Orientation and contrast tuning properties and temporal flicker fusion characteristics of primate superior colliculus neurons. In Preparation.



## **II. Summary**

Vision is an important sensory modality for primates. However, because of foveated retinal organization, vision requires repetitive eye movements to align the fovea with new objects. This creates interesting theoretical questions about perception in general, since eye movements themselves alter images on the retina even if there are no moving objects in the world. Thus, to study vision is to also study how vision operates during active behavior. In my dissertation, I have investigated the concept of “active vision” in a brainstem structure critical for eye movement generation, the superior colliculus (SC). The SC is a well-studied structure, with a prominent role in driving eye movements. However, this structure is also ultimately a visual structure, and it is the primary visual structure in lower animals. Given a relatively sparse interest in visual properties of the primate SC in the literature, and given the proximity of both visual and motor representations already together within the same structure, we have adopted the SC as an ideal locus for investigating active vision. We first characterized SC visual representations in the absence of eye movements. We found surprising asymmetries in visual representations between upper and lower visual fields, which have direct consequences on oculomotor behavior. We also performed analogs of visual neurophysiology experiments in structures like primary visual cortex (V1) or lateral geniculate nucleus (LGN), but this time to characterize SC spatial and temporal frequency tuning properties. We found remarkable tuning properties and response time profiles of SC neurons that we think allow this structure to be highly in-tune with the statistics of natural scenes. This in turn allows very efficient eye movement response times to spatial frequencies prominent in our environment. In the same set of studies, we also characterized center-surround interactions, orientation tuning, and temporal frequency tuning. To further explore the concept of “active vision”, we showed how visual representations in the SC are modulated around the time of eye movements. We discovered surprising and spatially far-reaching pre-movement enhancement of contrast sensitivity, which can provide a neural basis for attentional enhancements in behavior. We also found spatial-frequency-specific post-movement modulations of neural activity. The latter results are particularly interesting when related to classic perceptual phenomena of saccadic suppression, and also when considering different neuronal cell types. Finally, we tested how the eyes stabilize themselves after saccadic eye movements and found an enhanced ocular drift control even for the smallest possible saccades generated during fixation. The overall aggregation

## *Summary*

---

of our results creates several interesting new research avenues with important and solid foundations for future understanding of detailed circuit-mechanisms of SC function, and also for relating such mechanisms to perception and action.

### III. Synopsis

#### 1. Introduction

The superior colliculus (SC), an evolutionarily conserved structure, exists widely in vertebrates (Gaither and Stein, 1979; Stein, 1981; Saitoh et al., 2007; Kardamakis et al., 2015). It is referred to as the optic tectum in non-mammalian animals (Ingle, 1973; Stein and Gaither, 1983), and it has important contributions to vision (Wilson and Toyne, 1970; Perry and Cowey, 1984; Berson, 1988; Wylie et al., 2009; Huberman and Niell, 2011) and orienting behavior (Dean et al., 1989; Guitton, 1992; Masino, 1992; Isa and Sasaki, 2002; Huberman and Niell, 2011). In primates, specifically, this structure plays critical roles as an alternative visual pathway (Cowey and Stoerig, 1991; Ptito and Leh, 2007; Isa and Yoshida, 2009; Cowey, 2010; Lyon et al., 2010), as a center for eye movement control (Schiller, 1972; Wurtz and Albano, 1980; Fuchs et al., 1985; Sparks, 1986, 1990, 2002; Kalesnykas and Sparks, 1996; Moschovakis et al., 1996; Munoz, 2002; King, 2004; Optican, 2005; Gandhi and Katnani, 2011; Hafed, 2011; Otero-Millan et al., 2011), and also as a mediator of higher cognitive functions, like attention (Schall, 1995; Horwitz and Newsome, 1999; Dorris et al., 2002; Shipp, 2004; Bisley, 2011; Krauzlis et al., 2013; Hafed et al., 2015). This dissertation is about my research on the SC of macaque monkeys (*Macaca mulatta*). My main focus is on visual representation by the SC during active vision. I will start with introducing the basic anatomical structure and physiological properties of this important brain structure, and I will then highlight the main visual afferent and saccadic efferent projections to and from the SC, respectively. Finally, I will describe modulations of SC visual representations during active vision that have been reported in the literature. At the end of the introduction, I will point out the important questions that I will ask in this dissertation. I will answer these questions with a series of experiments, and at the end discuss the possible implications of my work, as well as future directions. For the sake of this dissertation, I will focus only on primate SC unless mentioned explicitly in the text.

## 1.1. Anatomical and physiological organization of the SC

### 1.1.1. Anatomy

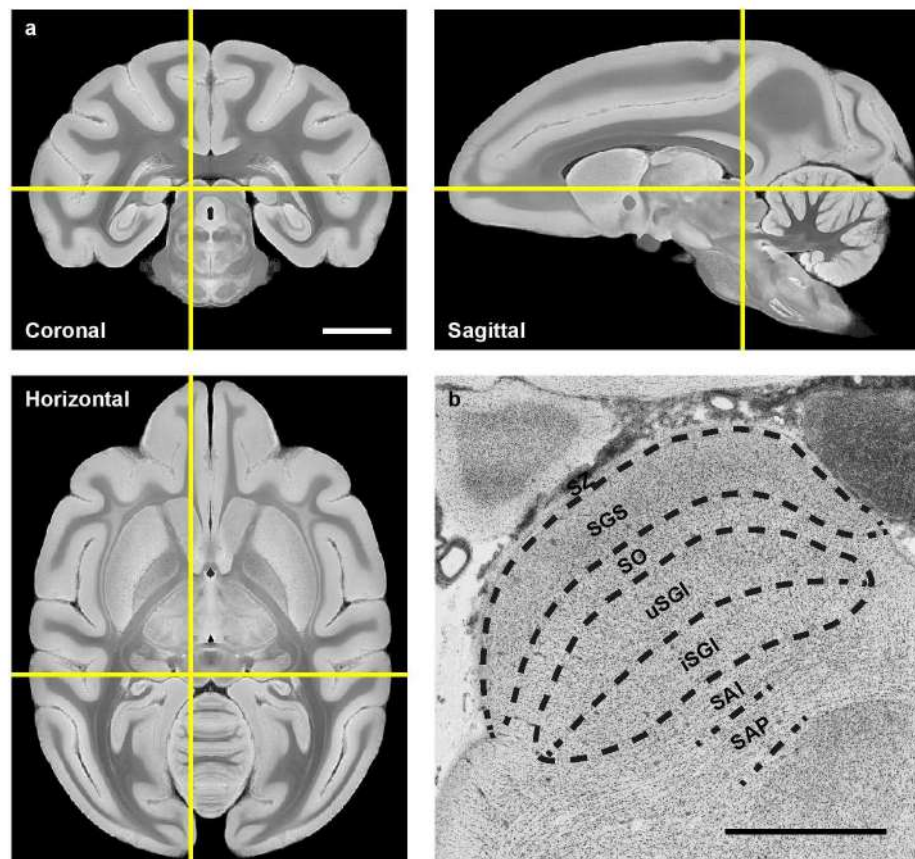


Figure 1. Anatomical location and lamination of the macaque SC. (a) Anatomical location of the SC in standard stereotaxic space. Upper left, upper right, and lower left show coronal, sagittal, and horizontal views of a macaque brain from a normalized high field (7T) MR image. The yellow crosshair marks the location of the left SC. Scale bar: 10 mm. Figure modified from (Calabrese et al., 2015). (b) Layered structure of the macaque SC. Macaque brain slice processed with Nissl staining. The layers are marked according to local landmarks. Scale bar: 2 mm. Figure modified from *The Rhesus Monkey Brain in Stereotaxic Coordinates*, Second Edition.

The SC is a layered midbrain structure that sits on top of the brainstem (Fig. 1a). Roughly speaking, the SC can be divided into two primary functional layers: the superficial layer and the deeper layer (Casagrande et al., 1972).

**Lamination** The superficial SC layer can be further divided into three sub-layers (Fig. 1b). The outermost layer, termed stratum zonale (SZ), is narrow and nearly cell free. Under this layer comes a gray layer with numerous small neurons, and it is

called stratum griseum superficiale (SGS), or superficial gray layer. Beneath it is the stratum opticum (SO). This layer contains some neurons, but it is predominantly comprised of optic fibers coming from retinal projections to the SC (Huber and Crosby, 1933; Wurtz and Albano, 1980; Huerta and Harting, 1984; May, 2006).

The deeper layer can also be subdivided into several layers (Fig. 1b). Right under SO is a layer filled with a variety of multipolar neurons. This layer, named stratum griseum intermediale (SGI), or intermediate gray layer, is sometimes divided into upper and lower layers (May, 2006). The layer beneath this is another layer with abundant fibers, called stratum album intermediale (SAI). Under SAI is the layer termed stratum griseum profundum (SGP). This layer is also called deeper gray layer because it contains mainly neurons. The most inner layer of the SC is a thin band of fibers sitting right on top of the periaqueductal gray, named stratum album profundum (SAP) (Huber and Crosby, 1933; Wurtz and Albano, 1980; May, 2006). All the neurons recorded in this thesis are from the SGS and SO of the superficial layer, and the SGI of the deeper layer.

***Intralaminar connections*** Presenting a large disc-like stimulus in the response field (RF) of an SGS neuron produces suppressed visual responses when compared to a small dot stimulus (Humphrey, 1968; Schiller and Koerner, 1971; Cynader and Berman, 1972; Goldberg and Wurtz, 1972a; Marrocco and Li, 1977). However, failing to induce any response using a ring-like stimulus avoiding the central part of the field suggests that the RF is not organized as a conventional Mexican hat type of center-surround RF (Schiller and Koerner, 1971; Cynader and Berman, 1972; Goldberg and Wurtz, 1972a). In any case, studies in SC have revealed long-range horizontal connections in SGS (Laemle, 1981) that may aid in this suppression. In addition, GABAergic inhibitory neurons have also been found (Mize et al., 1991), presumably having wide horizontal projections that can provide a suppressive signal from RF surrounds. In my dissertation, I also characterized surround suppression and found interesting slope changes in the contrast sensitivity functions instead of response gain modulations typically found with surround stimulation in other visual areas.

Related to the idea of horizontal connections, it has also been suggested that the SGI can be divided into rostral and caudal regions that are connected by a mutually inhibitory long-range projection (Munoz and Wurtz, 1993a, 1993b; Munoz and Fecteau, 2002). Although evidence from physiological recordings and electrical stimulation does show such a possibility (Munoz and Istvan, 1998), anatomical and physiological support for it is far from complete. Instead, what may happen is a pattern of relatively local excitatory interconnections, which may exhibit asymmetries that result

in apparent spreading of activity during saccadic eye movements (Nakahara et al., 2006). Such spreading of activity has been proposed to provide an online control of the eye position during a saccade until activity reaches the rostral SC pole and ends the saccade (Guitton, 1992; Munoz and Wurtz, 1995a; Port et al., 2000), but the problem is that this spread was always more “fuzzy” than a literal “moving hill” representing real-time saccade progress (Sparks, 1993; Anderson et al., 1998; Soetedjo et al., 2002). In my own research, I have re-examined this possibility and found that a surprising asymmetry between upper and lower visual field representations in the SC could be a critical reason for why some studies found such spreading of activity and some did not (Hafed and Chen, 2016). Anatomically, in the deeper SC, multiple populations of GABAergic neurons also exist (Mize et al., 1991), but their axonal trajectories remain to be determined. Only a rostral-to-caudal projection is known in cat (McIlwain, 1982) but not in the opposite direction. In the primate, no known long range inhibitory projections have been identified. Most likely, SGI neurons project to local interneurons to produce recurrent inhibition (Moschovakis et al., 1988a; Mize et al., 1991). In short, more observations are needed for intra-laminar connections within the deeper SC layer.

***Interlaminar connections*** Originally, there were some debates about whether the SC’s superficial and deeper layers are interconnected. Physiological characterization of SGS and SGI neurons in the same vertical column showed similar visual RF locations (Goldberg and Wurtz, 1972a). However, lesion or cooling in primary visual cortex impaired visual responses in only SGI neurons (Schiller et al., 1974) with SGS neurons left largely intact. This result suggests that SGS neurons receive both retinal and cortical visual input, whereas SGI neurons receive exclusively cortical input and have no direct input from the superficial layer (Wurtz and Albano, 1980; Sparks, 1986). However, more recent anatomical (Benevento and Fallon, 1975; Moschovakis et al., 1988a) and physiological (Wurtz and Goldberg, 1972a; Isa et al., 1998; Özen et al., 2000; Vokoun et al., 2010) work has demonstrated that such projection does exist. This suggests that a proper explanation for the previous studies of cooling of the primary visual cortex remains to be elusive. In the reverse direction, physiological recordings from slice work in rats suggest that there exists feedback from the deeper layer to the superficial layer (Vokoun et al., 2010; Phongphananee et al., 2011; Ghitani et al., 2014). While this projection has historically been viewed as being inhibitory to mediate saccadic suppression of visual responses in the superficial layer (to aid in perceptual stability across saccades), the evidence (including from one of my studies) suggests that the feedback might perform more sophisticated functions

(Chen and Hafed, 2017). For example, in rat work, it was found that the projection can be either excitatory or inhibitory. In any case, whether similar feedback connections can be found in the primate remains to be seen.

***Tectotectal connections*** There are also identified tectotectal connections (Benevento and Fallon, 1975; Moschovakis et al., 1988b; Olivier et al., 1998). These connections are mainly in SO, SGI, and SGP with either glutamatergic or GABAergic terminals targeting primarily the mirror image region of the other colliculus (Appell and Behan, 1990; Olivier et al., 2000). These tectotectal cells are found only in the rostral half of the SC (Appell and Behan, 1990; Olivier et al., 1998, 2000). Although there is no comprehensive explanation for their function, tectotectal connections have been proposed to be involved in generating different directions of saccades, or for executing orienting vs. avoidance behaviors. It has also been suggested that these connections allow implementing gaze fixation through balanced activity across the two SC's (Hafed and Krauzlis, 2008; Hafed et al., 2008, 2009; Goffart et al., 2012; Krauzlis et al., 2017).

### **1.1.2. Physiology**

The SC's function is complicated, because of various afferent and efferent projections. It receives sensory input ranging from visual, auditory, somatosensory, to vestibular information, and more (Stein et al., 2001; May, 2006). Some of the sensory inputs are specialized from species to species. It also projects to thalamus, brainstem eye movement related nuclei, cerebellum, and also cervical spinal cord (Wilson and Toyne, 1970; Benevento and Fallon, 1975; Harting, 1977; Huerta and Harting, 1984). However, to introduce all of the SC's functions is beyond the scope of this dissertation. Here, I will only focus on the physiological characteristics of superficial SGS and SO, neurons which are visually responsive, and deeper SGI neurons that are additionally involved in eye movement control (Fig. 2).

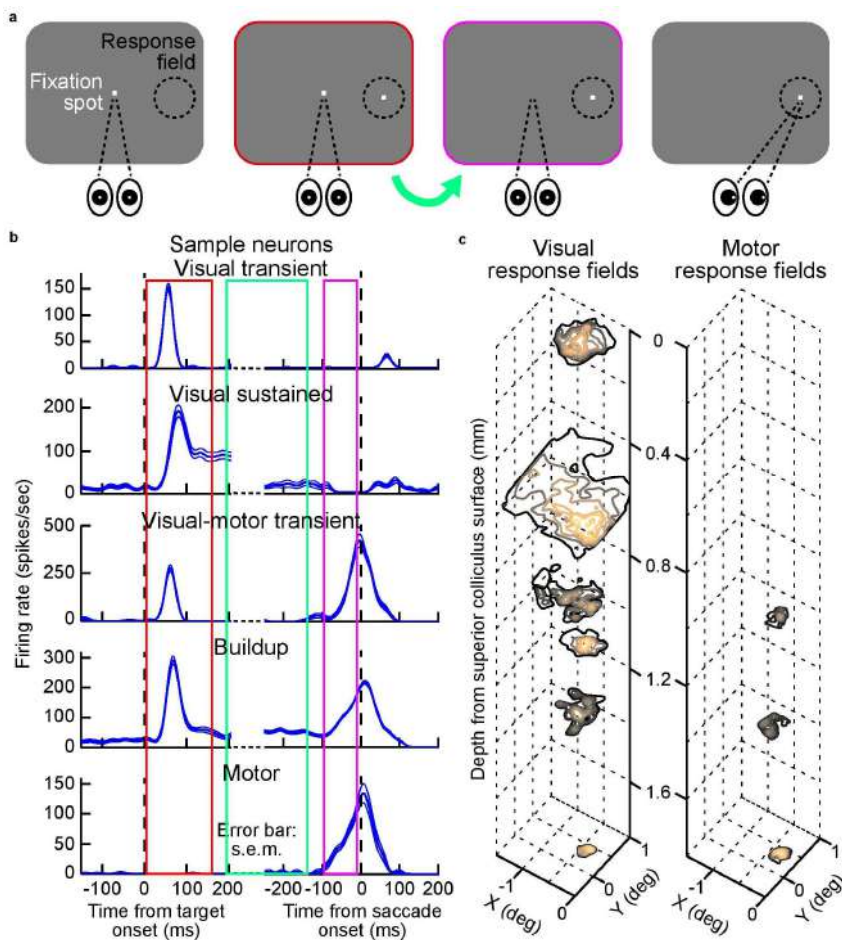


Figure 2. Physiological properties of neurons in the macaque SC.

(a) A typical behavioral paradigm for separating neuronal properties. The paradigm is a standard delayed saccade task. A monkey first fixates at a white fixation spot over a grey background on the screen. After a certain period of fixation, a stimulus appears within the response field (second left). After a delay period (indicated by a light green arrow), the fixation spot disappears (second right), and the monkey is required to make a speeded saccade to the stimulus to get a reward. (b) SC neurons with different physiological properties during the delayed saccade task. Neurons with increased activity after stimulus

onset are called visual neurons (red rectangle). Neurons with increased activity right before saccade onset are called motor neurons (magenta rectangle). Neurons with sustained activity during the delay period (light green) are called sustained neurons. Neurons without such activity are transient neurons. According to the definitions above, we can classify the neurons into visual transient, visual sustained, visual-motor transient, visual-motor sustained (buildup), and motor neurons. Error bar: s.e.m. (c) Response field properties in a single column. Neurons in this figure were collected from a single penetration, showing the depth profile of the visual and motor response fields. Neurons with visual response fields can be found from the SC surface to at least 1.6 mm deep. Neurons with motor response fields are found much deeper, starting from around 1 mm deep.

**Superficial SGS and SO neurons** Neurons in the superficial layer are almost exclusively visually responsive (Fig 2b, upper two traces) (Cynader and Berman, 1972). Although either one of the colliculi receives input from both retinæ (Pollack and Hickey, 1979), only the contralateral visual field is represented (Fig 3) (Cynader and Berman, 1972). This means that the SC is primarily binocular rather than monocular. The SC is also organized in a retinotopic manner, in which the foveal region is mapped onto the rostral lateral pole of the SC, the upper visual field is on the medial margin, and the lower visual field is on the lateral portion (Fig 3) (Cynader and Berman, 1972). It is known that the visual field in eccentricity is mapped onto the SC



surface using logarithmic warping along the rostral-caudal axis (Ottes et al., 1986). In the primate, the magnification factor of the foveal representation is large compared to other mammals. The central 10 degrees in the visual field cover more than 30% of the collicular surface (Fig 3b) (Cynader and Berman, 1972), although ongoing work related to my dissertation might suggest an even larger proportion especially for foveal eccentricities (unpublished observations). The upper and lower visual fields are also historically believed to be very similar in size, because visual angle from the horizontal is represented in a uniform fashion in the most popular model of SC retinotopic topography (Fig 3) (Ottes et al., 1986). However, this may be subject to debate given our recent discovery of large upper versus lower visual field asymmetries (Hafed and Chen, 2016).

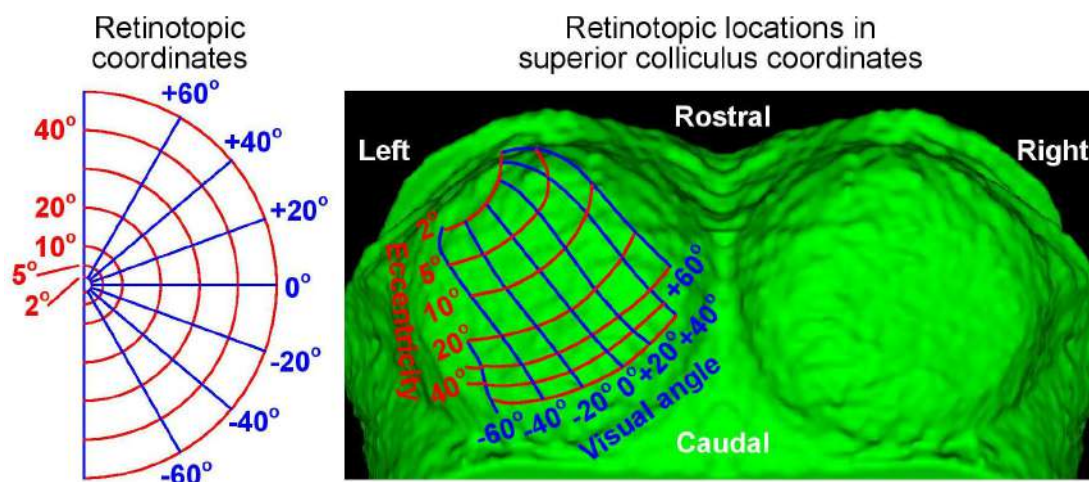


Figure 3. Retinotopy in the macaque SC. Retinotopic coordinates can be represented in visual angles (blue) and eccentricities (red). These retinotopic locations (left figure) can be mapped onto SC tissue (3D reconstructed from the MR in Figure 1) through logarithmic warping (right figure). The foveal representation is amplified and mapped onto the rostral superior colliculus. The retinotopic locations in SC coordinates used here were mapped by (Robinson, 1972) using electrical stimulation to evoke saccades. Specifically, the experiment was done by recording saccade vector dimensions induced by SC microstimulation. Later, it was shown that visual and motor RF's from the same neuron overlap. It is thus widely believed that the retinotopic map and the saccade vector map in the SC are similar. However, our work has shown that the map itself (whether visual or motor) might have asymmetries in representing upper and lower visual fields as well as larger foveal magnification, which are not accounted for by the Robinson map drawn in this figure.

SGS and SO neurons also receive cortical visual input and are topographically registered with the retinal input (Wilson and Toyne, 1970; Graham, 1982). Superficial neurons' responses to the transient onset and/or offset of a spot stimulus come after approximately 40-80 ms latency (Fig 2b, upper two traces). The responses are usually with transient bursts without additional background baseline activity (Fig 2b, upper two traces). Circular or ellipsoidal visual RF's consist of an activating center with in-

ternal summation property; that is, a progressively stronger visual responses and shorter response latencies are observed for increasing stimulus diameter (Humphrey, 1968; Schiller and Koerner, 1971; Cynader and Berman, 1972; Goldberg and Wurtz, 1972a; Marrocco and Li, 1977). However, our recent experiments further suggested that such latency effect could be dependent on contrast (unpublished observations included below in this dissertation). Around the activating center is a suppressive surround, which was described in an earlier paragraph. The size of the visual RF increases with eccentricity (Cynader and Berman, 1972). It is also known that neurons are sensitive to contrast with sharp sensitivity functions (Li and Basso, 2008). Most of the superficial neurons also respond to moving stimuli with either very broad or without directional tuning (Schiller and Koerner, 1971; Cynader and Berman, 1972; Goldberg and Wurtz, 1972a; Marrocco and Li, 1977). Although some neurons respond to stimulus velocity up to 800 deg/s, most neurons respond to maximally up to 30 deg/s. The neurons are also not sensitive to small changes in stimulus velocity or higher order shapes (Schiller and Koerner, 1971; Cynader and Berman, 1972; Goldberg and Wurtz, 1972a; Marrocco and Li, 1977). Only one study characterized the first order spatial frequency and temporal frequency tuning of superficial neurons in marmosets (Tailby et al., 2012). It shows that the neurons are with broad spatial frequency tuning, together with either low-pass or band-pass property; temporal tuning is also broad-band or low-pass with a population peak at around 10 Hz. However, these experiments were done on anaesthetized animals only. We examined the tuning properties of visually responsive neurons in awake macaques and found only low-pass spatial frequency tuning (unpublished observations included below in this dissertation). We also characterized other properties like temporal and orientation tunings. Recently, several studies have indicated that superficial neurons can discriminate color (Hendry and Reid, 2000; Tailby et al., 2012; Hall and Colby, 2014). However, more studies are needed to reconcile this with the previous assumption that the SC is color blind (Marrocco and Li, 1977; Sparks, 1986). One possibility is that color responses are really salience indicators but not real feature responsiveness to the property “color” (Herman and Krauzlis, 2017; Veale et al., 2017).

**Deeper SGI neurons** Multisensory neurons are common in SGI with either visual, somatosensory, or auditory responses. Some neurons are bimodal or even trimodal (Stein et al., 2001). However, in this dissertation, I will focus on neurons that are exclusively responsive to visual stimuli because these neurons discharge also prior to saccades (Fig 2b, lower three traces). These neurons are referred to as visual-motor neurons in the deeper layer. Some neurons without visual responses but responding to

saccades will also be included here. The visual responses can be either phasic or with sustained activity if the stimulus stays on in the visual RF or if the stimulus is task related in any way (either for a later saccade target or a location needed to be memorized) (Fig 2b, lower three traces) (Schiller and Koerner, 1971; Wurtz and Goldberg, 1972a; Mohler and Wurtz, 1976; Mays and Sparks, 1980; Munoz and Wurtz, 1993a, 1995b; Ignashchenkova et al., 2004). The stimulus off response becomes less prominent or disappears completely in these neurons. The neurons are also highly adaptive to repetitive stimuli with short intervals between successive stimuli (Goldberg and Wurtz, 1972b; Mayo and Sommer, 2008; Boehnke et al., 2011). The deeper the neuron is in the SGI layer, the weaker the visual response usually is, and also the smaller the visual RF becomes (Fig. 2c). Other visual properties like spatial frequency, temporal, and orientation tunings are quite similar to superficial neurons (unpublished observations included below in this dissertation).

Concerning motor responses, understanding of saccade-related properties in SGI began with early microstimulation studies (Apter, 1946; Robinson, 1972). It was shown that stimulating SGI produces contraversive conjugate saccades after a short 20-30 ms latency. Later, physiological studies confirmed that SGI neurons discharge maximally before a saccade with a particular direction and amplitude (Fig 2b, lower three traces) (Schiller and Koerner, 1971; Wurtz and Goldberg, 1971), thus forming (as a whole) a map of possible saccade endpoints. This map can be extended to also microsaccade amplitudes (Hafed et al., 2009). The visual and saccade maps are in register with each other (Fig 3) (Schiller and Koerner, 1971; Marino et al., 2008). This means that the saccade map is also topographically mapped onto the SC using logarithmic warping with a large amount of neurons being involved in microsaccades and small saccades. The neurons can further be mapped out with motor RF's using response strength in relation to saccade vector dimensions (Fig 2c) (Wurtz and Goldberg, 1972a), similar to the concept of a visual RF in relation to visual stimulus location. The two fields overlap, and the peak locations of the fields are aligned for neurons exhibiting both visual and motor fields (Fig 2c) (Marino et al., 2008). One distinct difference between the two RF's is that the motor RF can extend to the ipsilateral side of the visual RF if the recorded neuron represents a movement vector close to the vertical meridian (Sparks, 1986), but the visual RF is more confined and with almost no extension (Cynader and Berman, 1972), even deep within the foveal region (unpublished observations). Cells with movement RF's start discharging before saccade initiation by around 20 to 300 ms or longer, with either baseline activity or not (Fig 2b, lower three traces) (Munoz and Wurtz, 1995b). A small portion of these neurons exhibit saccade related responses only when the stimulus is present (Mohler

and Wurtz, 1976; Mays and Sparks, 1980). Most of these neurons have similar activity for saccades even in complete darkness (Schiller and Koerner, 1971; Wurtz and Goldberg, 1971). Based on these physiological properties, SGI neurons can further be divided into subgroups. Nevertheless, these properties seem to be more of a continuum in the SGI than clearly segregated categories (Fig 2b, lower three traces). Typically, if starting from the shallowest visual motor neurons, saccade-related activity is usually weak and with short lead time before saccade onset. These neurons are also mainly with low baseline activity and can be visually dependent for their saccade activity (i.e. they only emit the saccade burst if the target of the saccade is visible). The deeper the neuron is, the less visually dependent it is, and it normally also has stronger and longer leading activity before saccade onset (Fig 2b, lower three traces). In the meantime, these neurons start to have bigger movement RF's, weaker visual responses, and stronger baseline activity (Munoz and Wurtz, 1995b; unpublished observations). Even though after cooling or lesion of the primary visual cortex, visual responses are abolished in SGI neurons, their saccade-related activity remains present (Schiller et al., 1974). Monkeys can still make saccades to visual targets. This suggests that the visual response in the deeper layer may not be crucial for generating visually guided saccade behavior. However, as will be discussed later, the deeper layer is important for saccade initiation and also saccade metrics but encoded as a motor error. It may also signal behavioral relevance of stimuli (Krauzlis et al., 2017; Veale et al., 2017).

### 1.2. Role of the SC in vision

Because of a pronounced visual cortex in primates (VanEssen et al., 1992), the role of the SC in vision is relatively vague for normally behaving animals. However, the SC contribution for modulating visual perception during active vision as well as its possible role in mediating an alternative visual pathway are emphasized in the history of SC research. I will introduce the visual projections to the SC, separating retinal (Fig 3) and cortical projections (Fig 4), and then the visual thalamus connections with this structure (Fig 5). In the meantime, I will also introduce the role of the SC as an alternative visual pathway because this idea is related to the thalamic connections with the SC. I will also tap into the visual perceptual effects around saccadic eye movements in a later section, and highlight my contributions to all of these topics.

### **1.2.1. Retinal input**

The retinotectal projection is terminated primarily in SGS, with some in SO, and very sparsely in upper SGI (Pollack and Hickey, 1979; Beckstead and Frankfurter, 1983). The lateralization of which side of the retina projects to which side of the SC is rather complex. Both sides of the SC receive both information from both retinæ (Wilson and Toyne, 1970; Pollack and Hickey, 1979; Beckstead and Frankfurter, 1983). However, physiological mapping of the visual RF suggests that similar to the primary visual cortex (V1), each side of the SC only represents the contralateral side of the visual field (Fig. 3) (Cynader and Berman, 1972). There is limited representation crossing the vertical meridian (Fig. 3). Even at the foveal region, the visual RF's do not cross to the ipsilateral side (unpublished observation). The ganglion cell types projecting to the SC are either magnocellular (Y cell) or koniocellular (W cell) (Marrocco and Li, 1977). Recent studies have identified and physiologically characterized two types of Y cells, parasol and smooth monostriated cells (Crook et al., 2008a, 2008b). These cells also project to the lateral geniculate nucleus (LGN). However, further studies are needed for characterizing physiological properties in SC neurons to compare the similarity to the projecting retinal ganglion cells. Because of recent studies on color sensitivity of the SC (White et al., 2009; Tailby et al., 2012; Hall and Colby, 2014), it is also likely that some other ganglion cell types project to the SC. More anatomical studies are needed to clarify this possibility. Most of the retinotectal terminals are glutamatergic (Mize and Butler, 1996), with a small proportion (< 3%) of exception to be GABAergic (Andrade da Costa et al., 1997).

### **1.2.2. Cortical input**

The corticotectal projection is rather complex. First, I will describe projections to the superficial and upper SGI layers. V1, visual area two (V2), and visual area three (V3) all provide visual input to SGS (Wilson and Toyne, 1970; Lui et al., 1995), with a small extent of V3 projecting to upper SGI (Fig. 4) (Lui et al., 1995). The cortical visuotopic arrangement is aligned with the neurons in the projection region (Wilson and Toyne, 1970; Graham, 1982). Cortical cells projecting to the SC are pyramidal neurons originating mainly from layer V, with the exception of a small proportion of layer IV neurons (Fries, 1984; Lock et al., 2003). V1 neurons projecting to the SC are mainly complex cells with broad orientation tuning and a high degree of binocularity (Finlay et al., 1976). Medial temporal visual area (MT) also provides direct input to

SGS, suggesting possible motion sensitivity in neurons of the superficial layer (Fig. 4) (Fries, 1984; Lock et al., 2003). The axonal terminals are mainly glutamatergic like the retinotectal ones (Mize and Butler, 1996).

Possible visual inputs to the deeper layer in the SC are from visual area four (V4), visual area four transitional (V4t), and posterior inferior temporal area (TEO), again with preserved retinotopy (Fig. 4) (Lock et al., 2003). Other possible inputs from the fundus of the superior temporal area (FST), medial superior temporal area (MST), V3 visual complex part A (V3A), parieto-occipital area (PO), posterior intraparietal area (PIP), lateral intraparietal area (LIP), and dorso-posterior area (DP) to the deeper layer are less predictable from the visuotopic arrangement (Fig. 4) (Lock et al., 2003). These projections may contribute to visual-motor roles of the SC, which will be introduced in a later section, or to the multisensory component of SC activity, which will not be further discussed in this dissertation.

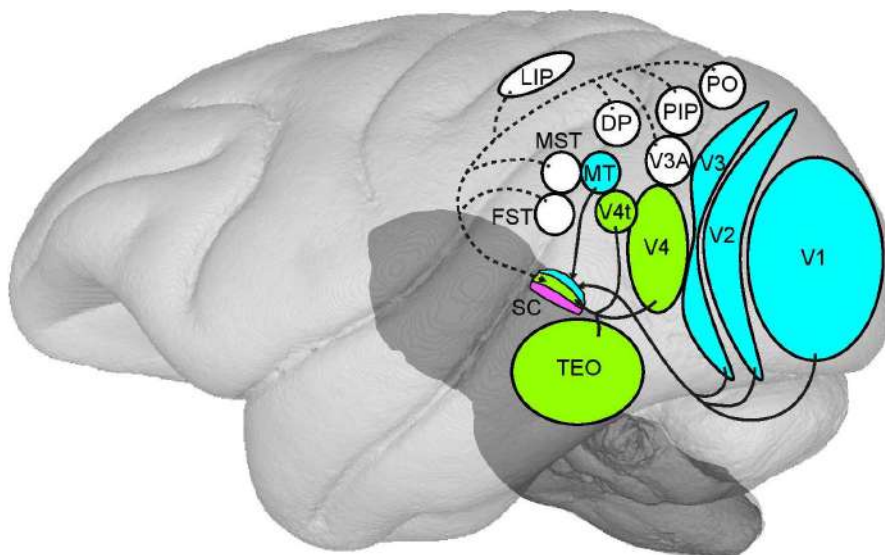


Figure 4. Cortical visual inputs to the macaque SC.

The cortical visual areas projecting to the SC are illustrated in this figure. The projections can be to superficial layer (cyan), or to the intermediate layer (green). The deep layer (magenta) does not receive input from cortical visual areas. The areas with matched retinotopic projections to the SC are colored with the same color of the projecting layer and also connected to the projecting layer through solid lines. The areas with less or no topographic projection are colored in white and connected to their projecting layer by dashed lines. As shown here, the superficial layer of the SC receives cortical inputs from V1, V2, V3, and MT with matched retinotopy. The intermediate layer receives cortical visual inputs from area V4, V4t, and TEO with also matched retinotopy. The inputs from area V3A, PO, PIP, DP, MST, FST, and LIP are less predicted by retinotopic organization.

## 1.2.3. Visual thalamus connections

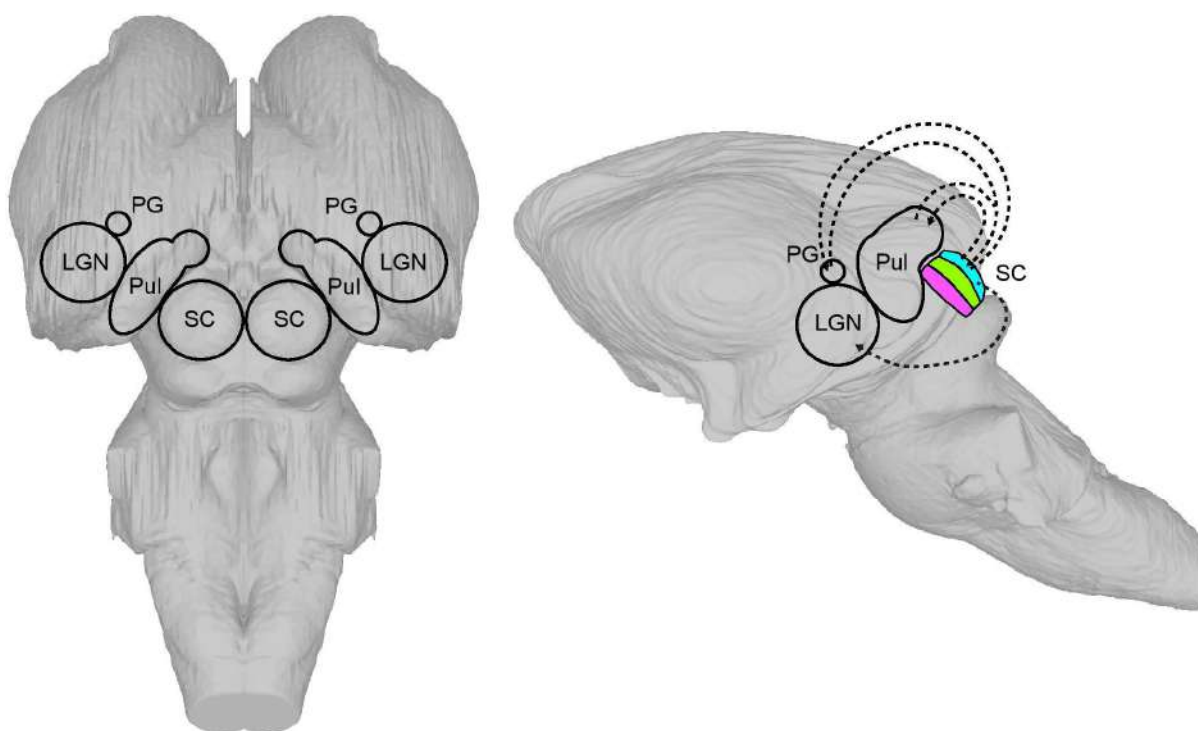


Figure 5. Subcortical visual areas connected to the macaque SC. There are several subcortical visual areas linked to the SC. LGN receives visual input from the superficial layer of the SC. There is no known projection going in the opposite direction. PG and pulvinar (Pul) also receive projections from the superficial layer and feedback to it. The only known retinotopic projection from the SC to the visual thalamus is to the inferior pulvinar. The other subcortical nuclei, like LGN, other parts of pulvinar, and PG are not aligned with SC retinotopy.

The superficial layer is connected with LGN (Fig. 5) (Harting et al., 1991; Wilson et al., 1995). LGN receives koniocellular (W cell) projections from SGS neurons and terminates on its own K-cells that are in between individual lamina (Harting et al., 1991). The physiological contribution of this projection remains to be determined. SGS neurons also project to pregeniculate (PG) and receive feedback from it (Fig. 5) (Harting et al., 1980; Livingston and Mustari, 2000). These neurons in PG mainly provide the SC with sustained discharge in the koniocellular (W cell) neurons (Hada et al., 1985). PG is suggested to act as a relay between parietal cortex and the SC because recordings in PG neurons showed early and late saccade related activity (Livingston and Fedder, 2003). SGS neurons also project to pulvinar (Fig. 5) (Benevento and Standage, 1983; Huerta and Harting, 1983). The main terminal zone in the inferior pulvinar is organized topographically. The medial, lateral pulvinar, and lateral posterior complex are also terminal zones for the superficial layer, but they are not topographically organized (Benevento and Standage, 1983; Stepniewska et al.,

2000). It has been shown recently that there is a bidirectional connection from the superficial layer of the SC to relay to the inferior pulvinar then to MT (Berman and Wurtz, 2008, 2010, 2011). The potential physiological signals that the relay neurons convey will be discussed in a later section.

Some literature concerning an interesting phenomenon called “blindsight” is also related to this pathway. Blindsight is a phenomenon that after lesion of primary visual cortex, with very little or sometimes no awareness of a stimulus presented in the blind field, patients can still perform discrimination tasks if they are forced to and be way above chance level, especially if the stimulus is salient (Weiskrantz et al., 1974; Cowey and Stoerig, 1991; Ptito and Leh, 2007; Cowey, 2010; Leopold, 2012). The visual stimuli that are optimal for these patients are critical. They perform the best with first-order low spatial frequency patches, with a cut off of around 3 cpd (Sahraie et al., 2002, 2010; Trevelyan and Sahraie, 2003). Transient stimuli are usually better, with a range around 10 to 33 Hz, peaking at around 20 Hz. These tuning properties are very similar to what we found in the SC neurons (unpublished observations included below in this dissertation). They can also perform color discrimination tasks (Boyer et al., 2005; Silvanto et al., 2008). It is also known that the pupillary reflex can be a reliable predictor of performance (Sahraie et al., 2002). Because the LGN and pulvinar project directly to extrastriate cortex, and because both of them also receive superficial SC and retinal input, it could be that blindsight reflects residual vision from this alternative visual pathway through LGN, SC, or pulvinar, or all of them to the extrastriate cortex (Cowey and Stoerig, 1991; Isa and Yoshida, 2009; Leopold, 2012).

### 1.3. Role of the SC in saccade and microsaccade control

As previously described, a direct link from the superficial layer to the deeper layer exists and could contribute to performing a sensory to motor transformation from vision to saccades (Wurtz and Goldberg, 1971; Benevento and Fallon, 1975; Moschovakis et al., 1988a; Özen et al., 2000; Vokoun et al., 2010). However, after cooling or lesion of the primary visual cortex, visual responses are abolished only in SGI neurons and not in SGS neurons (Schiller et al., 1974). Moreover, saccade-related activity is still present, and monkeys can still make saccades to visual targets (Isa and Yoshida, 2009). This suggests that the visual response in the deeper layer may not be crucial for visually guided saccade behavior (Wurtz and Albano, 1980; Sparks, 1986). However, this remains to be a topic of controversy. For example, a focal lesion in the



SGL layer was shown to prolong saccade reaction times to the lesion site, and saccade accuracy also decreases (Wurtz and Goldberg, 1972b; Mohler and Wurtz, 1977), although saccade reaction time recovers after some time. With a complete unilateral SC lesion, additional deficits of neglecting the contralateral visual field and hyperbolic saccades occur (Butter et al., 1978; Albano and Wurtz, 1982; Albano et al., 1982), and both saccade reaction time and accuracy deficits do not recover after prolonged time. A combined lesion of frontal eye field (FEF) and SC abolishes visually guided saccades completely (Schiller et al., 1979, 1980). If only cortical lesions combining FEF and LIP are made, intentional saccades are completely abolished leaving only spontaneous saccades intact (Lynch, 1992). All of these lesion studies show that the SC is not essential for saccade generation on its own. Saccade generation runs in parallel pathways and seems to be able to separate into intentional and reflexive saccade (Sparks, 1986; Pierrot-Deseilligny et al., 2004). But still, these studies demonstrate that the SC deeper layer is an important subcortical region for saccade control, especially for movement initiation and for computing saccade amplitude and direction.

The computation of saccade amplitude and direction extends down even to microsaccades. This means that during saccade-free fixation, there is a balance of activity among neurons that individually might prefer a certain saccadic vector (Hafed et al., 2009). When an overall imbalance occurs, say when a subset of neurons begins to increase its activity, a “motor error” is represented by the population of SC activity, and a subsequent saccade would be triggered based on the vector average of the entire active population (Sparks, 1986; Waitzman et al., 1988; Goossens and van Opstal, 2012). Subcortical nuclei later read out this population information into actual muscle contractions, and this results in a saccade to correct for the motor error (Moschovakis et al., 1996; Sparks, 2002; Horn, 2005; May, 2006; Hafed, 2016). This principle seems to be the same for saccades and microsaccades (VanGisbergen et al., 1981; Brien et al., 2009; Van Horn and Cullen, 2009; Hafed, 2011). Moreover, information integrated in the SC from cortical inputs may be thought of as performing a selection operation for potential saccade targets (Munoz, 2002; Pierrot-Deseilligny et al., 2004; Bisley, 2011; Pouget, 2015). In this sense, the deeper layer could act as a priority map for where the eyes should be focused on (Fecteau and Munoz, 2006; Serences and Yantis, 2006; Gottlieb, 2007; Boehnke and Munoz, 2008; Bisley and Goldberg, 2010; Veale et al., 2017). The following sections separate the cortical (Fig. 6) and the subcortical (Fig. 7) control of saccadic eye movements and describe them in more detail.

### 1.3.1. Cortical control of saccades

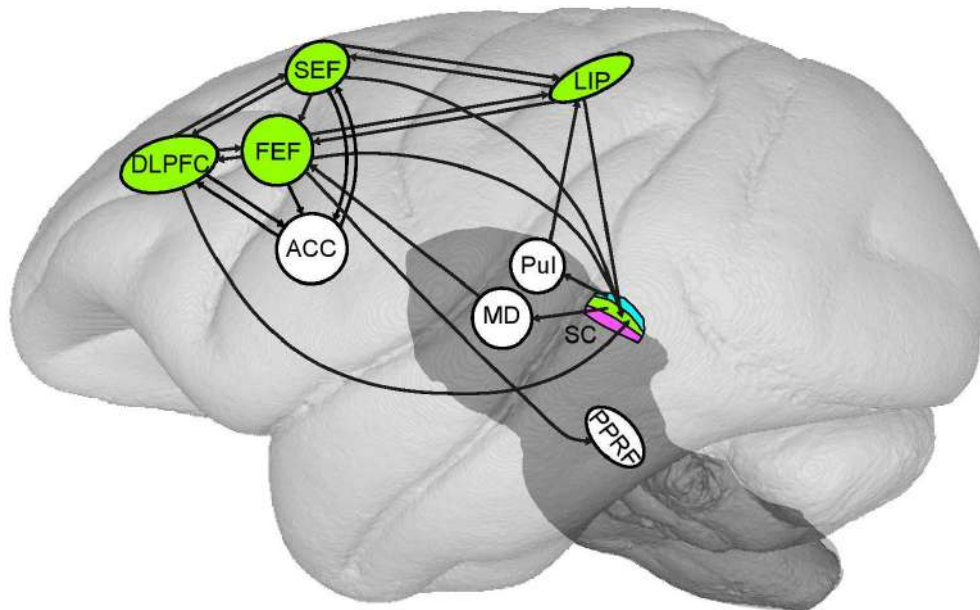


Figure 6. Cortical control of saccadic eye movements. The cortical saccade related areas are illustrated in this figure. Most of the areas have direct projections to the intermediate layer (green) in macaque SC. These areas, including FEF, SEF, LIP, and DLPFC, are colored in green, the same color as the intermediate layer. Only ACC does not have direct connection with SC. FEF and LIP receive feedback from the SC intermediate layer through MD and from superficial layer (cyan) through inferior pulvinar (Pul). All cortical areas interconnected with each other are also indicated with solid lines. FEF is the only cortical area having projections also bypassing the SC and directly to the downstream saccade generation nucleus, PPRF.

There are massive projections coming from cortex to the SC helping to control the generation of saccades (Fig. 6) (Schall, 2015). Some of the cortical areas also receive feedback from the SC. Here, I will describe the interconnections between critical cortical areas, their main function with regard to saccade preparation, and their connections with SC.

One important such cortical area is FEF, because microstimulation of FEF with low intensity can directly induce saccades with short latencies of around 25 ms (Robinson and Fuchs, 1969; Bruce et al., 1985), similar to SC microstimulation results (Apter, 1946; Robinson, 1972). This area was shown to be involved in a range of intentional saccade generation modes, including delayed, predictive, memory-driven, and anti- saccades (Schall, 1995; Moschovakis et al., 2004). This area has also been shown to be less involved in reflexive visually guided saccades. It projects to ipsilateral SGI in the SC (Leichnetz et al., 1981; Komatsu and Suzuki, 1985; Huerta et al., 1986; Stanton et al., 1988) with projections of large saccades mainly terminating in lower SGI and those of small saccades mainly terminating in upper SGI (Komatsu

and Suzuki, 1985; Stanton et al., 1988). Feedback from the inner SGI through medial dorsal thalamus relays information back to the FEF associated with saccades, and therefore subserves an important functional property related to “corollary discharge” (Fig. 6) (Huerta et al., 1986; Lynch et al., 1994; Sommer and Wurtz, 2006). This property will be elaborated on in a later section. FEF also bypasses SC and has direct projections to the downstream brainstem nuclei contributing to saccade generation (Fig. 6) (Schnyder et al., 1985; Huerta et al., 1986; Stanton et al., 1988). It also has topographic organization like the SC since stimulating different loci of the FEF results in inducing different directions and amplitudes of evoked saccades, whereas changing stimulation amplitude or frequency at a given site does not alter saccade vectors (Robinson and Fuchs, 1969; Bruce et al., 1985; Huerta et al., 1986; Stanton et al., 1988).

Stimulating the supplementary eye field (SEF) also induces saccades but with a longer latency of around 50 ms (Schlag and Schlag-Rey, 1987; Schall, 1991; Russo and Bruce, 2000). It is also topographically organized. A critical difference between FEF and SEF is that the elicited saccades by prolonged microstimulation of SEF often result in the eyes being directed to a particular orbital location instead of stair-case saccades as with FEF (Schall, 1991; Martinez-Trujillo et al., 2004; Park et al., 2006). SEF sends direct projections to the inner SGI and also to the FEF (Fig. 6) (Huerta and Kaas, 1990; Shook et al., 1990; Parthasarathy et al., 1992). It is demonstrated to be more involved in saccade preparation and sequential saccade programming (Isoda and Tanji, 2002; Lu et al., 2002) instead of the actual saccade command (Schiller and Chou, 2000; Stuphorn et al., 2010). It is also involved in suppressing unwanted reflexive saccades (Nakamura et al., 2005; Stuphorn and Schall, 2006).

LIP was also shown to be able to elicit saccades with latencies of around 120-140 ms using higher intensity microstimulation (Shibutani et al., 1984; Thier and Andersen, 1998; Constantin et al., 2007). With lower intensity, attentional shifts are observed without generating large saccades (Hanks et al., 2006; Mirpour et al., 2010). Whether microsaccades are generated in this scenario remains unknown. It is interconnected with SEF and FEF (Pandya and Seltzer, 1982; Petrides and Pandya, 1984; Cavada and Goldman-Rakic, 1989a, 1989b), and also projects to inner SGI (Fig. 6) (Fries, 1984; Lock et al., 2003). However, the main feedback from the SC back to LIP is from the SGS layer relaying through pulvinar (Fig. 6) (Clower et al., 2001).

The dorso-lateral prefrontal cortex (DLPFC) is also involved in saccade programming. It was shown to have direct projection to inner SGI (Fig. 6) (Leichnetz et al., 1981). It is also believed that DLPFC is important for saccade target selection as well as sequential saccade programming, short-term spatial memory, and suppressing un-

wanted reflexive saccades (Levy and Goldman-Rakic, 2000; Schall, 2013). It is interconnected with FEF and SEF (Fig. 6) (Selemon and Goldman-Rakic, 1988).

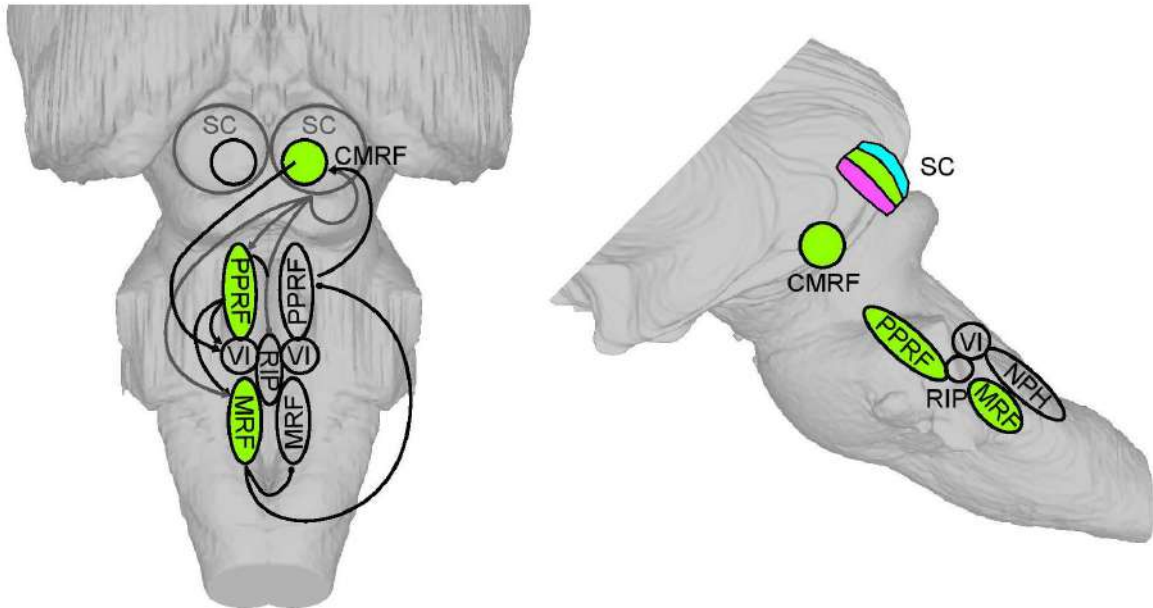
Finally, the anterior cingulate cortex (ACC), which does not have direct connections with the SC (Fig. 6), also has important roles in intentional saccades (Koval et al., 2014). It is interconnected with SEF and DLPFC, and also receives input from FEF (Fig. 6) (Selemon and Goldman-Rakic, 1988; Darian-Smith et al., 1999). The cortical control of microsaccades is still undefined except for recent evidence that FEF inactivation through cooling alters microsaccade directions, rates, and kinematics (Peel et al., 2016).

### 1.3.2. Subcortical control of saccades and microsaccades

Like with visual signals, the SC targets multiple motor related brain circuits and plays a crucial role in movement control, even for skeletal systems beyond the oculomotor system (Moschovakis et al., 1996; Horn, 2005; May, 2006). In this section, I will introduce the most studied, and also the most relevant, SC role, which is that in saccade control (Fig. 7).

The SC is interconnected with all of the important nuclei in the saccade circuits of the brainstem (Fig. 7) (Harting, 1977; Huerta and Harting, 1984). I will walk through these nuclei and introduce the projecting SC layer to these nuclei, starting with the horizontal component of a saccade (Fig. 7a). The primary target for the descending axons from the SC is to the contralateral paramedian zone of the pontine reticular formation (PPRF) (Fig. 7a) (Harting, 1977). Long-lead burst neurons (LLBN) and excitatory burst neurons (EBN) here receive this projection from the upper SGI and initiate saccade generation by generating high frequency bursts (Luschei and Fuchs, 1972; Keller, 1974; Van Gisbergen et al., 1981; Hepp and Henn, 1983). Inhibitory burst neurons (IBN) in the medullary reticular formation (MRF) receive both contralateral inner SGI and ipsilateral EBN projections and inhibit the EBN and IBN on the other side, forming a push-pull scenario (Fig. 7a) (Strassman et al., 1986; Scudder et al., 1988). In the meantime, the contralateral inner SGI, ipsilateral EBN, and LLBN also send activity to omnipause neurons (OPN) in the nucleus raphe interpositus (RIP) through inhibitory relays (Fig. 7a) (Luschei and Fuchs, 1972; Langer et al., 1986; Strassman et al., 1987; Büttner-Ennever et al., 1988). In this case, OPN's stop firing and release their strong inhibition on EBN's and IBN's. EBN's then send activity to motor neurons in the ipsilateral abducens nucleus and act as the main source to drive these neurons (Fig. 7a). The amplitude, velocity, and duration of a

**a** Subcortical pathway for horizontal saccades



**b** Subcortical pathway for vertical saccades

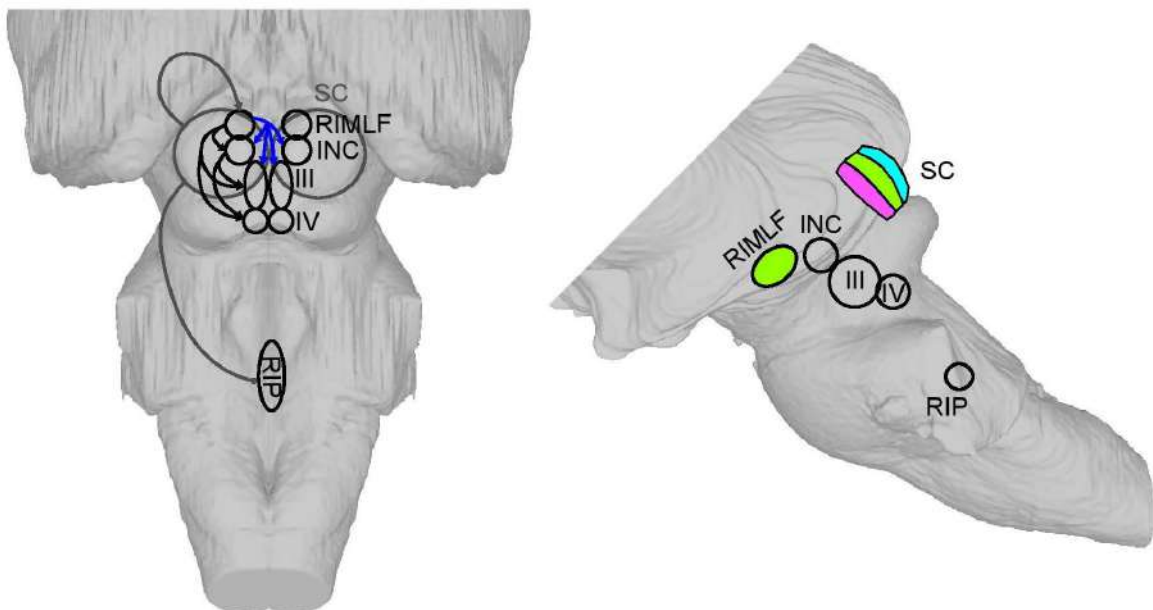


Figure 7. Simplified model for subcortical control of saccadic eye movements. Saccadic eye movements are decomposed into horizontal (a), and vertical (b) components at the subcortical level. These movements are controlled by different nuclei. (a) Nuclei controlling the horizontal component of saccades. The 3D reconstructed subcortical illustration (left figure) is a dorsal view tilted posteriorly 45° from a standard stereotaxic coordinate. Sagittal view (right figure) is without tilting the image. SC location and projections from it are indicated in grey. All the other nuclei related to horizontal saccadic eye movements are in black. The projections indicated in solid lines can be either excitatory (arrowhead) or inhibitory (round head). Nuclei in green are connected directly to the SC intermediate layer (green). The diagram is for generating a leftward saccade. (b) Nuclei controlling the vertical component of saccades. All the illustrations are the same as (a). The black or blue pathways indicate generating a downward or upward saccade, respectively. For vertical saccades, both sides of the SC are activated. Here, we mark only one side for simplification. III, oculomotor nucleus; IV, trochlear nucleus; VI, abducens nucleus.

saccade are proportional to the number of spikes, peak firing rate, and burst duration of the motor neurons, respectively (Fuchs and Luschei, 1970; Schiller, 1970; Luschei and Fuchs, 1972; Dean, 1997). There is a rare but existing direct projection from rostral SGI to motor neurons bilaterally, and also massive feedback projection back to SGI (Harting et al., 1980; Langer et al., 1986; Mays et al., 1986). However, the physiological function of such connections remains to be determined. One possibility is that feedback to the SC provides an estimate of instantaneous eye velocity and/or eye position during a saccade. Eye position is coupled with activity in nucleus prepositus hypoglossi (NPH) (McFarland and Fuchs, 1992; Zhou and King, 1998). Main projections to the NPH are from EBN in PPRF (Fig. 7a). There is no known projection from SC to NPH (Harting, 1977; Scudder et al., 1996), but there is bilateral preposito-collicular feedback (Hartwich-Young et al., 1990). Another important nucleus related to saccade vector and amplitude commands is the central mesencephalic reticular formation (CMRF) (Fig. 7a) (Cohen et al., 1985, 1986; Waitzman et al., 1996). CMRF receives massive projections from the ipsilateral upper SGI and feeds back bilaterally to inner SGI (Cohen and Büttner-Ennever, 1984; Moschovakis et al., 1988b; Chen and May, 2000). It also receives projections from EBN (Büttner-Ennever and Henn, 1976). CMRF targets a wide range of other saccade and head movement related nuclei including a direct projection to abducens motor neurons (Fig. 7a) (Robinson et al., 1994; Büttner-Ennever et al., 2001).

The generation of the vertical component of a saccade has been described more recently (Moschovakis et al., 1996). It starts from again the upper SGI output terminals arriving bilaterally on the medium-lead burst neurons (MLBN) (Moschovakis et al., 1991a, 1991b) in the rostral interstitial nucleus of the medial longitudinal fasciculus (RIMLF) (Büttner-Ennever and Büttner, 1978; Moschovakis et al., 1988b). In this case, either “up” or “down” MLBN’s in RIMLF will be activated based on the vector of the vertical component (Moschovakis et al., 1991a, 1991b). Also, in the meantime, the OPN’s receive inhibitory input originating from inner SGI and stop firing (Strassman et al., 1987). The down pathway, including the down motor neurons in the oculomotor and trochlear nucleus, determines saccade amplitude and velocity, and it receives input from the down MLBN in RIMLF (King and Fuchs, 1979; Moschovakis et al., 1991b; Horn and Büttner-Ennever, 1998). Its role is similar to the role of the abducens nucleus for horizontal saccades. The projection is purely ipsilateral. For the up pathway, the oculomotor nuclei and RIMLF are connected bilaterally to up MLBN’s in RIMLF (Moschovakis et al., 1991a). The interstitial nucleus of Cajal (INC) acts like the NPH encoding position signals for vertical saccades (King et al., 1981; Crawford et al., 1991; Fukushima et al., 1992). It receives mainly RIMLF input

and projects to vertical motor neurons (Kokkoroyannis et al., 1996). There is no known interconnection between INC and the SC.

There are also studies for microsaccade generation in the brainstem circuit (Hafed, 2011). Although the nuclei involved in generating the vertical component are not yet determined, the horizontal component of a microsaccade, involving the SC, EBN, LLBN, IBN, OPN, and CMRF, is controlled similarly to large saccades (Van Gisbergen et al., 1981; Brien et al., 2009; Hafed et al., 2009).

#### **1.4. The SC and active vision**

Primates are active animals with a fovea (Woollard, 1927; Provis et al., 2013). The fovea contains a high density of photoreceptors, and the density abruptly decreases when we go to the peripheral region. This means that our spatial resolution is the highest at the fovea. In order to obtain a clear image, we move our eyes constantly and point our fovea to where it interests us the most (Yarbus, 1967). The most common and efficient eye movement that we use for scanning a visual scene is the saccade (Dodge, 1903; Westheimer, 1954). As previously described, fast speeds and flexible amplitudes make saccades a very good tool to orient our gaze efficiently. However, there can be problems if we dissect this behavior carefully (Wurtz, 2008; Hafed et al., 2015). A series of processing steps need to take place in the brain before the eye even begins to move, and these steps include target selection, shifting of attentional processing resources to the target, and pre-analyzing the possible landing location. These steps are known to be related to cortical saccade generation processes, as described briefly in the above sections, but the SC is also involved. Once the saccade is initiated, a fast-moving retinal image to the counter direction of the saccade necessarily occurs. Suppressing this visual input is then necessary because otherwise, one would experience a blurry visual scene whenever a saccade starts. Right after a saccade, the oculomotor system should stabilize itself as fast as possible and gradually start to recover from this suppression. In the meantime, any visual information should be sent and analyzed as fast as possible in order to maintain a continuum of the visual representation. This concept should be able to apply to both saccades and microsaccades since they are very similar.

To understand all the mechanisms mentioned above, and which happen very briefly in time (around 200 ms in total) but frequently (around 1 to 4 times a second), researchers have conducted a great amount of experiments. Although some detailed mechanisms are still not completely understood, the overall picture for us to be able to

maintain visual stability is relatively clear. In this section, I will separate these phenomena into two main effects of spatial updating (Fig. 8) and saccadic suppression (Fig. 9), and I will discuss the known physiological evidences, possible mechanisms, and the unknown parts, some of which I have already addressed in my completed experiments.

### 1.4.1. Transsaccadic spatial updating, memory, and attentional shifts

It has been proposed for long that in order to maintain visual stability, the eye movement signal needs to be sent back to the brain for discriminating self-motion from real-world image motion (von Helmholtz, 1910; Sperry, 1950; von Holst and Mittelstaedt, 1950). Three possible sources were proposed and after a series of experiments, the most promising one was an extraretinal “corollary discharge” of the saccade command (Sperry, 1950; von Holst and Mittelstaedt, 1950; Guthrie et al., 1983). There are several elegant experiments done to prove that such a signal exists (Bridgeman et al., 1975; Stevens et al., 1976; Matin et al., 1982; Stark and Bridgeman, 1983; Bridgeman, 2007; Sommer and Wurtz, 2008). Before and after saccades, because of a change in the eye position, remapping the visual representation and a comparison of the visual scene before and after saccades is needed to make sure that the movement was caused by self-motion not image motion. At the same time, pre-processing of the saccade target is also necessary to later match perception before and after a saccade. Two important concepts, spatial updating and attentional shifts become essential for maintaining visual stability. I will introduce how spatial updating and attentional shifts can be achieved separately by making use of corollary discharge.

***Transsaccadic spatial updating*** There are two main hypotheses on how spatial updating is achieved (Breitmeyer et al., 1982). In one, which becomes necessary when visual representations are retinotopic, RF’s are shifted to their future location around the time of a saccade (Fig. 8a, b). In the other, each retinal image is projected to a higher order spatiotopic map in order to maintain the panorama of visual representation (Fig. 8c). Although each of these hypotheses has supporting neuronal evidence, shifting RF’s represent the main research tide of the field, especially in the numerous retinotopic visual areas. Shifting RF’s were first found in LIP (Duhamel et al., 1992; Colby et al., 1996; Kusunoki and Goldberg, 2003; Heiser and Colby, 2006) and later in FEF (Fig. 8a, b) (Umeno and Goldberg, 1997, 2001; Sommer and Wurtz, 2006;



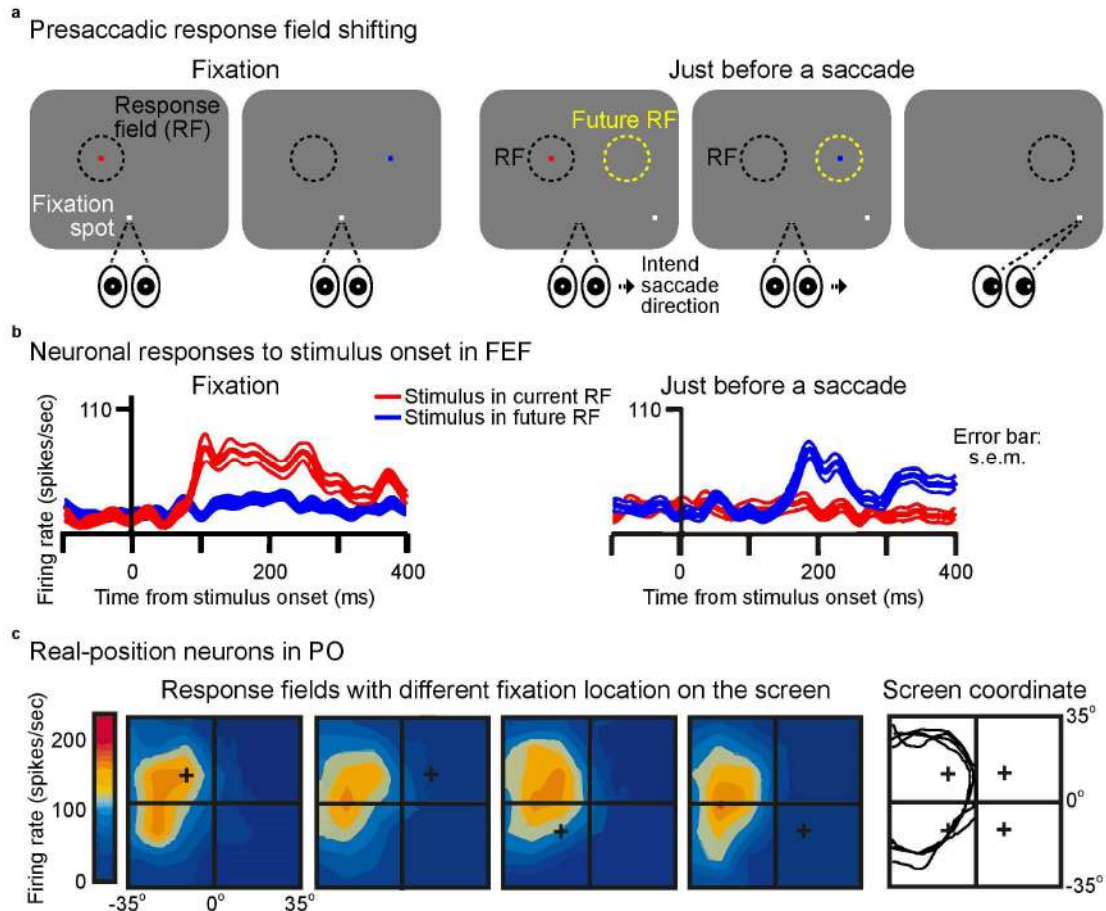


Figure 8. Two ways of maintaining visual stability around the time of saccades.

One way to maintain visual stability around the time of saccades is to shift the neurons' visual RF's before saccades to their future retinotopic location. Behavioral paradigm (a) and neuronal response of FEF neurons (b) shows how to probe presaccadic visual RF remapping. During fixation (left panel), the monkey fixates at the fixation spot (white spot) over a grey background on the screen. If you flash a visual stimulus (a, red dot, color notion is for later indicating neuronal response. In reality, most experiments use a white dot as the stimulus) in the visual RF of an FEF neuron, the neuron increases its activity (b, red trace in left panel). If the stimulus is outside the neuron's visual RF (a, left panel with blue dot, similar notion to red dot), the neuron is not sensitive to it (b, blue trace in left panel). We can do the same experiment right before a saccade and the saccade will bring the neuron's visual RF to the future retinotopic location indicated in yellow (right panel). Although the eyes have not moved yet, the neuron is no longer sensitive to the stimulus presented in the current RF (a and b, right panel with red dot and red trace, respectively). The neuron is already sensitive to the stimulus presented in the future location of where its visual RF will be (a and b, right panel with blue dot and blue trace, respectively). Error bar in (b): s.e.m. Another way to maintain visual stability around the time of saccades is to have higher order neurons forming an absolute spatial representation from each retinal image. (c) A real-position neuron found in PO in which the RF's remain at the same spatial location irrespective of eye position. Colored maps show the visual RF's mapped with four different fixation locations (black crosses) in screen coordinate (left panel). Contour plots in screen coordinates show almost perfect overlapping of the neuron's RF's mapped with different fixation locations (right panel). (a,b) modified from (Sommer and Wurtz, 2006). (c) modified from (Duhamel et al., 1997).

Zirnsak et al., 2014), V2, V3A (Nakamura and Colby, 2002), V4 (Tolias et al., 2001), and SC (Walker et al., 1995; Dunn et al., 2010; Churan et al., 2011). In this phenomenon, neurons start to have visual sensitivity for stimulus onset just before the saccade is executed in the neuron's future RF location, retinotopically bound to the landing

position of the saccade. This property makes these neurons a perfect candidate for comparing visual scenes before and after saccades. Also, these neurons must have the amplitude and direction information of the proceeding saccade in order to predictively shift their RF's even before the movement starts. This information can be conveyed by corollary discharge (Rao et al., 2016). There is also behavioral evidence suggesting that the brain is using this anticipatory change (Matin and Pearce, 1965; Ross et al., 2001; Melcher, 2005, 2007). After a possible corollary discharge pathway from the SGI via medial dorsal thalamus relay to FEF has been identified (Lynch et al., 1994; Sommer and Wurtz, 2004a), a crucial test to see if this is really functional would be to inactivate this pathway and record in the response field shifting neurons (Sommer and Wurtz, 2004b, 2006). The experiment turned out to be successful; after inactivation of the medial dorsal thalamus, the future RF location significantly reduced its sensitivity to visual stimuli without altering saccade generation. The corollary discharge relay to other brain areas remains to be determined.

The other hypothesis is that every single fixation is projected to a higher spatio-topic map (Fig. 8c) (Breitmeyer et al., 1982; Burr and Morrone, 2011; Melcher and Morrone, 2015). This is very tempting because it is exactly how we feel to have a continuous representation of the visual scene, instead of snapshots between individual saccades (Melcher and Morrone, 2015). Other body movements can also be integrated in this map. No such map has been identified in primates yet, but some neurons exhibit retinotopic maps with additional gain modulation in visual responses sensitive to eye position in orbit. These neurons are found in posterior parietal cortex (Andersen and Mountcastle, 1983; Zipser and Andersen, 1988), V1 (Trotter and Celebrini, 1999; Durand et al., 2010), V3A (Galletti and Battaglini, 1989), V4 (Bremmer, 2000), MT, MST (Bremmer et al., 1997), FEF (Cassanello and Ferrera, 2007), SEF (Schlag et al., 1992), and DLPFC (Funahashi and Takeda, 2002), meaning that a representation of object position relative to the head can be recovered irrespective of eye position. Other neurons that respond to a single spatial location instead of the retinal location are also found later in parietal cortex (Galletti et al., 1993), PO (Fig. 8c) (Galletti et al., 1995), and ventral intraparietal area (VIP) (Duhamel et al., 1997). The current working hypothesis is that these neurons form the map which cannot be identified at the single neuron level, but in a higher dimensional representation encoded in a population of neurons (Zipser and Andersen, 1988; Pouget et al., 1993; Colby and Goldberg, 1999; Melcher and Morrone, 2015). Additionally, hippocampus can have a spatial map that can guide eye movements based on non-retinotopic topography (Killian et al., 2012, 2015; Meister and Buffalo, 2016).

***Transsaccadic memory and attentional shifts*** Another possible mechanism to distinguish between self-motion and image motion relies on transsaccadic memory and attentional shifts (Wurtz et al., 2011; Higgins and Rayner, 2015; Rolfs, 2015). It is proposed that right before a saccade is executed, a memory of the future saccade end point and around it is built and stored temporarily (Rayner, 1978; Irwin, 1992). After the saccade is executed, a brief comparison of the memory and current visual representation occurs. If they match, this means that retinal signals were generated due to self-motion and the eye movement was accurate (Hollingworth et al., 2008). It has been first demonstrated that this mechanism is possible behaviorally (Deubel et al., 1996, 1998, 2002). Various experiments have been done and found that right before saccade execution, a visual processing enhancement is observed at the future saccade ending position and immediately around it (Hoffman and Subramaniam, 1995; Kowler et al., 1995; Deubel and Schneider, 1996). This indicates a shift in attentional resources to analyze the future location. As it is virtually impossible to make saccades to one location and pay attention to another, it is considered that spatial attention and saccades are closely coupled. As a matter of fact, attention and eye movements share very similar neuronal pathways (Corbetta et al., 1998). There is also behavioral evidence on spatial attention for limiting perception of selected locations for saccades (Rensink et al., 1997; Cavanaugh and Wurtz, 2004; Simons and Rensink, 2005). The neuronal evidence of such memory is not found yet, but enhanced visual responses at the saccade target before saccade execution in V4 are observed (Moore et al., 1998). The SC superficial layer also shows enhanced visual responses before saccades (Goldberg and Wurtz, 1972b). Also, the retinotopic remapping of the future RF, which was explained above, is a relevant neuronal effect because it suggests that more neuronal resources are dedicated towards the saccade target location (Fig. 8a, b). Furthermore, LIP neurons do not show RF shifts if attention is not directed to the saccade end point (Gottlieb et al., 1998). The other type of attentional shift, covert attention, can be directed to wanted spatial locations without changing eye position (Posner, 1980). However, recent evidence suggests that microsaccades can be correlated with the covertly attended locations (Hafed and Clark, 2002; Engbert and Kliegl, 2003). A detailed examination of the underlying mechanisms is needed, especially given how theoretical considerations suggest a highly interesting interpretation of such correlations (Hafed, 2013; Tian et al., 2016). We performed such experiments and found that signatures of covert visual attention can be found just before microsaccades, irrespective of attentional task requirements (Chen et al., 2015). This result provides a possible neural basis for covert attentional links to eye movements in general.

## 1.4.2. Saccadic suppression

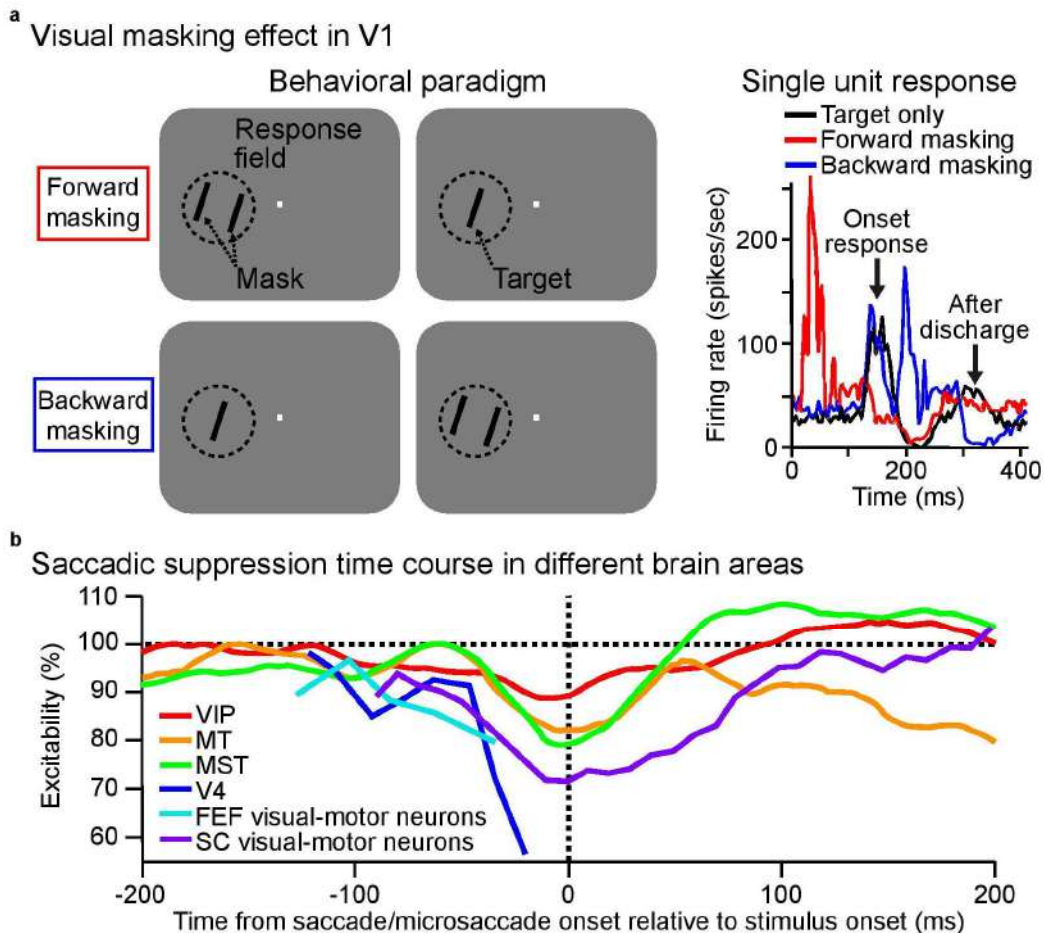


Figure 9. Saccadic suppression.

One possible mechanism for saccadic suppression is through a purely visual effect. (a) demonstrates such effect by showing the visual masking paradigm (left panel) and the neuronal response recorded in V1 (right panel). The behavioral paradigm can be separated into forward masking, in which the mask comes before the target, or backward masking, in which the mask comes right after the target. If the target is presented in a V1 neuron's RF (right panel, black trace), there will be a target onset response followed with a later after discharge. Forward masking can effectively suppress the onset response but leaving the after discharge unchanged (right panel, red trace). Backward masking on the other hand suppresses the after discharge (right panel, blue trace). The other possible mechanism is through an extraretinal signal from a saccade related region and broadcast the suppression signal to all other brain areas. (b) shows potential brain areas influenced by such a signal around the time of saccadic eye movements. The x-axis denotes the time aligned with either saccade or microsaccade onset. The y-axis denotes normalized visual response relative to a no movement condition, showing how visual sensitivity or excitability changes around the time of saccadic eye movements. As can be seen, the excitability drops before the movement starts and reaches a minimum around the time of movement onset for the brain areas listed here. The excitability gradually returns back to 100% after around 50 to 100 ms, meaning that the suppression can still be present shortly after the end of the movement. (a) modified from (Macknik and Livingstone, 1998). (b) modified from (Bremmer et al., 2009) for VIP, MT, and MST; (Han et al., 2009) for V4; (Krock and Moore, 2016) for FEF; (Hafed and Krauzlis, 2010) for SC. Note that data from SC is around the time of microsaccades; all other data are around the time of saccades.

Several behavioral experiments have suggested that starting around 50-100 ms before a saccade, our visual sensitivity starts to drop. During saccades, sensitivity drops to the lowest level. And after saccades, usually by around 100 ms, our visual sensitivity recovers to normal (Matin, 1974; Volkman, 1986; Bremmer et al., 2009). Besides the saccade target, as described previously with a shift of attention mechanism, the suppression effect is all over the visual field (Matin, 1974; Volkman, 1986; Bremmer et al., 2009). Several brain areas show suppressed visual responses around the time of saccades (Fig. 9b) (Robinson and Wurtz, 1976; Bremmer et al., 2009; Berman and Wurtz, 2011). There are two possible mechanisms for perceptual saccadic suppression; one is visual masking (Fig. 9a), and the other one is by extraretinal corollary discharge. Each of the two mechanisms has possible neuronal evidences to support it. Most likely, both mechanisms coexist. I will introduce first the neuronal and behavioral evidence for visual masking and then corollary discharge.

**Visual masking** This is a purely visual mechanism which is proposed to explain how we are unaware of blurry visual stimuli during saccades. Experimentally, it comes into two flavors: either a high contrast masking stimulus comes before saccades, thus blocking perception of a later test stimulus with low contrast of any kind; or a masking stimulus comes after saccades, thus blocking the previous test stimulus (Fig. 9a) (Matin et al., 1972; Campbell and Wurtz, 1978). This only happens with high contrast environments with critical spatial temporal edges of the mask. The neuronal substrates of visual masking were first found in V1 (Fig. 9a) (Judge et al., 1980; Macknik and Livingstone, 1998). Supragranular neurons in V1 greatly reduce their sensitivity for stimulus motion during saccades if a masking stimulus appears either before or after the movements. Even if the monkey fixates, the masking is still effective demonstrating that it is a purely visual effect. Similar effects are also found in the SC superficial layer (Wurtz et al., 1980; Bender and Davidson, 1986)

**Suppression via extraretinal signals** Reduced visual sensitivity could also occur if an extraretinal signal associated with the movement command is broadcast to the visual system (Fig. 9b). Several behavioral studies show that detection thresholds are elevated (Volkman, 1962; Latour, 2004), motion sensitivity is reduced (Bridgeman et al., 1975; Burr et al., 1982), and a selective reduction for low spatial frequencies takes place (Volkman et al., 1978; Burr et al., 1982, 1994). But saccadic suppression does not occur for colors, which has made scientists hypothesize a possible role of suppression specific to the magnocellular pathway in LGN (Burr et al., 1994). Moreover, afterimages on the retina are also suppressed during saccades, demonstrating possible

extraretinal signals from a corollary of the saccade commands mediating such suppression (Kennard et al., 1970). However, later neuronal recordings in the magnocellular pathway in LGN and V1 failed to demonstrate visual response suppression specific only to the magnocellular pathway; instead, there was modest suppression during saccades and a later large enhancement was observed after saccade end (Wurtz, 1968, 1969; Fischer et al., 1981; Ramcharan et al., 2001; Reppas et al., 2002). This does not mean that there is no neural signature of suppression. In fact, other brain areas involved in visual perception, primarily extrastriate cortex, including MT, MST, VIP, V4, FEF, pulvinar, and SC, show strong suppression (Fig. 9b) (Robinson and Wurtz, 1976; Bremmer et al., 2009; Berman and Wurtz, 2011)(Han et al., 2009; Krock and Moore, 2016). Suppression also occurs around the time of microsaccades (Fig. 9b) (Hafed and Krauzlis, 2010). It has been recently proposed that since a saccade command corollary is generated in the deeper SC, corollary discharge could be relayed up to the superficial layer with inter-laminar connection, and sent to inferior pulvinar (Berman and Wurtz, 2008; Wurtz et al., 2011). The inferior pulvinar projection conveys then the saccadic suppression signal to MT (Berman and Wurtz, 2010, 2011; Berman et al., 2016). However, the actual neurons that are interconnected in this pathway are relatively small in number. In fact, in the most recent study from (Berman et al., 2016), inactivating the SC superficial layers did not reduce suppression in MT, but inactivating deeper layers did. Although this is a possible pathway, more detailed characterization of the suppression signal, especially the selectivity to spatial frequency along this pathway, is needed. We found such selectivity was established in the deeper layer of SC but not in the superficial layer by looking at microsaccadic suppression (Chen and Hafed, 2017). This evidence is the first neural locus showing spatial frequency specific suppression similar to behavior. Furthermore, it suggests a possible method to track the pathway conveying suppression signals to cortical areas.

### 1.5. Open questions

It is not hard to find from the above detailed introduction that the SC is a historically popular brain area to study. It is involved in multiple important functions related to vision, attention, and orienting behavior. However, important questions remain still. In this dissertation, I have asked the following questions, with detailed answers provided in full manuscripts attached.

1) Motivated by findings related to the SC providing an alternative visual pathway for blindsight, and also motivated by the lack of details on visual representations of first order stimuli in the SC, I found it important to characterize the visual properties of the primate SC in awake behaving animals.

One important such aspect of visual properties relates to how upper and lower visual fields are segregated in the SC, and how they may physiologically differ. For example, in primary visual cortex, the upper and lower visual fields are physically segregated into ventral and dorsal parts due to wiring from the retina and LGN, and theoretical considerations have suggested possible functional differences between such fields (Previc, 1990). However, in the SC, it was assumed that upper and lower visual field representations are identical. This is not in line with the nature of the environment that we operate it. Specifically, primates encounter different object sizes in terms of retinal image projections, specifically small and far objects in the upper visual field and closer and bigger object in the lower visual field. According to this ecological constraint from the environment, it is hard to imagine that a purely symmetric upper and lower representation exists.

2) Concerning active vision, it is known that attentional shifts and saccades are tightly coupled and may contribute to visual stability. However, during fixation, microsaccades occur. Base on the similar generation pathway in subcortical nuclei between saccades and microsaccades, similar links for microsaccades to attention might be expected. During active fixation, a type of visual attention, called covert attention, could be linked with microsaccades in the same scenario as with attention and large saccades. This possibility needs to be tested in much more detail than has done so far in the literature.

3) Selective suppression of low spatial frequencies is thought to be an important phenomenon for understanding the neuronal substrates of saccadic suppression. However, the actual neuronal locus showing this selectivity has to date not yet been found. Since the SC is essential for generating corollary discharge to mediate saccadic suppression, I searched for selective suppression in the SC using microsaccades as an experimental model system.

4) It is known that after large saccades, a mechanism is activated to stabilize the eye from the recently moving scene. This mechanism has been proposed to contribute to visual stability after saccades. At this moment, the eyes are particularly sensitive to image motion. Since microsaccades and saccades share similar generation mechanisms up to the brainstem level, it is possible that such stabilizing mechanisms are also triggered after microsaccades. Nevertheless, there is no study demonstrating such possibility.

## 2. Main results

### 2.1. Visual responses to first order stationary stimuli in the SC

It has been shown since more than 50 years ago that SC neurons have visual responses. Almost in parallel with this finding, researchers recognized that the SC is also a crucial midbrain structure for orienting behavior, especially for saccadic eye movements. Right after, there was an explosion of studies in understanding subcortical connections of movement control and cortical neuronal substrates for eye movements. The visual properties, however, were left out after some simple characterizations using light dots and bars. Later research in saccadic patterns suggests that orienting efficiency and target selection can differ under a variety of visual conditions and in natural scene scenarios. This means that low level image statistics can massively influence saccade reaction time. One particularly interesting theory driven by image statistics, the saliency map, turned out to be able to predict target selection and eye movement patterns nicely. However, the timing of saccades is not investigated as heavily, and also the actual neuronal substrates for this purely hypothetical map remain debated. It may seem that SC is a good candidate for this map because visual topography in SC is naturally co-registered with deeper saccade topography. However, before we can go into evaluating this possibility, there is an urgent need to first characterize the low level visual responses of the SC. Such responses could be used to understand spatial frequency tuning, contrast sensitivity, center surround interaction, orientation tuning, and temporal resolution in superior colliculus. Here, we did exactly these experiments with various visual stimuli.

We trained our monkeys to fixate at the center of the monitor. After a random delay, various stimuli were presented in blocks in isolated SC neurons' visual RF's. These stimuli were sized as large as possible to elicit the strongest visual response. We recorded single units and local field potentials during these experiments. In a spatial frequency tuning block, we presented vertical, 80% contrast Gabor patches with different spatial frequencies ranging from 0.56 cycles per degree (cpd) to 11.11 cpd. In a contrast sensitivity block, we presented vertical, 2.22 cpd sine wave gratings with different contrasts ranging from 5% to 80%. For center surround interaction, we used similar gratings to the contrast sensitivity block, but with fixed 1 degree diameter in size. This is normally at least twice smaller than the visual RF. In an orientation tuning block, we presented 2.22 cpd, 80% contrast sine wave gratings with 6 different tilts covering a full range of orientations from horizontal to oblique to vertical. For a



temporal resolution block, we presented, vertical, 2.22 cpd Gabor patches with different temporal flickering frequencies, ranging from 3 to 60 Hz, for 2 seconds. The contrast of the flickering grating was set to gradually increase from 0% to 100% and then decrease back to 0% in order to avoid onset and offset transients. We analyzed peak visual responses, first spike latencies, tuning functions, and local field potentials for each of the experiments separately. For a separate behavioral study, we asked the monkeys to perform visually guided saccades to stimuli similar to those used in neuronal studies, and we correlated behavioral effects to neural ones.

We found spatial frequency tuning in the SC. The preferred spatial frequency varied the most when the neurons were close to the foveal representation. Gradually, the neurons showed less and less high spatial frequency preference when they represented more eccentric locations. The spatial frequency tuning curves were always low pass even for the highest spatial frequency preferring neurons. First spike latency was also the shortest for the lowest spatial frequency tested in all neurons, regardless of the preferred spatial frequency. A linear combination of first spike latency and peak visual response measured from the neurons could easily predict the result from behavior measurement of mean and variance in saccade reaction time obtained in completely different sessions. Moreover, center surround differences in contrast sensitivity appeared through a change in the slope of the psychometric function, not by changing the response gain or sensitivity. First spike latency also decreased with higher contrast but was statistically unchanged comparing large to small gratings. Highly orientation selective neurons were rare in the SC, and first spike latency was identical for the most preferred orientation and the least preferred orientation. The temporal resolution for all the neurons lied in between 10 to 20 Hz across eccentricities.

To conclude, we extensively characterized visual responses to first order stationary stimuli in the SC. We found neurons with low pass spatial frequency channels and weak orientation selectivity. We also found center surround interactions in the visual RF's different from early visual areas. Temporal filtering in the SC was around 10 to 20 Hz. This study is not just a thorough documentation of low level vision in the SC, but it can also be used to interpret behavioral results and the underlying mechanisms related to more complex stimuli, like natural images, and it can additionally give us insight in the visual capabilities of blindsight patients.

## **2.2. Differences between upper and lower visual fields in the SC**

It has been shown that the SC is critical for the sensorimotor transformation from retinal image features into gaze shift commands. Superficial SC layers contain retinotopic maps of the contralateral visual field, and deeper layers contain spatially registered eye-movement maps. Similar to the primary visual cortex, the SC magnifies foveal representations. Retinotopic eccentricity in visual space maps onto SC tissue using logarithmic warping. In this model, more tissue represents foveal locations and with higher resolution, but the upper and lower visual field representations are assumed to be identical. In our daily visual world, however, we encounter different sensory and motor conditions than the model suggested. For example, peri-personal “near” space is predominantly viewed through the lower visual field, whereas extra-personal “far” space encompasses the upper visual field. Thus, image features can differ between the lower and upper visual fields. In this study, we revisited the model and tested the hypothesis that SC retinotopic organization is in tune with the ecological constraints across the horizontal meridian.

We mapped neurons’ visual and motor RF’s while monkeys were performing saccade tasks. They were trained to fixate first at the center of the screen. After a certain delay, a peripheral target was presented. The target either stayed on or was only briefly flashed. After a second delay, the fixation spot was removed and the monkeys were required to saccade to either the still existing or remembered target location. The target locations were defined online using a real-time user interface allowing us to sample multiple locations that were needed to map out the RF’s. We defined the visual or motor RF size by first plotting the visual or motor response for each neuron in retinotopic coordinates and then calculating the area where responses were significantly above the activity before target onset. We also analyzed visual or motor response strength and visual response latency for all the neurons. For spatial frequency tuning or contrast sensitivity, we recorded a subpopulation of mapped neurons with vertical sine wave gratings presented in the neurons’ visual RF’s. The gratings were altered either in spatial frequency, ranging from 0.56 cpd to 11.11 cpd, with fixed 80% contrast, or in contrast, ranging from 5% to 80%, with fixed 2.22 cpd. To obtain spatial frequency tuning curves and contrast sensitivity curves, we analyzed peak visual responses to the stimuli and fitted the results with standard equations based on the previous literature.

We discovered a significant asymmetry across the horizontal meridian. Visual and motor RF sizes in the upper visual field were significantly smaller than in the lower visual field. The response strengths were also different, where visual responses were stronger in the upper visual field, but motor responses were stronger in the lower visual field. Visual response latency was shorter in the upper visual field. Moreover,

upper visual field neurons had higher spatial frequency tuning and contrast sensitivity. These results all indicated possible faster reaction times and more accurate target encoding in the upper visual field. We further analyzed a behavioral data set and found indeed that orienting to the upper visual field had shorter reaction times and more accurate landing positions comparing to the lower visual field. At the end, we modified the existing model of SC topography to add magnification of the upper visual field on top of magnification of foveal eccentricities.

Together, we found a sharper, stronger, and lower-latency upper visual field representation in the SC, and also explored the behavioral and neuroanatomical consequences of these observations. Our results suggest that representations in specific brain areas can be tuned to these areas' functions in interacting with the natural world, and also motivate a recasting of representation modalities in other brain areas in which models of their structure may have been over-simplified.

### 2.3. Neuronal response gain modulations around microsaccades in the SC

Neuronal modulations such as response gain enhancement and variability reduction are classically thought to reflect the allocation of covert visual attention to behaviorally relevant stimuli without eye movements. However, even during fixation, microsaccades constantly occur. Because large saccade and microsaccade generation are similar, it may be the case that the neuronal modulations observed during covert attention are related to the preparatory signals for microsaccades, as suggested in the premotor theory of attention. Here we tested this hypothesis by showing that these classic neuronal signatures of attention can occur during pure fixation tasks immediately before microsaccades without the requirement of allocating covert visual attention.

We trained our monkeys to perform a simple passive fixation task, while we presented vertical sine wave gratings with 2.2 cpd but different contrasts, ranging from 5 to 80%. The grating was presented in the visual RF of each recorded neuron in monkeys' SC. In the meantime, we recorded single unit neuronal activities. We analyzed visual responses after grating onset and separated trials based on whether such onset happened without microsaccades as a baseline, or within 100 ms before or after microsaccades. For comparison, we also analyzed SC neurons from two more monkeys, and FEF neurons from yet two more monkeys. For the latter four monkeys, the stimulus in the visual RF was a small spot and acted as a cue to a subsequent discrimination task.

In all six monkeys, we found robust microsaccadic enhancement of visual responses prior to the onset of a microsaccade, regardless of the task or area recorded. The enhancement was sensitive to the direction of ongoing microsaccades. Immediately after microsaccades, visual response suppression always occurred without directional dependency. Moreover, in the first two monkeys, we further analyzed contrast sensitivity functions to show that the change was a response gain change, not a sensitivity modulation. We also analyzed Fano factor to assess neuronal variability, and area under ROC curves to assess discriminability between baseline and microsaccade trials. All analyses revealed modulations that are classic signatures of covert visual attention (e.g. response gain enhancement, reductions in Fano factor and increases in ROC discriminability), but without any attentional task requirements. In addition, all of the above attentional signatures were also observed in later sustained visual responses period, and again without any attentional cueing.

In all, using six different monkeys and two different brain areas classically implicated in covert visual attention, we found that neuronal signatures of attention occur if stimuli appear immediately before microsaccades without the need for attentional tasks. Our results suggest that there is an obligatory link between premotor processes and neuronal signatures of selective visual processing, even for the smallest possible saccades, which may seem at first hand to be irrelevant to the neuronal modulations. It also suggests that we need to be more careful in interpreting our results even if we ask our subjects to maintain fixation during covert attentional tasks because microsaccades unavoidably happen during fixation.

### **2.4. Spatial frequency dependent microsaccadic suppression in the SC**

Saccadic eye movements happen several times per second. During these rapid eye movements, retinal images are shifted massively. But to our perception, this is normally unnoticed. Several possible theories on suppressing visual sensitivity immediately around the time of saccades have been proposed. Although it seems likely that a pure visual masking effect and an extra-retinal signal can both mediate saccadic suppression, controversies for saccadic suppression will not be resolved without further understanding of the underlying neuronal mechanisms. For example, one important behavioral study which demonstrated selective perceptual suppression in low spatial frequency stimuli implicated possible roles of the magno-cellular pathway in mediating saccadic suppression. However, later studies failed to establish such selective suppression in magno-cellular neurons in LGN and V1. Later, a corollary of the

saccade command, which has been shown to be generated in the deeper motor-related neurons in SC, was hypothesized to be relayed through the superficial visual neurons and further broadcast to other dorsal visual brain areas to suppress visual sensitivity. In light of this hypothesis, we designed a sensitive behavior paradigm and recorded single unit responses and local field potentials in both superficial and deeper SC neurons to look for behavioral and neuronal selective suppression.

In this study, instead of large saccades, we took advantage of microsaccades to study saccadic suppression. Because microsaccades are naturally small in amplitude, RF's are not displaced much after microsaccades. This advantage simplified the experimental design, data acquisition, and later data analysis. To establish a sensitive enough behavioral measurement of selective spatial frequency suppression, we trained our monkeys to perform visually guided saccades. Monkeys were first fixating at the center of the screen. After a delay, a real-time microsaccade detection algorithm was activated. After a microsaccade was detected, with various delays, a vertical Gabor patch with a range of different spatial frequencies, from 0.56 cpd to 11.11 cpd, was presented in the periphery and the fixation spot was removed simultaneously. The monkeys were trained to saccade to the grating after it appeared. We measured how reaction time was modulated as a function of when a particular grating appeared after a given microsaccade. In a separate session, we recorded visual responses to these gratings neuronally when they were presented in SC neurons' visual RF's. Monkeys in this case maintained fixation and never looked at the gratings. We analyzed response strength and latency of single unit and local field potentials and compared them with behavioral results.

Immediately after microsaccades, saccade reaction time for lower spatial frequency stimuli was selectively slowed down. This was similar to the previous original human study using a different perceptual measure and after large saccades. We found also after microsaccades that the visual responses of our single units were suppressed more with lower spatial frequency and less with higher spatial frequency. Moreover, we found that our behavioral measurement was better correlated with the suppression of visual-motor neurons than purely visual neurons. These results indicate that the behavioral cost in saccade reaction time was directly proportional to the suppression in visual-motor neurons. In field potential analyses, it was the change in the field potential latency which correlated the best with behavior, and again more so for visual-motor neuron locations in the SC. We also found a microsaccade related field potential change in both superficial and deeper SC layers.

In summary, these results indicate that visual-motor neurons in the deeper layers in the SC were more relevant to behavior than the superficial visual neurons. This is

in contrast to textbook views of how the SC might mediate saccadic suppression. We also found a wide spreading microsaccade related signal by analyzing field potentials in both neuronal types even if the neurons do not spike for microsaccades. This suggests that horizontal interactions in the SC can allow microsaccades to influence wide ranges of eccentricities, as was also found psychophysically in humans. In all, this study allows us to question the hypothetical function of the relay from deeper through superficial layers in SC, which has been strongly suggested in the literature to be part of the SC pathway for saccadic suppression.

### 2.5. Pre- and post-microsaccadic modulation of ocular drift gain control

Actively sampling visual environments consists of frequent transitions from rapid eye movements to fixation. These transitions exhibit a period of enhanced ocular drift immediately after large saccades before a gradual reduction to normal drift speed. During this period, restoring a reliable visual sensation is important because of interruptions of visual signals during saccades. It has been shown that during the enhanced drift period, a rapid gaze stabilizing mechanism is activated. The efficiency of this mechanism can be measured by analyzing the reflexive ocular following response to image motion presented to the eyes.

Even during fixation, the transition from microsaccades to slow ocular drifts puts our eyes in the same situation as with large saccades. However, whether the same enhanced ocular drift period and the stabilizing mechanism apply to immediately after microsaccades is unknown. Here we carefully analyzed the ocular drift pattern immediately before and after microsaccades and measured the efficiency of the stabilizing mechanism after microsaccades.

For ocular drift patterns, we collected eye movement data from two monkeys using scleral search coils while they fixated a fixation spot presented on a screen. We carefully determined the starting and ending point of a microsaccade by a pre-defined velocity and acceleration threshold and manually inspect and refined the result. For the efficiency of ocular following, in separate sessions, we trained the monkeys to fixate over a static, full field sine wave grating and activated an online microsaccade detection algorithm after they steadily fixated. When a microsaccade was detected, with a random delay, we triggered a horizontal motion of the grating. This image motion is known to drive an ultrashort-latency ocular following reflex that attempts to stabilize this motion on the retina. We collected eye movement data for one monkey using scleral search coils and the other one with a video eye tracker. We measured the

initial component of this ocular following response as a proxy for the efficiency of the retinal stabilizing mechanism.

We found that immediately after a microsaccade, there was enhanced ocular drift velocity lasting for 50 to 75 ms. During this period, the velocity gradually reduced to baseline slow drift velocity measured far from any microsaccade. The drifting trajectory immediately after a microsaccade was generally in the opposite direction from the preceded microsaccade. The ocular following response of the full field motion was also enhanced during this period. On the other hand, the ocular drifting velocity was stable and without systematic changes in trajectory immediately before microsaccades.

In summary, we demonstrated that even for microsaccades, the transition to subsequent fixation still consists of a short period of enhanced ocular drift, together with enhanced efficiency in stabilizing the gaze. These results not just add extra information to the similarity between saccades and microsaccades, but they also have implications on our understanding of motor control and the subsequent perceptual consequences.

### 3. Discussion

#### 3.1. The SC as an important neuronal locus for blindsight

From anatomical connections, lesion studies, and psychophysics, researchers speculated possible roles of the SC in blindsight. However, historically, the SC was mainly viewed as a motor structure with less emphasis on its visual functions. A detailed visual characterization of awake, behaving primate was never tested. Although some recent studies characterized color opponent and also spatial and temporal frequency tuning, they either tested only color related stimuli or anesthetized animals. Our work is the first report on first-order stationary stimuli in awake, behaving primates. I found that in the SC, neurons in both superficial and deeper SGI layers contain low-pass spatial frequency channels, together with higher and more various spatial frequency preferences in the fovea. These neurons are with low orientation tuning, atypical center-surround, and up to around 10 to 20 Hz temporal resolution. Since we know that practicing helps to restore the detectability of stimuli by blindsight patients, sometimes even awareness of the stimuli, and since the SC provides an alternative visual pathway, these visual properties that I characterized will help us to design possible training stimuli to more efficiently drive the alternative visual pathway for blindsight patients.

It is also suggested that our saccadic system is governed by a map encoding the salient features in the scene. Although we are not aware of it, this hypothetical map derived from analyzing image statistics and eye movement patterns does a pretty good job on predicting eye movement path. The visual properties of the SC seem to fit really nicely with this hypothetical map. It could be that the saliency map is encoded using the visual properties of SC neurons, since we are also unaware of the visual information processed in SC. This will also help us to understand more about saccades, especially the reflexive saccades, and to design better stimuli for blindsight patients.

Recently, it was shown that eye movements of blindsight monkeys can be well predicted from the saliency map. It is also worth noticing that the visual response properties, like peak visual response and also the response latency (first spike latency), seem to be well correlated with saccade reaction time. It is known that saccade reaction time is not dependent on the stimulus strength or protocol from microstimulation in SC. Together, this means that the speed of visual processing and the strength of a visual response seem to dictate how fast a saccade can be generated. Understanding the visual properties in SC becomes important because if we know how long the SC



needs to process a certain information and also how these neurons spike for visual stimuli, we know how fast the saccade reaction time is. In summary, I think that these results will improve our knowledge in blindsight, saliency maps, and saccadic eye movements.

### **3.2. Updated topography in the SC**

A difference in visually-guided saccade reaction time between upper and lower visual fields has been known for a while. A proper explanation, however, was never proposed. Motivated by the ecological constraints that we daily encounter, I found that visual RF's are smaller, with stronger visual responses, and also with shorter response latencies in the upper visual field. Together with the assumption that visual representation in the SC is directly correlated with saccade reaction time, it is almost expected to have faster reaction time and more accurate saccades in the upper visual field. It is to my surprise that the encoding of a certain target seems also dictated by the density of the SC neurons. In the memory saccade test, the landing accuracy proved this possibility. This means that possible memory function is presented in the SC for encoding visual information of a saccade-relevant target. Other visual areas show larger lower visual field representation, like V1, V2, and MT. I think that this is mainly because of different functions in these areas since they are mainly for object discrimination and location. In line with this, in human psychophysics, it is known that the lower visual field has better attentional resources. In the SC, like the research history of it, the main function is primarily related to saccade control. In this case, overrepresentation of the upper visual field in other cortical areas related to eye movements is possible, like FEF, SEF, and LIP. The motor RF in SGI is also smaller in the upper visual field, but with weaker motor response. It was shown from microstimulation results that the saccade reaction time is not dependent on the stimulation strength, meaning that weaker motor response likely does not contribute to saccade reaction time per se. Instead, it may change the actual dynamics of the saccades, including velocity and duration. Detailed analysis needs to be done to show this possibility.

At the end of my study, I proposed a scaled SC visual representation map with larger area for upper visual field based on both response field size and anatomical recording locations. Although this does not change the overall function and the connections to cortical and subcortical areas of SC, but its internal property, especially intra-laminar connection, could be differently interpreted. Some models which take

such internal connection into account, like saccade efficacy, visual-motor transformation in SC, and the moving hill hypothesis should implement such difference between up and down visual field. This would hopefully give better explanations on neuronal or behavioral results and also more insights on SC functions from models.

It would also be interesting to understand how the SC might be interconnected with other visual maps in which other types of magnification, for example for the lower visual field, exists. Taken together, in this study, I found sharper, stronger, fast upper visual field representation in the SC and I hope to motivate a recasting of the representation map in other brain areas according to ecological constraints.

### **3.3. Covert visual attention and microsaccades**

A tight link between saccades and overt attention is known. Another type of attention, called covert attention, which literally means attending to somewhere or something without overtly looking at it, is used by scientists to uncover the mechanisms of attention. By definition, for these experiments, subjects are always asked to maintain fixation. But even during fixation, microscopic eye movements occur. In this study, we took one of these microscopic eye movements, microsaccades, because we know that behaviorally, visual perception can be altered around the time of microsaccades similar to how it is altered around large saccades. We found that before microsaccades, visual-motor neurons increased their visual response to stimuli conjugate with the direction of a microsaccade. This increase in neuronal response was accompanied with better discriminability and without changes in neural variability. This is very similar to the known brain modulations for covert attention. This means that a possible obligatory link between microsaccades to covert attention may exist, extending the obligatory link between large saccades and attention to all saccade sizes. On the other hand, visual neurons showed non-directional specific enhancement with similar neuronal properties. It could be that the superficial neurons receive the enhancement signal from the deeper neurons. The SC could also well be an important locus for covert attention. Supporting this argument, others have shown that after SC inactivation, the behavioral advantage due to covert attention abolished. However, in these experiments, the cortical neuronal signatures of attention were not altered. If such possible attentional signal is a movement preparation signal, like corollary discharge originated from the deeper SC layers, sending back to the cortical area, one should observe weaker or no signatures of attention after SC inactivation. Based on the above, it is likely that the cortical modulations are not from such pre-motor signal.

Cortical areas, like MT and MST, could be modulated by other cortical areas related to attention, like prefrontal cortex (PFC). Later, the attentional signal is sent to SC for enhancing behavior. However, because of inactivating the SC, the integration from the cortical area to subcortical region is defected, making the behavioral advantage disappear. With this reasoning, the SC is still an essential locus to integrate and represent the retinotopic signal for covert visual attention. It is just that in this case, the signal driving force is not provided by the SC. In other cases, like in the current study, the preparation signal of a saccadic movement can be sent back to cortical areas and initiate a cascade of attentional signals. In brief, it is important to take good care of possible contamination of covert attentional experiment since fixation is required and microsaccades constantly happen during fixation.

### **3.4. Studying visual stability using microsaccades as a tool**

Transsaccadic integration and visual stability have been debated for decades. Researchers in the field are dedicated to finding the possible mechanisms for how we maintain the continuum of our stable vision in time and in space while at the same time sampling the world using our eye movements. In order to gain insight into this topic, scientists design visual stimuli and record brain activity. However, usually for a subject, not just humans, but also primates, a session with a couple of thousands of saccades is already reaching the limit. It is hard to collect more data, unless with more subjects and with more time. Making use of microsaccades can help to reduce this problem. Microsaccades are very similar to saccades in almost all aspects, including saccade dynamics, generation mechanisms in the brainstem, and the most important part, effects on visual perception. It was shown that around the time of microsaccades, saccadic suppression happens. And in my work, selective suppression in low spatial frequencies was replicated. Also, before microsaccades, a gating effect related to the future microsaccade direction, the enhanced visual processing and neuronal gain enhancement, are very similar to with large saccades. Using microsaccades as a tool for studying visual stability therefore gives advantages, especially because the stimulus no longer needs to be large or with complicated designs to be eye conjugated. Microsaccades are small enough to keep the stimulus well within the RF of a neuron. In addition, microsaccades automatically happen during prolonged fixational tasks. Thousands of saccades are not required anymore to have enough data for statistical tests. With pure fixation, we can collect more data than required. As a matter of fact, in this study, I demonstrated how studying microsaccades can contribute to our

knowledge of visual stability. First, I used saccade reaction time after microsaccades as a proxy to detection thresholds during microsaccadic suppression. Next, in a separate session, I recorded neurons in the superficial and deeper SC layer responding to visual stimuli while monkeys maintained pure fixation. By post-hoc analyzing the modulation in the visual response after microsaccades, I found selective suppression to low spatial frequencies in only deeper layer. The suppressed response was highly correlated with changes in saccade reaction time collected in a completely different session. In brief, it is a good demonstration that using microsaccades as a tool, we can improve our knowledge in visual stability. At the same time, we found a possible neuronal locus for saccadic suppression.

#### **3.5. Postmicrosaccadic enhancement contribution to visual stability**

It was demonstrated that after saccade, a postsaccadic enhancement of slow drift exists. One possible explanation is that it's related to an error signal to correct the eye back to its programmed end point. The real mechanism is not well understood. In this period, an enhanced reflexive ocular drift is also present. It was proposed that after saccades, the continuum of our vision was disrupted by this rapid eye movement and needed to be recovered as fast as possible. A way to do this would be to tune up the retinal reflex in response to the visual scene in order to stabilize our eyes to acquire the next retinal image. Again, the actual mechanism mediating this behavior is not well understood; it is proposed that the motion sensitive brain area, MST could be the mediator. Right after saccades, it is also shown that LGN, V1, V4, and LIP has an enhanced visual response. This could well be to facilitate processing of the following retinal image taken after saccade. In this study, we demonstrated that the enhanced drift can also happen to microsaccades, adding another piece of evidence that saccades and microsaccades are from the same continuum of eye movement just with different sizes. It is also important to note that even for a microsaccade that is so small, similar mechanisms for maintaining visual stability will also be activated. Another interesting aspect of this study is that before a microsaccade, we did not find changes in drift speed. It is known that for prolonged fixation without eye movements, the image fades away. Our retina is more sensitive to changes in visual environment. It is important to have fixational eye movements for us to prevent visual fading during fixation. Microsaccades are considered to be the most effective one because of its efficiency in moving retinal image. One study even proposed that microsaccades are triggered because of slow retinal image slip. However, in our study, we looked at drift

velocity prior to microsaccades; there was no sign of reduction, but if any, there was a sign of a small enhancement in eye velocity immediately before microsaccade onset. This can be caused by different eye measuring techniques. Another counter argument is that other fixational eye movements, like drifts and tremors can also move the retinal image sufficiently to restore vision. Additionally, no such reduction is observed for large saccades. We concluded that microsaccades are not triggered solely by slower retinal image slip, even though it is effective in restoring vision from prolonged fixation. In short, we found another piece of evidence showing saccade and microsaccade are similar.

## 4. Concluding remark

Although the SC has been a very popular structure for research due to its importance in many aspects, including its role in oculomotor control, alternative visual pathways, and attention, questions still remain. In my dissertation, I have studied some important topics in the SC. I started with characterization of SC visual responses using classical stimuli like those used in early V1 and LGN studies. These fundamental experiments were left out for the SC because it is not in the traditional visual pathways. I found that the SC is likely to be in-tune with the statistics of natural scenes, and showed similar tuning properties that blindsight patients also show behaviorally (in preparation). I also found surprising asymmetries between upper and lower visual fields in the SC, which directly link to effects in saccade reaction time and accuracy (Hafed and Chen, 2016). After studying the visual role of the SC without eye movements, I further took microsaccades as a tool to study active vision. I found enhanced visual responses in the SC prior to microsaccades (Chen et al., 2015). This phenomenon does not just mean that similar concepts for maintaining perceptual stability for large saccades can be extended to microsaccades, but I also showed that such enhancements could serve as a possible neural basis for linking covert visual attention to eye movement generation. Also, I found spatial frequency specific microsaccadic suppression in the SC, which is the first neuronal locus showing similar results to behavioral effects of spatial-frequency specificity (Chen and Hafed, 2017). At the end, I looked carefully at the oculomotor drifts before and after microsaccades and discovered that there is enhanced drift gain control to stabilize the eye even for the smallest possible saccades (Chen and Hafed, 2013).

Besides the above articles and manuscripts, which are all included below in my dissertation, I have also made additional substantial contributions to the literature. For example, taking the behavioral part of my data, I contributed to a recently published article from our lab about alteration of the microsaccadic velocity-amplitude main sequence (Buonocore et al., 2017). Moreover, by reanalyzing my neuronal data, I contributed another research article about behavioral performance oscillations after microsaccades (Bellet et al., under review). Recently, I have also started a major research project to characterize the foveal visual representation of the SC both physiologically and anatomically. Among other things, I found that the foveal magnification factor in the SC is greater than in LGN or V1. I will also analyze yet another dataset that I collected for RF shifts around the time of microsaccades in the near future. More broadly, and in order to summarize what I and my colleagues have found so far

related to active vision, we have also published a review article together about what we have learned so far through the lens of microsaccades about vision, perception and attention (Hafed et al., 2015). The knowledge that I have gained during my pursuit of my PhD degree also let me publish with my colleague a comment related to perceptual performance after microsaccades (Tian and Chen, 2015).

In all, I have several important published articles with several more to come, all uncovering interesting phenomena that I hope will propel the field of active perception forward.

## 5. Abbreviation

|       |  |       |  |
|-------|--|-------|--|
| ACC   | anterior cingulate cortex                          | RF    | response field   |
| CMRF  | central mesencephalic reticular formation          | RIMLF | rostral interstitial nucleus of the medial longitudinal fasciculus |
| DLPFC | dorsal lateral prefrontal cortex                   | RIP   | nucleus raphe interpositus   |
| DP    | dorso-posterior area                               | SAI   | stratum album intermediale   |
| EBN   | excitatory burst neurons                           | SAP   | stratum album profundum  |
| FEF   | frontal eye field                                  | SC    | superior colliculus  |
| FST   | superior temporal area                             | SEF   | supplementary eye field  |
| IBN   | inhibitory burst neurons                           | SGI   | stratum griseum intermediale                                       |
| INC   | interstitial nucleus of Cajal                      | SGP   | stratum griseum profundum  |
| LGN   | lateral geniculate nucleus                         | SGS   | stratum griseum superficiale                                       |
| LIP   | lateral intraparietal area                         | SO    | stratum opticum  |
| LLBN  | long-lead burst neurons                            | SZ    | stratum zonale   |
| MLBN  | medium-lead burst neurons                          | TEO   | posterior inferior temporal area                                   |
| MRF   | medullary reticular formation                      | V1    | primary visual cortex  |
| MST   | medial superior temporal area                      | V2    | visual area two  |
| MT    | medial temporal area                               | V3    | visual area three  |
| NPH   | nucleus prepositus hypoglossi                      | V3A   | V3 visual complex part A   |
| OPN   | omnipause neurons                                  | V4    | visual area four   |
| PFC   | prefrontal cortex                                  | V4t   | visual area four transitional                                      |
| PG    | pregeniculate                                      | VIP   | ventral intraparietal area   |
| PIP   | posterior intraparietal area                       |       |  |
| PO    | parieto-occipital area                             |       |  |
| PPRF  | paramedian zone of the pontine reticular formation |       |  |



## 6. Reference

- AlbanoJE, MishkinM, WestbrookLE, WurtzRH (1982) Visuomotor deficits following ablation of monkey superior colliculus. *J Neurophysiol* 48:338–351.
- AlbanoJE, WurtzRH (1982) Deficits in eye position following ablation of monkey superior colliculus, pretectum, and posterior-medial thalamus. *J Neurophysiol* 48:318–337.
- AndersenRA, MountcastleVB (1983) The influence of the angle of gaze upon the excitability of the light-sensitive neurons of the posterior parietal cortex. *J Neurosci* 3:532–548.
- AndersonRW, KellerEL, GandhiNJ, DasS (1998) Two-dimensional saccade-related population activity in superior colliculus in monkey. *J Neurophysiol* 80:798–817.
- Andrade da CostaBL, HokocJN, PinaudRR, GattassR (1997) GABAergic retinocollicular projection in the New World monkey *Cebus apella*. *Neuroreport* 8:1797–802.
- AppellPP, BehanM (1990) Sources of subcortical GABAergic projections to the superior colliculus in the cat. *J Comp Neurol* 302:143–158.
- ApterJT (1946) Eye movements following strychninization of the superior colliculus of cats. *J Neurophysiol* 9:73–86.
- BecksteadRM, FrankfurterA (1983) A direct projection from the retina to the intermediate gray layer of the superior colliculus demonstrated by anterograde transport of horseradish peroxidase in monkey, cat and rat. *Exp Brain Res* 52:261–268.
- BenderDB, DavidsonRM (1986) Global visual processing in the monkey superior colliculus. *Brain Res* 381:372–375.
- BeneventoLA, FallonJH (1975) The ascending projections of the superior colliculus in the rhesus monkey (*Macaca mulatta*). *J Comp Neurol* 160:339–361.
- BeneventoLA, StandageGP (1983) The organization of projections of the retinorecipient and nonretinorecipient nuclei of the pretectal complex and layers of the superior colliculus to the lateral pulvinar and medial pulvinar in the macaque monkey. *J Comp Neurol* 217:307–336.
- BermanRA, CavanaughJ, McAlonanK, WurtzRH (2016) A circuit for saccadic suppression in the primate brain. *J Neurophysiol*:jn.00679.2016.
- BermanRA, WurtzRH (2008) Exploring the pulvinar path to visual cortex. *Prog Brain Res* 171:467–473.

- BermanRA, WurtzRH (2010) Functional identification of a pulvinar path from superior colliculus to cortical area MT. *J Neurosci* 30:6342–6354.
- BermanRA, WurtzRH (2011) Signals conveyed in the pulvinar pathway from superior colliculus to cortical area MT. *J Neurosci* 31:373–384.
- BersonD (1988) Retinal and cortical inputs to cat superior colliculus: convergence and laminar specificity. *Prog Brain Res* 75:17–26.
- BisleyJW (2011) The neural basis of visual attention. *J Physiol* 589:49–57.
- BisleyJW, GoldbergME (2010) Attention, intention, and priority in the parietal lobe. *Annu Rev Neurosci* 33:1–21.
- BoehnkeSE, BergDJ, MarinoRA, BaldiPF, IttiL, MunozDP (2011) Visual adaptation and novelty responses in the superior colliculus. *Eur J Neurosci* 34:766–779.
- BoehnkeSE, MunozDP (2008) On the importance of the transient visual response in the superior colliculus. *Curr Opin Neurobiol* 18:544–551.
- BoyerJL, HarrisonS, RoT (2005) Unconscious processing of orientation and color without primary visual cortex. *Proc Natl Acad Sci U S A* 102:16875–16879.
- BreitmeyerBG, KropflW, JuleszB (1982) The existence and role of retinotopic and spatiotopic forms of visual persistence. *Acta Psychol (Amst)* 52:175–196.
- BremmerF (2000) Eye position effects in macaque area V4. *Neuroreport* 11:1277–1283.
- BremmerF, IlgUJJ, ThieleA, DistlerC, HoffmannK-P (1997) Eye position effects in monkey cortex. I. Visual and pursuit-related activity in extrastriate areas MT and MST. *J Neurophysiol* 77:944–961.
- BremmerF, KubischikM, HoffmannK-P, KrekelbergB (2009) Neural dynamics of saccadic suppression. *J Neurosci* 29:12374–12383.
- BridgemanB (2007) Efference copy and its limitations. *Comput Biol Med* 37:924–929.
- BridgemanB, HendryD, StarkL (1975) Failure to detect displacement of the visual world during saccadic eye movements. *Vision Res* 15:719–722.
- BrienDC, CorneilBD, FecteauJH, BellAH, MunozDP (2009) The behavioral and neurophysiological modulation of microsaccades in monkeys. *J Eye Mov Res* 3:1–12.
- BruceCJ, GoldbergME, BushnellMC, StantonGB (1985) Primate frontal eye fields. II. Physiological and anatomical correlates of electrically evoked eye movements. *J Neurophysiol* 54:714–734.
- BuonocoreA, ChenC-Y, TianX, IdreesS, MuenchT, HafedZM (2017) Alteration of the microsaccadic velocity-amplitude main sequence relationship after visual

- transients : implications for models of saccade control. *J Neurophysiol*:doi:10.1152/jn.00811.2016.
- BurrDC, HoltJ, JohnstoneJR, RossJ (1982) Selective depression of motion sensitivity during saccades. *J Physiol* 333:1–15.
- BurrDC, MorroneMC (2011) Spatiotopic coding and remapping in humans. *Philos Trans R Soc Lond B Biol Sci* 366:504–515.
- BurrDC, MorroneMC, RossJ (1994) Selective suppression of the magnocellular visual pathway during saccadic eye movements. *Nature* 371:511–513.
- ButterCM, WeinsteinC, BenderDB, GrossCG (1978) Localization and detection of visual stimuli following superior colliculus lesions in Rhesus monkeys. *Brain Res* 156:33–49.
- Büttner-EnneverJA, BüttnerU (1978) A cell group associated with vertical eye movements in the rostral mesencephalic reticular formation of the monkey. *Brain Res* 151:31–47.
- Büttner-EnneverJA, CohenB, PauseM, FriesW (1988) Raphe nucleus of the pons containing omnipause neurons of the oculomotor system in the monkey, and its homologue in man. *J Comp Neurol* 267:307–321.
- Büttner-EnneverJA, HennV (1976) An autoradiographic study of the pathways from the pontine reticular formation involved in horizontal eye movements. *Brain Res* 108:155–164.
- Büttner-EnneverJA, HornAKE, ScherbergerH, D’ascanioP (2001) Motoneurons of twitch and nontwitch extraocular muscle fibers in the abducens, trochlear, and oculomotor nuclei of monkeys. *J Comp Neurol* 438:318–335.
- CalabreseE, BadeaA, CoeCL, LubachGR, ShiY, StynerMA, JohnsonGA (2015) A diffusion tensor MRI atlas of the postmortem rhesus macaque brain. *Neuroimage* 117:408–416.
- CampbellFW, WurtzRH (1978) Saccadic omission: Why we do not see a grey-out during a saccadic eye movement. *Vision Res* 18:1297–1303.
- CasagrandeVA, HartingJK, HallWC, DiamondIT, MartinGF (1972) Superior colliculus of the tree shrew: a Structural and functional subdivision into superficial and deep layers. *Science* (80- ) 177:444–447.
- CassanelloCR, FerreraVP (2007) Computing vector differences using a gain field-like mechanism in monkey frontal eye field. *J Physiol* 582:647–664.
- CavadaC, Goldman-RakicPS (1989a) Posterior parietal cortex in rhesus monkey: I. Parcellation of areas based on distinctive limbic and sensory corticocortical connections. *J Comp Neurol* 287:393–421.

- CavadaC, Goldman-RakicPS (1989b) Posterior parietal cortex in rhesus monkey: II. Evidence for segregated corticocortical networks linking sensory and limbic areas with the frontal lobe. *J Comp Neurol* 287:422–445.
- CavanaughJ, WurtzRH (2004) Subcortical modulation of attention counters change blindness. *J Neurosci* 24:11236–11243.
- ChenB, MayPJ (2000) The feedback circuit connecting the superior colliculus and central mesencephalic reticular formation: a direct morphological demonstration. *Exp Brain Res* 131:10–21.
- ChenC-Y, HafedZM (2013) Postmicrosaccadic enhancement of slow eye movements. *J Neurosci* 33:5375–5386.
- ChenC-Y, HafedZM (2017) A neural locus for spatial-frequency specific saccadic suppression in visual-motor neurons of the primate superior colliculus. *J Neurophysiol* 117:1657–1673.
- ChenC-Y, IgnashchenkovaA, ThierP, HafedZM (2015) Neuronal response gain enhancement prior to microsaccades. *Curr Biol* 25:2065–2074.
- ChuranJ, GuittonD, PackCC (2011) Context dependence of receptive field remapping in superior colliculus. *J Neurophysiol* 106:1862–1874.
- ClowerDM, WestRA, LynchJC, StrickPL (2001) The inferior parietal lobule is the target of output from the superior colliculus, hippocampus, and cerebellum. *J Neurosci* 21:6283–6291.
- CohenB, Büttner-EnneverJA (1984) Projections from the superior colliculus to a region of the central mesencephalic reticular formation (cMRF) associated with horizontal saccadic eye movements. *Exp Brain Res* 57:167–176.
- CohenB, MatsuoV, FradinJ, RaphanT (1985) Horizontal saccades induced by stimulation of the central mesencephalic reticular formation. *Exp Brain Res* 57:605–616.
- CohenB, WaitzmanDM, Büttner-EnneverJA, MatsuoV (1986) Horizontal saccades and the central mesencephalic reticular formation. *Prog Brain Res* 64:243–256.
- ColbyCL, DuhamelJ-R, GoldbergME (1996) Visual, presaccadic, and cognitive activation of single neurons in monkey lateral intraparietal area. *J Neurophysiol* 76:2841–2852.
- ColbyCL, GoldbergME (1999) Space and attention in parietal cortex. *Annu Rev Neurosci* 22:319–349.
- ConstantinAG, WangH, Martinez-TrujilloJC, CrawfordJD (2007) Frames of reference for gaze saccades evoked during stimulation of lateral intraparietal cortex. *J Neurophysiol* 98:696–709.

- CorbettaM, AkbudakE, ConturoTE, SnyderAZ, OllingerJM, DruryHA, LinenweberMR, PetersenSE, RaichleME, VanEssenDC, ShulmanGL (1998) A common network of functional areas for attention and eye movements. *Neuron* 21:761–773.
- CoweyA (2010) The blindsight saga. *Exp Brain Res* 200:3–24.
- CoweyA, StoerigP (1991) The neurobiology of blindsight. *Trends Neurosci* 14:140–145.
- CrawfordJ, CaderaW, VilisT (1991) Generation of torsional and vertical eye position signals by the interstitial nucleus of Cajal. *Science* (80- ) 252:1551–1553.
- CrookJD, PetersonBB, PackerOS, RobinsonFR, GamlinPD, TroyJB, DaceyDM (2008a) The smooth monostratified ganglion cell : evidence for spatial diversity in the Y-cell pathway to the lateral geniculate nucleus and superior colliculus in the macaque monkey. *J Neurosci* 28:12654–12671.
- CrookJD, PetersonBB, PackerOS, RobinsonFR, TroyJB, DaceyDM (2008b) Y-cell receptive field and collicular projection of parasol ganglion cells in macaque monkey retina. *J Neurosci* 28:11277–11291.
- CynaderM, BermanN (1972) Receptive-field organization of monkey superior colliculus. *J Neurophysiol* 35:187–201.
- Darian-SmithC, TanA, EdwardsS (1999) Comparing thalamocortical and corticothalamic microstructure and spatial reciprocity in the macaque ventral posterolateral nucleus (VPLc) and medial pulvinar. *J Comp Neurol* 410:211–234.
- DeanP (1997) Simulated recruitment of medial rectus motoneurons by abducens internuclear neurons: synaptic specificity vs. intrinsic motoneuron properties. *J Neurophysiol* 78:1531–1549.
- DeanP, RedgraveP, WestbyGWM (1989) Event or emergency? Two response systems in the mammalian superior colliculus. *Trends Neurosci* 12:137–147.
- DeubelH, BridgemanB, SchneiderWX (1998) Immediate post-saccadic information mediates space constancy. *Vision Res* 38:3147–3159.
- DeubelH, SchneiderWX (1996) Saccade target selection and object recognition: Evidence for a common attentional mechanism. *Vision Res* 36:1827–1837.
- DeubelH, SchneiderWX, BridgemanB (1996) Postsaccadic target blanking prevents saccadic suppression of image displacement. *Vision Res* 36:985–996.
- DeubelH, SchneiderWX, BridgemanB (2002) Transsaccadic memory of position and form. *Prog Brain Res* 140:165–180.
- DodgeR (1903) Five types of eye movement in the horizontal meridian plane of the field of regard. *Am J Physiol* 8:307–329.

- DorrisMC, KleinRM, EverlingS, MunozDP (2002) Contribution of the primate superior colliculus to inhibition of return. *J Cogn Neurosci* 14:1256–1263.
- DuhamelJ-R, BremmerF, BenHamedS, GrafW (1997) Spatial invariance of visual receptive fields in parietal cortex neurons. *Nature* 389:845–848.
- DuhamelJ-R, ColbyCL, GoldbergME (1992) The updating of the representation of visual space in parietal cortex by intended eye movements. *Science* (80- ) 255:90–92.
- DunnCA, HallNJ, ColbyCL (2010) Spatial updating in monkey superior colliculus in the absence of the forebrain commissures: dissociation between superficial and intermediate layers. *J Neurophysiol* 104:1267–1285.
- DurandJB, TrotterY, CelebriniS (2010) Privileged processing of the straight-ahead direction in primate area V1. *Neuron* 66:126–137.
- EngbertR, KlieglR (2003) Microsaccades uncover the orientation of covert attention. *Vision Res* 43:1035–1045.
- FecteauJH, MunozDP (2006) Saliency, relevance, and firing: a priority map for target selection. *Trends Cogn Sci* 10:382–390.
- FinlayBL, SchillerPH, VolmanSF (1976) Quantitative studies of single-cell properties in monkey striate cortex. IV. Corticotectal cells. *J Neurophysiol* 39:1352–1361.
- FischerB, BochR, BachM (1981) Stimulus versus eye movements: comparison of neural activity in the striate and prelunate visual cortex (A17 and A19) of trained rhesus monkey. *Exp Brain Res* 43:69–77.
- FriesW (1984) Cortical projections to the superior colliculus in the macaque monkey: a retrograde study using horseradish peroxidase. *J Comp Neurol* 230:55–76.
- FuchsAF, KanekoCRS, ScudderCA (1985) Brainstem control of saccadic eye movements. *Annu Rev Neurosci* 8:307–337.
- FuchsAF, LuscheiES (1970) Firing patterns of abducens neurons of alert monkeys in relationship to horizontal eye movement. *J Neurophysiol* 33:382–392.
- FukushimaK, KanekoCRS, FuchsAF (1992) The neuronal substrate of integration in the oculomotor system. *Prog Neurobiol* 39:609–639.
- FunahashiS, TakedaK (2002) Information processes in the primate prefrontal cortex in relation to working memory processes. *Rev Neurosci* 13:313–345.
- GaitherNS, SteinBE (1979) Reptiles and mammals use similar sensory organizations in the midbrain. *Science* (80- ) 205:595–597.
- GallettiC, BattagliniPP (1989) Gaze-dependent visual neurons in area V3A of monkey prestriate cortex. *J Neurosci* 9:1112–1125.
- GallettiC, BattagliniPP, FattoriP (1993) Parietal neurons encoding spatial locations in craniotopic coordinates. *Exp Brain Res* 96:221–229.

- GallettiC, BattagliniPP, FattoriP (1995) Eye position influence on the parieto-occipital area PO (V6) of the macaque monkey. *Eur J Neurosci* 7:2486–2501.
- GandhiNJ, KatnaniHA (2011) Motor functions of the superior colliculus. *Annu Rev Neurosci* 34:205–231.
- GandhiNJ, KellerEL (1999) Comparison of saccades perturbed by stimulation of the rostral superior colliculus, the caudal superior colliculus, and the omnipause neuron region. *J Neurophysiol* 82:3236–3253.
- GhitaniN, BayguinovPO, VokounCR, McMahanS, JacksonMB, BassoMA (2014) Excitatory synaptic feedback from the motor layer to the sensory layers of the superior colliculus. *J Neurosci* 34:6822–6833.
- GoffartL, HafedZM, KrauzlisRJ (2012) Visual fixation as equilibrium : Evidence from superior colliculus inactivation. *J Neurosci* 32:10627–10636.
- GoldbergME, WurtzRH (1972a) Activity of superior colliculus in behaving monkey. I. Visual receptive fields of single neurons. *J Cogn Neurosci* 35:542–559.
- GoldbergME, WurtzRH (1972b) Activity of superior colliculus in behaving monkey. II. Effect of attention on neuronal responses. *J Neurophysiol* 35:560–574.
- GoossensHHL, vanOpstalAJ (2012) Optimal control of saccades by spatial-temporal activity patterns in the monkey superior colliculus. *PLoS Comput Biol* 8:e1002508.
- GottliebJ (2007) From thought to action: the parietal cortex as a bridge between perception, action, and cognition. *Neuron* 53:9–16.
- GottliebJP, KusunokiM, GoldbergME (1998) The representation of visual salience in monkey parietal cortex. *Nature* 391:481–484.
- GrahamJ (1982) Some topographical connections of the striate cortex with subcortical structures in *Macaca fascicularis*. *Exp Brain Res* 47:1–14.
- GuittonD (1992) Control of eye-head coordination during orienting gaze shifts. *Trends Neurosci* 15:174–179.
- GuthrieBL, PorterJD, SparksDL (1983) Corollary discharge provides accurate eye position information to the oculomotor system. *Science* (80-) 221:1193–1195.
- HadaJ, YamagataY, HayashiY (1985) Identification of ventral lateral geniculate nucleus cells projecting to the pretectum and superior colliculus in the cat. *Brain Res* 358:398–403.
- HafedZM (2011) Mechanisms for generating and compensating for the smallest possible saccades. *Eur J Neurosci* 33:2101–2113.
- HafedZM (2013) Alteration of visual perception prior to microsaccades. *Neuron* 77:775–786.

- HafedZM (2016) Saccades and smooth pursuit eye movements. In: From neuron to cognition via computational neuroscience (ArbibMA, BonaiutoJJ, eds), pp 559–584. MIT Press.
- HafedZM, ChenC-Y (2016) Sharper, stronger, faster upper visual field representation in primate superior colliculus. *Curr Biol* 26:1647–1658.
- HafedZM, ChenC-Y, TianX (2015) Vision, perception, and attention through the lens of microsaccades: mechanisms and implications. *Front Syst Neurosci* 9:167.
- HafedZM, ClarkJJ (2002) Microsaccades as an overt measure of covert attention shifts. *Vision Res* 42:2533–2545.
- HafedZM, GoffartL, KrauzlisRJ (2008) Superior colliculus inactivation causes stable offsets in eye position during tracking. *J Neurosci* 28:8124–8137.
- HafedZM, GoffartL, KrauzlisRJ (2009) A neural mechanism for microsaccade generation in the primate superior colliculus. *Science* (80- ) 323:940–943.
- HafedZM, KrauzlisRJ (2008) Goal representations dominate superior colliculus activity during extrafoveal tracking. *J Neurosci* 28:9426–9439.
- HafedZM, KrauzlisRJ (2010) Microsaccadic suppression of visual bursts in the primate superior colliculus. *J Neurosci* 30:9542–9547.
- HallN, ColbyC (2014) S-cone visual stimuli activate superior colliculus neurons in old world monkeys: implications for understanding blindsight. *J Cogn Neurosci* 26:1234–1256.
- HanX, XianSX, MooreT (2009) Dynamic sensitivity of area V4 neurons during saccade preparation. *Proc Natl Acad Sci* 106:13046–13051.
- HanksTD, DitterichJ, ShadlenMN (2006) Microstimulation of macaque area LIP affects decision-making in a motion discrimination task. *Nat Neurosci* 9:682–689.
- HartingJK (1977) Descending pathways from the superior colliculus: an autoradiographic analysis in the rhesus monkey (*Macaca mulatta*). *J Comp Neurol* 173:583–612.
- HartingJK, HuertaMF, FrankfurterAJ, StromingerNL, RoyceGJ (1980) Ascending pathways from the monkey superior colliculus: an autoradiographic analysis. *J Comp Neurol* 192:853–882.
- HartingJK, HuertaMF, HashikawaT, vanLieshoutDP (1991) Projection of the mammalian superior colliculus upon the dorsal lateral geniculate nucleus: organization of tectogeniculate pathways in nineteen species. *J Comp Neurol* 304:275–306.
- Hartwich-YoungR, NelsonJS, SparksDL (1990) The perihypoglossal projection to the superior colliculus in the rhesus monkey. *Vis Neurosci* 4:29–42.



- HeiserLM, ColbyCL (2006) Spatial updating in area LIP is independent of saccade direction. *J Neurophysiol* 95:2751–2767.
- HendrySHC, ReidRC (2000) The koniocellular pathway in primate vision. *Annu Rev Neurosci* 23:127–153.
- HeppK, HennV (1983) Spatial-temporal recording of rapid eye movement signals in the monkey paramedian pontine reticular formation (PPRF). *Exp Brain Res* 52:105–120.
- HermanJP, KrauzlisRJ (2017) Color-change detection activity in the primate superior colliculus. *eNeuro*:10.1523/ENEURO.0046-17.2017.
- HigginsE, RaynerK (2015) Transsaccadic processing: stability, integration, and the potential role of remapping. *Atten Percept Psychophys* 77:3–27.
- HoffmanJE, SubramaniamB (1995) The role of visual attention in saccadic eye movements. *Percept Psychophys* 57:787–795.
- HollingworthA, RichardAM, LuckSJ (2008) Understanding the function of visual short-term memory: transsaccadic memory, object correspondence, and gaze correction. *J Exp Psychol Gen* 137:163–181.
- HornAKE (2005) The reticular formation. *Prog Brain Res* 151:127–155.
- HornAKE, Büttner-EnneverJA (1998) Premotor neurons for vertical eye movements in the rostral mesencephalon of monkey and human: histologic identification by parvalbumin immunostaining. *J Comp Neurol* 392:413–427.
- HorwitzGD, NewsomeWT (1999) Separate signals for target selection and movement specification in the superior colliculus. *Science* 284:1158–1161.
- HuberGC, CrosbyEC (1933) A phylogenetic consideration of the optic tectum. *Proc Natl Acad Sci* 19:15–22.
- HubermanAD, NiellCM (2011) What can mice tell us about how vision works? *Trends Neurosci* 34:464–473.
- HuertaMF, HartingJK (1983) Sublamination within the superficial gray layer of the squirrel monkey: an analysis of the tectopulvinar projection using anterograde and retrograde transport methods. *Brain Res* 261:119–126.
- HuertaMF, HartingJK (1984) Connectional organization of the superior colliculus. *Trends Neurosci* 7:286–289.
- HuertaMF, KaasJH (1990) Supplementary eye field as defined by intracortical microstimulation: connections in macaques. *J Comp Neurol* 293:299–330.
- HuertaMF, KrubitzerLA, KaasJH (1986) Frontal eye field as defined by intracortical microstimulation in squirrel monkeys, owl monkeys, and macaque monkeys: I. Subcortical connections. *J Comp Neurol* 253:415–439.

- HumphreyNK (1968) Responses to visual stimuli of units in the superior colliculus of rats and monkeys. *Exp Neurol* 20:312–340.
- IgnashchenkovaA, DickePW, HaarmeierT, ThierP (2004) Neuron-specific contribution of the superior colliculus to overt and covert shifts of attention. *Nat Neurosci* 7:56–64.
- IngleD (1973) Evolutionary perspectives on the function of the optic tectum. *Brain Behav Evol* 8:211–223.
- IrwinDE (1992) Memory for position and identity across eye movements. *J Exp Psychol Learn Mem Cogn* 18:307–317.
- IsaT, EndoT, SaitoY (1998) The visuo-motor pathway in the local circuit of the rat superior colliculus. *J Neurosci* 18:8496–8504.
- IsaT, SasakiS (2002) Brainstem control of head movements during orienting; organization of the premotor circuits. *Prog Neurobiol* 66:205–241.
- IsaT, YoshidaM (2009) Saccade control after V1 lesion revisited. *Curr Opin Neurobiol* 19:608–614.
- IsodaM, TanjiJ (2002) Cellular activity in the supplementary eye field during sequential performance of multiple saccades. *J Neurophysiol* 88:3541–3545.
- JudgeS, WurtzR, RichmondB (1980) Vision during saccadic eye movements. I. Visual interactions in striate cortex. *J Neurophysiol* 43:1133–1155.
- KalesnykasRP, SparksDL (1996) The primate superior colliculus and the control of saccadic eye movements. *Neurosci* 2:284–292.
- KardamakisAA, SaitohK, GrillnerS (2015) Tectal microcircuit generating visual selection commands on gaze-controlling neurons. *Proc Natl Acad Sci*:E1956–E1965.
- KellerEL (1974) Participation of medial pontine reticular formation in eye movement generation in monkey. *J Neurophysiol* 37:316–332.
- KennardDW, HartmannRW, KraftDP, BoshesB (1970) Perceptual suppression of afterimages. *Vision Res* 10:575–585.
- KillianNJ, JutrasMJ, BuffaloEA (2012) A map of visual space in the primate entorhinal cortex. *Nature* 491:761–764.
- KillianNJ, PotterSM, BuffaloEA (2015) Saccade direction encoding in the primate entorhinal cortex during visual exploration. *Proc Natl Acad Sci* 112:15743–15748.
- KingAJ (2004) The superior colliculus. *Curr Biol* 14:R335–R338.
- KingWM, FuchsAF (1979) Reticular control of vertical saccadic eye movements by mesencephalic burst neurons. *J Neurophysiol* 42:861–876.

- KingWM, FuchsAF, MagninM (1981) Vertical eye movement-related responses of neurons in midbrain near interstitial nucleus of Cajal. *J Neurophysiol* 46:549–562.
- KokkoroyannisT, ScudderCA, BalabanCD, HighsteinSM, MoschovakisAK (1996) Anatomy and physiology of the primate interstitial nucleus of Cajal I. efferent projections. *J Neurophysiol* 75:725–739.
- KomatsuH, SuzukiH (1985) Projections from the functional subdivisions of the frontal eye field to the superior colliculus in the monkey. *Brain Res* 327:324–327.
- KovalMJ, HutchisonRM, LomberSG, EverlingS (2014) Effects of unilateral deactivations of dorsolateral prefrontal cortex and anterior cingulate cortex on saccadic eye movements. *J Neurophysiol* 111:787–803.
- KowlerE, AndersonE, DoshierB, BlaserE (1995) The role of attention in the programming of saccades. *Vision Res* 35:1897–1916.
- KrauzlisRJ, GoffartL, HafedZM (2017) Neuronal control of fixation and fixational eye movements. *Philos Trans R Soc Lond B Biol Sci* 372:20160205.
- KrauzlisRJ, LovejoyLP, ZénonA (2013) Superior colliculus and visual spatial attention. *Annu Rev Neurosci* 36:165–182.
- KrockRM, MooreT (2016) Visual sensitivity of frontal eye field neurons during the preparation of saccadic eye movements. *J Neurophysiol* 116:2882–2891.
- KusunokiM, GoldbergME (2003) The time course of perisaccadic receptive field shifts in the lateral intraparietal area of the monkey. *J Neurophysiol* 89:1519–1527.
- LaemleLK (1981) A Golgy study of cellular morphology in the superficial layers of superior colliculus man, Saimiri, and Macaca. *J Hirnforsch* 22:253–263.
- LangerT, KanekoCRS, ScudderCA, FuchsAF (1986) Afferents to the abducens nucleus in the monkey and cat. *J Comp Neurol* 245:379–400.
- LatourPL (2004) Visual threshold during eye movements. *Vision Res* 2:261–262.
- LeichnetzGR, SpencerRF, HardySGP, AstrucJ (1981) The prefrontal corticotectal projection in the monkey; An anterograde and retrograde horseradish peroxidase study. *Neuroscience* 6:1023–1041.
- LeopoldDA (2012) Primary visual cortex: awareness and blindsight. *Annu Rev Neurosci* 35:91–109.
- LevyR, Goldman-RakicPS (2000) Segregation of working memory functions within the dorsolateral prefrontal cortex. *Exp brain Res* 133:23–32.
- LiX, BassoMA (2008) Preparing to move increases the sensitivity of superior colliculus neurons. *J Neurosci* 28:4561–4577.

- LivingstonCA, FedderSR (2003) Visual-ocular motor activity in the macaque pregeniculate complex. *J Neurophysiol* 90:226–244.
- LivingstonCA, MustariMJ (2000) The anatomical organization of the macaque pregeniculate complex. *Brain Res* 876:166–179.
- LockTM, BaizerJS, BenderDB (2003) Distribution of corticotectal cells in macaque. *Exp Brain Res* 151:455–470.
- LuX, MatsuzawaM, HikosakaO (2002) A neural correlate of oculomotor sequences in supplementary eye field. *Neuron* 34:317–325.
- LuiF, GregoryKM, BlanksRHI, GiolliRA (1995) Projections from visual areas of the cerebral cortex to pretectal nuclear complex, terminal accessory optic nuclei, and superior colliculus in macaque monkey. *J Comp Neurol* 363:439–460.
- LuscheiES, FuchsAF (1972) Activity of brain stem neurons during eye movements of alert monkeys. *J Neurophysiol* 35:445–461.
- LynchJC (1992) Saccade initiation and latency deficits after combined lesions of the frontal and posterior eye fields in monkeys. *J Neurophysiol* 68:1913–1916.
- LynchJC, HooverJE, StrickPL (1994) Input to the primate frontal eye field from the substantia nigra, superior colliculus, and dentate nucleus demonstrated by transneuronal transport. *Exp Brain Res* 100:181–186.
- LyonDC, NassiJJ, CallawayEM (2010) A disynaptic relay from superior colliculus to dorsal stream visual cortex in macaque monkey. *Neuron* 65:270–279.
- MacknikSL, LivingstoneMS (1998) Neuronal correlates of visibility and invisibility in the primate visual system. *Nat Neurosci* 1:144–149.
- MarinoRA, RodgersCK, LevyR, MunozDP (2008) Spatial relationships of visuomotor transformations in the superior colliculus map. *J Neurophysiol* 100:2564–2576.
- MarroccoRT, LiRH (1977) Monkey superior colliculus: properties of single cells and their afferent inputs. *J Neurophysiol* 40:844–60.
- Martinez-CondeS, MacknikSL, TroncosoXG, HubelDH (2009) Microsaccades: a neurophysiological analysis. *Trends Neurosci* 32:463–475.
- Martinez-TrujilloJC, MedendorpWP, WangH, CrawfordJD (2004) Frames of reference for eye-head gaze commands in primate supplementary eye fields. *Neuron* 44:1057–1066.
- MasinoT (1992) Brainstem control of orienting movements: intrinsic coordinate systems and underlying circuitry. *Brain Behav Evol* 40:98–111.
- MatinE (1974) Saccadic suppression: a review and an analysis. *Psychol Bull* 81:899–917.
- MatinE, ClymerAB, MatinL (1972) Metacontrast and saccadic suppression. *Science* 178:179–182.

- MatinL, PearceDG (1965) Visual perception of direction for stimuli flashed during voluntary saccadic eye movements. *Science* (80- ) 148:1485–1488.
- MatinL, PicoultE, StevensJK, Edwards, M. W.J, YoungD, MacArthurR (1982) Oculoparalytic illusion: Visual-field dependent spatial mislocalizations by humans partially paralyzed with curare. *Science* (80- ) 216:198–201.
- MayPJ (2006) The mammalian superior colliculus: laminar structure and connections. *Prog Brain Res* 151:321–378.
- MayoJP, SommerMA (2008) Neuronal adaptation caused by sequential visual stimulation in the frontal eye field. *J Neurophysiol* 100:1923–1935.
- MaysLE, PorterJD, GamlinPD, TelloCA (1986) Neural control of vergence eye movements: neurons encoding vergence velocity. *J Neurophysiol* 56:1007–1021.
- MaysLE, SparksDL (1980) Dissociation of visual and saccade-related responses in superior colliculus neurons. *J Neurophysiol* 43:207–232.
- McFarlandJL, FuchsAF (1992) Discharge patterns in nucleus prepositus hypoglossi and adjacent medial vestibular nucleus during horizontal eye movement in behaving macaques. *J Neurophysiol* 68:319–332.
- McIlwainJT (1982) Lateral spread of neural excitation during microstimulation in intermediate gray layer of cat's superior colliculus. *J Neurophysiol* 47:167–178.
- MeisterMLR, BuffaloEA (2016) Getting directions from the hippocampus : The neural connection between looking and memory. *Neurobiol Learn Mem* 134:135–144.
- MelcherD (2005) Spatiotopic transfer of visual-form adaptation across saccadic eye movements. *Curr Biol* 15:1745–1748.
- MelcherD (2007) Predictive remapping of visual features precedes saccadic eye movements. *Nat Neurosci* 10:903–907.
- MelcherD, MorroneMC (2015) Nonretinotopic visual processing in the brain. *Vis Neurosci* 32:E017.
- MirpourK, OngWS, BisleyJW (2010) Microstimulation of posterior parietal cortex biases the selection of eye movement goals during search. *J Neurophysiol* 104:3021–3028.
- MizeRR, ButlerGD (1996) Postembedding immunocytochemistry demonstrates directly that both retinal and cortical terminals in the cat superior colliculus are glutamate immunoreactive. *J Comp Neurol* 371:633–648.
- MizeRR, JeonC-J, HamadaOL, SpencerRF (1991) Organization of neurons labeled by antibodies to gamma-aminobutyric acid (GABA) in the superior colliculus of the Rhesus monkey. *Vis Neurosci* 6:75–92.

- MohlerCW, WurtzRH (1976) Organization of monkey superior colliculus: intermediate layer cells discharging before eye movements. *J neuro* 39:722–744.
- MohlerCW, WurtzRH (1977) Role of striate cortex and superior colliculus in visual guidance of saccadic eye movements in monkeys. *J Neurophysiol* 40:74–94.
- MooreT, ToliaAS, SchillerPH (1998) Visual representations during saccadic eye movements. *Proc Natl Acad Sci U S A* 95:8981–8984.
- MoschovakisAK, GregoriouGG, UgoliniG, DoldanM, GrafW, GuldinW, HadjidimitrakisK, SavakiHE (2004) Oculomotor areas of the primate frontal lobes: a transneuronal transfer of rabies virus and [14C]-2-deoxyglucose functional imaging study. *J Neurosci* 24:5726–5740.
- MoschovakisAK, KarabelasAB, HighsteinSM (1988a) Structure-function relationships in the primate superior colliculus. I. Morphological classification of efferent neurons. *J Neurophysiol* 60:232–262.
- MoschovakisAK, KarabelasAB, HighsteinSM (1988b) Structure-function relationships in the primate superior colliculus. II. Morphological identity of presaccadic neurons. *J Neurophysiol* 60:263–302.
- MoschovakisAK, ScudderCA, HighsteinSM (1991a) Structure of the primate oculomotor burst generator I. Medium-lead burst neurons with upward on-directions. *J Neurophysiol* 65:203–217.
- MoschovakisAK, ScudderCA, HighsteinSM (1996) The microscopic anatomy and physiology of the mammalian saccadic system. *Prog Neurobiol* 50:133–254.
- MoschovakisAK, ScudderCA, HighsteinSM, WarrenJD (1991b) Structure of the primate oculomotor burst generator II. Medium-lead burst neurons with downward on-directions. *J Neurophysiol* 65:218–229.
- MunozD (2002) Saccadic eye movements: overview of neural circuitry. *Prog Brain Res* 140:89–96.
- MunozDP, FecteauJH (2002) Vying for dominance: dynamic interactions control visual fixation and saccadic initiation in the superior colliculus. *Prog Brain Res* 140:3–19.
- MunozDP, IstvanPJ (1998) Lateral inhibitory interactions in the intermediate layers of the monkey superior colliculus. *J Neurophysiol* 79:1193–1209.
- MunozDP, WurtzRH (1993a) Fixation cells in monkey superior colliculus. I. Characteristics of cell discharge. *J Neurophysiol* 70:559–575.
- MunozDP, WurtzRH (1993b) Fixation cells in monkey superior colliculus. II. Reversible activation and deactivation. *J Neurophysiol* 70:576–589.
- MunozDP, WurtzRH (1995a) Saccade-related activity in monkey superior colliculus. II. Spread of activity during saccades. *J Neurophysiol* 73:2334–2348.

- MunozDP, WurtzRH (1995b) Saccade-related activity in monkey superior colliculus. I. Characteristics of burst and buildup cells. *J Neurophysiol* 73:2313–2333.
- NakaharaH, MoritaK, WurtzRH, OpticanLM (2006) Saccade-related spread of activity across superior colliculus may arise from asymmetry of internal connections. *J Neurophysiol* 96:765–774.
- NakamuraK, ColbyCL (2002) Updating of the visual representation in monkey striate and extrastriate cortex during saccades. *Proc Natl Acad Sci* 99:4026–4031.
- NakamuraK, RoeschMR, OlsonCR (2005) Neuronal activity in macaque SEF and ACC during performance of tasks involving conflict. *J Neurophysiol* 93:884–908.
- OlivierE, CorvisierJ, PauluisQ, HardyO (2000) Evidence for glutamatergic tectotectal neurons in the cat superior colliculus: a comparison with GABAergic tectotectal neurons. *Eur J Neurosci* 12:2354–2366.
- OlivierE, PorterJD, MayPJ (1998) Comparison of the distribution and somatodendritic morphology of tectotectal neurons in the cat and monkey. *Vis Neurosci* 15:903–922.
- OpticanLM (2005) Sensorimotor transformation for visually guided saccades. *Ann N Y Acad Sci* 1039:132–148.
- Otero-MillanJ, MacknikSL, SerraA, LeighRJ, Martinez-CondeS (2011) Triggering mechanisms in microsaccade and saccade generation: a novel proposal. *Ann N Y Acad Sci* 1233:107–116.
- OttesFP, vanGisbergenJAM, EggermontJJ (1986) Visuomotor fields of the superior colliculus: a quantitative model. *26:857–873*.
- ÖzenG, AugustineGJ, HallWC (2000) Contribution of superficial layer neurons to premotor bursts in the superior colliculus. *J Neurophysiol* 84:460–471.
- PandyaDN, SeltzerB (1982) Intrinsic connections and architectonics of posterior parietal cortex in the rhesus monkey. *J Comp Neurol* 204:196–210.
- ParkJ, Schlag-ReyM, SchlagJ (2006) Frames of reference for saccadic command tested by saccade collision in the supplementary eye field. *J Neurophysiol* 95:159–170.
- ParthasarathyHB, SchallJD, Graybiel a M (1992) Distributed but convergent ordering of corticostriatal projections: analysis of the frontal eye field and the supplementary eye field in the macaque monkey. *J Neurosci* 12:4468–4488.
- PeelTR, HafedZM, DashS, LomberSG, CorneilBD (2016) A causal role for the cortical frontal eye fields in microsaccade deployment. *PLoS Biol* 14:e1002531.
- PerryVH, CoweyA (1984) Retinal ganglion cells that project to the superior colliculus and pretectum in the macaque monkey. *Neuroscience* 12:1125–1137.

- PetridesM, PandyaDN (1984) Projections to the frontal cortex from the posterior parietal region in the rhesus monkey. *J Comp Neurol* 228:105–116.
- Phongphanphaneep, MizunoF, LeePH, YanagawaY, IsaT, HallWC (2011) A circuit model for saccadic suppression in the superior colliculus. *J Neurosci* 31:1949–1954.
- Pierrot-DeseillignyC, MileaD, MüriRM (2004) Eye movement control by the cerebral cortex. *Curr Opin Neurol* 17:17–25.
- PollackJG, HickeyTL (1979) The distribution of retino-collicular axon terminals in rhesus monkey. *J Comp Neurol* 185:587–602.
- PortNL, SommerMA, WurtzRH (2000) Multielectrode evidence for spreading activity across the superior colliculus movement map. *J Neurophysiol* 84:344–357.
- PosnerMI (1980) Orienting of attention. *Q J Exp Psychol* 32:3–25.
- PougetA, FisherSA, SejnowskiTJ (1993) Egocentric spatial representation in early vision. *J Cogn Neurosci* 5:150–161.
- PougetP (2015) The cortex is in overall control of “voluntary” eye movement. *Eye* 29:241–245.
- PrevicFH (1990) Functional specialization in the lower and upper visual fields in humans : Its ecological origins and implications. *Behav Brain Sci* 13:519–575.
- ProvisJM, DubisAM, MaddessT, CarrollJ (2013) Adaptation of the central retina for high acuity vision: Cones, the fovea and the a vascular zone. *Prog Retin Eye Res* 35:63–81.
- PtitoA, LehSE (2007) Neural substrates of blindsight after hemispherectomy. *Neuroscientist* 13:506–518.
- RamcharanEJ, GnadtJW, ShermanSM (2001) The effects of saccadic eye movements on the activity of geniculate relay neurons in the monkey. *Vis Neurosci* 18:253–258.
- RaoHM, MayoJP, SommerMA (2016) Circuits for presaccadic visual remapping. *J Neurophysiol* 116:2624–2636.
- RaynerK (1978) Eye movements in reading and information processing. *Psychol Bull* 85:618–660.
- RensinkRA, O’ReganJK, ClarkJJ (1997) To see or not to see: The need for attention to perceive changes in scenes. *Psychol Sci* 8:368–373.
- ReppasJB, UsreyWM, ReidRC (2002) Saccadic eye movements modulate visual responses in the lateral geniculate nucleus. *Neuron* 35:961–974.
- RobinsonDA (1972) Eye Movements Evoked by Collicular Stimulation in the Alert Monkey. *Vision Res* 12:1795–1808.



- RobinsonDA, FuchsAF (1969) Eye movements evoked by stimulation of frontal eye fields. *J Neurophysiol* 32:637–648.
- RobinsonDL, WurtzRH (1976) Use of an extraretinal signal by monkey superior colliculus neurons to distinguish real from self-induced stimulus movement. *J Neurophysiol* 39:852–870.
- RobinsonFR, PhillipsJO, FuchsAF (1994) Coordination of gaze shifts in primates: brainstem inputs to neck and extraocular motoneuron pools. *J Comp Neurol* 346:43–62.
- RolfsM (2015) Attention in active vision: a perspective on perceptual continuity across saccades. *Perception* 44:900–919.
- RossJ, MorroneMC, GoldbergME, BurrDC (2001) Changes in visual perception at the time of saccades. *Trends Neurosci* 24:113–121.
- RussoGS, BruceCJ (2000) Supplementary eye field: representation of saccades and relationship between neural response fields and elicited eye movements. *J Neurophysiol* 84:2605–2621.
- SahraieA, HibbardPB, TrevethanCT, RitchieKL, WeiskrantzL (2010) Consciousness of the first order in blindsight. *Proc Natl Acad Sci* 107:21217–21222.
- SahraieA, WeiskrantzL, TrevethanC, CruceR, MurrayA (2002) Psychophysical and pupillometric study of spatial channels of visual processing in blindsight. *Exp Brain Res* 143:249–256.
- SaitohK, MénardA, GrillnerS (2007) Tectal control of locomotion, steering, and eye movements in lamprey. *J Neurophysiol* 97:3093–3108.
- SchallJD (1991) Neuronal activity related to visually guided saccadic eye movements in the supplementary motor area of rhesus monkeys. *J Neurophysiol* 66:530–558.
- SchallJD (1995) Neural basis of saccade target selection. *Rev Neurosci* 6:63–85.
- SchallJD (2013) Production, control, and visual guidance of saccadic eye movements. *ISRN Neurol* 2013:752384.
- SchallJD (2015) *Visuomotor Functions in the Frontal Lobe*.
- SchillerPH (1970) The discharge characteristics of single units in the oculomotor and abducens nuclei of the unanaesthetized monkey. *Exp Brain Res* 10:347–362.
- SchillerPH (1972) The role of the monkey superior colliculus in eye movement and vision. *Invest Ophthalmol* 11:451–460.
- SchillerPH, ChouIH (2000) The effects of anterior arcuate and dorsomedial frontal cortex lesions on visually guided eye movements in the rhesus monkey: 1. Single and sequential targets. *Vision Res* 40:1609–1626.
- SchillerPH, KoernerF (1971) Discharge characteristics of single units in superior colliculus of the alert rhesus monkey. *J Neurophysiol* 34:920–936.

## 6. Reference

---

- SchillerPH, StrykerM, CynaderM, BermanN (1974) Response characteristics of single cells in the monkey superior colliculus following ablation or cooling of visual cortex. *J Neurophysiol* 37:181–94.
- SchillerPH, TrueSD, ConwayJL (1979) Effects of frontal eye field and superior colliculus ablations on eye movements. *Science* (80- ) 206:590–592.
- SchillerPH, TrueSD, ConwayJL (1980) Deficits in eye movements following frontal eye-field and superior colliculus ablations. *J Neurophysiol* 44:1175–1189.
- SchlagJ, Schlag-ReyM (1987) Evidence for a supplementary eye field. *J Neurophysiol* 57:179–200.
- SchlagJ, Schlag-ReyM, PigareviI (1992) Supplementary eye field: Influence of eye position on neural signals of fixation. *Exp Brain Res* 90:302–306.
- SchnyderH, ReisineH, HeppK, HennV (1985) Frontal eye field projection to the paramedian pontine reticular formation traced with wheat germ agglutinin in the monkey. *Brain Res* 329:151–160.
- ScudderCA, FuchsAF, LangerTP (1988) Characteristics and functional identification of saccadic inhibitory burst neurons in the alert monkey. *J Neurophysiol* 59:1430–1454.
- ScudderCA, MoschovakisAK, KarabelasAB, HighsteinSM (1996) Anatomy and physiology of saccadic long-lead burst neurons recorded in the alert squirrel monkey. I. Descending projections from the mesencephalon. *J Neurophysiol* 76:332–352.
- SelemonLD, Goldman-RakicPS (1988) Common cortical and subcortical targets of the dorsolateral prefrontal and posterior parietal cortices in the rhesus monkey: evidence for a distributed neural network subserving spatially guided behavior. *J Neurosci* 8:4049–4068.
- SerencesJT, YantisS (2006) Selective visual attention and perceptual coherence. *Trends Cogn Sci* 10:38–45.
- ShibutaniH, SakataH, HyvarinenJ (1984) Saccade and blinking evoked by microstimulation of the posterior parietal association cortex of the monkey. *Exp Brain Res* 55:1–8.
- ShippS (2004) The brain circuitry of attention. *Trends Cogn Sci* 8:223–230.
- ShookBL, Schlag-ReyM, SchlagJ (1990) Primate supplementary eye field: I. Comparative aspects of mesencephalic and pontine connections. *J Comp Neurol* 301:618–642.
- SilvantoJ, CoweyA, WalshV (2008) Inducing conscious perception of colour in blindsight. *Curr Biol* 18:950–951.

- SimonsDJ, RensinkRA (2005) Change blindness: Past, present, and future. *Trends Cogn Sci* 9:16–20.
- SoetedjoR, KanekoCRS, FuchsAF (2002) Evidence against a moving hill in the superior colliculus during saccadic eye movements in the monkey. *J Neurophysiol* 87:2778–2789.
- SommerMA, WurtzRH (2004a) What the brain stem tells the frontal cortex. I. Oculomotor signals sent from superior colliculus to frontal eye field via mediodorsal thalamus. *J Neurophysiol* 91:1381–1402.
- SommerMA, WurtzRH (2004b) What the brain stem tells the frontal cortex. II. Role of the SC-MD-FEF pathway in corollary discharge. *J Neurophysiol* 91:1403–1423.
- SommerMA, WurtzRH (2006) Influence of the thalamus on spatial visual processing in frontal cortex. *Nature* 444:374–377.
- SommerMA, WurtzRH (2008) Brain circuits for the internal monitoring of movements. *Annu Rev Neurosci* 31:317–338.
- SparksDL (1986) Translation of sensory signals into commands for control of saccadic eye movements: role of primate superior colliculus. *Physiol Rev* 66:118–171.
- SparksDL (1990) Signal transformations required for the generation of saccadic eye movements. *Annu Rev Neurosci* 13:309–336.
- SparksDL (1993) Are gaze shifts controlled by a “moving hill” of activity in the superior colliculus? *Trends Neurosci* 16:214–216.
- SparksDL (2002) The brainstem control of saccadic eye movements. *Nat Rev Neurosci* 3:952–964.
- SperryRW (1950) Neural basis of the spontaneous optokinetic response produced by visual inversion. *J Comp Physiol Psychol* 43:482–489.
- StantonGB, GoldbergME, BruceCJ (1988) Frontal eye field efferents in the macaque monkey: II. Topography of terminal fields in midbrain and pons. *J Comp Neurol* 271:493–506.
- StarkL, BridgemanB (1983) Role of corollary discharge in space constancy. *Percept Psychophys* 34:371–380.
- SteinBE (1981) Organization of the rodent superior colliculus: some comparisons with other mammals. *Behav Brain Res* 3:175–188.
- SteinBE, GaitherNS (1983) Receptive-field properties in reptilian optic tectum : some comparisons with mammals. *Neurophysiology* 50:102–124.

- SteinBE, JiangW, WallaceMT, StanfordTR (2001) Nonvisual influences on visual-information processing in the superior colliculus. *Prog Brain Res* 134:143–156.
- StepniewskaI, QIH, KaasJH (2000) Projections of the superior colliculus to subdivisions of the inferior pulvinar in New World and Old World monkeys. *Vis Neurosci* 17:529–549.
- StevensJK, EmersonRC, GersteinGL, KallosT, NeufeldGR, NicholsCW, RosenquistAC (1976) Paralysis of the awake human: visual perceptions. *Vision Res* 16:93–98.
- StrassmanA, EvingerC, McCreaRA, BakerRG, HighsteinSM (1987) Anatomy and physiology of intracellularly labeled omnipause neurons in the cat and squirrel monkey. *Exp Brain Res* 67:436–440.
- StrassmanA, HighsteinSM, McCreaRA (1986) Anatomy and physiology of saccadic burst neurons in the alert squirrel monkey. II. Inhibitory burst neurons. *J Comp Neurol* 249:358–380.
- StuphornV, BrownJW, SchallJD (2010) Role of supplementary eye field in saccade initiation: executive, not direct, control. *J Neurophysiol* 103:801–816.
- StuphornV, SchallJD (2006) Executive control of countermanding saccades by the supplementary eye field. *Nat Neurosci* 9:925–931.
- TailbyC, CheongSK, PietersenAN, SolomonSG, MartinPR (2012) Colour and pattern selectivity of receptive fields in superior colliculus of marmoset monkeys. *J Physiol* 590:4061–4077.
- ThierP, AndersenR (1998) Electrical microstimulation distinguishes distinct saccade-related areas in the posterior parietal cortex. *J Neurophysiol* 80:1713–1735.
- TianX, ChenC-Y (2015) Probing Perceptual Performance after Microsaccades. *J Neurosci* 35:2842–2844.
- TianX, YoshidaM, HafedZM (2016) A microsaccadic account of attentional capture and inhibition of return in Posner cueing. *Front Syst Neurosci* 10:23.
- ToliasAS, MooreT, SmirnakisSM, TehovnikEJ, SiapasAG, SchillerPH (2001) Eye movements modulate visual receptive fields of V4 neurons. *Neuron* 29:757–767.
- TrevelyanCT, SahraieA (2003) Spatial and temporal processing in a subject with cortical blindness following occipital surgery. *Neuropsychologia* 41:1296–1306.
- TrotterY, CelebriniS (1999) Gaze direction controls response gain in primary visual-cortex neurons. *Nature* 398:239–242.
- UmenoMM, GoldbergME (1997) Spatial processing in the monkey frontal eye field. I. Predictive visual responses. *J Neurophysiol* 78:1373–1383.

- UmenoMM, GoldbergME (2001) Spatial processing in the monkey frontal eye field. II. Memory responses. *J Neurophysiol* 86:2344–2352.
- VanEssenDC, AndersonCH, FellemanDJ (1992) Information processing in the primate visual system: an integrated systems perspective. *Science* 255:419–423.
- VanGisbergenJAM, RobinsonDA, GielenS (1981) A quantitative analysis of generation of saccadic eye movements by burst neurons. *J Neurophysiol* 45:417–442.
- VanHornMR, CullenKE (2009) Dynamic characterization of agonist and antagonist oculomotor neurons during conjugate and disconjugate eye movements. *J Neurophysiol* 102:28–40.
- VealeR, HafedZM, YoshidaM (2017) How is visual salience computed in the brain? Insights from behaviour, neurobiology and modelling. *Philos Trans R Soc Lond B Biol Sci* 372:20160113.
- VokounCR, JacksonMB, BassoM a (2010) Intralaminar and interlaminar activity within the rodent superior colliculus visualized with voltage imaging. *J Neurosci* 30:10667–10682.
- VolkmanFC (1962) Vision during voluntary saccadic eye movements. *J Opt Soc Am* 52:571–578.
- VolkmanFC (1986) Human visual suppression. *Vision Res* 26:1401–1416.
- VolkmanFC, RiggsL a., WhiteKD, MooreRK (1978) Contrast sensitivity during saccadic eye movements. *Vision Res* 18:1193–1199.
- vonHelmholtzH (1910) *Handbuch der Physiologischen Optik*, III. Leopold Voss.
- vonHolstE, MittelstaedtH (1950) Das reafferenz princip. *Naturwissenschaften* 37:464–476.
- WaitzmanDM, MaTP, OpticanLM, WurtzRH (1988) Superior colliculus neurons provide the saccadic motor error signal. *Exp Brain Res* 72:649–652.
- WaitzmanDM, SilakovVL, CohenB (1996) Central mesencephalic reticular-formation (cMRF) neurons discharging before and during eye movements. *J Neurophysiol* 75:1546–1572.
- WalkerMF, FitzgibbonEJ, GoldbergME (1995) Neurons in the monkey superior colliculus predict the visual result of impending saccadic eye movements. *J Neurophysiol* 73:1988–2003.
- WeiskrantzBL, WarringtonEK, SandersMD, MarshallJ (1974) Visual capacity in the hemianopic field following a restricted occipital ablation. *Brain* 97:709–728.
- WestheimerG (1954) Mechanism of saccadic eye movements. *AMA Arch Ophthalmol* 52:710–724.

- WhiteBJ, BoehnkeSE, MarinoRA, IttiL, MunozDP (2009) Color-related signals in the primate superior colliculus. *J Neurosci* 29:12159–12166.
- WilsonJR, HendricksonAE, SherkH, TiggesJ (1995) Sources of subcortical afferents to the macaque's dorsal lateral geniculate nucleus. *Anat Rec* 242:566–574.
- WilsonME, ToyneMJ (1970) Retino-tectal and cortico-tectal projections in *Macaca Mulatta*. *Brain Res* 24:395–406.
- WoollardHH (1927) The differentiation of the retina in the primates. *Proc Zool Soc London* 97:1–18.
- WurtzR, RichmondB, JudgeS (1980) Vision during saccadic eye movements. III. Visual interactions in monkey superior colliculus. *J Neurophysiol* 43:1168–1181.
- WurtzRH (1968) Visual cortex neurons: response to stimuli during rapid eye movements. *Science* 162:1148–1150.
- WurtzRH (1969) Comparison of effects of eye movements and stimulus movements on striate cortex neurons of the monkey. *J Neurophysiol* 32:987–994.
- WurtzRH (2008) Neuronal mechanisms of visual stability. *Vision Res* 48:2070–2089.
- WurtzRH, AlbanoJE (1980) Visual-motor function of the primate superior colliculus. *Annu Rev Neurosci* 3:189–226.
- WurtzRH, GoldbergME (1971) Superior colliculus cell responses related to eye movements in awake monkeys. *Science* (80- ) 171:82–84.
- WurtzRH, GoldbergME (1972a) Activity of superior colliculus in behaving monkey. III. Cell discharging before eye movements. *J Neurophysiol* 35:575–586.
- WurtzRH, GoldbergME (1972b) Activity of superior colliculus in behaving monkey. IV. Effect of lesions on eye movements. *J Neurophysiol* 35:587–596.
- WurtzRH, JoinerWM, BermanRA (2011) Neuronal mechanisms for visual stability: progress and problems. *Philos Trans R Soc Lond B Biol Sci* 366:492–503.
- WylieDRW, Gutierrez-IbanezC, PakanJMP, IwaniukAN (2009) The optic tectum of birds: mapping our way to understanding visual processing. *Can J Exp Psychol* 63:328–338.
- YarbusAL (1967) *Eye movements and vision*.
- ZhouW, KingWM (1998) Premotor commands encode monocular eye movements. *Nature* 393:692–695.
- ZipserD, AndersenRA (1988) A back-propagation programmed network that simulates response properties of a subset of posterior parietal neurons. *Nature* 331:679–684.
- ZirnsakM, SteinmetzN a, NoudoostB, XuKZ, MooreT (2014) Visual space is compressed in prefrontal cortex before eye movements. *Nature* 507:504–507.

## IV. Statement of contributions

**Chen, C. -Y.** and Hafed, Z. M. (2013). Postmicrosaccadic enhancement of slow eye movements. *The Journal of Neuroscience*, Vol. 33, No. 12, pp. 5375-5386.

I and Z.M.H. designed research; I and Z.M.H. performed research; I and Z.M.H. analyzed data; Z.M.H. wrote the paper.

**Chen, C. -Y.**, Ignashchenkova, A., Thier, P., and Hafed, Z. M. (2015). Neuronal response gain enhancement prior to microsaccades. *Current Biology*, Vol. 25, No. 16, pp. 2065-2074.

I and Z.M.H. implemented and analyzed the SC experiments. I, A.I., and Z.M.H. analyzed the second SC data. A.I. and P.T. implemented the FEF experiments. A.I. analyzed the FEF data. Z.M.H. wrote the paper.

Hafed, Z. M. and **Chen, C. -Y.** (2016). Sharper, stronger, faster upper visual field representation in primate superior colliculus. *Current Biology*, Vol. 26, No. 13, pp. 1647-1658

Z.M.H. and I performed the experiments and analyzed the data. Z.M.H. wrote the paper.

**Chen, C. -Y.** and Hafed, Z. M. (2017). A neural locus for spatial-frequency specific saccadic suppression in visual-motor neurons of the primate superior colliculus. *Journal of Neurophysiology*. doi: 10.1152/jn.00911.2016

I and Z.M.H. designed research, performed research, and analyzed data; Z.M.H. wrote the paper.

**Chen, C. -Y.**, Sonnenberg, L., Weller, S., Witschel, T., and Hafed, Z. M. Spatial vision by macaque midbrain. In Preparation.

I and Z. M. H. performed the neural experiments and analyzed the data. L. S., S. W., T. W., and Z. M. H. performed the human experiments. Z. M. H. wrote the paper.

**Chen, C. -Y.** and Hafed, Z. M. Orientation and contrast tuning properties and temporal flicker fusion characteristics of primate superior colliculus neurons. In Preparation.

I and Z. M. H. performed the neural experiments and analyzed the data. Z. M. H. wrote the paper.

## **V. Appendix: Individual studies**

### **1. Postmicrosaccadic enhancement of slow eye movements**



# Postmicrosaccadic Enhancement of Slow Eye Movements

Chih-Yang Chen<sup>1,2,3</sup> and Ziad M. Hafed<sup>2,3</sup>

<sup>1</sup>Graduate School of Neural and Behavioural Sciences, International Max Planck Research School, Tuebingen, 72074 Germany, <sup>2</sup>Werner Reichardt Centre for Integrative Neuroscience, Tuebingen, 72076 Germany, and <sup>3</sup>Animal Physiology, Institute of Neurobiology, University of Tuebingen, Tuebingen, 72076 Germany

Active sensation poses unique challenges to sensory systems because moving the sensor necessarily alters the input sensory stream. Sensory input quality is additionally compromised if the sensor moves rapidly, as during rapid eye movements, making the period immediately after the movement critical for recovering reliable sensation. Here, we studied this immediate postmovement interval for the case of microsaccades during fixation, which rapidly jitter the “sensor” exactly when it is being voluntarily stabilized to maintain clear vision. We characterized retinal-image slip in monkeys immediately after microsaccades by analyzing postmovement ocular drifts. We observed enhanced ocular drifts by up to ~28% relative to premicrosaccade levels, and for up to ~50 ms after movement end. Moreover, we used a technique to trigger full-field image motion contingent on real-time microsaccade detection, and we used the initial ocular following response to this motion as a proxy for changes in early visual motion processing caused by microsaccades. When the full-field image motion started during microsaccades, ocular following was strongly suppressed, consistent with detrimental retinal effects of the movements. However, when the motion started after microsaccades, there was up to ~73% increase in ocular following speed, suggesting an enhanced motion sensitivity. These results suggest that the interface between even the smallest possible saccades and “fixation” includes a period of faster than usual image slip, as well as an enhanced responsiveness to image motion, and that both of these phenomena need to be considered when interpreting the pervasive neural and perceptual modulations frequently observed around the time of microsaccades.

## Introduction

Active visual exploration involves frequent transitions between rapid eye movements and fixation. Such transitions also happen even during extended periods of fixation, because tiny saccades, called microsaccades, continue to occur during such periods. Given that saccades and microsaccades alter retinal images, they both modulate neural activity in the visual system. In fact, neural enhancement after saccades/microsaccades has been observed in several areas, including lateral geniculate nucleus, V1, V4, and MT/MST (Bair and O’Keefe, 1998; Leopold and Logothetis, 1998; Martinez-Conde et al., 2000, 2002; Reppas et al., 2002; Ibbotson et al., 2008; Kagan et al., 2008; Rajkai et al., 2008; Bosman et al., 2009; Bremmer et al., 2009; Crowder et al., 2009; Herrington et al., 2009; Cloherty et al., 2010). Although part of this enhancement is due to active extraretinal mechanisms associated with movement generation (Rajkai et al., 2008), a significant component of it also reflects visual reafference after movement end (Martinez-Conde et al., 2000).

The mechanisms of visual reafference after microsaccades are not entirely clear. Specifically, since the eye is never still during

fixation (Barlow, 1952), the transition from microsaccades to fixation described above is in fact a more fuzzy transition from fast eye movements to slow, drift-like position displacements. This creates a problem for understanding what contributes to enhanced visual activity after microsaccades. For example, since slow drifts result in retinal-image slip that is within the range of motion sensitivity of the visual system (Verheijen, 1961; Kuang et al., 2012), might it be the case that such image slip is momentarily altered after microsaccades, and thus potentially contributes to the altered visual responses?

Motivated by classic results on large saccades, we have investigated this question by carefully analyzing the patterns of ocular drifts (or, equivalently, retinal-image slip) immediately after microsaccades. We describe two main novel phenomena. First, it is known that large saccades are followed by a period of enhanced ocular drift, sometimes called “glissade” in reference to the smooth change in eye position involved (Weber and Daroff, 1972; Bahill et al., 1978). In the first part of this paper, we demonstrate that glissades remarkably also happen after microsaccades. Second, because glissades alter retinal images exactly when gaze is supposed to be stable, saccades are known to activate a rapid gaze stabilization mechanism immediately after their end. The efficacy of such a mechanism can be observed by imposing retinal image motion on the visual system immediately after saccades and analyzing the ensuing reflexive ocular following eye movement (Kawano and Miles, 1986). In the second part of this paper, we also show that this same mechanism still applies for microsaccades.

In addition to adding to our understanding of the oculomotor and visual mechanisms associated with microsaccades, our work

Received Aug. 2, 2012; revised Feb. 5, 2013; accepted Feb. 14, 2013.

Author contributions: C.-Y.C. and Z.M.H. designed research; C.-Y.C. and Z.M.H. performed research; C.-Y.C. and Z.M.H. analyzed data; Z.M.H. wrote the paper.

We were funded by the Werner Reichardt Centre for Integrative Neuroscience, Tuebingen, Germany. We thank Alla Ignashchenkova for helpful comments on an earlier version of this manuscript.

Correspondence should be addressed to Ziad M. Hafed, Werner Reichardt Centre for Integrative Neuroscience, Otfried-Muller Strasse 25, Tuebingen, 72076 Germany. E-mail: ziad.m.hafed@cin.uni-tuebingen.de.

DOI:10.1523/JNEUROSCI.3703-12.2013

Copyright © 2013 the authors 0270-6474/13/335375-12\$15.00/0

more generally highlights an important component of oculomotor activity that studies of postsaccadic perceptual and neural phenomena need to consider: the fact that the transition from even the smallest possible saccades to fixation is not a discrete transition. These studies rightly recognize the importance of understanding postmovement processing for comprehending vision under natural “active” conditions (Rajkai et al., 2008). However, these studies do not always consider the important contributions of postsaccadic drifts to such processing, even though such drifts after large saccades have long been known to exist (Weber and Daroff, 1972; Bahill et al., 1978; Kawano and Miles, 1986).

## Materials and Methods

### Animal preparation

We collected data from two (N and P) adult, male rhesus monkeys (*Macaca mulatta*) that were 6 years of age and weighed 6–7 kg. All experimental protocols for the monkeys were in accordance with the guidelines for animal experimentation approved by the Regierungspräsidium (local governing committee) of the city of Tuebingen, Germany.

The monkeys were prepared using standard surgical techniques necessary for behavioral training. Under isoflurane anesthesia and aseptic conditions, we first attached a head-holder to the skull to allow stabilizing head position during the experiments. The head-holder consisted of a titanium implant that was embedded under the skin and attached to the skull using titanium skull screws. We then sutured the skin to cover this implant and allow it to integrate with the bone for several months. In a subsequent surgery, we made a small skin incision on top of the head and attached a metal connector to the previously implanted head-holder. This connector acted as the interface for fixing the head to a standard position in the lab during data collection. In the same surgery, a scleral search coil was implanted in one eye to allow measuring eye movements with high temporal and spatial precision using the magnetic induction technique (Fuchs and Robinson, 1966; Judge et al., 1980).

### Behavioral tasks

**Fixation task.** To study the characteristics of ocular drifts (or retinal-image slip) before and after microsaccades, we analyzed eye movements from a task in which the monkeys were steadily fixating a small white fixation spot similar to that described by (Hafed et al., 2009), and presented over a uniform gray background (in an otherwise dark room). Each trial lasted for 900–1500 ms, and the monkeys were rewarded for maintaining fixation to within 1–1.5° from the fixation spot. The spot itself was  $\sim 8.5 \times 8.5$  min arc in size, and its luminance was 72 Cd/m<sup>2</sup>. The background luminance was 21 Cd/m<sup>2</sup>. The fixation task we used also involved a brief,  $\sim 8$  ms luminance transient of the fixation spot (to black and then back to white), and a second brief peripheral white flash ( $\sim 50$  ms), both occurring at a random time during fixation. These flashes were used to increase microsaccade frequency (Hafed and Clark, 2002; Hafed et al., 2011), for a second ongoing study unrelated to this one, but we are confident that they do not explain the ocular drift results that we present here. In fact, in preliminary analyses, we also tested for premicrosaccadic and postmicrosaccadic alterations in ocular drifts in a second fixation task that did not contain luminance transients, and we found similar results to those presented here.

To compare perimicrosaccadic ocular drifts to those around large saccades, we also measured eye movements in one monkey (P) during a delayed, visually guided saccade task. In this task, the monkey fixated while a peripheral spot was presented (at 5–15° of eccentricity). Once the fixation spot disappeared, the monkey initiated a visually guided saccade to the peripheral spot.

**Ocular following task.** To study the sensitivity of early motion processing to retinal-image slip after microsaccades, we presented, in different blocks of trials, a full-field image motion stimulus that was triggered at different times after real-time microsaccade detection. The procedure for this behavioral task was as follows. A static stimulus was first presented to allow the monkeys to fixate the center of the display. This stimulus consisted of a fixation spot presented over the same uniform gray back-

ground as described above, along with a large, vertical sine wave grating of 0.25 cycles per degree and 50% contrast relative to the background luminance. The sine wave grating covered the entire extent of the display, except for a horizontal strip of thickness 22 min arc and centered vertically on the fixation spot. This strip was of background luminance, and we used it so that the fixation spot was always clearly visible to the monkeys, regardless of the sine wave grating (see Fig. 6A). After the monkeys steadily fixated the central spot (to within 1.5°) for at least 500 ms, we enabled a process to detect microsaccades in real-time using eye velocity criteria (see below), and to trigger a pure horizontal motion (rightward or leftward) of the grating contingent on such detection. During the motion, which lasted for 225 ms, the entire grating was shown without the horizontal strip of background luminance. We triggered the motion 0 ms, 25 ms, 50 ms, 75 ms, 100 ms, 150 ms, or 200 ms after real-time microsaccade detection, and the motion itself consisted of a horizontal translation of the sine wave grating by 1/4 cycles every 42 ms (resulting in an effective stimulus speed of 24°/s). If no microsaccade was detected for 500 ms after enabling the process to detect these movements, we triggered the full-field motion anyway. The fixation spot always disappeared at the same time as motion onset, releasing the monkey from the requirement to fixate, and we analyzed the resulting initial ocular following response to this motion as a proxy for early motion processing (Miles et al., 1986; Masson and Perrinet, 2012; Quaia et al., 2012). We relaxed the fixation constraint of 1.5° (to 4.5°) during stimulus motion to avoid unnecessarily penalizing the monkeys for the ocular following responses that we were interested in measuring. Finally, the initial phase of the sine wave grating was randomly selected on every trial from eight possible equally spaced phases.

We also tested this task on large saccades in one monkey (P), to replicate classic results (Kawano and Miles, 1986). In this variant of the task, the fixation spot initially appeared 10° to the right or left of the center of the display. Once the monkey fixated this spot, the spot jumped to the center of the display (to its normative position in Fig. 6A), and the monkey initiated a visually guided saccade to follow it (i.e., a 10° saccade). We removed the spot and triggered full-field image motion of the sine wave grating at different times after real-time detection of the 10° saccade onset, as described above. Thus, this task variant tested for postsaccadic ocular following responses after large, horizontal 10° eye movements.

We analyzed 1567 trials from monkey N and 2818 trials from monkey P in the microsaccade version of our ocular following task, and we analyzed 1667 more trials from monkey P in the large saccade variant of it.

### Experimental control system and real-time microsaccade detection

We used a custom-built experimental control system that drove stimulus presentation and ensured monkey behavioral monitoring and reward delivery, as well as implemented real-time microsaccade detection. The core of the system consisted of a real-time signal processor from National Instruments (cRIO-9024), paired to high-speed digital I/O and analog-to-digital converter cards. The system ran at 1 kHz, and it communicated with our graphics system by sending display update commands using a high-speed universal-data-packet protocol over Ethernet cables. The graphics system in turn consisted of a Mac Pro workstation (Apple) running the Psychophysics Toolbox extension of MATLAB (Brainard, 1997; Pelli, 1997). The graphics system updated display frames at 120 Hz, meaning that our display updated with a maximum possible latency of  $\sim 8$  ms (1 frame) after microsaccade/saccade detection. All eye movement data and behavioral task events (such as microsaccade detections and display update time stamps) were saved digitally using a dedicated data acquisition system (Multichannel Acquisition Processor; Plexon). We also confirmed (and saved) stimulus update times by measuring display frames using a photodiode aimed at the bottom right corner of the graphics display.

Our system detected microsaccades in real time by obtaining a real-time estimate of radial eye velocity. This estimate used a variant of a previously described algorithm to differentiate the incoming position signals into velocity estimates (Janabi-Sharifi et al., 2000). Briefly, at every time sample, we obtained the slope of a best fitting line to the latest 5 ms of input eye position data. We then reduced noise in the velocity calculation by obtaining the median of the three latest slope measure-

ments and using that as our real-time estimate of eye velocity. After estimating eye velocity, we identified microsaccades as the eye movements that exceeded a user-adjustable threshold on this velocity. We manually adjusted the eye-velocity threshold during experiments based on the signal-to-noise ratio in the digitized eye position data. In *post hoc* analyses, including all analyses presented in this paper, we obtained eye velocities using a more sophisticated “acausal” differentiating filter (odd-symmetric FIR filter with a smoothing 3 dB cutoff at 54 Hz) (Hafed et al., 2009; Lovejoy and Krauzlis, 2010) because in these analyses, we had the luxury of using both past and future eye position samples to estimate derivatives. Such *post hoc* analyses demonstrated that we could reliably detect microsaccades as small as 3 min arc in real time (median amplitude:  $\sim 12$  min arc), and that the earliest possible display update after true microsaccade onset was  $\sim 12$  ms (this included the time for the real-time estimator of velocity to calculate eye speed and the time for the graphics system to start the display update on the next frame). Thus, these *post hoc* analyses showed that we could reliably start the motion stimulus during tiny microsaccades (whose average duration was  $38 \pm 5.9$  ms SD), as well as after them, with precise time delays exactly as our experimental design dictated.

For one of our monkeys (P), and in only one analysis in Figure 7B, eye movements in the full-field motion task (not the main fixation task above) were collected using a video-based eye tracker (EyeLink 1000; SR-Research) rather than scleral search coils, because the search coil had to be removed from this monkey. The tracker consisted of a high-speed video camera placed under the display and aimed at the monkey's left eye, and its output was directed to the real-time processor exactly as described above. Microsaccades (Otero-Millan et al., 2012) and ocular following responses (Boström and Warzecha, 2009) can both be reliably detected using this system, and we confirmed this with our analyses (see Results) and confirming their similarity to the results with monkey N using scleral search coils (Figs. 6, 7). We should emphasize, again, that this use of the video-based eye tracker was only restricted to one single analysis (Fig. 7B) involving smooth ocular following eye movements much faster than fixational drift, and that all other analyses of slow fixational drifts were performed using the more precise scleral search coils. This was important because we found that using a video-based eye tracker like the EyeLink system can cause interpretational ambiguities for slow fixational drifts, as we discuss at length (see Discussion; Fig. 8) and as was also recently found (Kimmel et al., 2012).

### Data analysis

**Eye movement detection and classification.** Eye movements were sampled at 1 kHz. Microsaccades were detected in *post hoc* analyses using velocity and acceleration thresholds as described by (Krauzlis and Miles, 1996; Hafed et al., 2009). Briefly, for any given microsaccade, we first identified all time samples of the movement in which radial eye velocity exceeded a threshold of  $5^\circ/\text{s}$ . This threshold was chosen to be low enough to detect even the smallest microsaccades, but high enough to exclude eye tracker noise. We then refined the start and end points of the microsaccade by using an acceleration threshold of  $250^\circ/\text{s}^2$ . Specifically, after the initial velocity thresholding, we kept marching backward in time (for microsaccade onset) or forward in time (for microsaccade end) below the velocity threshold until absolute eye acceleration was below the acceleration threshold. The latter threshold was again chosen to exclude eye tracker noise from erroneously marking noise samples as parts of microsaccades. In our analyses, we considered as microsaccades all fixational saccades that were  $\leq 1^\circ$  in radial amplitude. However, in reality, the great majority of these movements were in fact much smaller. Specifically, the overall median microsaccade amplitude in monkey N was 11 min arc across all detected microsaccades, and it was 9 min arc in monkey P. These values are consistent with previous reports of microsaccade amplitudes in monkeys (Kagan et al., 2008; Hafed et al., 2009, 2011, 2013; Hafed and Krauzlis, 2010, 2012) and humans (Poletti and Rucci, 2010; Otero-Millan et al., 2012; Hafed, 2013). Moreover, the amplitude distributions of these microsaccades were similar to those published previously, in both monkeys (Kagan et al., 2008; Hafed et al., 2009) and humans (Poletti and Rucci, 2010; Chericci et al., 2012; Otero-Millan et al., 2012; Hafed, 2013), and they showed a skew toward small movement amplitudes. For example,

the insets in Figure 2 show such sample amplitude distributions from a subset of our collected microsaccades (those used in the analysis of that figure). As can be seen, the distributions were clearly skewed to small movements, again as previously found (although note that the small sample sizes in these figure insets compared with earlier studies meant that it was even less likely to observe “large microsaccades” in these insets than in previous reports: large microsaccades are normally rare and would thus be even less likely with small sample sizes).

Our use of acceleration criteria to refine microsaccade onset and end times (Krauzlis and Miles, 1996) was critical for the current study because it extended the endpoint of a microsaccade well beyond the endpoint classically identified using methods that only employ eye velocity thresholds. This was of great importance for us because the basic result of our analyses was an enhanced ocular drift velocity after microsaccades (see Results). Thus, we wanted to be as conservative as possible (by extending microsaccade end forward in time) so that we do not attribute velocities that are part of the microsaccade itself (which are necessarily higher than premovement drifts) to our measured postmicrosaccadic drifts. In addition, we added one final step in identifying microsaccade onset and end times. We did so by manually inspecting all detected microsaccades and using all of eye position, eye velocity, and eye acceleration inspection to refine the movement parameters. Our refinement was always toward the conservative side by extending our estimate of movement end forward as much as possible, especially if a microsaccade had a small, but rapid, dynamic overshoot that could contaminate our estimate of postmicrosaccadic drift. For example, the first two sample microsaccades in Figure 1A (from left to right) are movements in which we manually extended their endpoint forward in time beyond the acceleration threshold criterion. We did this to avoid erroneously attributing the small dynamic overshoot present in these movements to postmicrosaccadic drift. Thus, such a conservative approach of using acceleration criteria combined with manual inspection makes us confident that the postmicrosaccadic enhancements of drifts that we report in this paper are not artifacts of erroneously marking the end of a given microsaccade too early, and thus including high velocities from the movement itself in our measurements (see Fig. 1 for example microsaccades and their premovement and postmovement drifts and Fig. 5 for a measurement of eye trajectory after microsaccade end, confirming that the trajectory was not forward in microsaccade direction, as might be expected from a premature marking of microsaccade end).

**Time course of premicrosaccadic and postmicrosaccadic drifts.** Retinal-image slip is directly related to slow drift velocity during fixation (if the eye drifts in one direction, then the retinal-image “slips” in the opposite direction). Thus, even though earlier studies of premicrosaccadic retinal-image slip have relied on eye position to infer such slip (Engbert and Mergenthaler, 2006), we directly analyzed drift velocity. We measured radial eye velocity during 50 ms time windows before microsaccade onset or after microsaccade end. To obtain a time course of drift velocity relative to the movement, we slid these time windows backward in time (before microsaccade onset) or forward in time (after microsaccade offset) by 10 ms steps. To get a statistical estimate of postmicrosaccadic enhancement of drift velocity, we used drift velocity in the 50 ms period centered at 125 ms before microsaccade onset as the baseline to which we compared postmicrosaccadic drifts. Moreover, we ensured that any changes in drift velocity (i.e., retinal-image slip) were not contaminated by other microsaccades before or after the movement we were analyzing. We did this by only analyzing premicrosaccadic and postmicrosaccadic drifts for microsaccades that were not preceded by a second movement within 300 ms and also not followed by a second movement within 300 ms. This ensured that changes in drift velocity associated with a given microsaccade were not artifacts of other nearby eye movements (which necessarily have higher eye velocity than slow drifts), but it meant that the microsaccades analyzed in the current study constituted only a subset of all microsaccades that the monkeys made in our experiments. For some analyses, we extended these time periods even more to 500–600 ms before movement onset (see Results). We used a similar strategy when analyzing large saccade data.

In some of our analyses, we reported relative measures of drift velocity after microsaccades. That is, we normalized eye velocity relative to the

baseline velocity measurement made at a time point centered on 125 ms before movement onset. This approach ensured that our results were not dependent on our particular choice for estimating eye velocity. For example, depending on the amount of smoothing performed during eye position differentiation in different algorithms, the absolute measure of eye velocity during slow drifts can be variable (Cherici et al., 2012). However, by using relative measures and a single algorithm for all analysis time windows, it was still possible to reliably identify relative changes in postmicrosaccadic drift as a function of time after microsaccades. Having said that, in Figures 1 and 2, we also analyzed absolute measures of eye velocity without any normalization, and we confirmed that the basic results we are reporting were unaltered by such normalization procedure.

To further confirm our results on postmicrosaccadic changes in drift, we also assessed such drift using a second method completely independent of a specific algorithm for eye velocity estimation. Specifically, and like previous studies of premicrosaccadic retinal-image slip that have used eye position as a proxy for this slip (Engbert and Mergenthaler, 2006), we analyzed premicrosaccadic and postmicrosaccadic image slip by directly analyzing eye positions. We used the same “box-counting” procedure used earlier (Engbert and Mergenthaler, 2006), but we extended it to measure eye drift after microsaccades, not just before them. This box-counting procedure may be thought of as “path integration” of eye trajectory. Briefly, within a given 50 ms time period relative to microsaccade onset or end, the 2D locations of eye position in this period are spatially binned (0.01° bin width), and the count of spatial bins (box-count) covered by the eye trajectory during this 50 ms time period provides an estimate of how much “space” the eye has traversed along its “path.” If the eye drifts faster than usual, then the box-count is increased, and vice versa if the eye drifts slower than usual. We compared the results of this box-counting procedure to our results with direct measures of retinal-image slip (through measures of ocular drift velocity), to confirm our interpretation of postmicrosaccadic enhancements using two different techniques.

Finally, we used eye position to also investigate the spatial trajectory of ocular drift immediately after microsaccades. We simply measured eye position in every millisecond after microsaccade end, and we averaged all such measurements for all detected microsaccades, but only after rotating all microsaccades (and the postmovement measurements) to align all data for a “canonical” microsaccade ending direction. Thus, the measured postmicrosaccadic drift positions were calculated relative to the direction of the final quarter of the antecedent microsaccade. This averaging technique allowed us to conclude whether postmicrosaccadic ocular drift (and thus retinal-image slip) was systematically related to the trajectory of the antecedent movement or not. If it is, then this averaging technique should reveal a consistent trajectory. Otherwise, it should not. We then repeated the same procedure for the drift trajectory immediately before microsaccade onset. In this case, we rotated all measurements to measure eye position relative to the direction of the initial quarter of microsaccade trajectory.

**Time course of ocular following responses after microsaccades.** To test for a possible consequence of postmicrosaccadic drift on the visual system, we used our full-field image motion task to artificially simulate full-field retinal-image slip at different times after microsaccades. Full-field image motion is known to drive an ultrashort-latency ocular following reflex that attempts to stabilize this motion (Miles et al., 1986; Gellman et al., 1990; Masson and Perrinet, 2012). The initial component of this ocular following response is an “open-loop” response that is not influenced by visual feedback caused by ongoing eye movements, and thus acts as a proxy for the very initial motion processing of the full-field (retinal) image motion (Masson and Perrinet, 2012; Quaia et al., 2012). Thus, we analyzed only the initial ocular following response after full-field motion onset. For every trial, we measured the peak eye velocity during the time period between 80 and 100 ms after motion onset. To measure the time course of modulations in this response after microsaccades, we manually inspected all microsaccades as described above, and we binned trials based on when the motion started after microsaccade offset. We then plotted the magnitude of the ocular following response (peak eye velocity

in the period between 80 and 100 ms after motion onset) as a function of the time of motion onset relative to microsaccade offset.

## Results

### Ocular drift (or retinal-image slip) was constant before microsaccades but enhanced immediately afterward

We analyzed 2314 microsaccades from two male rhesus macaques fixating a small fixation spot. For each of these microsaccades, whose overall median amplitude was 8.24 min arc for monkey N and 4.54 min arc for monkey P, we analyzed slow ocular drift velocity before and after the movements. This allowed us to infer the pattern of retinal-image slip around the time of even the smallest of microsaccades. We carefully measured eye movements in both monkeys using the magnetic induction technique (Fuchs and Robinson, 1966; Judge et al., 1980), which was critical for interpreting our results. Not only does this technique have unparalleled spatial and temporal resolution, but it also has the added advantage of not exhibiting postmovement ringing that is frequently observed with video-based measurements of eye position; these video-based measurements are affected by factors such as ocular lens distortions during rapid eye movements, which become particularly prominent at the ends of the movements (Deubel and Bridgeman, 1995), and which would otherwise potentially mask the postmovement effects that we were studying.

Postmicrosaccadic drift velocity was consistently enhanced relative to premovement levels, even for the tiniest eye movements. Figure 1A shows three sample microsaccades of different sizes and directions, for which a clear postmovement ocular drift was observed in both eye position and eye velocity traces. The figure plots horizontal and vertical eye position (top row) as well as radial eye velocity (middle row) and acceleration (bottom row) before, during, and after these tiny saccadic eye movements. The eye position, velocity, and acceleration samples marked in green in the figure represent the microsaccadic component of the eye movement, and the other samples show premovement or postmovement drift. As can be seen, for all of these sample microsaccades, there was a clear enhancement of ocular drift velocity immediately after microsaccades relative to before the rapid eye movements (highlighted with a black diagonal arrow for each microsaccade), and this enhancement was also evident in the eye position traces as well. In fact, the eye position traces revealed that such faster postmicrosaccadic drifts could be characterized as so-called “glissadic overshoots” (in which the eye drifts backward immediately after movement end) commonly observed after much larger saccades (Bahill et al., 1978). An example of such a glissadic overshoot after large saccades from our own dataset is illustrated in Figure 1B, in which we document a postmovement drift after a large 15° visually guided saccade generated by monkey P. Thus, our analysis of the sample microsaccades in Figure 1A shows that, just like for their much larger counterparts (Fig. 1B), ocular drift, and necessarily retinal-image slip, was markedly enhanced (i.e., faster) after these tiny eye movements, despite the fact that these movements (like the first two in Fig. 1A) could be smaller than even the strictest definitions for microsaccades (Collewijn and Kowler, 2008; Hafed et al., 2009; Hafed and Krauzlis, 2012).

Postmicrosaccadic enhancement of ocular drift velocity was consistently observed in each of the two monkeys. For every detected microsaccade in one sample session from each of our monkeys, we analyzed premicrosaccadic and postmicrosaccadic ocular drift velocity as we did for the three sample movements of Figure 1A above. We specifically measured radial eye velocity

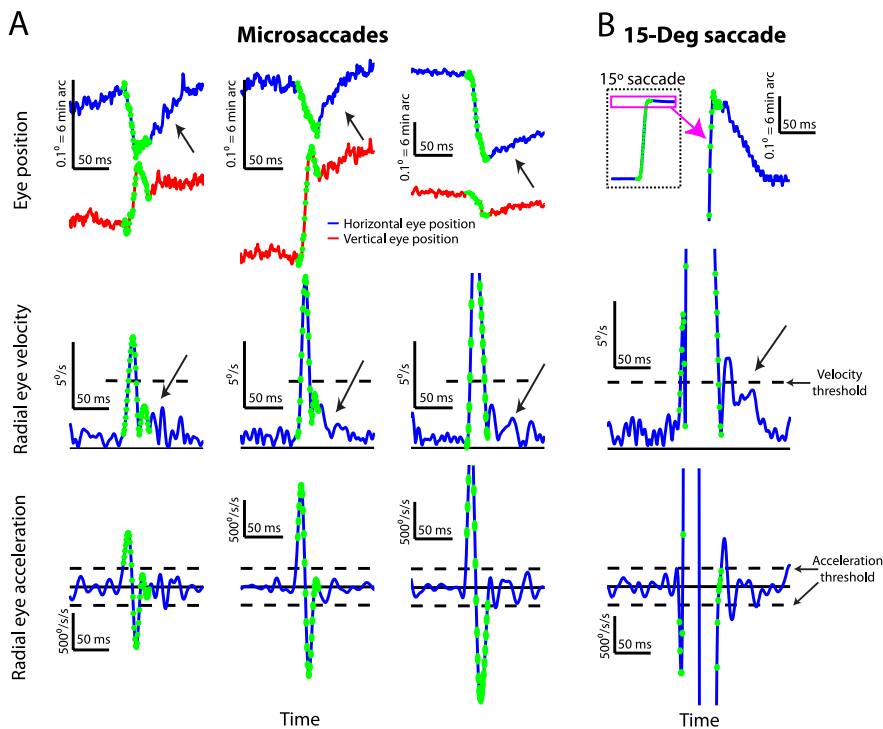


**Figure 1.** Postmicrosaccadic enhancement of slow eye movements. **A**, Three example microsaccades of increasing size (from left to right) and different directions showing differences between premovement and postmovement drift. The top row shows horizontal (blue) and vertical (red) eye position, the middle row shows radial eye velocity, and the bottom row shows radial eye acceleration. The dashed horizontal lines in the middle and bottom rows indicate the velocity (middle) and acceleration (bottom) thresholds we used to mark microsaccade onset and end (see Materials and Methods), and the green samples are those that were flagged as part of a microsaccade. Note that for the first two microsaccades, we manually extended microsaccade end forward in time to ensure that the small dynamic overshoot in vertical eye position did not artifactually bias our estimates of postmicrosaccadic drifts (see Materials and Methods). The black diagonal arrows highlight a period of clear enhancement of postmicrosaccadic drift (compare position and velocity traces after microsaccades to a similar period before them). **B**, An illustration of postsaccadic drift (Weber and Daroff, 1972; Bahill et al., 1978) for a large, 15° saccade. A conceptually identical postmovement drift was observed as in the case of the microsaccades in **A**, albeit with a larger overall magnitude and duration. In all the eye-position plots, upward deflections in the traces denote rightward and upward changes in eye position, respectively.

during the first 50 ms after microsaccade end (i.e., during a 50 ms time window centered on 25 ms after movement end) and compared it to radial eye velocity during a 50 ms time window centered around 125 ms before microsaccade onset. Across the analyzed population of microsaccades in these two sample sessions, there was a robust enhancement in ocular drift velocity immediately after microsaccades relative to the premovement baseline (Fig. 2*A,C*) ( $p < 0.0001$  for monkey N and  $p < 0.0001$  for monkey P; paired  $t$  test). Specifically, the average drift velocity in monkey N was  $\sim 1^\circ/\text{s}$  before microsaccades but  $\sim 1.28^\circ/\text{s}$  immediately after the movements ( $\sim 28\%$  enhancement), and it was  $\sim 0.74^\circ/\text{s}$  before microsaccades but  $\sim 0.91^\circ/\text{s}$  after them for monkey P ( $\sim 23\%$  enhancement). Moreover, this effect was specific to the postmovement period, because a similar analysis but now measuring radial eye velocity during two premicrosaccade intervals showed no significant enhancement or reduction (Fig. 2*B,D*) ( $p = 0.1$  for monkey N and  $p = 0.6$  for monkey P; paired  $t$  test). Thus, immediately after microsaccade end, ocular drift (and thus retinal-image slip) was consistently enhanced in both monkeys, and this effect was linked to the antecedent eye movement because no change in ocular drift was apparent before the movement.

The above analyses compared ocular drift velocity before and after microsaccades to demonstrate a possible postmicrosaccadic enhancement effect. However, it may be argued that the enhance-

ment we observed in Figures 1 and 2 after microsaccades was simply an artifact of reduced “retinal-image slip” before the movements, as was recently suggested to happen (Engbert and Mergenthaler, 2006). In other words, it could be argued that postmicrosaccadic ocular drift is not enhanced, but it is simply the premicrosaccadic drift that is suppressed instead. To rule this possibility out, we analyzed the full-time course of premicrosaccadic and postmicrosaccadic ocular drifts, rather than just during two temporal windows before and after the movement as we did above in Figure 2. The results of this analysis are shown in Figure 3*A,B* for each monkey individually (black curves). To obtain this figure, we measured radial eye velocity (or the radial velocity of retinal-image slip) during 50 ms time windows that were centered at 10 ms time steps relative to either microsaccade onset or microsaccade end. To facilitate comparisons of eye velocity at different time windows, we normalized all measurements to the radial eye velocity during the 50 ms window centered on  $-125$  ms relative to microsaccade onset. As can be seen, we saw no evidence for a reduction in drift velocity before microsaccade onset and for up to 200 ms before such onset. Instead, drift velocity remained relatively constant, and it was strongly enhanced for a short interval after the end of the microsaccades. For example, monkey N showed a  $25.7 \pm 1.1\%$  SEM enhancement in ocular drift velocity during the first 50 ms after microsaccade end, and monkey P showed a  $17.6 \pm 0.7\%$  SEM enhancement in the same time window. We also noticed that both monkeys showed a modest enhancement immediately before microsaccade onset, but this enhancement was much smaller than that observed after microsaccade end. Moreover, these effects did not depend on microsaccade size, because they persisted for movements that were only smaller than the median amplitude in our population (green curves) as well as movements that were only larger than the median amplitude (red curves). We also analyzed large 5–15° saccades from monkey P (Fig. 3*B*, blue curves in the insets), and we found that our microsaccadic results were conceptually identical to those of classic “glissades” after large saccades (consistent with Fig. 1*B*), although they were smaller and more short-lived. Thus, the postmicrosaccadic enhancement in ocular drift velocity that we observed above (Figs. 1, 2) was directly linked to the microsaccade, and it was not an artifact of premovement reductions in retinal-image slip, as was recently suggested (Engbert and Mergenthaler, 2006).

We further analyzed the time course of premicrosaccadic and postmicrosaccadic ocular drift, this time by analyzing eye position using the exact same path integration (or box-counting) algorithm as that used in (Engbert and Mergenthaler, 2006) (see Materials and Methods). To further confirm that retinal-image slip was relatively unaltered before microsaccades and only increased after the movements, we extended for this analysis our time intervals for measuring premovement and postmovement

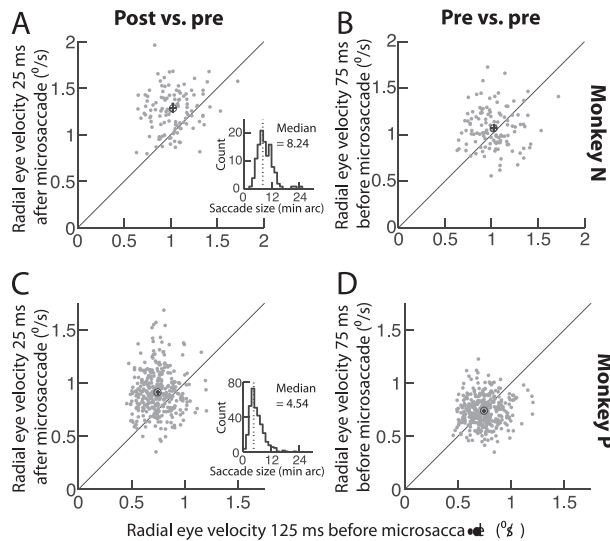


**Figure 2.** Postmicrosaccadic enhancement occurred in both monkeys. **A, C**, Comparison of radial eye velocity during a 50 ms time window immediately after microsaccade end (i.e., centered on 25 ms after the microsaccade) ( $y$ -axis) to radial eye velocity during a 50 ms time window well before microsaccade onset (i.e., centered on  $-125$  ms relative to movement onset) ( $x$ -axis). In each panel, the individual symbols correspond to individual microsaccades in monkey N (**A**) or monkey P (**C**). The black hollow circle in each panel shows mean values. Error bars around this circle (horizontal and vertical), when visible, indicate 95% confidence intervals. As can be seen, there was a robust enhancement in drift velocity after microsaccades relative to before them. The inset in each panel shows the amplitude distribution of the microsaccades in this figure (note that such distribution was skewed to small microsaccades, consistent with previous reports, but that this skew is particularly more obvious here because of the small sample size: large microsaccades are normally already rare, so they are even less likely to be observed with such a small sample size). **B, D**, Similar analyses from the same session in each monkey, but now comparing eye velocity during two time windows that were both before microsaccade onset. No enhancement or reduction occurred.

drift. Specifically, in Figure 3A and B above, we only measured drift velocity from 200 ms before microsaccade onset to 200 ms after microsaccade end. However, for the present analysis, we picked only the microsaccades that were not preceded by other microsaccades by up to 500–600 ms. This allowed us to analyze box-counts during longer time intervals spanning from 400 to 500 ms before microsaccade onset. For both monkeys, the box-count obtained during 50 ms ocular drift intervals was significantly increased in the immediate postmovement interval relative to premicrosaccade levels, consistent with our previous observations above, but it was again virtually unaltered for the entire 400–500 ms before microsaccade onset (Fig. 4A, C). Thus, contrary to (Engbert and Mergenthaler, 2006), we saw no evidence that retinal-image slip is reduced before microsaccades. Instead, the most obvious observation in our data was that post-movement slip was significantly enhanced. We further confirmed this by measuring ocular drift velocity on the same movements analyzed in Figure 4, A and C, and having the same longer pre-movement analysis intervals (Fig. 4B, D). Both eye position and eye velocity analyses revealed relatively stable drift before microsaccades and a strong, but short-lived postmicrosaccadic enhancement.

#### Postmicrosaccadic ocular drift was related to the direction of the antecedent microsaccade

Since our analyses above suggested that postmicrosaccadic enhancement of ocular drift velocity was directly related to the immediate generation of an antecedent microsaccade, we next asked whether the trajectory of the eye after the movement was in any

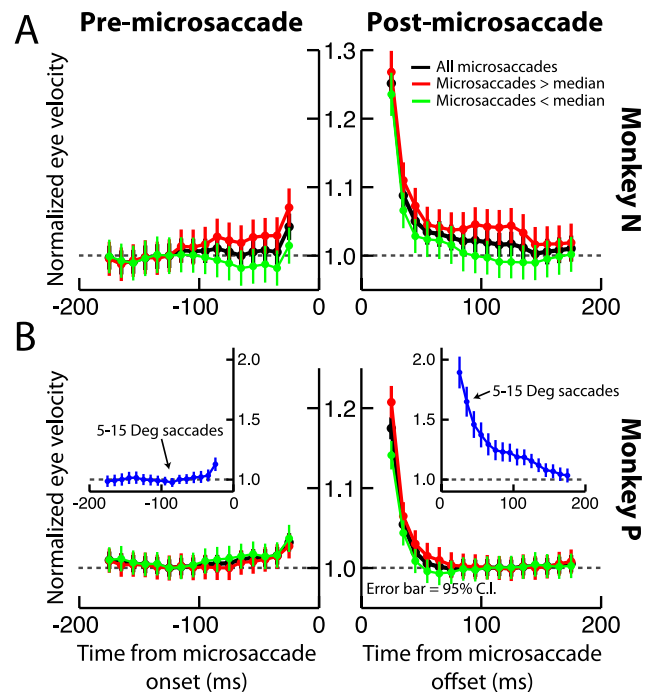


**Figure 3.** **A, B**, Perimicrosaccadic drift velocities were relatively constant long before microsaccades, but enhanced after them. In each panel, we plotted in black radial eye velocity for each monkey as a function of time from microsaccade onset (left subgraph) or microsaccade end (right subgraph). All eye velocities were first normalized to the velocity measured during a 50 ms time window centered on  $-125$  ms from microsaccade onset. We then measured eye velocities in similar 50 ms time windows that were translated in time. Drift velocity was relatively constant before microsaccade onset, but it increased immediately after the movements. The red curves show the same analysis but only for microsaccades larger than the median amplitude, and the green curves show it for microsaccades smaller than the median amplitude. The blue curves in the inset for monkey P show data from  $\sim 450$  large ( $5\text{--}15^\circ$ ) saccades made by this monkey. These additional curves demonstrate that the basic conceptual results did not depend on movement amplitude. Error bars in all parts indicate 95% confidence intervals.

way related to the direction of the microsaccade that was just completed (as we observed in the sample microsaccades of Fig. 1A). In other words, is postmicrosaccadic drift corrective in nature (i.e., does the eye drift back opposite the microsaccade direction?) or does it exhibit momentum (i.e., does the eye drift forward in the same direction as a microsaccade?) or is it completely unrelated to the antecedent movement? To answer this question, we measured for every microsaccade the position of the eye in every millisecond after movement end. Because our monkeys made microsaccades in all directions (Fig. 1), and to combine microsaccades of different directions in the same summary analysis, we first applied a coordinate transformation (rotation) such that all microsaccades (and subsequent drifts) were aligned to a “canonical” direction based on the direction of the final trajectory of the microsaccades (see Materials and Methods). Our motivation for this analysis was as follows: if postmicrosaccadic drift is completely unrelated to the antecedent microsaccade trajectory, then averaging across all movements should not result in any systematic pattern of postmovement drift. However, if the postmovement drift is consistently related to the direction of the previous microsaccade, then averaging should reveal a consistent path. Figure 5, A and C, shows the result of this analysis for each monkey. In this figure, we plotted the average horizontal and vertical eye position of the monkey relative to the ending position of a microsaccade (indicated schematically as the origin of the figure), and we rotated all axes such that positive horizontal axes

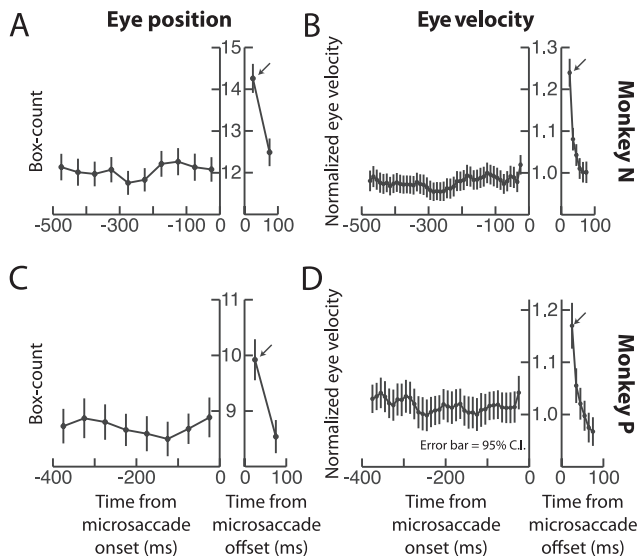


**Figure 4.** Postmicrosaccadic enhancement was also observed using eye position estimates of ocular drift. **A, C**, For each monkey, we implemented the box counting path integration algorithm by Engbert and Mergenthaler (2006). However, in our case, we measured box counts both after micro-saccade end as well as before micro-saccade onset, instead of just in the latter interval. Box counts of eye position drift were constant before movement onset, unlike in the data of Engbert and Mergenthaler (2006). However, consistent with our earlier analyses above, box counts were larger after micro-saccade end. **B, D**, We further tested the same eye movements in **A** and **C**, but this time by analyzing eye velocities similar to our procedure in Figure 3. Consistent with **A** and **C**, eye velocity for these same movements was constant for up to 500 ms before micro-saccade onset, and it was enhanced immediately after movement end. Error bars in all plots indicate 95% confidence intervals. Note that monkey P made frequent micro-saccades, so it was virtually impossible to find fixation intervals in which a single micro-saccade was not preceded by an earlier movement for a full 500 ms. Thus, for this monkey, we restricted the premicrosaccadic interval to 400 ms, to avoid contamination of ocular drift measurements by other previous micro-saccades.

in the figure were drifts in the same direction as the final micro-saccade trajectory and positive vertical axes were drifts orthogonal (and counterclockwise) to the direction of the antecedent micro-saccade. As can be seen, in both monkeys, postmicrosaccadic drift had a corrective component to it. Specifically, in both monkeys, the eye consistently drifted backward directly opposite the antecedent micro-saccade's ending trajectory. Note how the enhancement in postmicrosaccadic drift velocity is also obvious in this figure, evidenced by the larger displacement of the average eye position in every millisecond of time during the initial period after the movement end. Also note that this analysis confirms that we did not prematurely mark micro-saccade end, and thus erroneously treat saccadic components of eye velocity as postmicrosaccadic drift, because in this case Figure 5, **A** and **C**, should reveal a trajectory along the path of the yet-to-end micro-saccade rather than opposite it as we observed. Thus, in both monkeys, not only was postmicrosaccadic drift faster than normal, but it also exhibited a corrective component relative to the antecedent movement direction, as is the case with so-called glissadic overshoots in much larger saccades (Bahill et al., 1978; Fig. 1*B*). Such corrective component was also seen in the sample micro-saccades of Figure 1*A*. For comparison, we also plotted in Figure 5, **B** and **D**, results of the same analysis but now for premicrosaccadic drift instead. In this case, we plotted pre-movement horizontal and vertical average eye position relative to the starting point of a micro-saccade, and all micro-saccades were again rotated such that the horizontal axis reflected positions along the initial direction of the upcoming movement and the vertical axis reflected positions or-

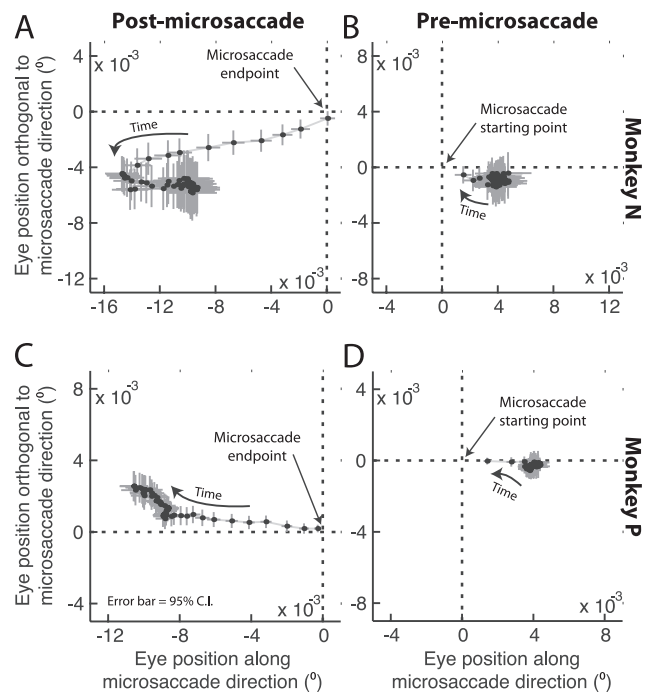


**Figure 5.** Postmicrosaccadic drift trajectory was related to the antecedent micro-saccade direction. **A, C**, We plotted average eye position in every millisecond following micro-saccade end. Each panel plots the first 50 ms of eye drift after micro-saccades. Each symbol shows the average  $\pm 95\%$  confidence intervals, and the first point after micro-saccade end is the point closest to the origin in the figure. The progression of time after a micro-saccade is indicated graphically by an arrow. As mentioned in the text, before averaging such eye positions, we first re-aligned all micro-saccades according to the direction of the final quarter of micro-saccade trajectory, such that rightward horizontal displacements in the figure now correspond to drifts along the same direction as the antecedent micro-saccade and upward vertical displacements in the figure correspond to drifts orthogonal to the direction of the antecedent micro-saccade. For both monkeys, postmicrosaccadic drift was consistently opposite the final direction of the antecedent eye movement. **B, D**, Similar analyses but now for eye positions immediately before micro-saccade onset. This time, we aligned movements according to the initial micro-saccade trajectory such that rightward displacements in the figure are displacements along the upcoming micro-saccade direction. Notice how premicrosaccadic drift was slow (strong clustering of the points together) compared with postmicrosaccadic drift, and that it did not exhibit a consistent trajectory.

thogonal to its direction. As can be seen, no consistent pattern of eye position, or enhancement, was seen before micro-saccades. Thus, the analyses in Figure 5 combined confirm that retinal-image slip is enhanced immediately after micro-saccades, and they also show that the direction of such slip has a corrective component to the slip caused by the antecedent eye movements. Such corrective component was also recently observed in humans immediately after micro-saccades (Cherici et al., 2012).

#### Ocular following responses to full-field image motion were also enhanced after micro-saccades

One possible hypothesis about the postmicrosaccadic enhancement described above is that the faster retinal-image slip it gives rise to can activate visual circuitry in the retina and early visual system with full-field image motion caused by the drifting eye movement. This full-field image motion can in turn galvanize a “field-holding reflex” mediated by activity in the early visual system in response to such image motion, as is hypothesized to happen for much larger saccades (Kawano and Miles, 1986). If this is the case, then artificially altering the full-field image motion impinging on the retina immediately after micro-saccades, to simulate larger than usual retinal-image slip, should tap into the

same putative “microsaccade-activated” field-holding reflex. This would in turn become reflected in subsequent reflexive eye movements that attempt to stabilize the retinal image of the now artificially generated full-field motion. We tested this hypothesis explicitly by designing a task that probed low-level motion sensitivity in the visual system immediately after microsaccades. The task relied on a stimulus like that shown in Figure 6A, consisting of a low-frequency, full-field sine wave grating (Sheliga et al., 2008; Quaia et al., 2012). Whenever we detected a microsaccade during fixation, we triggered a horizontal motion of this sine wave grating either during the movement itself or at different times after it (see Materials and Methods). Such horizontal full-field image motion is known to drive an ultrashort-latency ocular following response (Miles et al., 1986; Gellman et al., 1990; Matsuura et al., 2008; Sheliga et al., 2008; Masson and Perrinet, 2012), which is thought to reflect motion responses in the early visual system (Quaia et al., 2012). Our goal was to find out whether such a response can be modulated by antecedent microsaccades.

Full-field horizontal image motion resulted in a short-latency ocular following response without any microsaccades, as is expected from prior work (Miles et al., 1986). We first confirmed the presence of ocular following responses in our monkeys by analyzing the eye velocity in response to full-field image motion whenever this motion started after at least 213 ms from the end of any previous microsaccades. Figure 6B shows the average eye velocity for all trials in which this was the case from one of our monkeys (N). As can be seen, radial eye velocity was stable for several tens of milliseconds before the full-field motion onset. However, starting ~80 ms after motion onset, there was an initial increase in eye velocity in response to the motion (arrow) (note that there was an even earlier bump in eye velocity at ~50 ms, but we elected to analyze the slightly later increase to avoid any possible contamination by eye tracker noise). This initial increase represents a rapid image-stabilizing reflex by the visual system (Miles et al., 1986), and it reflects pooling of early motion signals to drive the eye in the same direction as the motion (Masson and Perrinet, 2012), and thus effectively reduce the motion’s slip on the retina.

If microsaccades do indeed cause faster than usual retinal-image slip after their end (Figs. 1–5), then one might expect that these eye movements would activate a field-holding reflex to quickly stabilize such slip, just like larger saccades do (Kawano and Miles, 1986). We thus asked whether the basic ocular following reflex in Figure 6B was in any way modulated by microsaccades. To do this, we plotted radial eye velocity in the same manner as in Figure 6B, but now for only the trials in which the motion of the sine wave grating started within a specific time interval relative to microsaccade end. An example of one such interval is shown in Figure 6C, in which we only considered all the trials with the motion starting immediately upon microsaccade detection (i.e., the motion started during a microsaccade) (black

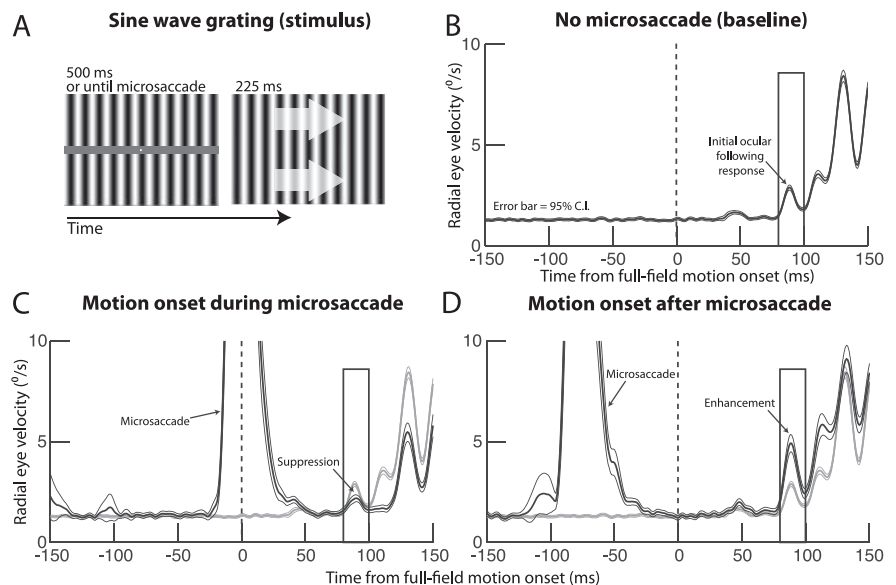


**Figure 6.** Testing the influence of microsaccades on early visual motion processing. **A**, Our ocular following paradigm aimed to simulate full-field retinal-image motion at different times relative to microsaccades. Monkeys first fixated a stationary stimulus consisting of a fixation point and a vertical sine wave grating (left). After steady fixation, we enabled a process to detect microsaccades, and we triggered a horizontal (rightward or leftward) motion of the grating at different times relative to microsaccade detection (right; the arrows are just an illustration of grating motion and were not actually visible). **B**, Average radial eye velocity of one monkey (N) aligned on motion onset of the grating. Full-field image motion elicited a short-latency increase in radial eye velocity. We analyzed the peak of the initial upswing of this velocity (in the shown rectangular analysis window) as our “open-loop” response. **C**, Same analysis as in **B** but for the case in which the motion was triggered during microsaccades (black curve; note the upswing in average eye velocity around motion onset, corresponding to the velocity of the triggering microsaccades). Compared with the baseline with no microsaccades (gray curve; identical to that in **B**), there was a strong and long-lasting suppression of the initial ocular following response (arrow labeled suppression). **D**, When the image motion was started ~50 ms after the end of a microsaccade (black curve), the initial ocular following response was greatly enhanced. Error bars in all plots indicate 95% confidence intervals.

curve). For comparison, we show in the same figure the ocular velocity after motion onset when no microsaccades occurred (gray curve; which is an identical copy of the curve in Fig. 6B but placed here to facilitate comparison). As can be seen, whenever the motion onset started during microsaccades, the subsequent ocular following responses were dramatically suppressed, and for a prolonged period of time. This is consistent with the detrimental visual effects of rapid eye movements, and the possible involvement of active suppressive mechanisms associated with these movements (Hafed and Krauzlis, 2010). However, when we repeated the same analysis but now for the trials in which the motion started within ~50 ms after microsaccade end, we found a large, almost twofold enhancement in ocular following response (Fig. 6D). Thus, full-field retinal-image motion that was presented immediately after microsaccades resulted in a much-enhanced magnitude of the image-stabilizing reflex by the oculomotor system, compared with identical full-field retinal-image motion that was presented without any antecedent microsaccades.

Similar to the postmicrosaccadic enhancement of ocular drift velocity we observed earlier (Figs. 1–4), the postmicrosaccadic enhancement of ocular following responses to full-field image motion was also time locked to movement end, and it was consistent across both monkeys. For each monkey, we analyzed the initial ocular following response (peak eye velocity in the period between 80 and 100 ms after motion onset; see Materials and Methods), and we plotted the magnitude of this response as a function of when the full-field motion started relative to microsaccade end (Fig. 7A, B). Consistent with the sample data in Fig-



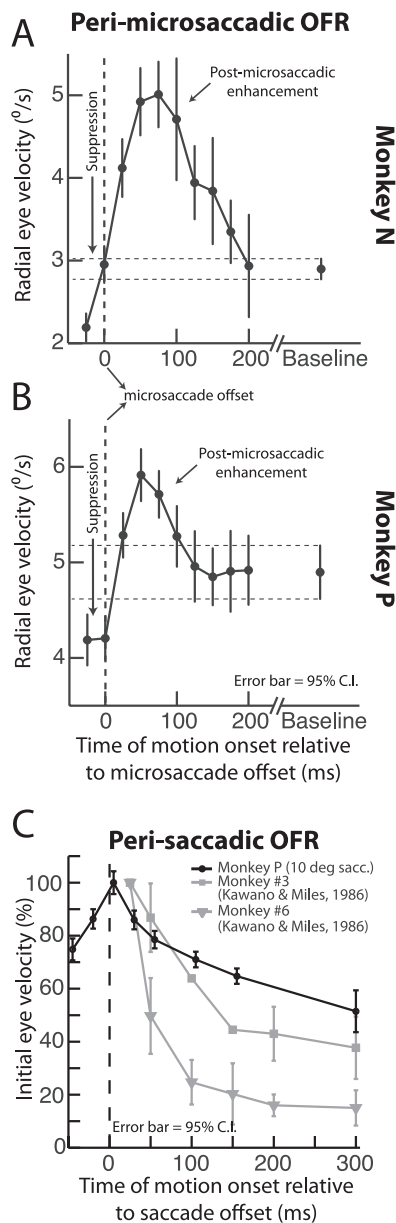


**Figure 7.** Time course of ocular following response magnitude relative to microsaccades. *A, B*, We plotted the magnitude of the initial ocular following response (see measurement box in Fig. 6*B–D* and Materials and Methods) as a function of the time of full-field motion onset relative to microsaccade end. Consistent with the sample data of Figure 6, motion onset during microsaccades was associated with a strong suppression in the ocular following response (notice the response for negative time values on the *x*-axis). However, motion onset immediately in the wake of microsaccades was associated with strong enhancement in sensitivity to the full-field motion stimulus. This enhancement was then followed by a gradual return to baseline ocular following performance. *C*, Data from monkey P (black) showing ocular following response magnitude after 10° saccades instead of microsaccades. The data are plotted in a format identical to that used classically (Kawano and Miles, 1986), to facilitate comparison to classic results. We also replicated (with permission from the publisher) representative data from two monkeys reported by Kawano and Miles (1986) to demonstrate the consistency of our results. Similar to Figure 3, large saccades exhibited a conceptually identical result to microsaccades, albeit stronger and longer lived. Note that idiosyncratic differences in time course for monkey P relative to the monkeys of Kawano and Miles (1986) likely reflect the different motion stimuli used, as well as the differences in algorithms used for detecting exact saccade end. Error bars in all panels indicate 95% confidence intervals.

ure 6*B–D*, image motion that started during microsaccades was strongly suppressed in terms of its influence on subsequent ocular following (compare the response to that without any nearby antecedent saccades; rightmost Baseline point in each panel).

However, whenever the image motion started within ~50–75 ms after microsaccade end, there was a large and significant enhancement in eye velocity compared with Baseline. This enhancement and its time course were similar to the enhancement known to happen after much larger saccades, although it was smaller in absolute magnitude, peaking at ~73% as opposed to ~100–400% for much larger saccades according to the classic literature (Kawano and Miles, 1986). We also confirmed this observation by testing monkey P using a “large-saccade” variant of the same full-field image motion task (see Materials and Methods). We found that this monkey exhibited similar postsaccadic enhancement as observed classically (Kawano and Miles, 1986), and that the peak enhancement was bigger than for microsaccades. In particular, Figure 7*C* plots this monkey’s large-saccade ocular following responses in a manner identical to that shown in (Kawano and Miles, 1986, their Fig. 2). For comparison, we also included in this figure data from two of the monkeys used in that earlier classic study. As can be seen, our monkey showed a ~100% peak magnitude postsaccadic enhancement of ocular following responses relative to ~300 ms after saccades, which is similar to some monkeys in the earlier classic study (e.g., Monkey #3) (Kawano and Miles, 1986), and which is larger than the post-microsaccadic enhancement. Thus, not only did we observe an enhancement in postmicrosaccadic ocular drift (Figs. 1–5), but we also found postmicrosaccadic enhancement in image-stabilizing ocular responses (Figs. 6, 7), which are presumed to be helpful for quickly counteracting such postmicrosaccadic drift under normal conditions. Moreover, these responses were conceptually similar to those after much larger saccades.

## Summary

In summary, our results above demonstrate two main findings. First, the transition between even the tiniest of saccades and subsequent fixation is not a discrete one, but it includes a period of short-lived enhancement of ocular drift (or retinal-image slip) that likely alters visual responses in the retina and beyond. Second, microsaccades and their postmovement drift act to modulate visual sensitivity to full-field image motion, which is presumed to normally aid the visual and oculomotor systems to rapidly stabilize the world immediately after these rapid, flick-like eye movements.

## Discussion

In this paper, we studied the characteristics of ocular drifts, and necessarily retinal-image slip, around the time of microsaccades. We found a period of enhanced retinal-image slip immediately after these movements, with no large change in such slip (either enhancement or reduction) before them. Moreover, we discovered that microsaccades also cause postmovement enhancement of early motion sensitivity, evidenced by a much more responsive ocular following response to full-field image motion when this motion starts immediately after microsaccades than when it starts without them. These results have implications on our understanding of the motor control of microsaccades, as well as their neural and perceptual consequences.

## Origins of postmicrosaccadic enhancement

Our observation of postmicrosaccadic enhancement of ocular drift is similar to classic observations of enhanced drifts immediately after much larger saccades (Figs. 1*B*, 3*B*, blue). Such classically observed postsaccadic drifts, or glissades (Weber and Daroff, 1972; Bahill et al., 1978), could either appear as backward eye position drifts opposite the saccade direction or as forward

ones. Glissades were therefore initially described as corrective movements (Weber and Daroff, 1972), perhaps even being centrally programmed. However, the exact origin of postsaccadic drifts is not entirely known, with another possibility being related to small mismatches or variability in the oculomotor drive signals generating saccades (Easter, 1973; Bahill et al., 1978). Specifically, saccadic eye velocities are achieved at the level of brainstem oculomotor neurons by a “pulse-step” motor command: a strong initial pulse of action potentials that rapidly moves the eye at saccadic velocities, and a subsequent tonic discharge (step command) that maintains the eye at the saccade endpoint (Van Gisbergen et al., 1981). According to one view of postsaccadic drifts, if there is a small mismatch between the position that the eye lands on as a result of the “pulse” command and the “desired” position specified by the “step” command, then a slow eye movement might be expected to occur until the mismatch is corrected for (Easter, 1973; Bahill et al., 1978).

Whatever the origin of postsaccadic drifts, the remarkable observation of postmovement drifts even for the smallest microsaccades suggests that a similar mechanism must be at play for these tiny eye movements. This is consistent with observations that the brainstem control of saccades and microsaccades is shared (Van Gisbergen et al., 1981; Hafed et al., 2009; Hafed, 2011; Goffart et al., 2012; Hafed and Krauzlis, 2012). This would also be consistent with the hypothesis that microsaccades can cause a “gain change” in early motion processing as we saw in our data for the ocular following task (Figs. 6, 7), because larger saccades are also known to increase the gain of visuomotor transformations for ocular following (Kawano and Miles, 1986) (Fig. 7C) and smooth pursuit (Lisberger, 1998). Under normal circumstances, such a gain change is useful because it would allow the visual system to quickly stabilize gaze in the face of full-field image motion caused by postmicrosaccadic (and postsaccadic) drift.

#### Are microsaccades triggered by reduced retinal-image slip?

Regardless of what causes postmicrosaccadic (and postsaccadic) enhancement of ocular drift, our results also clarify an important question about what triggers microsaccades. Specifically, and using two different analysis approaches, we found no reductions in retinal-image slip, and for an extended period of up to 400–500 ms before microsaccade onset (Figs. 3, 4). This is in direct contrast to an earlier result arguing that microsaccades are triggered by low retinal-image slip (Engbert and Mergenthaler, 2006; Engbert et al., 2011), but it is in agreement with later experiments that directly manipulated image visibility and found that microsaccades are not necessarily triggered by image fading (which would be the expected perceptual consequence of reduced retinal-image slip) (Poletti and Rucci, 2010).

We think that our results are different from those by (Engbert and Mergenthaler, 2006) because these authors used a video-based eye tracker (tracking pupil position in a video image), whereas we used scleral search coils in both monkeys for this sensitive analysis. Video-based eye trackers that measure pupil position are susceptible to small position artifacts due to changes in pupil diameter (Wyatt, 2010; Kimmel et al., 2012). In fact, when we directly re-analyzed monkey P’s video-based eye tracker data for premicrosaccadic ocular drifts as in Figure 4A, we could indeed replicate the Engbert and Mergenthaler (2006) result (Fig. 8B), suggesting an interpretational ambiguity caused by the video-based data (Kimmel et al., 2012). This re-analysis then prompted us to collect even more fixation data from monkey N, and now using simultaneous recording of the same eye with both

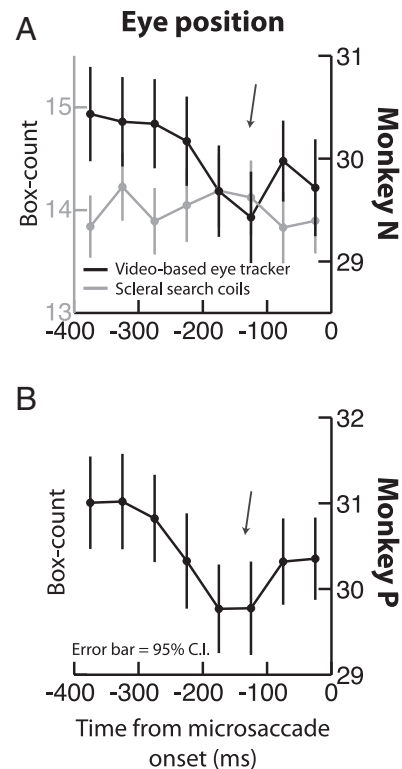


**Figure 8.** *A, B*, Premicrosaccadic ocular drifts using different eye tracking techniques. We repeated the same box counting procedure of Engbert and Mergenthaler (2006) on both monkeys, but now using the video-based eye tracker (black curves). In monkey N (*A*), we also measured the same eye simultaneously using scleral search coils (gray curve; note that the box counts for the coils are lower than those for the video-based eye tracker because coils are much less noisy). In both monkeys, the video-based data showed an apparently artifactual reduction in ocular drift  $\sim 200$  ms before microsaccade onset, replicating Engbert and Mergenthaler (2006). This reduction was not present in simultaneously measured search coil data (*A*, gray) and in all our other analyses with coils (Figs. 1–5). This discrepancy likely reflects the limitation of video-based eye tracking for measuring slow ocular drifts (Kimmel et al., 2012). All conventions are similar to Figure 4A and C.

scleral search coils and video-based eye tracking. Again, we could replicate the Engbert and Mergenthaler (2006) results in this second monkey, but only when we used the video-based tracker data (Fig. 8A, black); no reduction in premicrosaccadic retinal-image slip could be detected in the simultaneously recorded scleral search coil data (Fig. 8A, gray), consistent with our earlier results (Fig. 4). We therefore conclude that microsaccades are not necessarily triggered by reductions in retinal-image slip, consistent with other studies that directly tested the relationships between visual percepts of fading and microsaccades (Poletti and Rucci, 2010). This conclusion adds to the currently emerging picture of a decidedly varied and complex role of microsaccades in vision (Hafed et al., 2009, 2011; Rolfs, 2009; Hafed and Krauzlis, 2010; Ko et al., 2010; Kuang et al., 2012; McCamy et al., 2012; Hafed, 2013).

#### Perceptual consequences of microsaccades

Our results do indicate, however, that microsaccades indeed have perceptual consequences regardless of how they get triggered. In addition to the expected alteration of retinal images caused by microsaccades shifting the line of sight from one point in foveal space to another, our results indicate that retinal images are significantly modulated after microsaccades. This has implications on interpreting some neural and perceptual phenomena attrib-

uted to microsaccades, because it indicates that the visual system experiences faster full-field image motion after microsaccades than otherwise. For example, there have been some conflicting observations about the neural consequences of microsaccades in the primary visual cortex (V1), with some studies emphasizing bursting after microsaccades (Martinez-Conde et al., 2000) and others reporting more varied responses (Kagan et al., 2008). Similar discrepancies have also been observed in extrastriate area V4 (Leopold and Logothetis, 1998; Bosman et al., 2009). Since the retinal-image motions associated with ocular drift can affect all of these early visual areas, our results may reconcile some of these discrepancies. For example, it could be the case that if responses in V1 are aligned on microsaccade end, some of the varied response patterns observed in (Kagan et al., 2008) can be explained by whether ocular drift moves images in preferred or nonpreferred neuronal directions.

Our results can also clarify the contribution of microsaccades to some perceptual phenomena. For example, the “rotating snakes” illusion is a motion illusion that has been hypothesized to be triggered by slow eye movements (Murakami et al., 2006). More recently, however, an additional contribution of microsaccades, and even blinks, was also demonstrated (Otero-Millan et al., 2012). Since our results show that enhanced slow eye movements follow microsaccades anyway, these results support a functional link between the two interpretations.

### Implications for active vision

Finally, our results suggest that studies of active vision in the broader context, beyond just microsaccades, need to consider postsaccadic drifts in eye position and their potential contributions to altering neural and behavioral data. For example, neurons in area MST, which is implicated in mediating postsaccadic enhancement of ocular following (Takemura and Kawano, 2006; Ibbotson et al., 2007) (and presumably the postmicrosaccadic enhancement that we observed here), exhibit increases in spontaneous activity immediately after saccades, and particularly under well lit conditions (Ibbotson et al., 2008). These increases could reflect postsaccadic drifts that move the visual world over the receptive fields of these neurons. In fact, our observation of both postmicrosaccadic enhancement of ocular drift and postmicrosaccadic enhancement of ocular following responses suggest that under natural conditions, eye movements have the majority of the impact on neural processing in the visual brain. Specifically, the combination of postsaccadic enhancement as well as active extraretinal mechanisms associated with eye movements (including microsaccades), such as saccadic suppression (Diamond et al., 2000; Hafed and Krauzlis, 2010), saccadic compression (Ross et al., 1997; Hafed, 2013), and postsaccadic enhancement of motion sensitivity, suggests that the mere generation of a rapid eye movement can result in altered responses in the visual system for up to 250–300 ms around each movement. Given that eye movements can take place approximately three times a second, this suggests that perception is essentially under a constant influence of the retinal and extraretinal processes associated with moving the eye. If one also considers the constant perpetual drift that never ceases to occur between saccades, as well as the remarkable influence it might have on image statistics impinging on the retina (Kuang et al., 2012), one is compelled to consider the role of eye movements in any study associated with visual perception. Adopting such a view to research on “active” vision can be tremendously helpful for fully understanding visual function under natural conditions.

### References

- Bahill AT, Hsu FK, Stark L (1978) Glissadic overshoots are due to pulse width errors. *Arch Neurol* 35:138–142. [CrossRef Medline](#)
- Bair W, O’Keefe LP (1998) The influence of fixational eye movements on the response of neurons in area MT of the macaque. *Vis Neurosci* 15:779–786. [Medline](#)
- Barlow HB (1952) Eye movements during fixation. *J Physiol* 116:290–306. [Medline](#)
- Bosman CA, Womelsdorf T, Desimone R, Fries P (2009) A microsaccadic rhythm modulates gamma-band synchronization and behavior. *J Neurosci* 29:9471–9480. [CrossRef Medline](#)
- Boström KJ, Warzecha AK (2009) Ocular following response to sampled motion. *Vision Res* 49:1693–1701. [CrossRef Medline](#)
- Brainard DH (1997) The Psychophysics Toolbox. *Spat Vis* 10:433–436. [CrossRef Medline](#)
- Bremmer F, Kubischik M, Hoffmann KP, Krekelberg B (2009) Neural dynamics of saccadic suppression. *J Neurosci* 29:12374–12383. [CrossRef Medline](#)
- Cherici C, Kuang X, Poletti M, Rucci M (2012) Precision of sustained fixation in trained and untrained observers. *J Vis* 12(6):pii:31.
- Cloherly SL, Mustari MJ, Rosa MG, Ibbotson MR (2010) Effects of saccades on visual processing in primate MSTd. *Vision Res* 50:2683–2691. [CrossRef Medline](#)
- Collewijn H, Kowler E (2008) The significance of microsaccades for vision and oculomotor control. *J Vis* 8(14):20 1–21. [CrossRef Medline](#)
- Crowder NA, Price NS, Mustari MJ, Ibbotson MR (2009) Direction and contrast tuning of macaque MSTd neurons during saccades. *J Neurophysiol* 101:3100–3107. [CrossRef Medline](#)
- Deubel H, Bridgeman B (1995) Fourth Purkinje image signals reveal eye-lens deviations and retinal image distortions during saccades. *Vision Res* 35:529–538. [CrossRef Medline](#)
- Diamond MR, Ross J, Morrone MC (2000) Extraretinal control of saccadic suppression. *J Neurosci* 20:3449–3455. [Medline](#)
- Easter SS Jr (1973) A comment on the “glissade.” *Vision Res* 13:881–882.
- Engbert R, Mergenthaler K (2006) Microsaccades are triggered by low retinal image slip. *Proc Natl Acad Sci U S A* 103:7192–7197. [CrossRef Medline](#)
- Engbert R, Mergenthaler K, Sinn P, Pivovskiy A (2011) An integrated model of fixational eye movements and microsaccades. *Proc Natl Acad Sci U S A* 108:E765–E770. [CrossRef Medline](#)
- Fuchs AF, Robinson DA (1966) A method for measuring horizontal and vertical eye movement chronically in the monkey. *J Appl Physiol* 21:1068–1070. [Medline](#)
- Gellman RS, Carl JR, Miles FA (1990) Short latency ocular-following responses in man. *Vis Neurosci* 5:107–122. [CrossRef Medline](#)
- Goffart L, Hafed ZM, Krauzlis RJ (2012) Visual fixation as equilibrium: evidence from superior colliculus inactivation. *J Neurosci* 32:10627–10636. [CrossRef Medline](#)
- Hafed ZM (2011) Mechanisms for generating and compensating for the smallest possible saccades. *Eur J Neurosci* 33:2101–2113. [CrossRef Medline](#)
- Hafed ZM (2013) Alteration of visual perception prior to microsaccades. *Neuron* 77:775–786. [CrossRef](#)
- Hafed ZM, Clark JJ (2002) Microsaccades as an overt measure of covert attention shifts. *Vision Res* 42:2533–2545. [CrossRef Medline](#)
- Hafed ZM, Krauzlis RJ (2010) Microsaccadic suppression of visual bursts in the primate superior colliculus. *J Neurosci* 30:9542–9547. [Medline](#)
- Hafed ZM, Krauzlis RJ (2012) Similarity of superior colliculus involvement in microsaccade and saccade generation. *J Neurophysiol* 107:1904–1916. [CrossRef Medline](#)
- Hafed ZM, Goffart L, Krauzlis RJ (2009) A neural mechanism for microsaccade generation in the primate superior colliculus. *Science* 323:940–943. [CrossRef Medline](#)
- Hafed ZM, Lovejoy LP, Krauzlis RJ (2011) Modulation of microsaccades in monkey during a covert visual attention task. *J Neurosci* 31:15219–15230. [CrossRef Medline](#)
- Hafed ZM, Lovejoy LP, Krauzlis RJ (2013) Superior colliculus inactivation alters the relationship between covert visual attention and microsaccades. *Eur J Neurosci*. Advance online publication. Retrieved Jan. 21, 2013. doi: 10.1111/ejn.12127. [CrossRef](#)
- Herrington TM, Masse NY, Hachmeh KJ, Smith JE, Assad JA, Cook EP (2009) The effect of microsaccades on the correlation between neural

- activity and behavior in middle temporal, ventral intraparietal, and lateral intraparietal areas. *J Neurosci* 29:5793–5805. [CrossRef Medline](#)
- Ibbotson MR, Price NS, Crowder NA, Ono S, Mustari MJ (2007) Enhanced motion sensitivity follows saccadic suppression in the superior temporal sulcus of the macaque cortex. *Cereb Cortex* 17:1129–1138. [Medline](#)
- Ibbotson MR, Crowder NA, Cloherty SL, Price NS, Mustari MJ (2008) Saccadic modulation of neural responses: possible roles in saccadic suppression, enhancement, and time compression. *J Neurosci* 28:10952–10960. [CrossRef Medline](#)
- Janabi-Sharifi F, Hayward V, Chen C-SJ (2000) Discrete-time adaptive windowing for velocity estimation. *IEEE Trans Control Sys Tech* 8:1003–1009. [CrossRef](#)
- Judge SJ, Richmond BJ, Chu FC (1980) Implantation of magnetic search coils for measurement of eye position: an improved method. *Vision Res* 20:535–538. [CrossRef Medline](#)
- Kagan I, Gur M, Snodderly DM (2008) Saccades and drifts differentially modulate neuronal activity in V1: effects of retinal image motion, position, and extraretinal influences. *J Vis* 8(14):19–25. [CrossRef Medline](#)
- Kawano K, Miles FA (1986) Short-latency ocular following responses of monkey. II. Dependence on a prior saccadic eye movement. *J Neurophysiol* 56:1355–1380. [Medline](#)
- Kimmel DL, Mammo D, Newsome WT (2012) Tracking the eye non-invasively: simultaneous comparison of the scleral search coil and optical tracking techniques in the macaque monkey. *Front Behav Neurosci* 6:49. [Medline](#)
- Ko HK, Poletti M, Rucci M (2010) Microsaccades precisely relocate gaze in a high visual acuity task. *Nat Neurosci* 13:1549–1553. [CrossRef Medline](#)
- Krauzlis RJ, Miles FA (1996) Release of fixation for pursuit and saccades in humans: evidence for shared inputs acting on different neural substrates. *J Neurophysiol* 76:2822–2833. [Medline](#)
- Kuang X, Poletti M, Victor JD, Rucci M (2012) Temporal encoding of spatial information during active visual fixation. *Curr Biol* 22:510–514. [CrossRef Medline](#)
- Leopold DA, Logothetis NK (1998) Microsaccades differentially modulate neural activity in the striate and extrastriate visual cortex. *Exp Brain Res* 123:341–345. [CrossRef Medline](#)
- Lisberger SG (1998) Postsaccadic enhancement of initiation of smooth pursuit eye movements in monkeys. *J Neurophysiol* 79:1918–1930. [Medline](#)
- Lovejoy LP, Krauzlis RJ (2010) Inactivation of primate superior colliculus impairs covert selection of signals for perceptual judgments. *Nat Neurosci* 13:261–266. [CrossRef Medline](#)
- Martinez-Conde S, Macknik SL, Hubel DH (2000) Microsaccadic eye movements and firing of single cells in the striate cortex of macaque monkeys. *Nat Neurosci* 3:251–258. [CrossRef Medline](#)
- Martinez-Conde S, Macknik SL, Hubel DH (2002) The function of bursts of spikes during visual fixation in the awake primate lateral geniculate nucleus and primary visual cortex. *Proc Natl Acad Sci U S A* 99:13920–13925. [CrossRef Medline](#)
- Masson GS, Perrinet LU (2012) The behavioral receptive field underlying motion integration for primate tracking eye movements. *Neurosci Biobehav Rev* 36:1–25. [CrossRef Medline](#)
- Matsuura K, Miura K, Taki M, Tabata H, Inaba N, Kawano K, Miles FA (2008) Ocular following responses of monkeys to the competing motions of two sinusoidal gratings. *Neurosci Res* 61:56–69. [CrossRef Medline](#)
- McCamy MB, Otero-Millan J, Macknik SL, Yang Y, Troncoso XG, Baer SM, Crook SM, Martinez-Conde S (2012) Microsaccadic efficacy and contribution to foveal and peripheral vision. *J Neurosci* 32:9194–9204. [CrossRef Medline](#)
- Miles FA, Kawano K, Optican LM (1986) Short-latency ocular following responses of monkey. I. Dependence on temporospatial properties of visual input. *J Neurophysiol* 56:1321–1354. [Medline](#)
- Murakami I, Kitaoka A, Ashida H (2006) A positive correlation between fixation instability and the strength of illusory motion in a static display. *Vision Res* 46:2421–2431. [CrossRef Medline](#)
- Otero-Millan J, Macknik SL, Martinez-Conde S (2012) Microsaccades and blinks trigger illusory rotation in the “rotating snakes” illusion. *J Neurosci* 32:6043–6051. [CrossRef Medline](#)
- Pelli DG (1997) The VideoToolbox software for visual psychophysics: transforming numbers into movies. *Spat Vis* 10:437–442. [CrossRef Medline](#)
- Poletti M, Rucci M (2010) Eye movements under various conditions of image fading. *J Vis* 10(3):6–18. [CrossRef Medline](#)
- Quaia C, Sheliga BM, Fitzgibbon EJ, Optican LM (2012) Ocular following in humans: spatial properties. *J Vis* 12(4) pii:13. [CrossRef Medline](#)
- Rajkai C, Lakatos P, Chen CM, Pincze Z, Karmos G, Schroeder CE (2008) Transient cortical excitation at the onset of visual fixation. *Cereb Cortex* 18:200–209. [Medline](#)
- Reppas JB, Usrey WM, Reid RC (2002) Saccadic eye movements modulate visual responses in the lateral geniculate nucleus. *Neuron* 35:961–974. [CrossRef Medline](#)
- Rolfs M (2009) Microsaccades: small steps on a long way. *Vision Res* 49:2415–2441. [CrossRef Medline](#)
- Ross J, Morrone MC, Burr DC (1997) Compression of visual space before saccades. *Nature* 386:598–601. [CrossRef Medline](#)
- Sheliga BM, Fitzgibbon EJ, Miles FA (2008) Spatial summation properties of the human ocular following response (OFR): evidence for nonlinearities due to local and global inhibitory interactions. *Vision Res* 48:1758–1776. [CrossRef Medline](#)
- Takemura A, Kawano K (2006) Neuronal responses in MST reflect the postsaccadic enhancement of short-latency ocular following responses. *Exp Brain Res* 173:174–179. [CrossRef Medline](#)
- Van Gisbergen JA, Robinson DA, Gielen S (1981) A quantitative analysis of generation of saccadic eye movements by burst neurons. *J Neurophysiol* 45:417–442. [Medline](#)
- Verheijen FJ (1961) A simple after image method demonstrating the involuntary multidirectional eye movements during fixation. *Opt Acta* 8:309–311. [CrossRef Medline](#)
- Weber RB, Daroff RB (1972) Corrective movements following refixation saccades: type and control system analysis. *Vision Res* 12:467–475. [CrossRef Medline](#)
- Wyatt HJ (2010) The human pupil and the use of video-based eyetrackers. *Vision Res* 50:1982–1988. [CrossRef Medline](#)

## **2. Neuronal response gain enhancement prior to microsaccades**

# Current Biology

## Neuronal Response Gain Enhancement prior to Microsaccades

### Highlights

- SC and FEF neurons exhibit stronger visual bursts for stimuli before microsaccades
- Suppressed visual bursts occur for stimuli after microsaccades
- The modulations are highly dependent on microsaccade direction
- Response gain enhancement is not accompanied by increased noise in representations

### Authors

Chih-Yang Chen, Alla Ignashchenkova, Peter Thier, Ziad M. Hafed

### Correspondence

ziad.m.hafed@cin.uni-tuebingen.de

### In Brief

Chen et al. show that superior colliculus (SC) and frontal eye fields (FEFs) exhibit stronger responses when visual stimuli appear immediately before tiny fixational eye movements called microsaccades. The enhancement is spatially specific and independent of behavioral tasks, showing that microsaccades can have strong impacts on neuronal activity.



# Neuronal Response Gain Enhancement prior to Microsaccades

Chih-Yang Chen,<sup>1,2,3</sup> Alla Ignashchenkova,<sup>1,3,4</sup> Peter Thier,<sup>4</sup> and Ziad M. Hafed<sup>1,3,\*</sup>

<sup>1</sup>Werner Reichardt Centre for Integrative Neuroscience, Tuebingen University, 72076 Tuebingen, Germany

<sup>2</sup>International Max Planck Graduate School of Behavioral and Neural Sciences, Tuebingen University, 72076 Tuebingen, Germany

<sup>3</sup>Animal Physiology Unit, Institute for Neurobiology, Tuebingen University, 72076 Tuebingen, Germany

<sup>4</sup>Hertie Institute for Clinical Brain Research, Tuebingen University, 72076 Tuebingen, Germany

\*Correspondence: [ziad.m.hafed@cin.uni-tuebingen.de](mailto:ziad.m.hafed@cin.uni-tuebingen.de)

<http://dx.doi.org/10.1016/j.cub.2015.06.022>

## SUMMARY

Neuronal response gain enhancement is a classic signature of the allocation of covert visual attention without eye movements. However, microsaccades continuously occur during gaze fixation. Because these tiny eye movements are preceded by motor preparatory signals well before they are triggered, it may be the case that a corollary of such signals may cause enhancement, even without attentional cueing. In six different macaque monkeys and two different brain areas previously implicated in covert visual attention (superior colliculus and frontal eye fields), we show neuronal response gain enhancement for peripheral stimuli appearing immediately before microsaccades. This enhancement occurs both during simple fixation with behaviorally irrelevant peripheral stimuli and when the stimuli are relevant for the subsequent allocation of covert visual attention. Moreover, this enhancement occurs in both purely visual neurons and visual-motor neurons, and it is replaced by suppression for stimuli appearing immediately after microsaccades. Our results suggest that there may be an obligatory link between microsaccade occurrence and peripheral selective processing, even though microsaccades can be orders of magnitude smaller than the eccentricities of peripheral stimuli. Because microsaccades occur in a repetitive manner during fixation, and because these eye movements reset neurophysiological rhythms every time they occur, our results highlight a possible mechanism through which oculomotor events may aid periodic sampling of the visual environment for the benefit of perception, even when gaze is prevented from overtly shifting. One functional consequence of such periodic sampling could be the magnification of rhythmic fluctuations of peripheral covert visual attention.

## INTRODUCTION

Covert visual attention refers to the brain's ability to selectively process behaviorally relevant stimuli [1, 2]. Such selective pro-

cessing arises through changes in stimulus representation. For example, neuronal response is enhanced if a stimulus was attended [3–12]. Concomitant reductions in variability also take place [13], and when attention deviates away from the stimulus, during inhibition of return (IOR) [2, 14, 15], suppression occurs [6, 11, 16]. These sensory modulations are signatures of selective covert visual attention.

Inherent in covert attention is a requirement to fixate. However, subliminal gaze shifts continuously occur [17–19]. Microsaccades are modulated in an automatic manner by any stimulus, whether or not attentionally relevant [19, 20]. Moreover, these eye movements are generated using similar mechanisms to larger saccades [21, 22], and they are also associated with peri-movement changes in vision, similar to those accompanying saccades [23, 24]. Given these peri-movement changes, it may be expected that at least some changes in stimulus representation during gaze fixation (for example, during attentional allocation) might be time locked to microsaccades, reflecting peri-movement changes. It might also be the case that these changes share characteristics with changes observed when attentional allocation is instructed. For example, if microsaccade-related preparatory activity in the superior colliculus (SC) [21] were to provide a “gain” modulation signal for visually evoked neuronal activity [24], similar to how it might do with large saccades [25–30], then response enhancement could potentially be observed for stimuli appearing before microsaccades, independent of whether a task involved attention. Thus, response enhancement, an attentional signature, can also occur in tight synchrony with individual microsaccades. Starting from this hypothesis, using behavioral and computational studies, we recently found that spatial attentional performance was modulated peri-microsaccadically [19, 24]; the largest attentional effects occurred when targets appeared around microsaccades, during a period in which visual perception is altered [24]. Here, we investigated possible neuronal correlates of these findings.

We describe robust response enhancement if stimuli appear before microsaccades, independent of whether or not an attentional task is used. Moreover, there is often sustained activity elevation, similar to sustained attentional modulations [5]. Finally, such enhancement is not associated with increased neuronal variability, but rather decreased variability in some cases. Thus, pre-microsaccadic alterations in visual representations both contribute to and modulate neuronal signatures of covert attention. While these results have strong implications on the interpretation of a large body of literature [24], they do not deny the concept of attention. Instead, they uncover a tight temporal

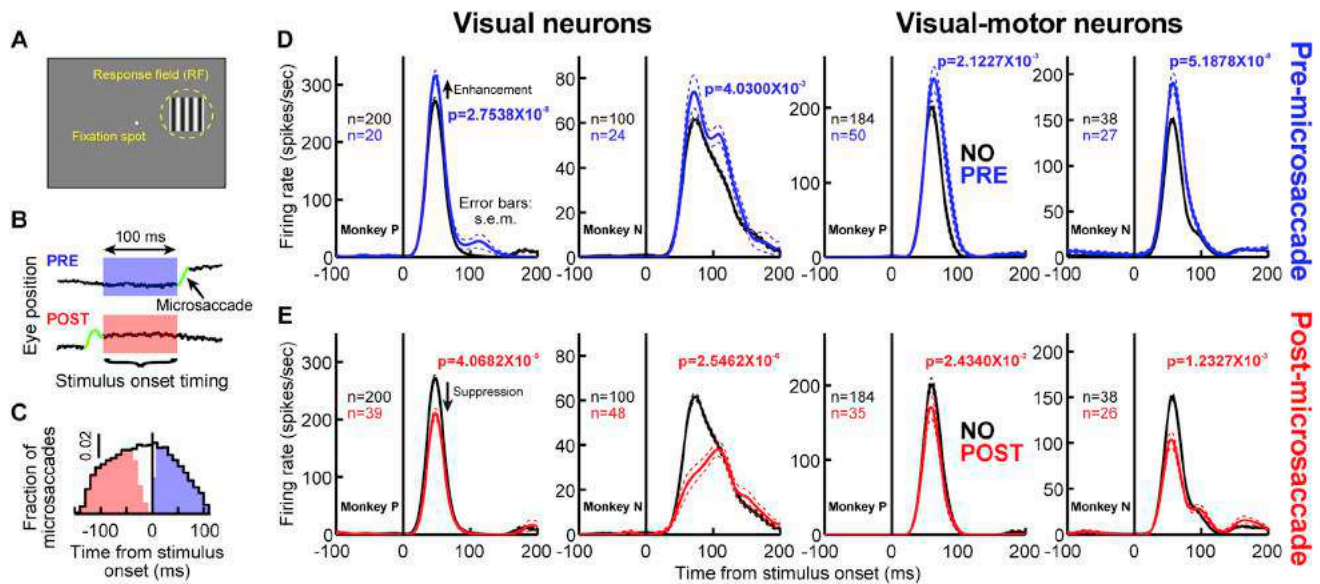


**Figure 1. Pre-microsaccadic Response Gain Enhancement**

(A) Monkeys fixated on a spot, and a sine wave grating appeared inside a neuron's response field (RF).

(B) Our analysis approach is as follows: if the grating appeared  $<100$  ms before microsaccade onset, the trial had a pre-microsaccadic stimulus (pre); if it appeared  $<100$  ms after microsaccade end, it was a post-microsaccade trial (post). "Baseline" trials had no microsaccades  $\pm 100$  ms from the grating onset.

(C) Across all trials and sessions, microsaccades occurred around stimulus onset, allowing us to explore pre- and post-microsaccadic modulations. Red denotes microsaccades in which the stimulus appeared after microsaccade end (post); blue denotes microsaccades with stimuli appearing before microsaccade onset (pre). We did not include trials with stimulus onset during microsaccades (unshaded region).

(D) Four sample superior colliculus (SC) neurons (two from each monkey), in which responses were enhanced for stimuli appearing before microsaccades directed toward their hemifield. Black curves show no-microsaccade responses; blue curves show enhanced responses for pre-microsaccadic stimuli (t test; p values and numbers of trials are shown in the figure; [Experimental Procedures](#)).

(E) The same neurons were suppressed on post-microsaccade trials. This figure shows responses to 80% contrast. [Figure 5](#) shows results from full contrast sensitivity curves. Error bars denote SEM.

relationship between attentional effects and individual microsaccades. Thus, even during fixation, perception is periodically interjected with momentary increases or decreases in visual sensitivity, which are time locked to individual microsaccades, and which will not only affect attentional performance [24] but also generally influence perception [24, 31] and action [23].

## RESULTS

### Response Enhancement for Stimuli before Microsaccades

We first describe results from two monkeys, P and N, performing a pure fixation task. After fixating on a spot for 400–550 ms, the spot transiently dimmed for 50 ms, which reset microsaccadic rhythms [19] without inducing a spatial bias in microsaccades. After 110–320 ms, a vertical sine wave grating (2.22 cycles/°) appeared for 300 ms within a neuron's response field (RF) ([Figure 1A](#)). Monkeys were rewarded only for maintaining fixation, and we investigated how grating-induced visual responses were modulated around microsaccades ([Figure 1B](#)): we analyzed response strength when the grating appeared without any microsaccades within  $\pm 100$  ms from stimulus onset or when it appeared  $<100$  ms before (blue) or after (red) microsaccades. Across all trials, microsaccades occurred at different times relative to stimulus onset ([Figure 1C](#)), allowing us to map the time course of peri-microsaccadic changes in neuronal activity.

Visually responsive SC neurons showed enhanced responses for stimuli appearing before microsaccades, even though these microsaccades never placed the monkey's gaze at the stimuli. [Figure 1D](#) shows the activity of four example neurons and demonstrates such enhancement for a high-contrast (80%) grating. When the grating appeared  $<100$  ms before a microsaccade directed toward its hemifield (blue), enhancement occurred, similar to SC enhancement in covert attention tasks [6, 7, 9, 11, 29], but we observed it merely during fixation.

Response enhancement was restricted to pre-movement intervals. If the same stimulus appeared  $<100$  ms after microsaccades, suppression occurred ([Figure 1E](#), red), analogous to microsaccadic suppression [23]. Thus, both visual and visual-motor SC neurons showed pre-microsaccadic enhancement and post-microsaccadic suppression, consistent with behavioral evidence [24] and reminiscent of SC neuronal response gain changes during covert attention [6, 7, 9, 11, 16, 29].

Across the population, we computed a modulation index normalizing activity on trials with microsaccades to activity on trials without. [Figure 2A](#) plots this index for all visual neurons as a function of their preferred eccentricity. For stimulus onsets  $<100$  ms before microsaccades, there was  $\sim 15\%$  (median) enhancement ([Figure 2A](#), blue histogram;  $p = 2.3 \times 10^{-5}$ , paired signed-rank test); 18/31 (58%) neurons were individually significant ( $p < 0.05$ ). For stimulus onsets  $<100$  ms after microsaccades ([Figure 2C](#), red),  $\sim 2.4\%$  (median) suppression occurred



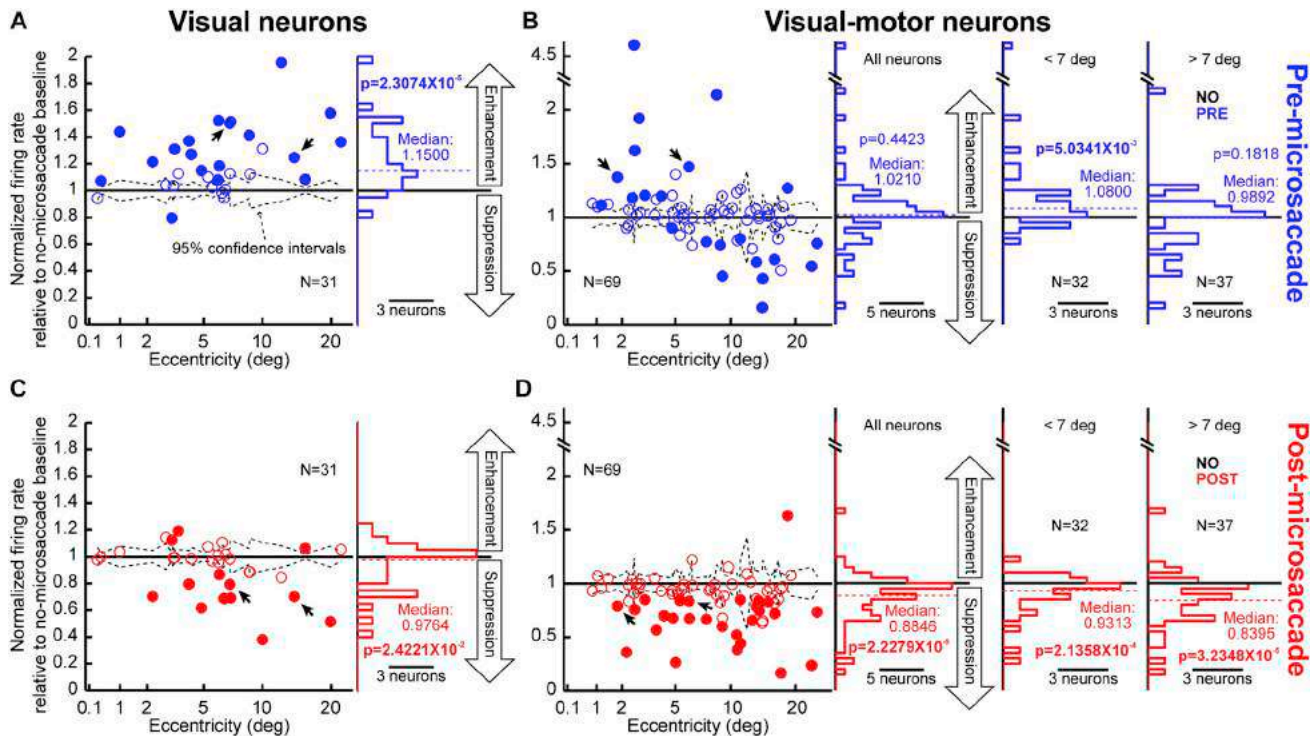


**Figure 2. SC Population Summary**

(A) Normalized activity on pre-microsaccade trials against neuronal preferred eccentricity. Eccentricity is plotted on a logarithmic scale representing SC topography (Experimental Procedures). Points above one are neurons with enhanced responses. Filled symbols indicate significant modulations ( $p < 0.05$ ; t test; Experimental Procedures). Dashed lines around one are 95% confidence intervals for the no-microsaccade baselines computed for each neuron. The marginal histogram summarizes the population result. The two arrows point to the two-sample visual neurons of Figure 1.

(B) The same as in (A), except for visual-motor neurons. Similar observations were made, except that eccentric neurons ( $>7^\circ$ ) do not show enhancement. The marginal histograms show neuronal modulation indices for all neurons (leftmost histogram) or for either central (middle histogram) or eccentric (rightmost histogram) neurons.

(C and D) The same as in (A) and (B), except for post-microsaccade trials. Suppression occurred and was strongest for peripheral visual-motor neurons. In all panels, neuron numbers are indicated, and p values are from paired signed-rank tests (Experimental Procedures). Colored dashed lines indicate median values. See also Figures S1–S3.

( $p = 2.4 \times 10^{-2}$ , paired signed-rank test). Importantly, pre-microsaccadic enhancement occurred in neurons at all tested eccentricities; microsaccades were associated with response enhancement even for neurons at  $>20^\circ$ .

Visual-motor SC neurons behaved similarly (Figure 2B), but pre-microsaccadic enhancement was now eccentricity dependent. Neurons with RF centers  $<7^\circ$  exhibited enhancement; more eccentric neurons showed no modulation or suppression. The leftmost histogram in Figure 2B describes all neurons ( $n = 69$ ), and the middle and rightmost histograms show modulation indices for RF centers less ( $n = 32$ ) or greater ( $n = 37$ ) than  $7^\circ$ . More central neurons exhibited  $\sim 8\%$  (median) enhancement ( $p = 5 \times 10^{-3}$ , paired signed-rank test); more eccentric ones did not exhibit enhancement ( $p = 0.1818$ ). Suppression occurred for post-microsaccadic stimuli (Figure 2D).

Therefore, we found pre-microsaccadic enhancement in both visual and visual-motor SC neurons, only under simple fixation. We also checked whether the monkeys may have sustained attention at the RF location by analyzing pre-stimulus microsaccade directions. If monkeys sustained attention at that location, because of its predictability, previous work [17, 18] suggests strong microsaccade direction biases toward it. This was not

the case (Figure S1A). Moreover, if the stimulus appeared after a microsaccade (Figures 1 and 2), there was suppression; thus, the modulations were time locked to movement generation, rather than reflecting a sustained RF-directed bias. Post-stimulus microsaccades were also not affected by stimulus location (Figure S1B), consistent with their short onset times (Figure 1C) and suggesting that they were not visually triggered by the grating.

Our results are also not due to peri-microsaccadic modulations, either in the absence (Figure S2A) or presence (Figure S2B) of RF stimuli, and they still occurred with brief RF stimuli (Figure S2C). We also confirmed that our results are not due to displacements of stimuli by microsaccades relative to RF centers (Figure S3). Finally, no stimulus-foveating saccades occurred. Microsaccade amplitude was  $<0.25\times$  the nearest stimulus eccentricity and much more often  $>10\times$  smaller.

#### Dependence on Microsaccade Direction

We asked whether microsaccade direction relative to the RF matters, as predicted recently [24]. We plotted (Figures 3A and 3B) each neuron's response if a stimulus appeared before a microsaccade toward (y axis) or away from (x axis) the stimulus

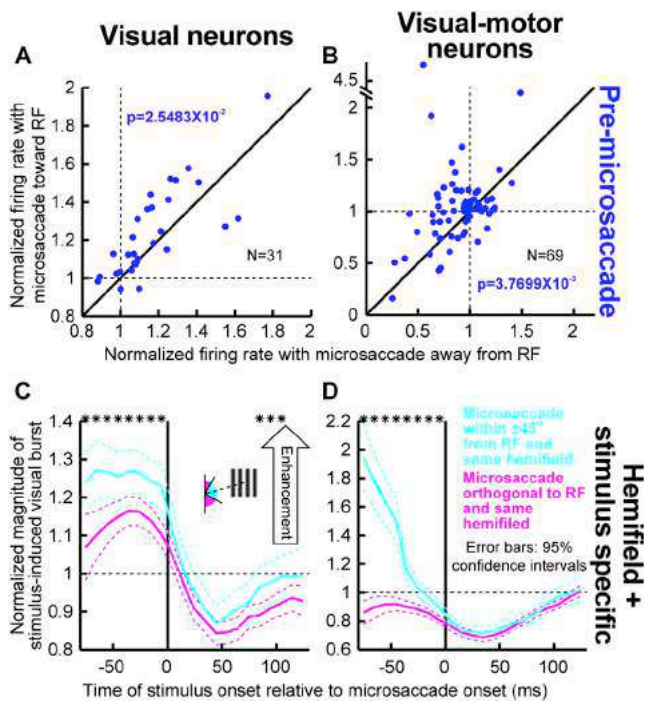


**Figure 3. Differential Influence of Microsaccade Direction on Pre-microsaccadic Enhancement in the SC**

(A and B) Normalized firing rate (relative to no-microsaccade baselines) on trials with a stimulus before a microsaccade toward the hemifield (y axis) of the stimulus versus the opposite (x axis) is shown. For pure visual neurons (A), even though opposite trials still showed enhancement (x axis points above one), the enhancement was stronger if the microsaccade was toward the hemifield of the stimulus. This effect was even stronger for visual-motor neurons (B), which often showed suppression before “opposite” microsaccades (x axis points below one) but enhancement before “toward” movements (y axis points above one). p values are from paired signed-rank tests.

(C and D) Time courses of peri-microsaccadic response modulation. Both visual (C) and visual-motor (D) neurons show pre-microsaccadic enhancement, which was strongest for microsaccades within  $<45^\circ$  in direction relative to the RF stimulus location. Notice how for visual-motor neurons (D), even movements within the same hemifield but orthogonal to the stimulus location exhibited pre-microsaccadic suppression (magenta). Thus, pre-microsaccadic enhancement (in both visual and visual-motor neurons) was best for microsaccades specifically “pointing” toward the stimulus location. Asterisks illustrate times with a significant difference between toward and “away” ( $p < 0.05$ ). The icon in (C) indicates the analysis logic: we considered all microsaccades toward (cyan) the hemifield of the grating and within  $<45^\circ$  in direction from grating location, and we compared them to microsaccades within the same hemifield but pointing “away” from the grating location (magenta). Error bars in (C) and (D) denote 95% confidence intervals. See also Figure S4.

hemifield. For visual neurons, microsaccades toward were associated with stronger enhancement than microsaccades opposite (Figure 3A;  $p = 2.5 \times 10^{-2}$ , paired signed-rank test), even though opposite trials still showed enhancement (x axis points lying above one). Visual-motor neurons showed an even stronger directional effect: there was suppression before opposite microsaccades (x axis points lying below one) but enhancement toward (y axis points lying above one) (Figure 3B;  $p = 3.8 \times 10^{-3}$ , paired signed-rank test). Thus, an upcoming microsaccade was associated with sensitization of visual responses to

stimuli in the same direction, but weaker sensitization or suppression opposite. These results are reminiscent of direction-dependent pre-microsaccadic behavioral effects [24].

The full time course of response modulation further demonstrated direction dependence. We measured responses as a function of when stimuli appeared relative to microsaccade onset [23], and we asked whether even movements within the same hemifield but orthogonal to the RF location had differential effects from movements specifically directed toward the RF location. There was a distinct time course of pre-microsaccadic enhancement followed by post-microsaccadic suppression, and the enhancement was always stronger (visual neurons) or only present (visual-motor neurons) for movements directed toward the stimulus (Figures 3C and 3D). Note that our time range in this analysis was dictated by having sufficient trials with a stimulus appearing within a given time window. Because stimulus onsets result in microsaccadic inhibition  $\sim 75$ – $100$  ms later [19, 20] (Figure 1C), we could not map times  $< -75$  ms. Nonetheless, the analysis sufficiently demonstrated pre-microsaccadic enhancement. Most interestingly, visual and visual-motor neurons showed qualitative differences, with visual-motor neurons showing an earlier effect. In fact, Figure S4 suggests that even visual-motor neurons at large eccentricities can still exhibit enhancement (an effect masked in Figure 2 with a less sensitive time-window analysis), indicating that visual-motor enhancement was not due to a “microsaccade-related” motor discharge restricted in the foveal SC (Figure S2A).

Thus, microsaccades were associated with spatially specific SC response enhancement. Next, we explore the generalizability of this phenomenon and describe additional corroborations of it.

### Generalizability across Tasks and Areas

In a study of the SC’s role in covert attention [7], activity was modulated after attentional cue onset. We re-analyzed 60 neurons from this study and asked whether cue-induced activity was also modulated around microsaccades. Even though these experiments were not designed to focus on microsaccades, thus not allowing individual-neuron statistics (Experimental Procedures), we still found robust population results: two additional monkeys (B and Z) showed similar pre-microsaccadic enhancement (Figures 4A and 4E, blue) and post-microsaccadic suppression (Figures 4C and 4E, red). Thus, all four monkeys, regardless of whether or not a stimulus was an attentional cue, showed enhancement.

We also ran the same task [7] using two additional monkeys (A and C), now recording in the frontal eye fields (FEFs) [10, 32, 33]. Once again, qualitatively and quantitatively similar modulations occurred (Figures 4B, 4D, and 4F), and these results were also similar when we analyzed visual and visual-motor neurons separately.

Therefore, in six monkeys and two areas implicated in attention [6, 7, 9–11, 33, 34], pre-microsaccadic enhancement occurred, and with different stimulus types (gratings versus spots). These results confirm that pre-microsaccadic enhancement can occur in attentional tasks [24].

### Changes in Contrast Sensitivity

In monkeys P and N, we also presented different contrasts. Figure 5A (left) shows contrast sensitivity curves for an example

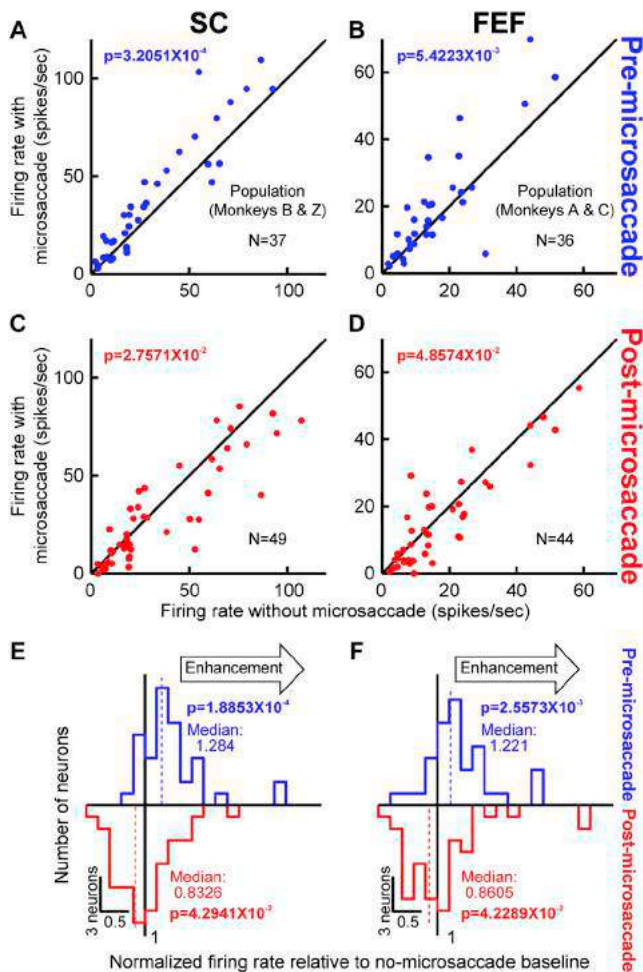


**Figure 4. Generalizability of Pre-microsaccadic Enhancement across Monkeys, Areas, and Tasks**

(A) Cue-induced SC visual bursts from a previously published [7] attentional cueing task. We plotted activity on trials with cue onset before microsaccades versus activity without microsaccades (as in Figures 1 and 2; Experimental Procedures). Across the population, significant enhancement occurred (paired signed-rank test). Thus, pre-microsaccadic SC enhancement occurred in four monkeys, in different tasks (fixation in Figures 1, 2, and 3; attentional cueing in this figure), and with different stimuli (gratings in Figures 1, 2, and 3; spots in this figure).

(B) Similar results from the same cueing task but in the FEFs and with two additional monkeys are shown. The neurons in this analysis had similar eccentricities as those in (A) and also similar proportions of visual and visual-motor neurons (Experimental Procedures).

(C and D) If the cue appeared after microsaccades, both SC and FEF neurons were suppressed.

(E and F) Neuronal modulation indices are shown in a manner similar to Figure 2, except for the data in (A)–(D). Blue histograms show pre-microsaccadic indices and demonstrate enhancement. Red histograms show post-microsaccadic indices and demonstrate suppression. All population-level statistics are from paired signed-rank tests. Only neurons that had enough measurements of both no-microsaccade and either pre- or post-microsaccade trials were included (Experimental Procedures). Colored dashed lines indicate median values.

neuron from Figure 1B. For stimuli <100 ms before microsaccades toward their hemifield (blue), the curve was scaled upward. Also in Figure 5A, the right curves show population results

(Experimental Procedures), and Figure 5B repeats this for visual-motor neurons. In all cases, whenever enhancement occurred, the multiplicative gain parameter in our psychometric curve fits (Experimental Procedures) was the parameter that was significantly altered compared to no-microsaccade psychometric curves ( $p < 0.05$ , bootstrapping). For stimuli after microsaccades, contrast sensitivity curves were scaled downward (Figures 5C and 5D). Whether pre- or post-microsaccade, there was no statistically significant shift in semi-saturation sensitivity points ( $p > 0.05$ , bootstrapping). For microsaccades opposite the stimulus, pre-microsaccadic enhancement was reduced or eliminated (Figure S5), consistent with Figure 3. Therefore, response gain enhancement for our stimuli appeared to be primarily governed by multiplicative modulation, although we acknowledge that enhancement at low contrasts was less strong in our data compared to cortical studies of attention.

### Lack of Variability Increases

If enhancement is accompanied by increased variability, readout of neuronal populations could be muddled by noise [13]. In monkeys P and N, from which we had enough data to explore this, we performed receiver operating characteristic curve (ROC) analyses, to assess whether enhancement resulted in significant discriminability of neuronal responses between no-microsaccade and microsaccade trials. Figures 6A and 6B show the area under the ROC curve for trials with 80% gratings appearing before a microsaccade toward RF hemifield. In both visual and visual-motor neurons, enhanced responses were highly discriminable from baseline (and across contrasts; Figure S6).

We also analyzed fano factor and plotted data as performed previously in the SC [35]. Figure 6C shows results from visual neurons, comparing trials with a stimulus before a microsaccade toward the RF hemifield (y axis) to trials without microsaccades (x axis). Each color represents a single contrast, and each faint dot represents data from a single neuron; dots with saturated colors summarize population results. Visual neurons showed reduced fano factors ( $p = 0.015817$ ), which was also observed previously for large saccades (albeit anecdotally) [9]. Visual-motor neurons (Figure 6D) showed no modulation.

Thus, pre-microsaccadic enhancement was accompanied by putatively equal- or higher-fidelity sensory representations. In our case, this happened without attentional tasks and demonstrated instead tight synchrony between microsaccades and altered visual representations.

### A Sustained Enhancement

Some of our SC neurons possessed sustained activity (Experimental Procedures). For these neurons in monkeys P and N, we asked whether sustained enhancement could still be observed. Figure 7A shows data from one such neuron (80% grating). For stimuli before microsaccades toward the RF hemifield, the neuron showed both burst enhancement and sustained elevation (blue; shaded region), similar to sustained elevations with attention [5]. For post-microsaccadic stimuli (Figure 7C), the effect disappeared. These observations were consistent across 30 neurons (27/100; plus three neurons recorded for this analysis) (Figures 7B, 7D, and S7), and they were again accompanied by significant ROC discriminability (Figure 7E). Moreover, fano factor analyses revealed a subtle variability

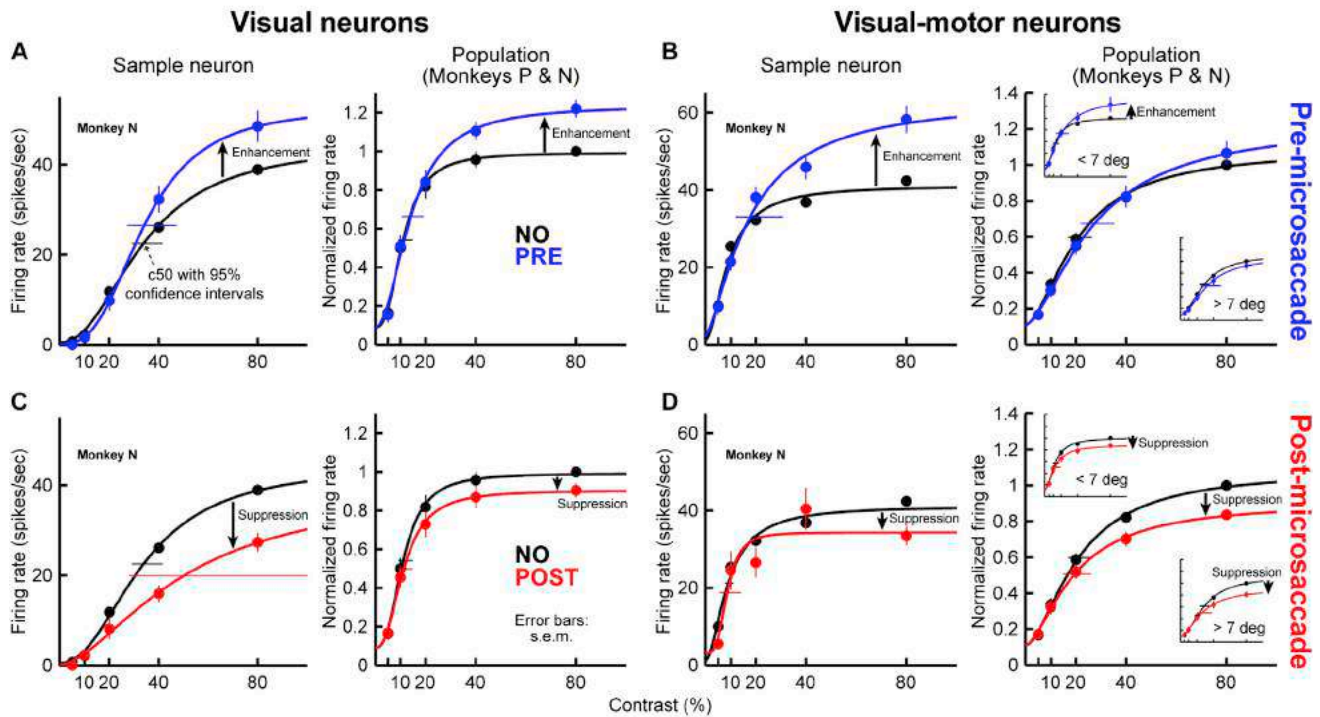


**Figure 5. SC Contrast Sensitivity Changes around Microsaccades**

(A) Left shows responses of the visual neuron of Figure 1B from monkey N. Black shows responses on no-microsaccade trials. Blue shows responses for stimuli <100 ms before a microsaccade toward the hemifield of the stimulus. Error bars denote SEM, and horizontal bars show 95% confidence intervals for the semi-saturation contrasts (c50) (Experimental Procedures). Right shows results from the population of visual neurons in monkeys P and N. Before combining neurons, each neuron's curve was normalized based on the no-microsaccade baseline curve (Experimental Procedures).

(B) The same as in (A), except for visual-motor neurons from monkeys P and N. The sample neuron shown is the visual-motor neuron of Figure 1B from monkey N. Visual-motor neurons also show enhancement, but the effect was strongest for more central neurons (insets).

(C and D) Both visual (C) and visual-motor (D) neurons show significant suppression for stimuli after microsaccades.

See also Figure S5.

decrease ( $p = 0.00143$ ) (Figure 7F). We did not have enough trials from monkeys B, Z, A, and C to repeat these analyses, but we did notice population-level evidence that cueing trials with sustained post-cue activity elevations [7] were ones with pre-microsaccadic cue onsets.

Thus, previously observed single-neuron correlates of covert attention can also be observed during simple fixation. Because microsaccades occur systematically during spatial attention tasks, this indicates that pre-microsaccadic processes may be tightly correlated with covert attentional modulations.

### Relationship to Behavior

Previous behavioral work strongly motivated our study [24]. More recently, we tested monkeys P and N on a prediction of the current data: if visual bursts are modulated on pre-microsaccade trials in a spatially specific manner (Figure 3), then reaction times (RTs) to stimuli might also be affected. We indeed found that RTs were faster if a stimulus appeared before microsaccades toward the stimulus than away from it (X. Tian, M. Yoshida, and Z.M.H., unpublished data; data not shown).

We also analyzed behavior from monkeys B, Z, A, and C. We reasoned that if cue-induced activity was modulated as we observed, then final performance might also change. We indeed

found that if the cue appeared <100 ms before a microsaccade toward its direction, performance was 80% correct; if the microsaccade was away, performance was 66.4% ( $p = 0.0185$ ;  $\chi^2$  test;  $\chi^2$  statistic: 5.5489;  $n = 143$  trials for toward and 105 trials for opposite). Performance on no-microsaccade trials was in between (73.4%). It is truly remarkable that this result was obtained at all, especially because in these attentional tasks, task difficulty was continuously adjusted from trial-to-trial [7], which likely muted our effect.

Thus, combined with these and earlier behavioral [24] and computational (X. Tian, M. Yoshida, and Z.M.H., unpublished data; data not shown) studies, our results suggest that behavioral and neuronal signatures of attention can be observed around microsaccades. Peri-microsaccadic alterations in vision, regardless of their origin, can modulate and potentially magnify [24] behavioral and neuronal signatures of covert attention.

### DISCUSSION

Because microsaccades occur systematically in attentional tasks [17–20], our results suggest that attentional modulations may be modified around microsaccades. These results do not in any way deny the concept of attention, but they highlight a

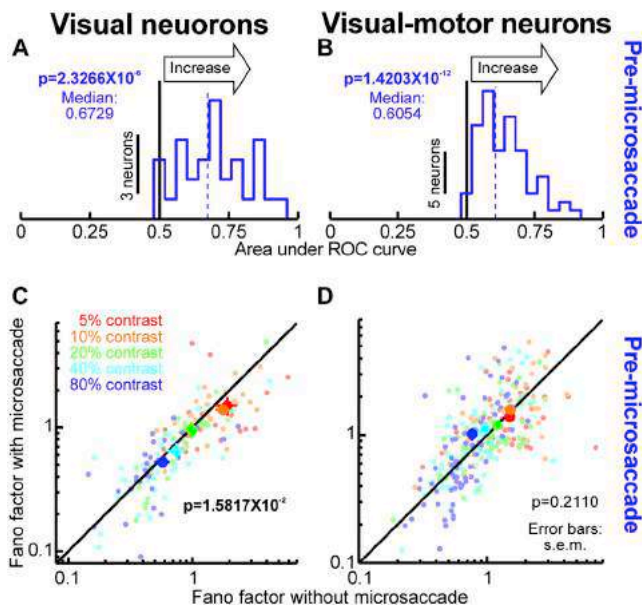


**Figure 6. SC Neuronal Discriminability and Variability with Pre-microsaccadic Stimuli**

(A) For pure visual neurons of monkeys P and N, we plotted area under the ROC curve comparing pre- and no-microsaccade trials. Values  $>0.5$  indicate above-chance discriminability. Data from 80% gratings are shown. See also Figure S6 for other contrasts and data for microsaccades opposite the RF hemifield.

(B) The same as in (A), except for visual-motor neurons.

(C and D) Fano factors on trials with and without microsaccades. Each dot shows data from a neuron, and each color denotes a single contrast. The dots with saturated colors show means (and SEM) across neurons for a given contrast. The p value shows statistical test results across all neurons and all contrasts, similar to the approach of [35]. Visual neurons show reduced fano factors when response gain was increased (for microsaccades toward the RF hemifield); visual-motor neurons show neither a reduction nor increase. All statistics are from paired signed-rank tests.

possible mechanism through which attentional effects may be magnified.

While our results do not establish causality in either direction, one possible mediator of synchrony between microsaccades and neuronal or behavioral [24] signatures of selective processing could be corollary discharge. For example, SC activity for large saccades is sent to cortex to update spatial representations [36]. Given that models of such updating invoke an oculomotor-derived “gain” signal [24, 26], our results could reflect the influence of such a signal [24]. Indeed, within the SC, an excitatory pathway from motor to sensory layers exists [37]. Interestingly, in this pathway, there is widespread influence, akin to a saccade toward one eccentricity influencing visual representations at different eccentricities. This is consistent with our observation of peripheral enhancement more eccentric than the microsaccade endpoint and also consistent with large-saccade dissociations of enhancement [9, 29].

Alternatively, or perhaps additionally, continuous brain-state fluctuations [38] likely also contribute to our results. These fluctuations happen independently of attentional task requirements and only get reset by attentional cues. Since cues reset microsaccadic rhythms [19, 39], and since microsaccades themselves

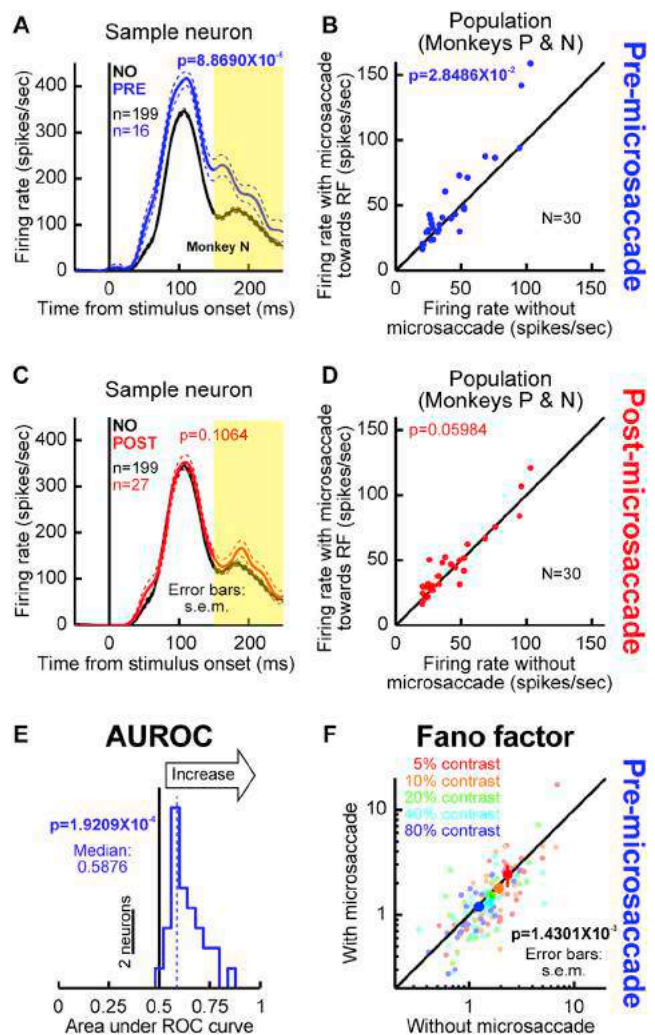


**Figure 7. A Sustained Influence of Pre-microsaccadic SC Modulations**

(A) A sample visual neuron from monkey N with 80% contrast is shown. The neuron had a sustained response (black curve, shaded region). If the stimulus appeared before a microsaccade toward its hemifield, this response was enhanced (blue) even though the microsaccade had long ended. Error bars denote SEM.

(B) Summary of sustained interval measurements from neurons with sustained activity in the no-microsaccade condition. This sustained activity was consistently enhanced for pre-microsaccadic stimuli (paired signed-rank test). (C and D) This effect disappeared when the stimulus appeared after microsaccades. See also Figure S7.

(E and F) Summaries of ROC (similar to Figures 6A and 6B) and fano factor (similar to Figures 6C and 6D) analyses performed on the sustained interval highlighted in (A). Pre-microsaccadic enhancement was accompanied by significant discriminability (ROC) and (a subtle) decreased variability (fano factor) even in the sustained response interval.

reset brain fluctuations [39] (probably through the pre- and post-motor changes we report here), synchrony between microsaccades and attentional modulations is expected [24]. Importantly, such synchrony suggests that a saccadic-rhythmicity model only employing pre-microsaccadic sensitivity changes is sufficient to generate “attentional capture” and “IOR” in Posner

cueing (X. Tian, M. Yoshida, and Z.M.H., unpublished data; data not shown). Finally, synchrony between neuronal excitability and microsaccades makes functional sense: saccades and attention are obligatorily synchronized under natural conditions, and microsaccades are a subset of saccades.

The idea of pre-motor links to attention has a rich history, with behavioral [40] and neurophysiological [25] support. Structures critical for saccades, like SC [34] and FEFs [32], are influential for attention. Our results extend these observations, suggesting that even under fixation, pre-motor modulations may contribute to neuronal and behavioral [24] modulations. In fact, microsaccades, like saccades, disrupt visual information flow. Thus, as part of a generalized perceptual stability mechanism, the brain could “attentionally sample” the world just before microsaccades. Indeed, microsaccades cause perceptual mislocalizations that are believed to be a hallmark of perceptual stability mechanisms [24]. Therefore, attention may be a general component of peri-saccadic perceptual stability [27].

Our sustained activity elevations are particularly intriguing (Figures 7 and S7). In this case, the microsaccade had long ended. This suggests that neuronal analyses of attentional modulations may miss possible influences of earlier microsaccades and that a microsaccade can have prolonged impact [24].

Equally interesting is the role of microsaccade directions. Pre-microsaccadic enhancement is spatially specific and strongest for stimuli congruent with microsaccade direction (Figure 3). We think that this effect, reminiscent of the focal nature of spatial attention, could arise because of an interaction between two signals: a gain-modulation signal that is potentially provided by corollary discharge [24, 37] and a spatially specific stimulus-induced burst. It would be interesting to further test this hypothesis with multiple simultaneous stimuli. In this case, for visual-motor SC neurons, microsaccades need to be congruent with one stimulus at a time to be associated with enhancement for each of the stimuli, reminiscent of sequential attentional sampling [38, 41]. If a pre-microsaccadic “gain” signal were to now be broadcast to visual areas at multiple hierarchies (e.g., to V1 with small RFs and V4 with larger ones), then this mechanism could also result in additional RF modulations: RF size in a higher area might appear to “shrink” around the stimulus location congruent with a microsaccade because with multiple stimuli, earlier visual areas with small RFs (each “seeing” only one of the stimuli) would either be enhanced or suppressed based on the microsaccade direction relative to its RF stimulus. This effect would then trickle toward the higher visual area, now pooling an enhanced response from one stimulus and a suppressed response from another. As for superficial SC layers, we found pre-microsaccadic enhancement regardless of microsaccade direction, albeit with direction-dependent differences (Figure 3A). Thus, a single microsaccade could subserve simultaneous enhancement, as with “divided attention.”

Finally, we observed consistent FEF modulations, which are interesting in light of the role of FEFs in attention [33]. In fact, V4 exhibits similar modulations before saccades to their modulations during attention [42], presumably mediated by FEFs. Our results add to these findings the observation that FEFs may also mediate synchrony between microsaccades and visual cortical neuronal modulations. Even when target selection oc-

curs without overt actions, covert processing may nonetheless intrinsically remain an “active perception” phenomenon.

## EXPERIMENTAL PROCEDURES

Ethics committees approved all experiments.

### Animal Preparation

Monkeys P and N (male, *Macaca mulatta*, aged 7 years) were prepared for behavior earlier [43]. We placed SC chambers on the midline, aimed at 1 mm posterior of and 15 mm above the inter-aural line. Chambers were tilted posterior of vertical (38° and 35° for P and N, respectively).

The methods used for monkeys B and Z were described earlier [7]. Monkeys A and C (C, female, aged 10 years; A, male, aged 9 years) were prepared in the same laboratory [7].

### Behavioral Tasks

Monkeys P and N fixated only. In each trial, a white spot (~8.5 × 8.5 min arc) appeared over a gray background [43]. We presented a vertical sine wave grating [30]. Grating contrast ( $L_{max} - L_{min} / L_{max} + L_{min}$ ) was 5%, 10%, 20%, 40%, or 80%, and phase was randomized. Grating size (filling the RF) was large enough to avoid a potential “micro” form of changing/shifting RFs around saccades [27, 28]. If such changes occur around microsaccades, they would be small and canceled with large stimuli.

We analyzed 103 SC neurons (1,075 ± 326 SD trials per neuron). We collected >20 no-microsaccade trials per contrast per neuron (average: 97.8 ± 68.1 SD) and >9 pre- or post-microsaccade trials (average: 21.9 ± 8.5 SD).

For monkeys B and Z, we re-analyzed data from [7], in which monkeys performed a covert spatial attention task. They fixated on a spot, while a peripheral cue appeared, followed by a landolt C at the cued location. Monkeys reported the direction of C opening.

Monkeys A and C performed the same peripheral cueing task [7], except during FEF recordings. We placed the cue inside a neuron’s RF and collected 85.7 trials ± 32.4 SD per neuron.

Before the main experiment, we classified SC neurons from monkeys P and N using saccade-related tasks. For delayed saccades [44], a spot appeared, after which time a target was presented. After 500–1,000 ms, the spot disappeared, releasing fixation. Across trials (>23; average: 136 ± 82.2 SD), we moved the target location to map visual and motor RFs. We also used a memory-guided saccade task. The target only appeared for ~50 ms. A memory interval (300–1,100 ms) then ensued before fixation was released. The monkey made a memory saccade (to within 3°) and maintained gaze for 200 ms, after which time the target re-appeared. We ran this task with saccades to the RF center (>35 trials).

Neurons from monkeys B, Z, A, and C were classified based on memory-guided saccades [7].

### Identifying SC and FEFs

We identified SC and FEFs using anatomical and physiological markers. For FEFs, during the last eight sessions from monkey C and three sessions from monkey A, we confirmed electrode locations by applying (on random trials) bipolar electrical stimulation (25 pulses at 350 Hz) to evoke short-latency saccades (38–63 ms after stimulation onset). In all experiments, we evoked saccades on >61% of stimulation trials using currents ≤40 μA [45].

### Neuron Classification

We recorded from all visually responsive SC neurons. A neuron was “visual” if activity 0–200 ms after target onset in the delayed saccade task was higher than 0–200 ms before target onset ( $p < 0.05$ , paired t test). The neuron was “visual motor” if its pre-saccadic activity (within 50 ms) was additionally elevated for either delayed or memory-guided saccades relative to an earlier interval (100–175 ms pre-saccade) [30].

We classified 60 SC neurons from monkeys B and Z in the same way, but using memory-guided saccades [7]. Using the current classification, “visuo-memory” and “visuo-motor” neurons in [7] were now visual-motor (35/60).

For FEFs, we analyzed four time windows for the location eliciting maximal visual response in memory-saccade trials: baseline (100 ms after fixation onset

to 100 ms before target onset), visual (70 ms after target onset to 70 ms after target offset), memory (100 ms after target offset to fixation-spot offset), and motor (0–200 ms after fixation-spot offset). Activity within each interval was normalized to the maximum. A neuron was visual if only visual-interval activity was >0.5. Visual-motor neurons had both visual and motor intervals >0.5. We found similar results for visual (16) and visual-motor (38) neurons and thus combined them to improve statistics. RFs had 8°–16° eccentricities (10.8 ± 2.1 SD), which was within the range tested in SC. Moreover, the relative proportions of visual and visual-motor neurons were similar to those in the SC data re-analyzed from [7]. Thus, Figure 4 data from the same laboratory [7] were comparable as much as possible.

### Data Analysis

In visual burst analyses from monkeys P and N, we measured activity 50–150 ms after grating onset. Our choice of a visual burst interval ensured measuring responses to stimulus onset, regardless of microsaccades. If a microsaccade occurred while a stimulus was on (e.g., pre-microsaccade trials), we were still measuring response to stimulus onset and not to microsaccade-induced image motion of the stimulus, because afferent delays would need to ensue after the microsaccade before image motion could influence neurons. Thus, potential re-afference would appear after our measured bursts. Moreover, we replicated our main results in some neurons with only brief stimulus flashes (Figure S2), and we also checked that microsaccade-related modulations with or without an RF stimulus were not sufficient to explain our results (Figure S2).

We compared activity with no microsaccades to activity from pre- or post-microsaccade trials using two-tailed t tests. For population summaries, we computed a modulation index normalizing activity on pre- or post-microsaccade trials to no-microsaccade trials. For Figure 2, we plotted eccentricity logarithmically using the afferent mapping of the SC [46].

For fano factors, we counted spikes in a 70-ms interval starting at 30 (visual neurons) or 40 ms (visual-motor neurons), and we normalized spike count variability by firing rate. We also created ROC curves based on firing rates from no-microsaccade and pre- or post-microsaccade trials.

Population summaries were tested using paired signed-rank tests. We performed analyses for microsaccades toward the stimulus or away from it. For time courses (Figures 3C and 3D), we used previous procedures [23].

For contrast sensitivity curves, we fit visual burst measurements to

$$f.r.(c) = R * \frac{c^n}{c50^n + c^n} + B, \quad (\text{Equation 1})$$

where  $c$  is contrast,  $R$  is a multiplicative term,  $c50$  is semi-saturation contrast,  $n$  determines curve steepness, and  $B$  is baseline activity (obtained from a 50-ms pre-stimulus interval). To obtain 95% confidence intervals for fit parameters, we used bootstrapping (1,000 bootstraps). When combining neurons, we first normalized activity to that of no-microsaccade trials with the highest contrast.

For sustained analyses (Figure 7), we analyzed activity 150–250 ms after grating onset. We only included neurons if activity 150–250 ms after 80% grating onset was >20 spikes/s on no-microsaccade trials.

For monkeys B, Z, A, and C, we computed a similar modulation index to above (Figure 4), averaging activity 30–80 ms (SC) or 60–120 ms (FEFs) after cue onset. These experiments were not originally designed for microsaccade analysis; they employed significantly fewer trials per neuron. Thus, we restricted analyses to population levels with no claims about individual neuron significance. This approach is equivalent to employing a multi-unit activity (e.g., [5]). Individual neurons were only analyzed if they had >1 trial with either pre- or post-microsaccade stimulus (average pre-stimulus: three trials; post-stimulus: five trials).

### SUPPLEMENTAL INFORMATION

Supplemental Information includes seven figures and can be found with this article online at <http://dx.doi.org/10.1016/j.cub.2015.06.022>.

### AUTHOR CONTRIBUTIONS

C.-Y.C. and Z.M.H. implemented and analyzed the SC experiments. C.-Y.C., A.I., and Z.M.H. analyzed the second SC data. A.I. and P.T. implemented the FEF experiments. A.I. analyzed the FEF data. Z.M.H. wrote the paper.

### ACKNOWLEDGMENTS

We thank P.W. Dicke for help with the FEF experiments. We were supported by the Werner Reichardt Centre for Integrative Neuroscience (CIN), which was funded through Excellence Cluster funds (EXC 307) from the German Research Association (DFG).

Received: April 8, 2015

Revised: June 1, 2015

Accepted: June 9, 2015

Published: July 16, 2015

### REFERENCES

- Egeth, H.E., and Yantis, S. (1997). Visual attention: control, representation, and time course. *Annu. Rev. Psychol.* 48, 269–297.
- Posner, M.I. (1980). Orienting of attention. *Q. J. Exp. Psychol.* 32, 3–25.
- Desimone, R., and Duncan, J. (1995). Neural mechanisms of selective visual attention. *Annu. Rev. Neurosci.* 18, 193–222.
- Reynolds, J.H., and Chelazzi, L. (2004). Attentional modulation of visual processing. *Annu. Rev. Neurosci.* 27, 611–647.
- Roelfsema, P.R., Lamme, V.A., and Spekreijse, H. (1998). Object-based attention in the primary visual cortex of the macaque monkey. *Nature* 395, 376–381.
- Fecteau, J.H., and Munoz, D.P. (2005). Correlates of capture of attention and inhibition of return across stages of visual processing. *J. Cogn. Neurosci.* 17, 1714–1727.
- Ignashchenkova, A., Dicke, P.W., Haarmeier, T., and Thier, P. (2004). Neuron-specific contribution of the superior colliculus to overt and covert shifts of attention. *Nat. Neurosci.* 7, 56–64.
- Schall, J.D. (2004). On the role of frontal eye field in guiding attention and saccades. *Vision Res.* 44, 1453–1467.
- Goldberg, M.E., and Wurtz, R.H. (1972). Activity of superior colliculus in behaving monkey. II. Effect of attention on neuronal responses. *J. Neurophysiol.* 35, 560–574.
- Wurtz, R.H., and Mohler, C.W. (1976). Enhancement of visual responses in monkey striate cortex and frontal eye fields. *J. Neurophysiol.* 39, 766–772.
- Fecteau, J.H., Bell, A.H., and Munoz, D.P. (2004). Neural correlates of the automatic and goal-driven biases in orienting spatial attention. *J. Neurophysiol.* 92, 1728–1737.
- Reynolds, J.H., and Heeger, D.J. (2009). The normalization model of attention. *Neuron* 61, 168–185.
- Mitchell, J.F., Sundberg, K.A., and Reynolds, J.H. (2007). Differential attention-dependent response modulation across cell classes in macaque visual area V4. *Neuron* 55, 131–141.
- Klein, R.M. (2000). Inhibition of return. *Trends Cogn. Sci.* 4, 138–147.
- Song, K., Meng, M., Chen, L., Zhou, K., and Luo, H. (2014). Behavioral oscillations in attention: rhythmic  $\alpha$  pulses mediated through  $\theta$  band. *J. Neurosci.* 34, 4837–4844.
- Dorris, M.C., Klein, R.M., Everling, S., and Munoz, D.P. (2002). Contribution of the primate superior colliculus to inhibition of return. *J. Cogn. Neurosci.* 14, 1256–1263.
- Hafed, Z.M., and Clark, J.J. (2002). Microsaccades as an overt measure of covert attention shifts. *Vision Res.* 42, 2533–2545.
- Engbert, R., and Kliegl, R. (2003). Microsaccades uncover the orientation of covert attention. *Vision Res.* 43, 1035–1045.
- Hafed, Z.M., and Ignashchenkova, A. (2013). On the dissociation between microsaccade rate and direction after peripheral cues: microsaccadic inhibition revisited. *J. Neurosci.* 33, 16220–16235.
- Rolfs, M., Kliegl, R., and Engbert, R. (2008). Toward a model of microsaccade generation: the case of microsaccadic inhibition. *J. Vis.* 8, 1–23.
- Hafed, Z.M., Goffart, L., and Krauzlis, R.J. (2009). A neural mechanism for microsaccade generation in the primate superior colliculus. *Science* 323, 940–943.

22. Hafed, Z.M. (2011). Mechanisms for generating and compensating for the smallest possible saccades. *Eur. J. Neurosci.* *33*, 2101–2113.
23. Hafed, Z.M., and Krauzlis, R.J. (2010). Microsaccadic suppression of visual bursts in the primate superior colliculus. *J. Neurosci.* *30*, 9542–9547.
24. Hafed, Z.M. (2013). Alteration of visual perception prior to microsaccades. *Neuron* *77*, 775–786.
25. Kustov, A.A., and Robinson, D.L. (1996). Shared neural control of attentional shifts and eye movements. *Nature* *384*, 74–77.
26. Zirnsak, M., Lappe, M., and Hamker, F.H. (2010). The spatial distribution of receptive field changes in a model of peri-saccadic perception: predictive remapping and shifts towards the saccade target. *Vision Res.* *50*, 1328–1337.
27. Zirnsak, M., and Moore, T. (2014). Saccades and shifting receptive fields: anticipating consequences or selecting targets? *Trends Cogn. Sci.* *18*, 621–628.
28. Zirnsak, M., Steinmetz, N.A., Noudoost, B., Xu, K.Z., and Moore, T. (2014). Visual space is compressed in prefrontal cortex before eye movements. *Nature* *507*, 504–507.
29. Wurtz, R.H., and Mohler, C.W. (1976). Organization of monkey superior colliculus: enhanced visual response of superficial layer cells. *J. Neurophysiol.* *39*, 745–765.
30. Li, X., and Basso, M.A. (2008). Preparing to move increases the sensitivity of superior colliculus neurons. *J. Neurosci.* *28*, 4561–4577.
31. Snodderly, D.M. (2014). A physiological perspective on fixational eye movements. *Vision Res.* S0042-6989(14)00318-6. Published online December 20, 2014. <http://dx.doi.org/10.1016/j.visres.2014.12.006>.
32. Moore, T., and Armstrong, K.M. (2003). Selective gating of visual signals by microstimulation of frontal cortex. *Nature* *421*, 370–373.
33. Squire, R.F., Noudoost, B., Schafer, R.J., and Moore, T. (2013). Prefrontal contributions to visual selective attention. *Annu. Rev. Neurosci.* *36*, 451–466.
34. Krauzlis, R.J., Lovejoy, L.P., and Zénon, A. (2013). Superior colliculus and visual spatial attention. *Annu. Rev. Neurosci.* *36*, 165–182.
35. Li, X., and Basso, M.A. (2011). Cues to move increased information in superior colliculus tuning curves. *J. Neurophysiol.* *106*, 690–703.
36. Sommer, M.A., and Wurtz, R.H. (2002). A pathway in primate brain for internal monitoring of movements. *Science* *296*, 1480–1482.
37. Ghitani, N., Bayguinov, P.O., Vokoun, C.R., McMahon, S., Jackson, M.B., and Basso, M.A. (2014). Excitatory synaptic feedback from the motor layer to the sensory layers of the superior colliculus. *J. Neurosci.* *34*, 6822–6833.
38. Busch, N.A., and VanRullen, R. (2010). Spontaneous EEG oscillations reveal periodic sampling of visual attention. *Proc. Natl. Acad. Sci. USA* *107*, 16048–16053.
39. Gaarder, K., Koresko, R., and Kropfl, W. (1966). The phasic relation of a component of alpha rhythm to fixation saccadic eye movements. *Electroencephalogr. Clin. Neurophysiol.* *21*, 544–551.
40. Sheliga, B.M., Riggio, L., and Rizzolatti, G. (1994). Orienting of attention and eye movements. *Exp. Brain Res.* *98*, 507–522.
41. Fiebelkorn, I.C., Saalman, Y.B., and Kastner, S. (2013). Rhythmic sampling within and between objects despite sustained attention at a cued location. *Curr. Biol.* *23*, 2553–2558.
42. Steinmetz, N.A., and Moore, T. (2014). Eye movement preparation modulates neuronal responses in area V4 when dissociated from attentional demands. *Neuron* *83*, 496–506.
43. Chen, C.Y., and Hafed, Z.M. (2013). Postmicrosaccadic enhancement of slow eye movements. *J. Neurosci.* *33*, 5375–5386.
44. Hafed, Z.M., and Krauzlis, R.J. (2008). Goal representations dominate superior colliculus activity during extrafoveal tracking. *J. Neurosci.* *28*, 9426–9439.
45. Russo, G.S., and Bruce, C.J. (1993). Effect of eye position within the orbit on electrically elicited saccadic eye movements: a comparison of the macaque monkey's frontal and supplementary eye fields. *J. Neurophysiol.* *69*, 800–818.
46. Ottes, F.P., Van Gisbergen, J.A., and Eggemont, J.J. (1986). Visuomotor fields of the superior colliculus: a quantitative model. *Vision Res.* *26*, 857–873.



**Current Biology**

**Supplemental Information**

**Neuronal Response Gain Enhancement  
prior to Microsaccades**

**Chih-Yang Chen, Alla Ignashchenkova, Peter Thier, and Ziad M. Hafed**

## Supplemental Figures

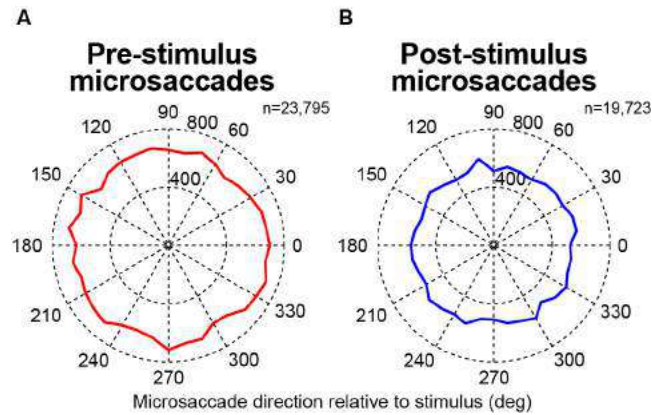


**Figure S1, Related to Figure 2** Distribution of pre-stimulus and post-stimulus microsaccade directions, demonstrating a lack of endogenous (A) or stimulus-driven (B) biases towards RF locations. Microsaccade directions can be very strongly biased towards peripheral locations. (A) To test whether our neuronal modulations were due to a sustained endogenous attentional bias towards the RF stimulus location, we analyzed the directions of microsaccades occurring <100 ms before stimulus onset. If there was a sustained endogenous attentional bias towards the RF stimulus location, then these microsaccades should be strongly directed towards that location. For each session, we rotated all data such that stimulus location was represented at 0 deg, and we then pooled all pre-stimulus microsaccades from all sessions. There was no strong peak of pre-stimulus microsaccade directions near 0 deg, as might be expected if there was a generalized sustained attentional bias towards the RF location. (B) Similarly, there was no directional bias for the microsaccades occurring immediately after stimulus onset (i.e. the microsaccades that were associated with neuronal response gain enhancement), suggesting that these microsaccades were not visually-triggered.

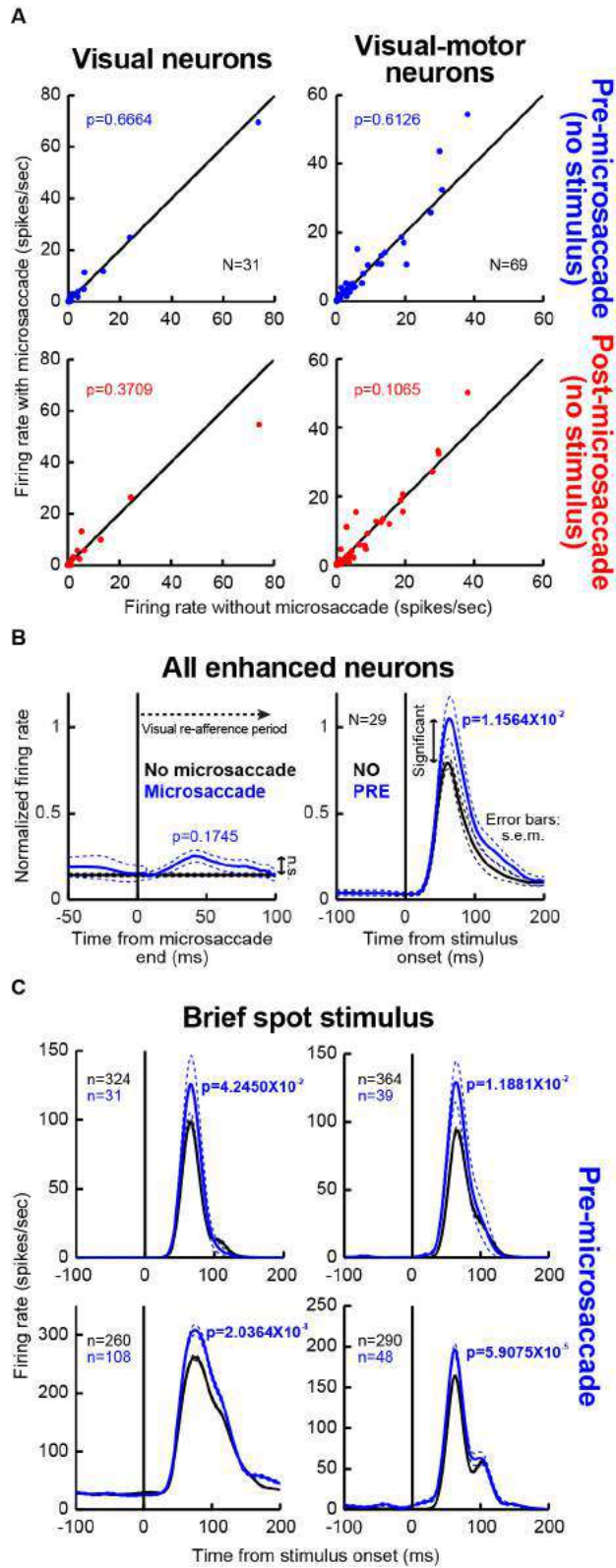


**Figure S2, Related to Figure 2** Exploring *microsaccade-only* (A) or *microsaccade-stimulus* (B, C) interactions in our results. (A) Lack of influence of microsaccades on

neuronal activity *without* the presence of an RF stimulus. To rule out the possibility that pre-microsaccadic enhancement in the main text was observed because our neurons were simply sensitive to microsaccade generation, we analyzed peri-microsaccadic changes in neuronal activity during a pre-stimulus fixation epoch. For each neuron, we analyzed microsaccades occurring 0-300 ms before stimulus onset. For each microsaccade, we measured neuronal activity in the interval 0-100 ms before microsaccade onset (top two panels), and we plotted it against activity from a similar interval but containing no microsaccades (0-100 ms before stimulus onset). We also repeated the same analysis but for an interval 0-50 ms after microsaccade end (bottom two panels), and compared it to a 50-ms interval without microsaccades (0-50 ms before stimulus onset). Most neurons were inactive without an RF stimulus, whether there was a microsaccade or not. For the few that did possess *baseline* activity, the activity was statistically unaltered by microsaccades. Each panel shows the number of neurons and p-value for the shown comparison (paired signed rank test, Experimental Procedures). Note that this figure includes data from *all* neurons. However, because a lot of these neurons were silent without a stimulus, a majority of them in the present analysis (i.e. without a stimulus in the RF) lied on the origin of the plots shown in this figure. **(B)** Comparing peri-microsaccadic modulations in the *presence* of an RF stimulus to the enhancement effects that we saw in the main text. For all neurons that individually exhibited statistically significant enhancement (Figs. 1-2), we normalized activity to the peak firing rate after stimulus onset on no-microsaccade trials (black, right panel), and we then averaged across neurons. The right panel shows population results, demonstrating strong visual-burst enhancement if a stimulus appeared <100 ms before a microsaccade towards the stimulus' hemifield (consistent with the main text). In the left panel, for the *same* neurons, we picked an interval 150-250 ms after stimulus onset and investigated possible visual re-afferent responses to microsaccades occurring within this interval (i.e. with the stimulus still present over the RF). The blue curve shows neuronal activity aligned on microsaccade end (for microsaccades towards the RF stimulus' hemifield; similar results were obtained for opposite microsaccades). The black curve shows neuronal activity from an interval of the same length (200-300 ms) when no microsaccades occurred. There was no statistically significant visual re-afferent response in the interval 0-100 ms after microsaccade end compared to no-microsaccade baselines; on the other hand, the right panel shows robust visual burst enhancement with an analysis interval of identical length. Thus, visual burst enhancement was not accounted for by visual re-afferent neuronal responses. **(C)** To further support this idea, we recorded from SC visual-motor neurons while we presented only *brief* flashes (50-ms spots) rather than our longer-duration gratings. We still observed strong enhancement, as can be seen from four sample neurons illustrated in this panel. In fact, with these brief flashes, we were able to pick specific times of microsaccade onsets that resulted in *no* overlap with a stimulus presentation over the RF (i.e. the stimulus had appeared and disappeared *before* the eye movement began). We still observed strong enhancement. Thus, **B-C** demonstrate that pre-microsaccadic response gain enhancement was not accounted for by visual re-afferent neuronal responses. All conventions in **B-C** are like in the main text (Figs. 1-2).

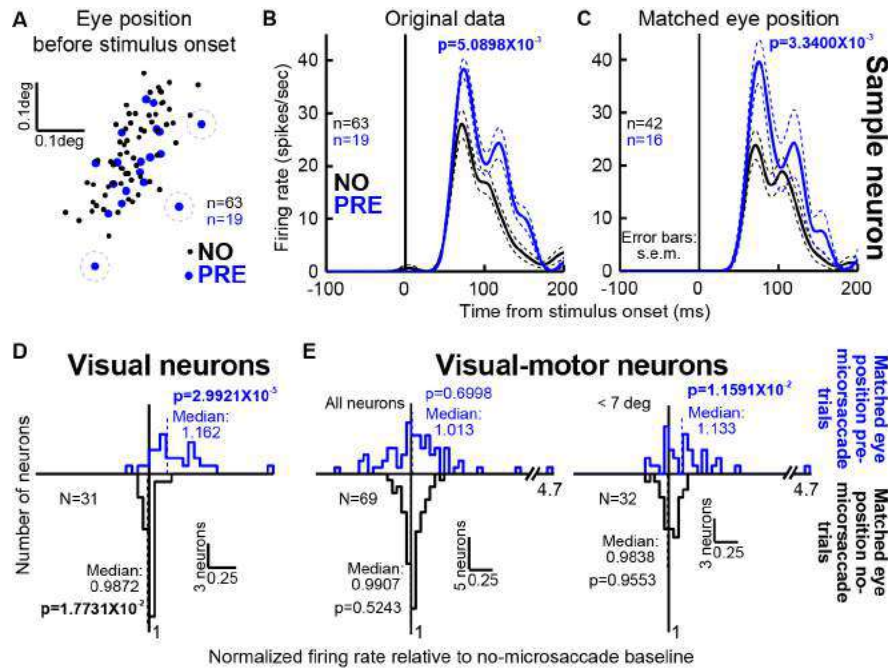


**Figure S3, Related to Figure 2** Independence of our modulations from a potential role of instantaneous eye position at stimulus onset. It could be argued that the modulations we saw were explained by changes in eye position across trials, which can change the position of the presented stimulus over the RF. For example, if no-microsaccade trials had a certain eye position at stimulus onset that was different from the eye position on pre-microsaccade trials, then it could be argued that eye position on pre-microsaccade trials was always such that when the stimulus appeared, it was placed at a more preferred RF location than when it appeared for no-microsaccade trials (thus giving higher firing rates). While this is highly unlikely given the specific patterns of effects that we saw (e.g. Fig. 3), we ruled it out by repeating our analyses but after “matching” eye position on no-microsaccade and microsaccade trials. **(A)** Data from an example session demonstrating a large overlap in eye position on no-microsaccade and pre-microsaccade trials. We collected all 80% grating trials from a sample session, and we measured average eye position 0-50 ms before grating onset. The black dots show eye position from no-microsaccade trials, and the blue dots show eye position from trials in which the stimulus appeared <100 ms before a microsaccade towards the grating’s hemifield. The circled trials are trials in which eye position on microsaccade trials did not fall within the region of overlap of no-microsaccade trials. Only 3 such trials existed in this session. **(B, C)** We performed our analysis of Fig. 1B for the sample session in **A**, which was obtained from a pure visual neuron. In **B**, we performed the original analysis. In **C**, we excluded each “pre-microsaccade” trial that did not have any neighboring “no-microsaccade” trials within 1.8 min arc radius (the 3 circled trials in **A**), and we also excluded each “no-microsaccade” trial that did not have any neighboring “microsaccade” trials (within a similar radius). Thus, in panel **C**, eye position at stimulus onset was “matched” across the no-microsaccade and microsaccade trials. As can be seen, response gain enhancement was still robustly observed. Thus, the effects in Figs. 1-2 were not due to different RF

stimulus positions caused by differences in eye position at grating onset. Error bars denote s.e.m. **(D, E)** Across the population, we compared our neuronal modulation indices in “matched” eye position data sets to the original no-microsaccade baseline data from Fig. 2 (i.e. from all no-microsaccade trials before “matching”). “Matched” pre-microsaccade trials showed robust enhancement even after removing eye position outliers (blue histograms). “Matched” no-microsaccade trials were statistically indistinguishable from original no-microsaccade trials (black histograms), suggesting that our subsampling of no-microsaccade trials to obtained “matched” sets did not alter our no-microsaccade baseline reference. Thus, our effects in this paper were not due to differences in eye position between no-microsaccade and microsaccade trials. All other conventions are similar to Fig. 2. Note that we also repeated the above analyses for microsaccades away from the grating location, and also for grating onsets after microsaccades. In all cases, the conclusions presented in the main text (Figs. 2-3) were unaltered.

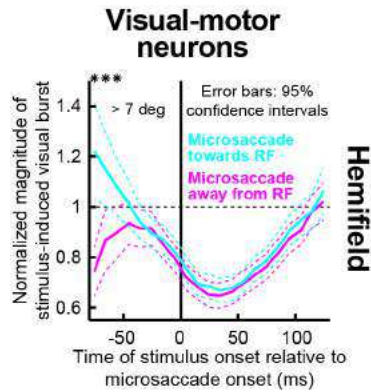


**Figure S4, Related to Figure 3** Pre-microsaccadic response gain enhancement for peripheral visual-motor SC neurons. This figure is similar to Fig. 3D. However, in this case, we only show data from visual-motor SC neurons with preferred eccentricities >7 deg. Also, for simplicity, we classified microsaccade directions in this analysis as either being towards the hemifield of the RF stimulus or opposite it. As can be seen, even these eccentric visual-motor neurons showed differential modulation based on microsaccade direction, as well as pre-microsaccadic enhancement of response gain for microsaccades towards the hemifield of the stimulus. Thus, pre-microsaccadic enhancement was a robustly observed phenomenon, even in eccentric visual-motor neurons. All conventions are similar to those in Fig. 3D.

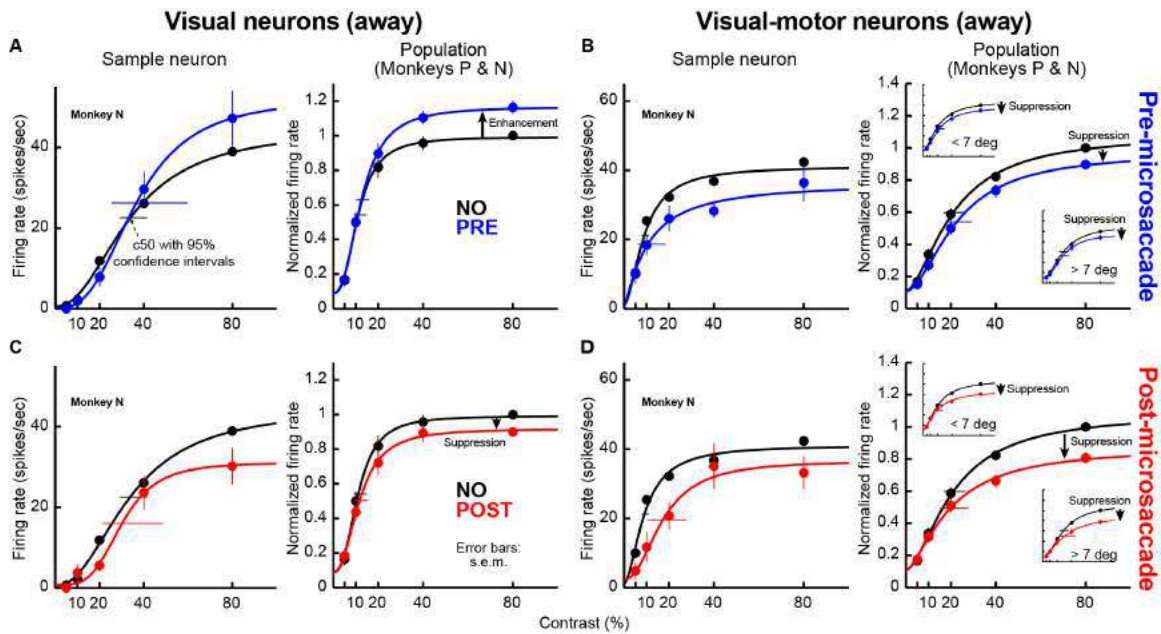


**Figure S5, Related to Figure 5** Contrast sensitivity curves like in Fig. 5 but for microsaccades opposite the hemifield of a stimulus (i.e. away from the stimulus). The figure has formatting and conventions identical to Fig. 5. Consistent with all of our earlier analyses (e.g. Fig. 3), microsaccades away from the stimulus were associated with either weaker enhancement for visual neurons or significant suppression for visual-motor neurons when the stimulus appeared before microsaccades (**A**, **B**). After microsaccades, suppression was always consistently observed (**C**, **D**).



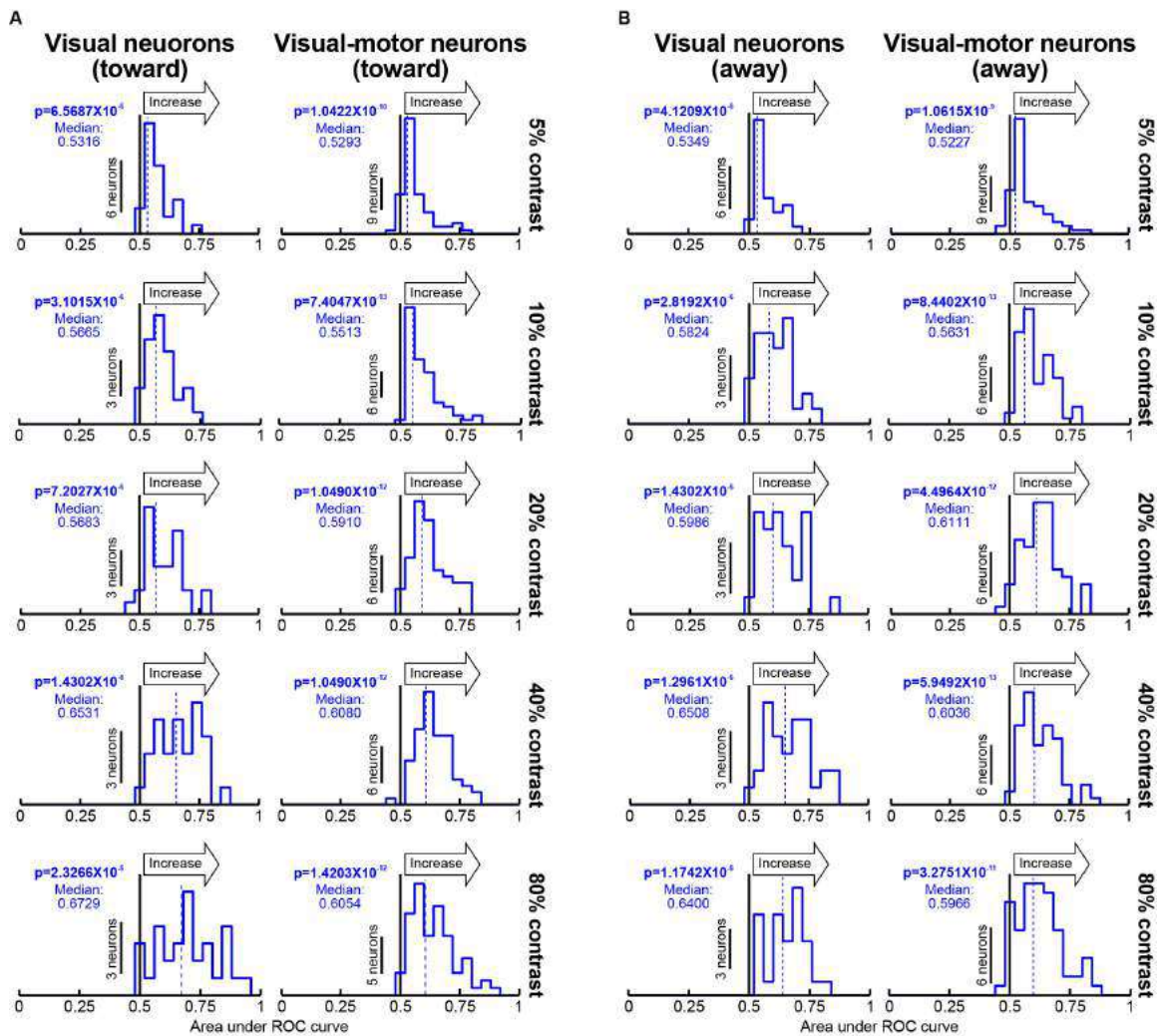


**Figure S6, Related to Figure 6** Analyses similar to Fig. 6A, B but for all stimulus contrasts (A), and also for microsaccades opposite the hemifield of a stimulus (B). (A) Area under the ROC curve comparing activity on pre-microsaccade trials to activity on no-microsaccade trials. The left column shows pure visual SC neurons, and the right column shows visual-motor neurons. Each row shows results from a single grating contrast, and all panels show results for microsaccades towards the hemifield of the RF location. In all cases, activity on microsaccade trials was discriminable from that on no-microsaccade trials. (B) Similar analyses for microsaccades opposite the stimulus' hemifield. For these microsaccades, our earlier analyses (e.g. Fig. 3) showed that pure visual SC neurons still showed pre-microsaccadic response gain enhancement (albeit weaker), whereas visual-motor neurons showed pre-microsaccadic response gain suppression. Consistent with these results, this figure shows that whenever firing rates were either enhanced or suppressed, our ROC analyses revealed above-chance discriminability of neuronal activity between microsaccade and no-microsaccade trials. All conventions are similar to Fig. 6A, B.

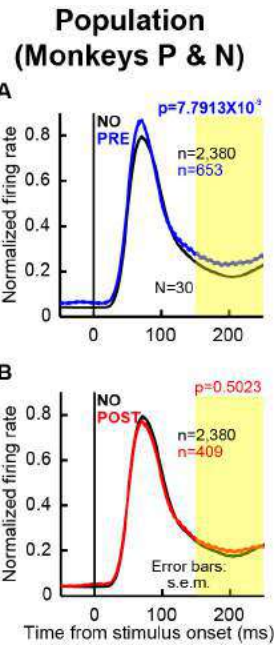


**Figure S7, Related to Figure 7** Normalized population firing rate curves from the data in Fig. 7. For all neurons with a sustained response on no-microsaccade trials (Fig. 7, Experimental Procedures), we normalized all firing rates to each neuron's peak firing rate on no-microsaccade trials. We then pooled all data to obtain a single normalized population firing rate curve. We obtained such a curve for no-microsaccade trials (black) and also for trials with a stimulus appearing before (blue) or after a microsaccade (red). In this figure, we show data from the highest contrast grating. This figure shows similar results to those in Fig. 7A, C. The p-value is for the shaded analysis interval, and error bars denote s.e.m.

**3. Sharper, stronger, faster upper visual field representation  
in primate superior colliculus**

# Current Biology

## Sharper, Stronger, Faster Upper Visual Field Representation in Primate Superior Colliculus

### Highlights

- Smaller upper visual field SC visual and saccade-related response fields
- Higher spatial-frequency tuning and contrast sensitivity in the upper visual field
- Over-representation of the upper visual field in visual and saccade-related SC maps
- SC tuning to smaller image features typically encountered in upper visual fields

### Authors

Ziad M. Hafed, Chih-Yang Chen

### Correspondence

ziad.m.hafed@cin.uni-tuebingen.de

### In Brief

Hafed and Chen show that the superior colliculus (SC) contains a functional discontinuity in spatial resolution and neural sensitivity between upper (UVF) and lower (LVF) visual field representations. This recasts prior knowledge of SC topography, assuming UVF/LVF symmetry, and demonstrates how the SC can support more accurate, lower-latency UVF saccades.



# Sharper, Stronger, Faster Upper Visual Field Representation in Primate Superior Colliculus

Ziad M. Hafed<sup>1,\*</sup> and Chih-Yang Chen<sup>1,2</sup><sup>1</sup>Werner Reichardt Centre for Integrative Neuroscience, Tuebingen University, Tuebingen BW 72076, Germany<sup>2</sup>Graduate School of Neural and Behavioural Sciences, International Max Planck Research School, Tuebingen University, Tuebingen BW 72074, Germany\*Correspondence: [ziad.m.hafed@cin.uni-tuebingen.de](mailto:ziad.m.hafed@cin.uni-tuebingen.de)<http://dx.doi.org/10.1016/j.cub.2016.04.059>

## SUMMARY

Visually guided behavior in three-dimensional environments entails handling immensely different sensory and motor conditions across retinotopic visual field locations: peri-personal (“near”) space is predominantly viewed through the lower retinotopic visual field (LVF), whereas extra-personal (“far”) space encompasses the upper visual field (UVF). Thus, when, say, driving a car, orienting toward the instrument cluster below eye level is different from scanning an upcoming intersection, even with similarly sized eye movements. However, an overwhelming assumption about visuomotor circuits for eye-movement exploration, like those in the primate superior colliculus (SC), is that they represent visual space in a purely symmetric fashion across the horizontal meridian. Motivated by ecological constraints on visual exploration of far space, containing small UVF retinal-image features, here we found a large, multi-faceted difference in the SC’s representation of the UVF versus LVF. Receptive fields are smaller, more finely tuned to image spatial structure, and more sensitive to image contrast for neurons representing the UVF. Stronger UVF responses also occur faster. Analysis of putative synaptic activity revealed a particularly categorical change when the horizontal meridian is crossed, and our observations correctly predicted novel eye-movement effects. Despite its appearance as a continuous layered sheet of neural tissue, the SC contains functional discontinuities between UVF and LVF representations, paralleling a physical discontinuity present in cortical visual areas. Our results motivate the recasting of structure-function relationships in the visual system from an ecological perspective, and also exemplify strong coherence between brain-circuit organization for visually guided exploration and the nature of the three-dimensional environment in which we function.

## INTRODUCTION

The primate superior colliculus (SC) is a layered midbrain structure critical for visual-motor processing, target selection, and

attention [1–11], and it is particularly important for sensorimotor transformations from retinal image features into gaze shift commands [5–7, 12]. Superficial SC layers contain retinotopic maps of the contralateral visual field, and deeper layers contain spatially registered eye-movement maps [13–15]. Visual, visual-motor, and motor neurons possess response fields (RFs) confined to a region of visual (afferent) or movement (efferent) space, and RF sizes are often large. This means that the SC may use coarse population coding to ensure accurate localization [16–19].

Much like primary visual cortex, the SC magnifies foveal representations [13, 14]. Such magnification affords smaller and more abundant RFs dedicated to processing small retinotopic eccentricities [13], which increases spatial resolution [16]. Indeed, RFs associated with microsaccades, which precisely relocate gaze on a miniature scale [20, 21], are smaller than peripheral RFs associated with large saccades [22, 23]. Observations like these have led to a universally accepted model [19] in which retinotopic eccentricity morphs onto SC tissue using logarithmic warping. In this model, more tissue represents central locations, and with higher resolution, but upper (UVF) and lower (LVF) visual field representations are identical.

However, our environment dictates different constraints on eye-movement exploration between the UVF and LVFs [24]. For example, the LVF encompasses peri-personal “near” space, in which objects project larger retinal images, whereas UVF objects are generally “far” and project small features (Figures 1A and S1A) [24]. In this study, we hypothesized that SC organization might be “in tune” with such ecological constraints on eye-movement exploration [24]. We discovered a significant asymmetry across the horizontal meridian, spanning both anatomical mapping as well as physiological and behavioral properties. This asymmetry is such that SC visual-motor processing allows more accurate and lower-latency saccades to UVF image features.

We will show, among other things, that UVF SC RFs are smaller than LVF RFs. This suggests UVF magnification in neural tissue, similar in principle to foveal magnification. We will thus propose a revised model more accurately representing SC topography than the universally accepted model [14, 19]. Our revised understanding of SC topography is not only in line with behavioral effects, but it may also be a critical missing link for resolving some long-standing debates about SC saccade-related dynamics [9, 25–27]. More broadly, our results motivate recasting of structure-function relationships in the visual system from an ecological perspective [24]. This sentiment is contrary to common practice. For example, because dorsal cortex (primarily

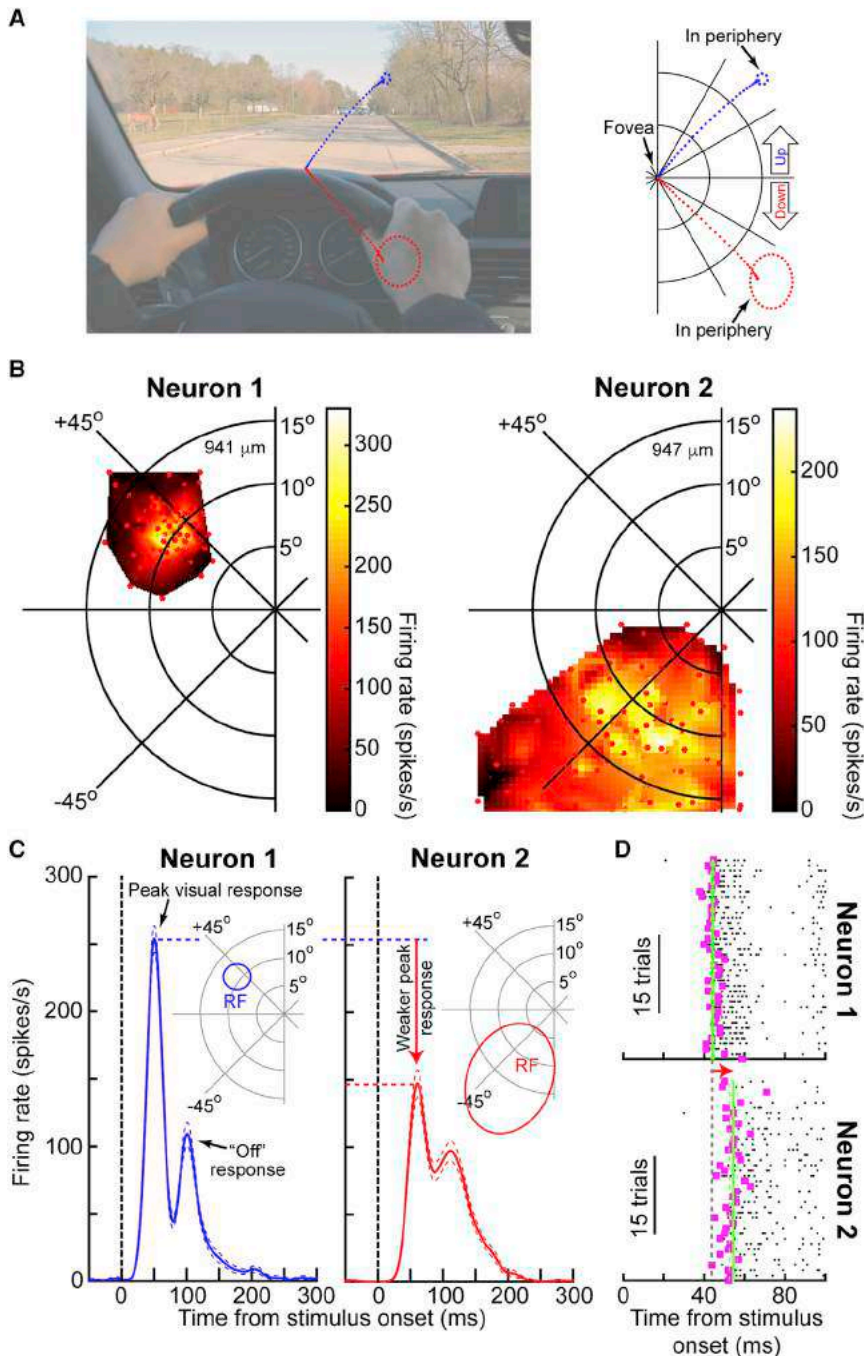


**Figure 1. Sharper, Stronger, Faster UVF SC Representation**

(A) In retinotopic coordinates, UVF features are generally farther and smaller than LVF features [24]. In this example, a driver initially looks down near the instrument cluster. A bird on a treetop might attract his gaze, requiring an upward saccade; a similarly sized saccade can be made to the LVF (if, for example, something itches on his hand). The spatial scales at the ends of the two, otherwise identical, saccades differ (dashed circles). Also see Figure S1A.

(B) Visual RFs from two example visual neurons (the depth from the SC surface is indicated in each panel). Individual dots show sampled stimulus locations. The neurons were matched for animal, side of space, depth, and hotspot eccentricity (i.e., eccentricity of peak response), but the UVF RF was smaller.

(C) Firing rates of the same neurons for a flashed spot at the preferred RF hotspot. The UVF neuron had a stronger response (measured as the peak response within 30–150 ms after stimulus onset). Note that the neurons showed a later “off” response because of the brief stimulus flash. Error bars, which are indicated by thin dashed lines around the data curves, indicate the SEM.

(D) The same visual responses but shown as spike rasters. Each dot is a spike; each row is a trial. The first stimulus-evoked spike is magenta, and green vertical lines indicate the mean/SEM first-spike latency. Visual responses occurred faster for the UVF neuron. The arrow indicates the time difference between the mean latency of neuron 1 and the mean latency of neuron 2

Also see Figure S1.

S1B–S1E) and was balanced, with 52.21% of neurons preferring UVF RF locations and 47.79% preferring LVF RF locations.

We observed a large change in visual RF area as a function of visual field location. Figure 1B shows RFs from two example visual neurons recorded from the same SC side, same animal, same electrode depth from the SC surface, and, most importantly, same RF hotspot eccentricity (defined as the stimulus location giving maximal visual response). In each panel, we plotted visual burst

representing the LVF) is more readily accessible experimentally, there exists a strong bias to study only the LVF. Such bias might mask interesting UVF versus LVF dissociations [24].

## RESULTS

We recorded from 419 neurons (157 visual, 251 visual-motor, and 11 motor) in two monkeys performing visual and saccade-related tasks (Experimental Procedures). We analyzed visual and saccade-related activity as well as RF properties. Our database spanned a range of eccentricities and directions (Figures

strength as a function of stimulus location from a delayed visually guided saccade task used to map RFs (Experimental Procedures). The figure shows locations with significant visual responses above each neuron’s no-stimulus baseline (Experimental Procedures). The UVF RF (neuron 1) was ~76% smaller than the LVF RF (neuron 2) (60.43 degrees<sup>2</sup> versus 251 degrees<sup>2</sup>).

This effect was accompanied by stronger and lower-latency responses. For the same neurons, we analyzed visual responses when the monkeys fixated, and we presented a briefly flashed spot at each neuron’s preferred hotspot (Experimental

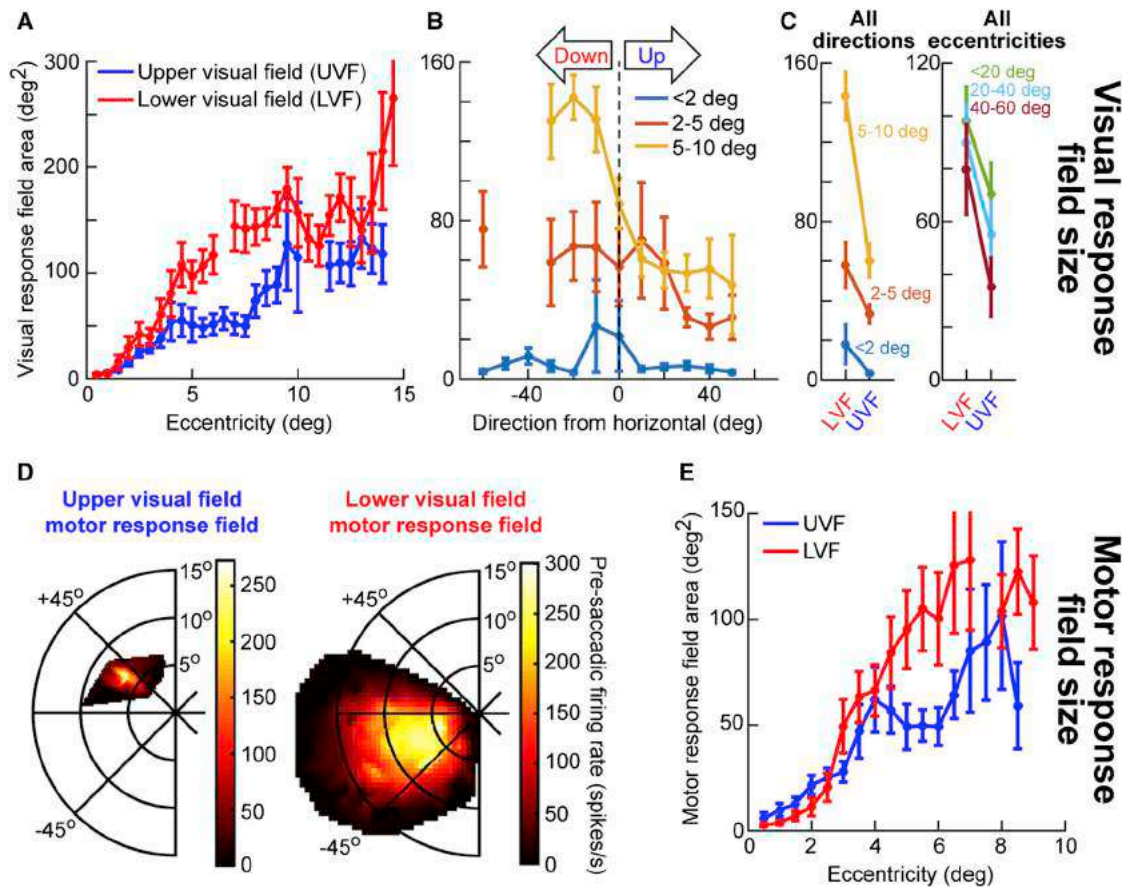


**Figure 2. Higher-Resolution UVF Spatial Representation**

(A) Visual RF area (Experimental Procedures) increased with eccentricity [13], but more dramatically for LVF neurons.

(B) Same data as in (A), but as a function of RF direction from horizontal.

(C) Same data, but collapsing across directions or eccentricities.

(D) Example eccentricity-matched motor RFs showing a similar asymmetry. All conventions are similar to Figure 1B, but here we measured pre-saccadic (0–50 ms before saccade onset) firing rate.

(E) Like (A), but for motor RFs.

Error bars indicate the SEM. Also see Figures S2–S4.

Procedures). We measured peak response 30–150 ms after stimulus onset and found that the UVF neuron had  $\sim 1.66$  times the response of the LVF neuron (Figure 1C;  $p < 0.05$ , two-tailed t test). Moreover, latency to first stimulus-induced spike was lower (Figure 1D;  $p < 0.05$ , two-tailed t test). Thus, UVF SC representations have smaller RFs and stronger, lower-latency visual responses.

We next describe the robustness of these findings, their relation to motor RF properties, as well as their implications for behavioral properties of saccades and SC topographic representations.

#### Higher-Resolution Coverage of the Upper Visual Field

We plotted visual RF area (Experimental Procedures) as a function of hotspot eccentricity (Figure 2A). RF area increased with eccentricity [13], but the increase was stronger for LVF RFs (two-way ANOVA,  $p < 0.05$  for both main effects of eccentricity and UVF/LVF location). We also analyzed RF area as a function of direction from horizontal (Figure 2B): both direction and ec-

centricity had an impact (two-way ANOVA,  $p < 0.05$  for both main effects of eccentricity and direction). The same conclusion was reached when collapsing across directions (Figure 2C, left; two-way ANOVA,  $p < 0.05$ ); moreover, for individual eccentricity bins, 2- to 5-degree and 5- to 10-degree eccentricities each had larger LVF RFs than UVF RFs ( $p < 0.05$ , two-tailed t tests; Figure 2C, left). The effect was weakest for foveal eccentricities, for which RF sizes are already small. Similar analyses when collapsing across eccentricities (Figure 2C, right) also revealed a main effect of UVF/LVF location ( $p < 0.05$ , two-way ANOVA). However, this time, there was no main effect of direction ( $p > 0.05$ ), suggestive of a categorical change across the horizon (i.e., even directions  $< 20$  degrees showed an area difference between UVF and LVF).

Because RF area increases with depth from the SC surface [28], we also confined analyses to the most superficial layers ( $< 1$  mm below the surface [8]) and still observed UVF/LVF differences (Figure S2A). Thus, Figures 2A–2C are not an artifact of combining different depths. We also found similar UVF/LVF

asymmetries in either right or left SC individually (Figure S2B). Moreover, for neurons with predominantly vertical RF hotspots, LVF RFs were uncharacteristically elongated, almost forming an edge-like representation (Figure S2C). Finally, for deeper visual-motor and motor neurons, even UVF saccade-related motor RFs were smaller. This is illustrated in Figure 2D for two eccentricity-matched visual-motor neurons recorded during the same delayed visually guided saccade task as that in Figure 1B. Pre-saccadic firing rate was plotted as a function of saccade endpoint (Experimental Procedures), and the LVF neuron still had a larger motor RF; this was also consistent across the population (Figures 2E and S3; two-way ANOVA,  $p < 0.05$  for both main effects of eccentricity and UVF/LVF location).

Therefore, even when separately analyzing different depths, individual SCs, and saccade-related RFs, UVF/LVF RF area differences persisted and extended to efferent representations.

With larger LVF RFs, a given stimulus or saccade endpoint would activate neurons with RF hotspots at significantly more retinotopic locations than a similarly eccentric UVF stimulus. We confirmed this for visual (Figure S4A) and saccade-related (Figure S4B) representations. Such a difference in spatial pooling is reminiscent of psychophysical differences in illusory contour integration between the UVF and LVFs [29].

### Higher Spatial-Frequency Tuning and Contrast Sensitivity in the Upper Visual Field

Another implication of a sharper UVF spatial representation (i.e., with smaller RFs) is that it might extend to other aspects of spatial vision. We hypothesized that sensitivity to fine spatial structure might be higher in the SC's UVF representation. We therefore characterized SC spatial-frequency tuning properties (Experimental Procedures). The monkeys fixated while we presented a stationary grating within an RF. We observed individual preferences for individual spatial frequencies (Figure 3A). Like in primary visual cortex [30, 31], individual eccentricities had neurons representing multiple spatial frequencies, and tuning curves became increasingly low pass eccentrically (Figure S5). Remarkably, beyond the parafovea, UVF neurons exhibited more tuning to higher spatial frequencies (Figures 3A and 3B). Thus, the existence of multiple spatial-frequency channels at a given eccentricity persists farther out in the periphery for UVF representations. We statistically confirmed this by testing for a larger UVF dispersion of preferred frequencies (Figure 3B;  $p < 0.05$ , median-subtracted Ansari-Bradley test for dispersions).

We also tested contrast sensitivity using the task of [32]. Once again, UVF neurons had higher sensitivity (i.e., lower semi-saturation contrasts;  $p < 0.05$ , two-tailed t test) and larger dynamic range ( $p < 0.05$ , two-tailed t test) (Figures 3C and 3D). Thus, UVF SC visual RFs are smaller, more finely tuned to spatial structure, and more sensitive to image contrast.

### Stronger, Lower-Latency Upper Visual Field Visual Responses

We explored the increased sensitivity property further by analyzing visual response strength for a briefly flashed spot at the RF hotspot while the monkeys fixated (from the same task used in Figure 1C; Experimental Procedures). Peak UVF re-

sponses were  $\sim 1.33$  times stronger than peak LVF responses (Figure 4A;  $p < 0.05$ , two-tailed t test), and this effect persisted for different directions from horizontal (Figures 4B and 4C;  $p < 0.05$ , one-way ANOVA with direction as the main factor). Like in the example neurons (Figure 1), we also confirmed that UVF neurons also exhibited lower visual response latencies (Figures 4D and 4E;  $p < 0.05$ , two-tailed t test; also demonstrated in Figure 4F;  $p < 0.05$ , one-way ANOVA with direction as the main factor). Given that SC visual bursts strongly correlate with saccadic reaction times (RTs) [33–35], these observations (Figures 4A–4F) help explain previously reported decreases in UVF visually guided saccade RTs [36, 37]. Such effects, which we replicated (Figure S6A, left panel; Figure S6B, leftmost panel), have eluded a neurobiologically plausible mechanism for several decades [24].

Interestingly, stronger UVF activity was specific for visual responses. Saccade-related activity showed the opposite effect: across directions, pre-saccadic activity was weaker in the UVF (Figure 4G;  $p < 0.05$ , two-tailed t test), and there was a direction main effect (Figures 4H and 4I;  $p < 0.05$ , one-way ANOVA). Thus, in the UVF, it is visual SC modulations that are particularly strong.

Given that the SC receives inputs from several cortical visual areas [38], in which there is a physical discontinuity between UVF and LVF representations [39, 40], we hypothesized that an SC functional discontinuity in visual representations might parallel a cortical structural discontinuity. We analyzed visually evoked local field potentials (LFPs) as a proxy for aggregate synaptic activity after stimulus onset (Experimental Procedures). We did this for the same task for which we analyzed visually evoked spiking (Figures 1C, 1D, and 4A–4F). An even stronger UVF asymmetry emerged: across eccentricities, stimulus-evoked LFP modulation was  $\sim 2.5$  times stronger for UVF RFs compared to LVF RFs (Figure 5A;  $p < 0.05$ , two-tailed t test). Additionally, there was a categorical change in response strength across the horizontal meridian (Figure 5B): for all UVF direction bins, LFP response was much stronger than for all LVF bins, and the effect was approximately equal for different directions (Figures 5B–5D) and eccentricities (Figures 5D and 5E). We confirmed this statistically: two-way ANOVAs with UVF/LVF location as one factor and eccentricity or direction as the other revealed a main effect of only UVF/LVF location ( $p < 0.05$ ). This suggests a categorical change, or functional discontinuity, across the horizontal meridian.

### Lower-Latency, More Accurate Upper Visual Field Saccades

Using visually guided saccades (Experimental Procedures), we confirmed that UVF saccades are not only lower latency (as stated above) but also more accurate (Figure S6A; Figure S6B, two leftmost panels). The RT effect is likely a consequence of visual response effects (Figures 4 and 5), and the accuracy effect probably reflects smaller UVF motor RFs (Figures 2D, 2E, and S3).

Using visually guided saccades, we also discovered that express saccades (with RTs  $< 100$  ms) [41] were 9–14 times more likely for UVF rather than LVF targets (Figure S6B, rightmost panel). This large effect is surprising given that express saccades should be rare (if not absent) in this task [41].



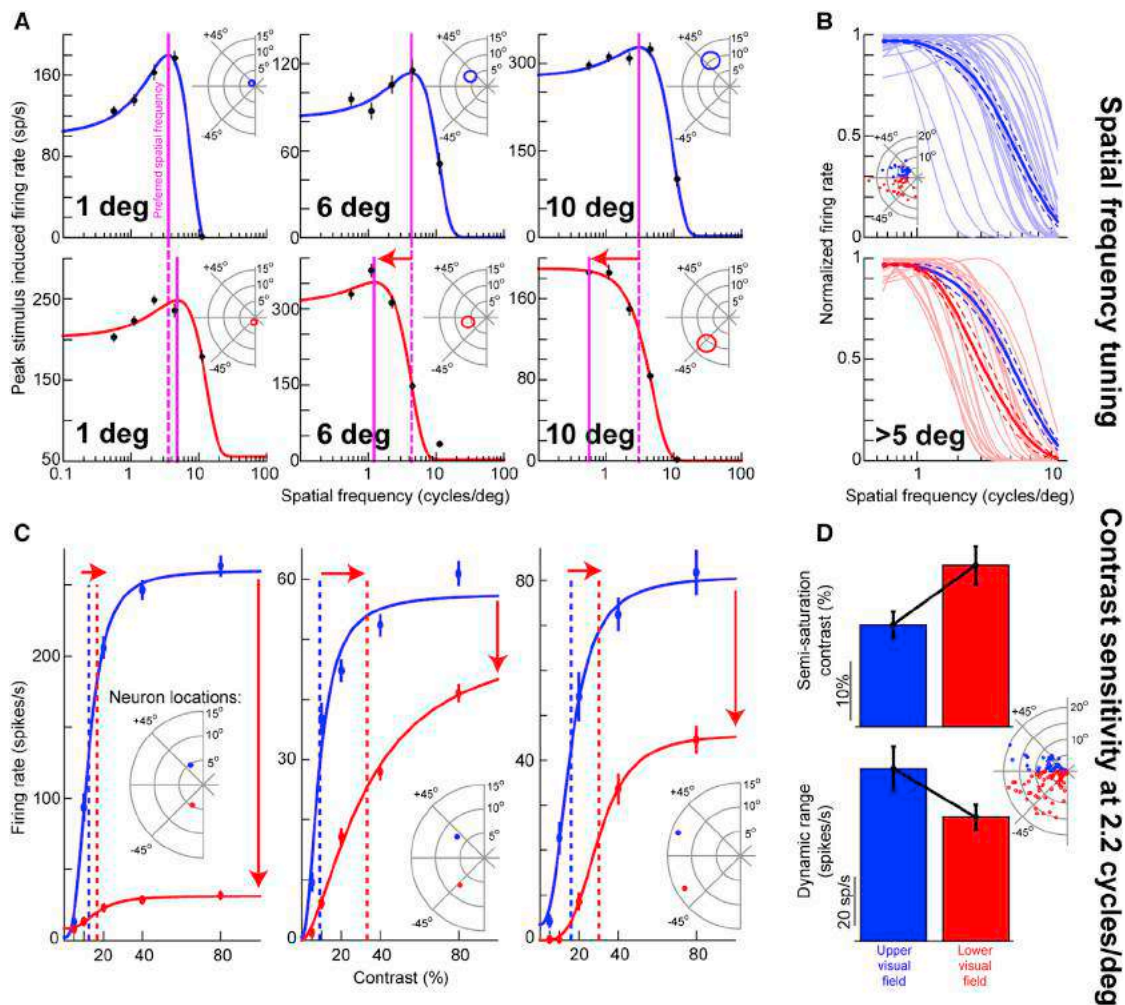


**Figure 3. Higher UVF Spatial-Frequency Tuning and Contrast Sensitivity**

(A) Sample spatial-frequency tuning curves for three eccentricity-matched pairs of UVF/LVF neurons. Each column shows one eccentricity, and the top and bottom rows show UVF and LVF neurons, respectively. UVF eccentric neurons (6 and 10 degrees) had higher preferred spatial frequency (magenta lines) than LVF neurons. The insets show neuron locations.

(B) Normalized tuning curves for all eccentric neurons (>5 degrees; inset). The range of preferred spatial frequencies was higher for UVF neurons. Saturated colors show the mean/SEM of the individual curves. Also see Figure S5.

(C) Contrast sensitivity curves for three eccentricity-matched pairs of UVF/LVF neurons. Vertical lines indicate semi-saturation contrasts. UVF neurons had higher sensitivity.

(D) Summary of all contrast sensitivity curves. UVF neurons had lower semi-saturation contrasts and larger dynamic ranges. Error bars indicate the SEM.

We also hypothesized that for memory-guided saccades (Experimental Procedures), RTs should not be affected by UVF/LVF location, because of stimulus absence and the deliberate task nature. However, UVF landing error should still decrease because of smaller motor RFs. We confirmed this (Figures S6C and S6D). Thus, our neural results have direct consequences for visual-motor behavior.

### Anatomical Over-Representation of the Upper Visual Field

Finally, if UVF RFs are smaller than LVF RFs, then ensuring coverage of the UVF in a topographic map should recruit more neural tissue, analogous to foveal magnification. This suggests

that the UVF should be over-represented. We found evidence for this by analyzing eccentricities and directions preferred by multi-unit visual activity first encountered at the SC surface (Experimental Procedures). We were noticeably more likely to encounter UVF than LVF locations. For example, Figure 6A shows a continuous run of daily recordings from one monkey, in which we systematically moved our recording electrode (laterally within a chamber) by 100- $\mu$ m steps (or small multiples thereof). The figure shows electrode track locations along with directions and eccentricities encoded by multi-unit activity at the SC surface. A larger area of sites was dedicated to the UVF (Figure 6A, right panel), at least within the SC region that we could map given our display-system limits. Meta-analysis

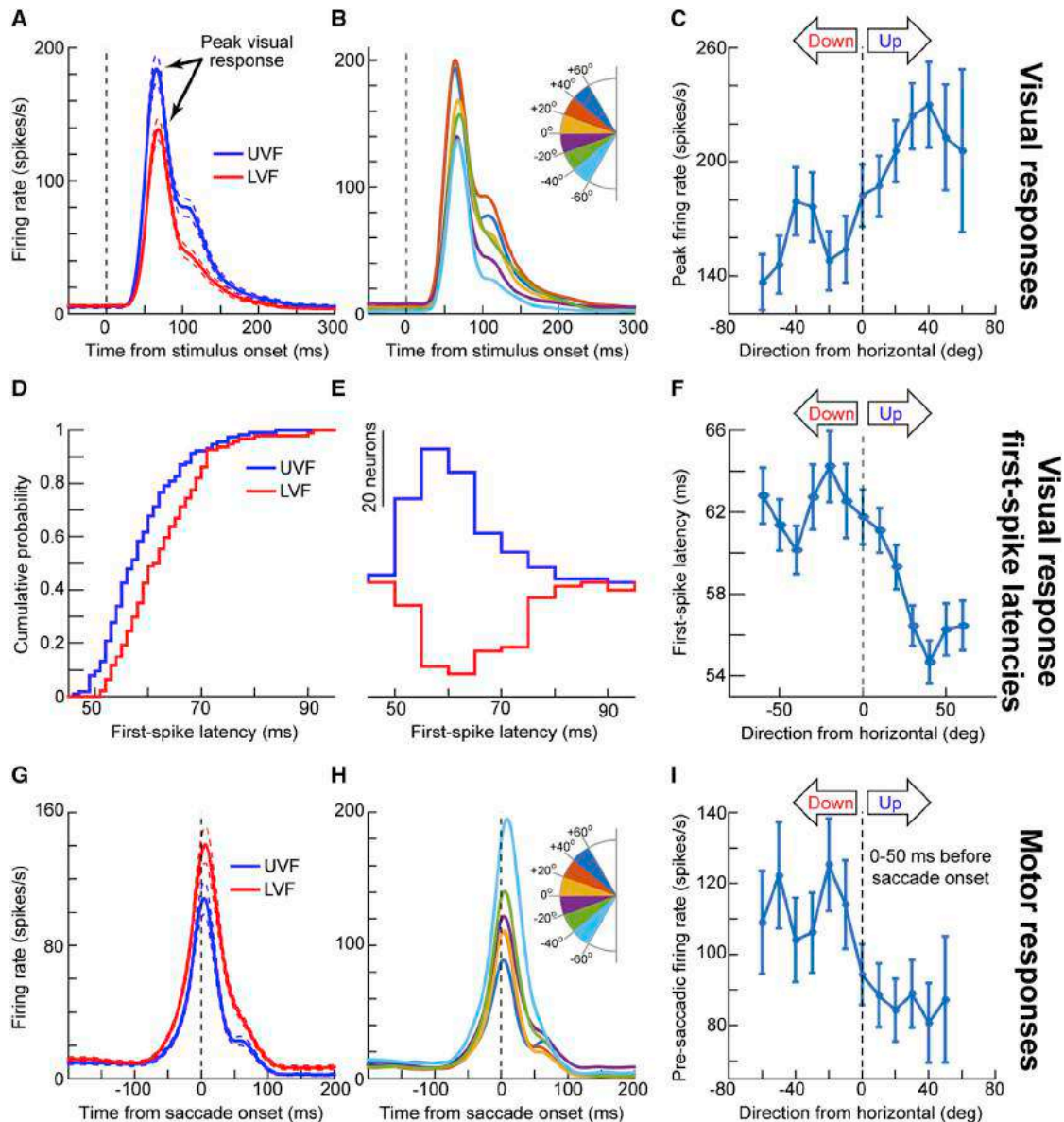


**Figure 4. Stronger, Lower-Latency UVF Visual Responses**

(A) Stimulus-evoked firing rate for UVF (blue) or LVF (red) neurons. In each neuron, the stimulus was a briefly flashed spot at the preferred RF hotspot. Peak firing rate was stronger in the UVF.

(B) Same data, but neurons were separated according to RF direction from horizontal (indicated by the color-coded legend). UVF responses were systematically higher.

(C) Same data, now summarized as a plot of peak stimulus-evoked firing rate versus RF direction from horizontal (similar binning to Figure 2B).

(D) Cumulative histograms of UVF or LVF first-spike latency (as computed in Figure 1D, and from the same task).

(E) Raw histograms of the data in (D). UVF responses occurred systematically sooner than LVF responses.

(F) Summary of first-spike latency as a function of RF direction from horizontal, as in (C).

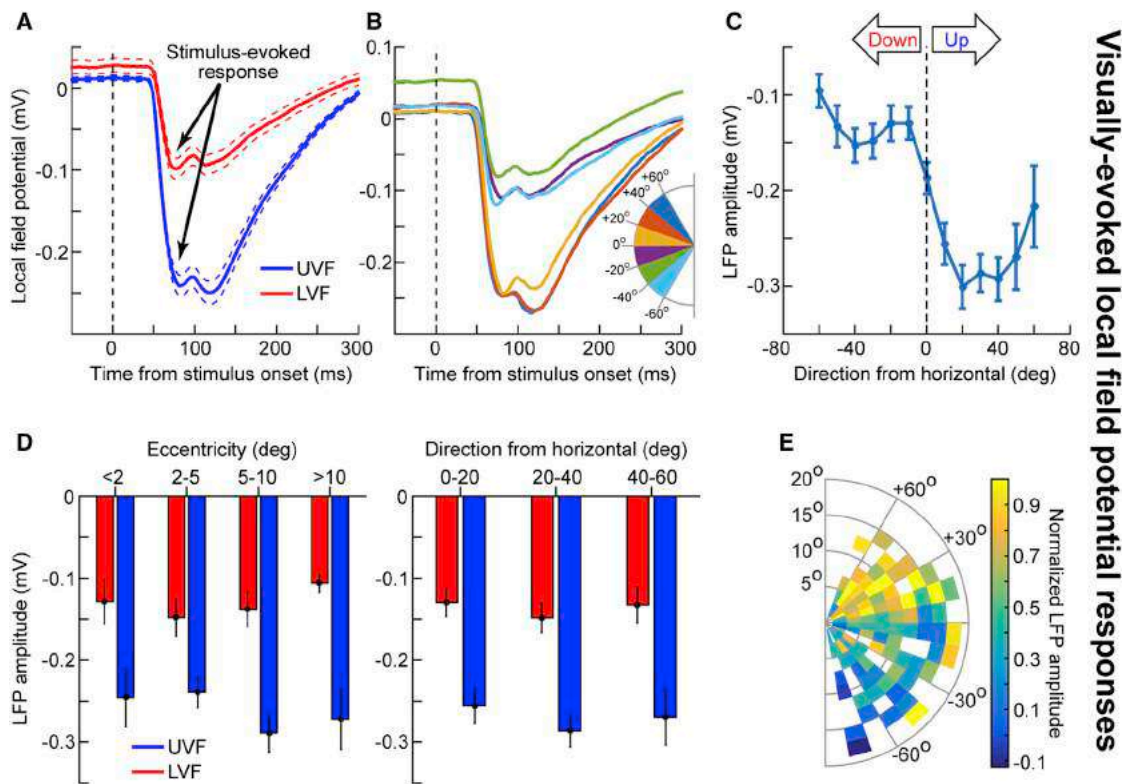
(G–I) Same analyses as in (A)–(C), but for saccade-aligned firing rates during the delayed visually guided saccade task. Saccade-related activity showed the opposite patterns from visual activity (A–C).

Error bars indicate the SEM. Also see Figures 5, S4, and S6.

of electrode locations from an earlier study [13] revealed very similar results (Figure 6B). Thus, our observations are robust, even though they are very different from the universally accepted model of SC mapping [19], having identical UVF/LVF representations (Figure 6C). We therefore revised (Experimental Proce-

dures) the model (Figure 6D) by including a functional discontinuity across the horizontal meridian.

An interesting consequence of our revised model is that it allows “equalizing” the size of the active SC population in anatomical coordinates, despite large changes in RF area as a function



Visually-evoked local field potential responses

### Figure 5. Stronger UVF Visually Evoked LFP Modulations

(A–C) Same analyses as in Figures 4A–4C, but for LFPs (Experimental Procedures). Peak LFP amplitude deflection (a negative-going deflection) was stronger in the UVF.

(D) We also separated electrode tracks according to their visual RF hotspot eccentricity and direction (x axis in each panel). Stronger negative deflections occurred in the UVF, regardless of eccentricity or direction. The LFP effect was much stronger than the firing rate effect (Figures 4A–4C).

(E) LFP visually evoked amplitude as a function of two-dimensional electrode location in the SC map (Experimental Procedures). The LFP response was stronger above the horizontal meridian.

Error bars indicate the SEM.

of either eccentricity or UVF/LVF location (e.g., Figure 2A). Specifically, in visual coordinates, UVF RFs are smaller than LVF RFs (Figures 7A and 7D), but our model suggests that there may be UVF magnification in SC coordinates, which compensates for this. We confirmed this in Figure 7. We projected visual RFs from retinotopic coordinates (Figures 7A and 7D) into SC anatomical coordinates using either the Ottes et al. model [19] (Figures 7B and 7E) or our revised model (Figures 7C and 7F). According to the original model, eccentricity is warped using logarithmic mapping. Thus, for either the UVF or LVF individually, RF sizes across eccentricities are equalized [9, 19] (compare eccentricities in each row individually in Figure 7B). However, because the original model is symmetric across the horizontal meridian, UVF RFs (upper row) are still smaller than the LVF RFs (bottom row). With our revised model (Figure 7C), over-representation of the UVF means that smaller UVF RFs in visual coordinates become “magnified” in SC coordinates. Thus, the SC can still equalize RF area both in terms of eccentricity (compare neurons in either the UVF or LVF individually in Figure 7C) and in terms of UVF or LVF location (compare neurons within a given column). Thus, even with UVF/LVF asymmetries, it may still be true that the same SC population size would be activated for different stimulus locations or saccade endpoints (Figure 7F), as was hy-

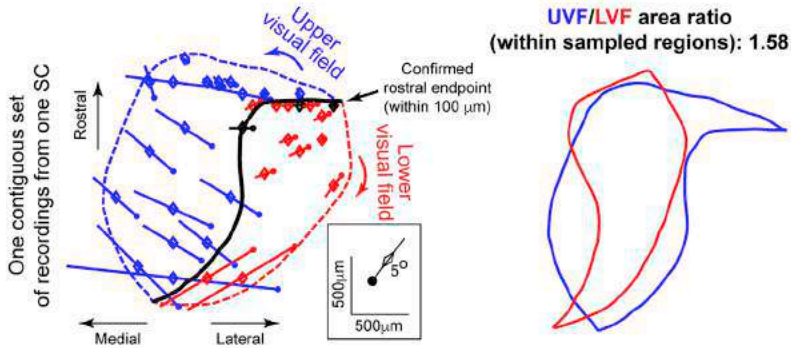
pothesized earlier using horizontal saccades [9, 19]. Moreover, because motor RFs show similar effects to visual RFs (Figure 2), this also applies for the SC’s motor map (Figure S7).

### DISCUSSION

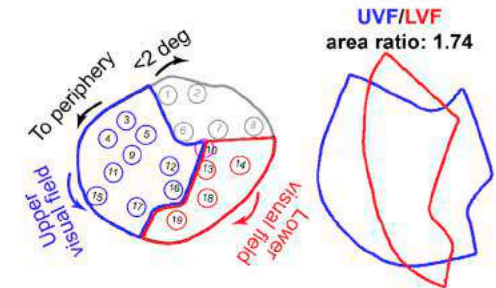
We observed a sharper, stronger, and lower-latency UVF representation in the primate SC, and also explored the behavioral and neuroanatomical consequences of these observations. Our results, showing an over-representation of the UVF (Figure 6), highlight the importance of analyzing structure-function relationships in the visual system.

Our results also motivate revisiting classic controversies about SC saccade-related dynamics. Specifically, peri-saccadic spreading of SC activity was hypothesized [9], but these results were hard to interpret and/or replicate [25]. These difficulties may have arisen exactly because of visual field locations. For example, much work on this issue used only horizontal saccades [9] or has used analyses assuming UVF/LVF symmetry [25]. However, if there are different UVF and LVF spatial pooling patterns (Figures 2, S3, and S4) and dynamics (Figures 4 and 5), then different “spreading” patterns (a hallmark of spatial pooling and lateral interaction [26]) may be expected to occur for UVF

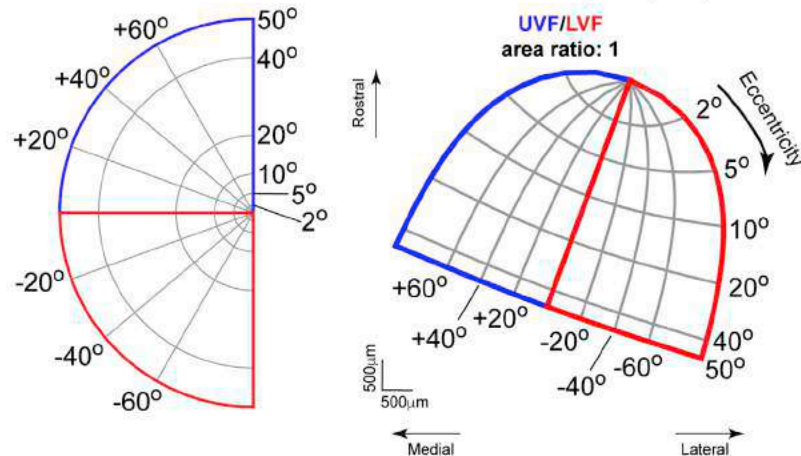
### A Preferred eccentricity and direction at SC surface for different electrode locations - Monkey N, Right SC



### B Cynader & Berman, 1972



### C Polar coordinates Ottes et al., 1986 model; based on the “Robinson (1972) map”



### D Model amended to include an over-representation of the UVF

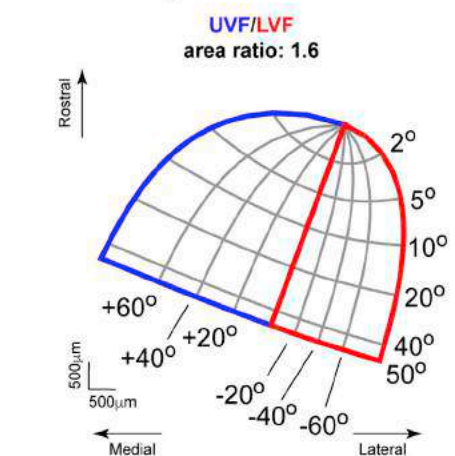


#### Figure 6. Over-Representation of the UVF in the Primate SC

(A) The left panel shows eccentricity and direction at the SC surface from one contiguous set of electrode penetrations. We mapped the rostral (foveal) SC with 100- $\mu\text{m}$  resolution and a significant chunk of the caudal (peripheral) region. Each diamond indicates an electrode location; each colored line indicates eccentricity (length of line) and direction (direction of line, starting from the filled circle) encoded at the SC surface. Eccentricity is scaled according to the 5-degree diagonal line in the inset. Colors delineate UVF and LVF. The UVF representation was larger: the right panel summarizes the area within contours delineating UVF and LVF electrode tracks. Note that due to foveal magnification, neighboring locations in the rostral sites of the left panel appear to have similar directions and eccentricities to each other. However, we confirmed that preferred direction still consistently changes as a function of medio-lateral SC location across eccentricities (data not shown). In fact, in the most caudal sites of the left panel, where there is less foveal magnification, clearer medio-lateral changes in preferred directions can be seen [14].

(B) Meta-analysis of Cynader and Berman [13]. Shown are electrode locations, which we color coded according to the UVF and LVF (left). Because foveal neurons (gray color) were not described in [13], we excluded them from the meta-analysis. The UVF region is larger, and the area ratio of blue and red contours (right) is consistent with (A). Modified with permission from [13].

(C) A popular model of SC mapping, from Ottes et al. [19] and based on Robinson [14], having identical UVF/LVF representations.

(D) Our proposed revised model (Experimental Procedures).

Also see Figures 7 and S7.

versus LVF saccades. In fact, even though we did not explicitly sample deep “buildup” neurons showing the most convincing spreading [9], we nonetheless identified differences in UVF/LVF saccade-related spreading (Figure S4B). This result is further supported by a theoretical hypothesis on the effect of asymmetries in internal SC connections on population dynamics [26]. Thus, the UVF/LVF asymmetry that we uncovered can have a substantial impact on our understanding of saccade control by the SC.

Our results may also help identify functional sources of residual visual capabilities after brain lesions. For example, subjects without primary visual cortex lose conscious perception but still exhibit “blindsight” [42]. Blindsight, a residual visual capability, could primarily arise through a retino-tectal pathway [43] traversing the SC or an extra-striate retino-geniculate pathway through LGN [44]. Given that the SC UVF asymmetry may be the exact opposite [24] (see below) of potential asymmetries that are present in at least some cortical visual areas, like MT

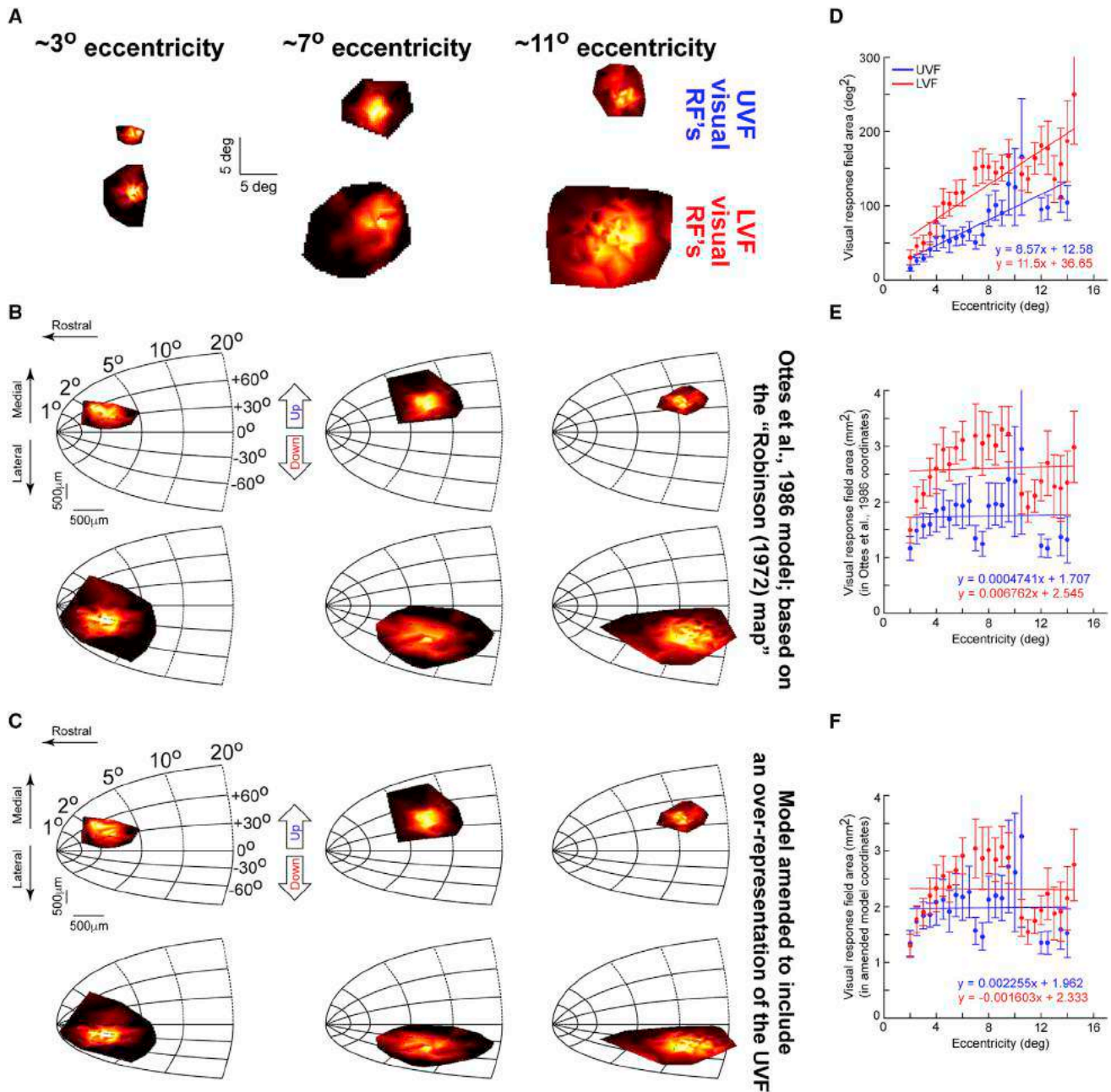


**Figure 7. Implications of UVF Over-Representation on the Active SC Population Size for a Given Stimulus Location**

(A) Example visual RFs from three eccentricity-matched pairs of UVF (top row) or LVF (bottom row) neurons. RF area increased with eccentricity and was larger in the LVF (Figure 2).

(B) The same RFs projected onto anatomical SC tissue using the Ottes et al. model [19] of the Robinson SC topographic map [9, 14, 19]. In each row (i.e., for either UVF or LVF neurons individually), RF sizes across the three eccentricities were roughly equalized (the most eccentric RF was decreased in size and the most central RF was magnified due to logarithmic warping). This is consistent with observations [9] made for horizontal saccades, and suggests that the size of the active SC population for a given saccade may be equalized in tissue coordinates [9, 19]. However, when different directions are considered, RFs cannot be equalized (compare the two rows).

(C) With our revised model (Figure 6D), the UVF is magnified. Thus, RF area can be equalized both in terms of eccentricity (compare neurons in either the UVF or LVF individually) and UVF/LVF location (compare neurons in a given eccentricity across the UVF or LVF).

(D) Population analysis similar to [9], showing dependence of RF area (in visual coordinates) on eccentricity and UVF/LVF location.

(E) The same data as in (D) plotted in SC coordinates using the original Ottes et al. model [19]. RF area was roughly equalized [9] in either the UVF or LVF (horizontal regression lines), but there was still a UVF/LVF asymmetry (the two regression lines are apart).

(F) The same data as in (D) and (E) plotted in revised SC coordinates. RF area was now roughly equalized not just for eccentricity but also for UVF/LVF location. Note that if the UVF magnification factor of the revised model is optimized further, the UVF/LVF differences that remain in this panel can be further reduced.

Error bars indicate the SEM. Also see Figure S7.

[45], it could be the case that patterns of UVF versus LVF visual abilities/deficits exhibited in blindsight may help clarify on which alternative pathways blindsight subjects rely. For example, inspecting published saccade data from blindsight monkeys [46], we found that their patterns of landing errors were strongly consistent with what our results predict if the SC were a primary determinant of their performance. Thus, our results could resolve historical debates about the functional importance of the SC's visual analysis properties, some of which, like spatial-frequency tuning, are yet to be fully investigated.

Related to the above, it is not yet entirely clear which (or whether) early visual cortical areas would exhibit strong UVF/LVF asymmetries. It is sometimes assumed that V1 is symmetric [47], although there is variability among studies. It was also shown that MT over-represents the LVF [45]. However, because of an experimental bias to record from dorsal cortical tissue, and because work investigating detailed cortical topographies is quite old [45], much still remains to be learned about detailed UVF/LVF asymmetries in different visual and motor areas. Given Previc's hypotheses about ecological constraints on functional specialization in the visual system [24], one might make predictions. Specifically, Previc has hypothesized that areas analyzing properties of retinal images that typically occupy near space (e.g., having motion and stereo disparity patterns associated with near objects) might over-represent the LVF, and that areas needed for exploration of far space might over-represent the UVF [24]. Given this, the frontal eye field (FEF), implicated in eye-movement exploration, might exhibit UVF over-representation like the SC. Interestingly, in a recent study characterizing FEF RFs [48], ~70% of neurons were UVF neurons (51/73 in Figure 2D of [48]). Likewise, saccade-direction cells in entorhinal cortex exhibit a strong bias toward upward saccades [49]. Thus, UVF over-representation may emerge in a variety of areas implicated in visual exploration.

More generally, our results demonstrate that even for simple two-dimensional image maps, there exists remarkable optimization that goes well beyond foveal magnification. This idea is in line with emerging evidence that the visual system is well adapted to its environment. For example, mouse retinal photoreceptor distributions and spectral responses provide near-optimal sampling of the environment above and below the horizon [50]. Similarly, some mouse retinal ganglion cells have non-uniform topographies allowing them to preferentially enhance sampling of, say, frontal visual fields [51]. Finally, the mouse SC itself over-represents the UVF [52]. Thus, detailed specialization patterns within individual brain regions may be more pervasive than previously thought.

Finally, our results run contrary to a universally accepted model of SC topography [14, 19], which is used heavily to document, analyze, and interpret results. However, such interpretation might be misguided by pure symmetry assumptions. Our revised model (Figures 6D and 7) provides what we hope is a more useful tool for future studies of this important brain structure.

## EXPERIMENTAL PROCEDURES

### Animal Preparation

Ethics committees at the Tuebingen regional governmental offices approved the experiments. Monkeys P and N (male, *Macaca mulatta*, aged 7 years) were prepared earlier [32, 53, 54].

### Behavioral Tasks

#### Visually Guided Saccade Task

A spot [32, 53, 54] was presented for 300–3,600 ms (monkey N) or 420–3,150 ms (monkey P). A white saccade target (1-degree-diameter circle) then appeared (5-degree eccentricity) in one of eight directions, and fixation was released. This task was used for behavioral tests (Figures S6A and S6B). We analyzed 24,396 (monkey N) and 17,446 (monkey P) trials.

#### Delayed Visually Guided Saccade Task

A spot was presented for 300–1,000 ms. An eccentric spot was then presented. The fixation spot was removed 500–1,000 ms later. Monkeys oriented to the eccentric spot. We collected >100 trials per neuron and varied target location to map visual and saccade-related RFs.

#### Memory-Guided Saccade Task

A spot was presented for 300–1,000 ms. An eccentric spot was flashed for ~50 ms. The fixation spot remained on for 300–1,100 ms before disappearing. Monkeys oriented toward the remembered flash location (within <2.5 degrees). We collected >45 trials per neuron, and placed the flash at the RF hotspot (assessed from the delayed visually guided saccade task or the fixation visual RF mapping task).

We used this task for classifying neurons as visual, visual-motor, or motor [32]. We also used it to study visual response strength and first-spike latency (Figures 1C, 1D, 4A–4F, and 5) because we had a well-controlled, repeatable stimulus location across trials (we also confirmed the observations with other tasks). Finally, we also analyzed additional saccade properties (see Figures S6C and S6D). We collected this task in 277 neurons.

#### Fixation Visual RF Mapping Task

In 78 neurons, we confirmed visual RF maps from the delayed visually guided saccade task by using a similar task involving fixation. The same sequence of events happened, except that the fixation spot was not removed at trial end. In a minority of neurons, we used this task instead of the saccade version for visual RF mapping. However, the two tasks were identical in the stimulus-induced phase.

#### Spatial-Frequency Tuning

Monkeys fixated a spot while we flashed a stationary vertical Gabor grating (80% contrast) filling the RF. Grating frequency was 0.56, 1.11, 2.22, 4.44, or 11.11 cycles/degree. Grating phase was randomized. We collected data from 106 neurons in this task.

#### Contrast Sensitivity

We analyzed data anew from [32], plus seven newly recorded neurons (total 110 neurons).

### Data Analysis

When analyzing visual responses, we combined data from visual and visual-motor neurons because they showed similar results. Similarly, when analyzing motor responses, we combined motor and visual-motor neurons.

#### RF Areas

From the delayed visually guided saccade task or the fixation visual RF mapping task, we measured peak firing rate 30–150 ms after stimulus onset. We classified stimulus locations with activity >3 SDs from baseline (0–200 ms before stimulus onset) as being within the visual RF (e.g., dots in Figure 1B). We also Delaunay triangulated locations and linearly interpolated to generate three-dimensional surfaces (e.g., Figure 1B). We measured the area of all significant locations. The RF hotspot was the location with maximal activity. For motor RFs, we repeated the same procedure but measured mean pre-saccadic (within 50 ms) firing rate.

For Figures 2A and 2E, we binned eccentricities into 1.5-degree bins (with running windows of 0.5-degree step size and a minimum of seven neurons per bin). We could not map RF area at very large eccentricities because of display-system constraints. For a given eccentricity range (Figure 2B), we also binned RF directions into 20-degree bins (in steps of 10 degrees and a minimum of ten neurons per bin).

#### Spatial-Frequency Tuning

We only analyzed trials without microsaccades <100 ms from stimulus onset. We measured peak visual response 20–150 ms after grating onset. We constructed tuning curves according to

$$f.r.(sf) = a_1 e^{-\left(\frac{sf-b_1}{c_1}\right)^2} - a_2 e^{-\left(\frac{sf-b_2}{c_2}\right)^2} + B, \quad (\text{Equation 1})$$

where  $f.r.$  is firing rate,  $sf$  is spatial frequency,  $B$  is baseline firing rate, and  $a_1$ ,  $b_1$ ,  $c_1$ ,  $a_2$ ,  $b_2$ , and  $c_2$  are parameters. The spatial frequency for which Equation 1 peaked was the preferred spatial frequency. To facilitate visualizing preferences across neurons (e.g., Figure 3B), we normalized curves by their maximum.

#### Contrast Sensitivity

We fit mean visual response 50–150 ms after grating onset using [32]

$$f.r.(c) = R \frac{c^n}{c_{50}^n + c^n} + B, \quad (\text{Equation 2})$$

where  $c$  is contrast. For dynamic range, we calculated the difference between maximum and minimum in a fitted curve. We also only analyzed no-microsaccade trials.

#### First-Spike Latency

We analyzed neurons with zero baseline activity (i.e., the majority). We manually defined time ranges after stimulus onset and searched for first spikes. Figure 4F binning was like in Figure 2B.

LFP analyses, population reconstruction, SC surface topography estimates, and modeling are described in detail in the Supplemental Experimental Procedures.

### SUPPLEMENTAL INFORMATION

Supplemental Information includes Supplemental Experimental Procedures and seven figures and can be found with this article online at <http://dx.doi.org/10.1016/j.cub.2016.04.059>.

### AUTHOR CONTRIBUTIONS

Z.M.H. and C.-Y.C. performed the experiments and analyzed the data. Z.M.H. wrote the paper.

### ACKNOWLEDGMENTS

The authors were funded by the Werner Reichardt Centre for Integrative Neuroscience (CIN) at the Eberhard Karls University of Tuebingen. The CIN is an Excellence Cluster funded by the Deutsche Forschungsgemeinschaft (DFG) within the framework of the Excellence Initiative (EXC 307).

Received: February 12, 2016

Revised: March 23, 2016

Accepted: April 22, 2016

Published: June 9, 2016

### REFERENCES

- Wurtz, R.H., and Albano, J.E. (1980). Visual-motor function of the primate superior colliculus. *Annu. Rev. Neurosci.* **3**, 189–226.
- Gandhi, N.J., and Katnani, H.A. (2011). Motor functions of the superior colliculus. *Annu. Rev. Neurosci.* **34**, 205–231.
- Krauzlis, R.J., Lovejoy, L.P., and Zénon, A. (2013). Superior colliculus and visual spatial attention. *Annu. Rev. Neurosci.* **36**, 165–182.
- Dash, S., Yan, X., Wang, H., and Crawford, J.D. (2015). Continuous updating of visuospatial memory in superior colliculus during slow eye movements. *Curr. Biol.* **25**, 267–274.
- Klier, E.M., Wang, H., and Crawford, J.D. (2001). The superior colliculus encodes gaze commands in retinal coordinates. *Nat. Neurosci.* **4**, 627–632.
- Goossens, H.H., and van Opstal, A.J. (2012). Optimal control of saccades by spatial-temporal activity patterns in the monkey superior colliculus. *PLoS Comput. Biol.* **8**, e1002508.
- Goossens, H.H., and Van Opstal, A.J. (2006). Dynamic ensemble coding of saccades in the monkey superior colliculus. *J. Neurophysiol.* **95**, 2326–2341.
- Munoz, D.P., and Wurtz, R.H. (1995). Saccade-related activity in monkey superior colliculus. I. Characteristics of burst and buildup cells. *J. Neurophysiol.* **73**, 2313–2333.
- Munoz, D.P., and Wurtz, R.H. (1995). Saccade-related activity in monkey superior colliculus. II. Spread of activity during saccades. *J. Neurophysiol.* **73**, 2334–2348.
- McPeck, R.M., and Keller, E.L. (2004). Deficits in saccade target selection after inactivation of superior colliculus. *Nat. Neurosci.* **7**, 757–763.
- Carello, C.D., and Krauzlis, R.J. (2004). Manipulating intent: evidence for a causal role of the superior colliculus in target selection. *Neuron* **43**, 575–583.
- Sadeh, M., Sajad, A., Wang, H., Yan, X., and Crawford, J.D. (2015). Spatial transformations between superior colliculus visual and motor response fields during head-unrestrained gaze shifts. *Eur. J. Neurosci.* **42**, 2934–2951.
- Cynader, M., and Berman, N. (1972). Receptive-field organization of monkey superior colliculus. *J. Neurophysiol.* **35**, 187–201.
- Robinson, D.A. (1972). Eye movements evoked by collicular stimulation in the alert monkey. *Vision Res.* **12**, 1795–1808.
- Sparks, D.L., and Nelson, I.S. (1987). Sensory and motor maps in the mammalian superior colliculus. *Trends Neurosci.* **10**, 312–317.
- Hinton, G.E., McClelland, J.L., and Rumelhart, D.E. (1986). Distributed representations. In *Parallel Distributed Processing: Explorations in the Microstructure of Cognition, Volume 1: Foundations*, D.E. Rumelhart, and J.L. McClelland, eds. (MIT Press), pp. 77–109.
- Pouget, A., Dayan, P., and Zemel, R. (2000). Information processing with population codes. *Nat. Rev. Neurosci.* **1**, 125–132.
- Lee, C., Rohrer, W.H., and Sparks, D.L. (1988). Population coding of saccadic eye movements by neurons in the superior colliculus. *Nature* **332**, 357–360.
- Ottes, F.P., Van Gisbergen, J.A., and Eggermont, J.J. (1986). Visuomotor fields of the superior colliculus: a quantitative model. *Vision Res.* **26**, 857–873.
- Ko, H.K., Poletti, M., and Rucci, M. (2010). Microsaccades precisely relocate gaze in a high visual acuity task. *Nat. Neurosci.* **13**, 1549–1553.
- Tian, X., Yoshida, M., and Hafed, Z.M. (2016). A microsaccadic account of attentional capture and inhibition of return in Posner cueing. *Front. Syst. Neurosci.* **10**, 23.
- Hafed, Z.M., Goffart, L., and Krauzlis, R.J. (2009). A neural mechanism for microsaccade generation in the primate superior colliculus. *Science* **323**, 940–943.
- Hafed, Z.M., and Krauzlis, R.J. (2012). Similarity of superior colliculus involvement in microsaccade and saccade generation. *J. Neurophysiol.* **107**, 1904–1916.
- Previc, F.H. (1990). Functional specialization in the lower and upper visual fields in humans: its ecological origins and neurophysiological implications. *Behav. Brain Sci.* **13**, 519–542.
- Anderson, R.W., Keller, E.L., Gandhi, N.J., and Das, S. (1998). Two-dimensional saccade-related population activity in superior colliculus in monkey. *J. Neurophysiol.* **80**, 798–817.
- Nakahara, H., Morita, K., Wurtz, R.H., and Optican, L.M. (2006). Saccade-related spread of activity across superior colliculus may arise from asymmetry of internal connections. *J. Neurophysiol.* **96**, 765–774.
- Choi, W.Y., and Guitton, D. (2009). Firing patterns in superior colliculus of head-unrestrained monkey during normal and perturbed gaze saccades reveal short-latency feedback and a sluggish rostral shift in activity. *J. Neurosci.* **29**, 7166–7180.
- Goldberg, M.E., and Wurtz, R.H. (1972). Activity of superior colliculus in behaving monkey. I. Visual receptive fields of single neurons. *J. Neurophysiol.* **35**, 542–559.
- Rubin, N., Nakayama, K., and Shapley, R. (1996). Enhanced perception of illusory contours in the lower versus upper visual hemifields. *Science* **271**, 651–653.

30. De Valois, K.K., De Valois, R.L., and Yund, E.W. (1979). Responses of striate cortex cells to grating and checkerboard patterns. *J. Physiol.* *291*, 483–505.
31. De Valois, R.L., and De Valois, K.K. (1980). Spatial vision. *Annu. Rev. Psychol.* *31*, 309–341.
32. Chen, C.Y., Ignashchenkova, A., Thier, P., and Hafed, Z.M. (2015). Neuronal response gain enhancement prior to microsaccades. *Curr. Biol.* *25*, 2065–2074.
33. Boehnke, S.E., and Munoz, D.P. (2008). On the importance of the transient visual response in the superior colliculus. *Curr. Opin. Neurobiol.* *18*, 544–551.
34. Hafed, Z.M., Chen, C.-Y., and Tian, X. (2015). Vision, perception, and attention through the lens of microsaccades: mechanisms and implications. *Front. Syst. Neurosci.* *9*, 167.
35. Hafed, Z.M., and Krauzlis, R.J. (2010). Microsaccadic suppression of visual bursts in the primate superior colliculus. *J. Neurosci.* *30*, 9542–9547.
36. Schlykova, L., Hoffmann, K.P., Bremmer, F., Thiele, A., and Ehrenstein, W.H. (1996). Monkey saccadic latency and pursuit velocity show a preference for upward directions of target motion. *Neuroreport* *7*, 409–412.
37. Zhou, W., and King, W.M. (2002). Attentional sensitivity and asymmetries of vertical saccade generation in monkey. *Vision Res.* *42*, 771–779.
38. Cerkevich, C.M., Lyon, D.C., Balaram, P., and Kaas, J.H. (2014). Distribution of cortical neurons projecting to the superior colliculus in macaque monkeys. *Eye Brain* *2014*, 121–137.
39. Van Essen, D.C. (1979). Visual areas of the mammalian cerebral cortex. *Annu. Rev. Neurosci.* *2*, 227–263.
40. Felleman, D.J., and Van Essen, D.C. (1991). Distributed hierarchical processing in the primate cerebral cortex. *Cereb. Cortex* *1*, 1–47.
41. Fischer, B., and Boch, R. (1983). Saccadic eye movements after extremely short reaction times in the monkey. *Brain Res.* *260*, 21–26.
42. Leopold, D.A. (2012). Primary visual cortex: awareness and blindsight. *Annu. Rev. Neurosci.* *35*, 91–109.
43. Kato, R., Takaura, K., Ikeda, T., Yoshida, M., and Isa, T. (2011). Contribution of the retino-tectal pathway to visually guided saccades after lesion of the primary visual cortex in monkeys. *Eur. J. Neurosci.* *33*, 1952–1960.
44. Schmid, M.C., Mrowka, S.W., Turchi, J., Saunders, R.C., Wilke, M., Peters, A.J., Ye, F.Q., and Leopold, D.A. (2010). Blindsight depends on the lateral geniculate nucleus. *Nature* *466*, 373–377.
45. Van Essen, D.C., Maunsell, J.H., and Bixby, J.L. (1981). The middle temporal visual area in the macaque: myeloarchitecture, connections, functional properties and topographic organization. *J. Comp. Neurol.* *199*, 293–326.
46. Yoshida, M., Takaura, K., Kato, R., Ikeda, T., and Isa, T. (2008). Striate cortical lesions affect deliberate decision and control of saccade: implication for blindsight. *J. Neurosci.* *28*, 10517–10530.
47. He, S., Cavanagh, P., and Intriligator, J. (1996). Attentional resolution and the locus of visual awareness. *Nature* *383*, 334–337.
48. Mayo, J.P., DiTomasso, A.R., Sommer, M.A., and Smith, M.A. (2015). Dynamics of visual receptive fields in the macaque frontal eye field. *J. Neurophysiol.* *114*, 3201–3210.
49. Killian, N.J., Potter, S.M., and Buffalo, E.A. (2015). Saccade direction encoding in the primate entorhinal cortex during visual exploration. *Proc. Natl. Acad. Sci. USA* *112*, 15743–15748.
50. Baden, T., Schubert, T., Chang, L., Wei, T., Zaichuk, M., Wissinger, B., and Euler, T. (2013). A tale of two retinal domains: near-optimal sampling of achromatic contrasts in natural scenes through asymmetric photoreceptor distribution. *Neuron* *80*, 1206–1217.
51. Bleckert, A., Schwartz, G.W., Turner, M.H., Rieke, F., and Wong, R.O. (2014). Visual space is represented by nonmatching topographies of distinct mouse retinal ganglion cell types. *Curr. Biol.* *24*, 310–315.
52. Dräger, U.C., and Hubel, D.H. (1976). Topography of visual and somatosensory projections to mouse superior colliculus. *J. Neurophysiol.* *39*, 91–101.
53. Chen, C.Y., and Hafed, Z.M. (2013). Postmicrosaccadic enhancement of slow eye movements. *J. Neurosci.* *33*, 5375–5386.
54. Hafed, Z.M., and Ignashchenkova, A. (2013). On the dissociation between microsaccade rate and direction after peripheral cues: microsaccadic inhibition revisited. *J. Neurosci.* *33*, 16220–16235.



**Current Biology, Volume 26**

**Supplemental Information**

**Sharper, Stronger, Faster Upper Visual Field  
Representation in Primate Superior Colliculus**

**Ziad M. Hafed and Chih-Yang Chen**

## Supplemental Figures

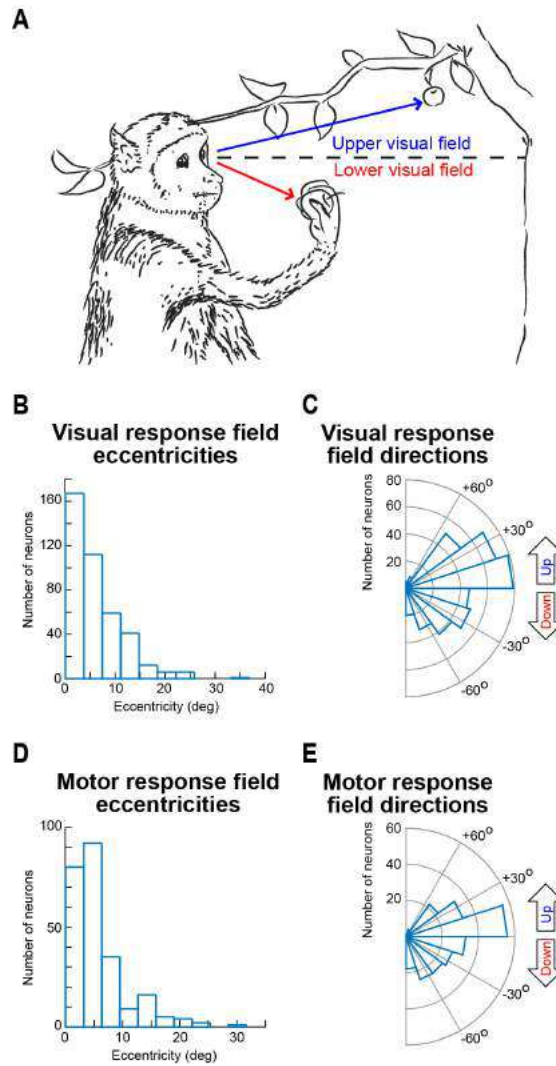


**Figure S1, Related to Figure 1.** (A) A situation similar to that shown in Fig. 1A, but using an example of a monkey in its natural habitat (modified with permission from [S1]). Relative to the line of sight (dashed black line), the apple in the LVF is closer to the monkey than the apple in the UVF. The LVF apple would thus project a larger retinal image. (B-E) Locations of SC visual and motor (saccade-related) RF's recorded for the current study. (B, D) RF hotspot eccentricities across neurons. (C, E) RF hotspot directions from horizontal. Note that we sampled neurons in both the right and left SC in both monkeys. However, in (C, E), we show directions collapsed together into one side of space, in order to facilitate presentation of the range of UVF/LVF directions that we sampled. Fig. S2 shows controls when only the right or left SC was analyzed. Also, note that we collected samples in many directions (from predominantly pure down to predominantly pure up). However, we had relatively fewer samples beyond  $\pm 60$  deg from horizontal. Thus, even though we still showed individual examples from beyond  $\pm 60$  deg (e.g. Fig. S2C), our summary plots were primarily restricted to the directions with maximal support in our population (and similarly for eccentricity summaries).

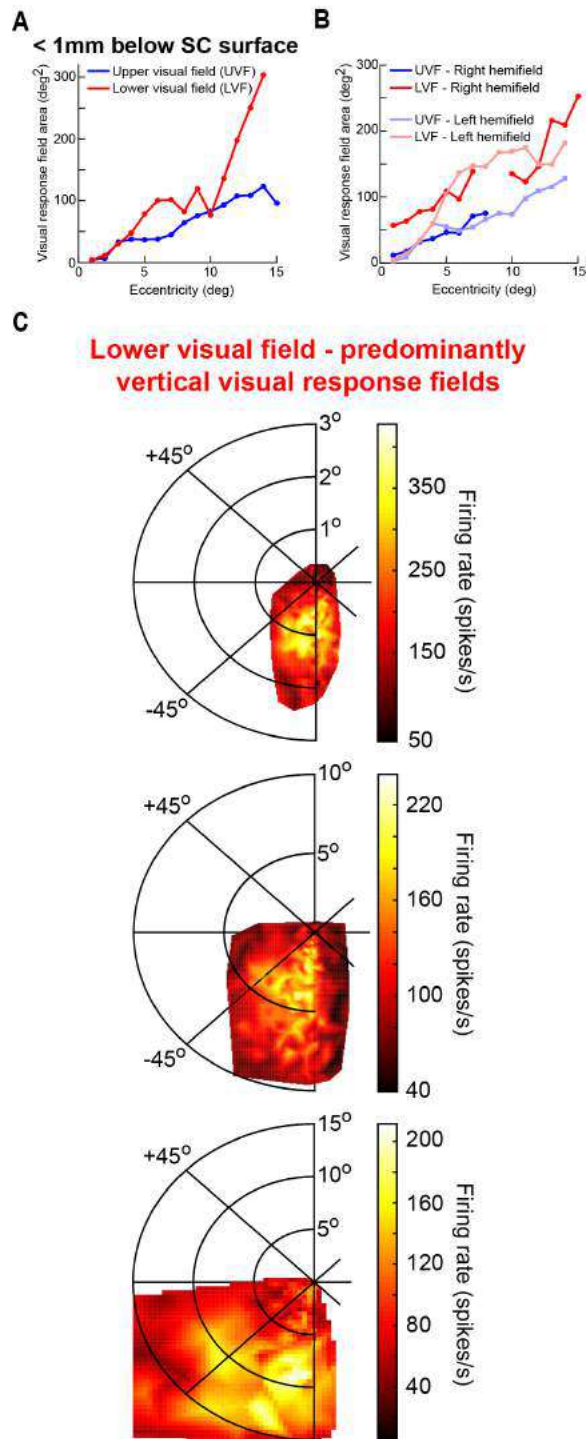


**Figure S2, Related to Figure 2.** (A, B) Analyses similar to those in Fig. 2A, but restricted to only superficial SC layers (A) or one side of space (B). (A) indicates that even the most superficial layer neurons show an UVF/LVF asymmetry in RF area. A 2-way ANOVA revealed statistically significant main effects of both eccentricity and UVF/LVF location ( $p < 0.05$  for each main factor). Similar analyses for deeper neurons ( $> 1$  mm) also revealed significant main effects of eccentricity and UVF/LVF location. Thus, the effect in Fig. 2A is not an artifact of sampling deeper neurons with larger RF's. Also, note that our behavioral effects (Fig. S6), as well as motor RF area effects (Figs. 2D,E, S3), support the conclusion that

the asymmetry seen in Fig. 2A is a functional property of SC architecture and not an analysis artifact. The sample neurons presented in Fig. 1 (having similar depth and RF hotspot eccentricity) also support this conclusion. **(B)** indicates that a similar UVF/LVF asymmetry in RF area existed in either the left or right SC, representing either the right or left visual hemifield, respectively. We confirmed this statistically: for either the right or left hemifield individually, a 2-way ANOVA confirmed that RF area depended on both main factors of eccentricity and UVF/LVF location ( $p < 0.05$  for each main effect). **(C)** Example visual RF's for predominantly vertical neurons in the LVF. We noticed elongated RF shapes for such neurons, and the RF's had a relatively large extent even for the top-most central neuron (notice the eccentricity scale bar for each neuron). In our experiments, predominantly vertical UVF neurons did not seem to exhibit such elongation and size increase, at least not in our recorded sample of neurons.

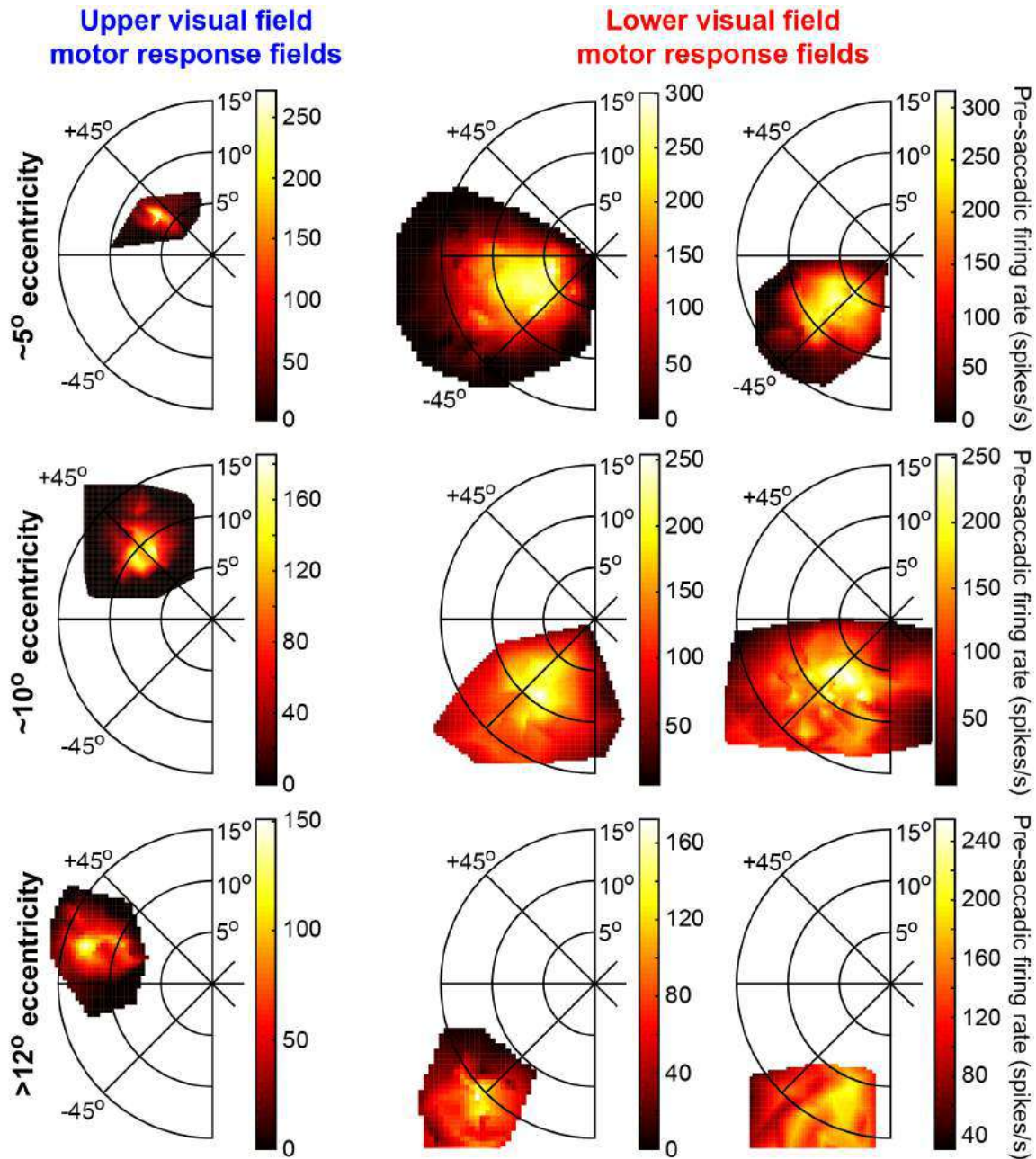


**Figure S3, Related to Figure 2.** Example saccade-related motor RF's for UVF and LVF SC neurons. Each row shows 3 example neurons from a given RF hotspot eccentricity. In each row, the leftmost neuron is an UVF neuron, and the rightmost two neurons are LVF neurons closely matched in eccentricity. As can be seen, the UVF neurons had motor RF's that were consistently smaller than the motor RF's of LVF neurons. Thus, higher-resolution UVF spatial representation in the primate SC extends to the efferent saccade-related maps of this structure (also see Fig. 2E). This is consistent with behavioral properties of saccades, even in the absence of a visual stimulus (Fig. S6). Note that in the top row, the leftmost two example neurons shown here are the same as those shown in Fig. 2D. They are included here to facilitate comparison to the rightmost neuron having a closely matched motor RF hotspot eccentricity.

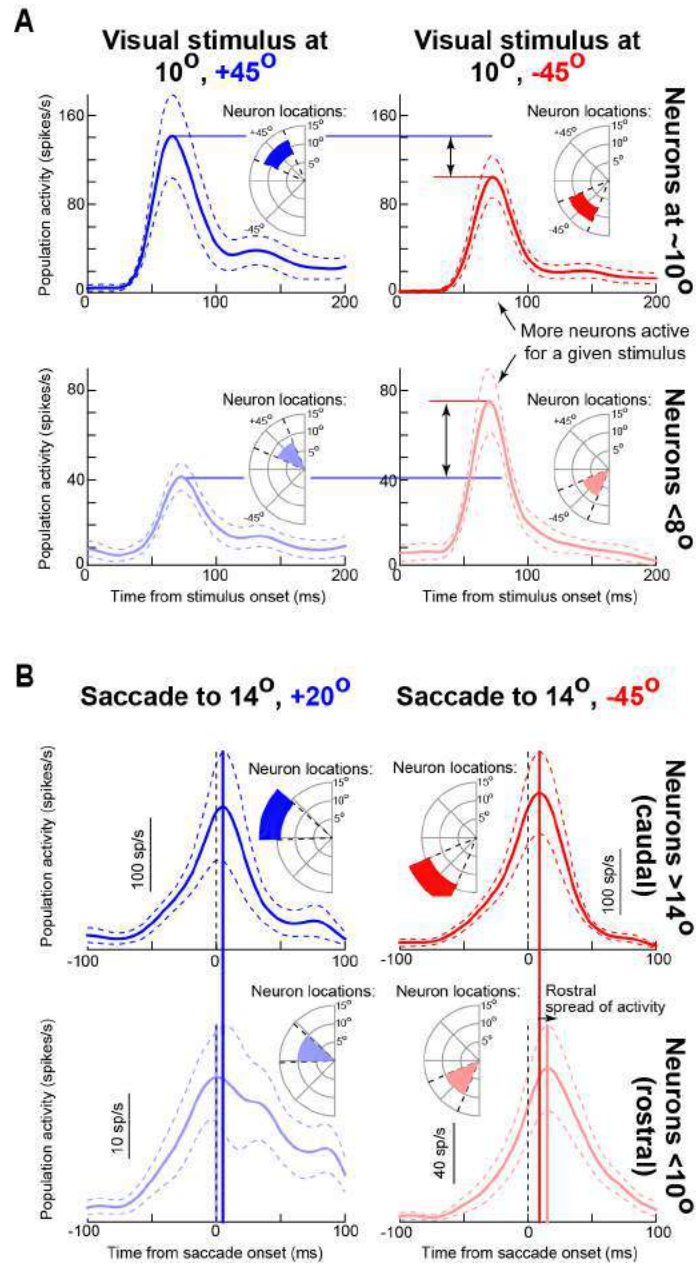


**Figure S4, Related to Figures 2, 4, 5.** Population reconstruction of SC activity following the presentation of a visual stimulus at a single location (**A**) or during the generation of a saccade to a specific endpoint (**B**). (**A**) In the left column, we asked how different SC neurons would be activated for a stimulus presented at 10 deg eccentricity and +45 deg above the horizontal meridian (from the delayed visually-guided saccade task, Experimental Procedures). For all presentations of this stimulus, we measured the activity of all neurons regardless of their visual RF hotspot location. We then plotted the responses of neurons with RF hotspots either close to the stimulus location (upper row, saturated blue) or of neurons with more central RF hotspot locations (bottom row, faint blue). We repeated the same analysis in the right column, but for a stimulus (and neurons) in the LVF. As can be seen, in the UVF, the more central neurons were much less active than the neurons with hotspot location near the stimulus location (compare the bottom and top panels in the left column). This is expected since more central neurons prefer more central locations than 10 deg, and UVF RF's are small (Figs. 1-2). However, for the LVF condition (right column), the change in firing rate between the top and bottom panels is smaller. This indicates that, because of their larger RF's, neurons whose RF hotspot locations are farther away from the stimulus would be more likely to still "see" the

stimulus in the LVF than in the UVF. Thus, our results of UVF/LVF differences in visual RF area have implications on population coding schemes in the SC (also see Figs. 7, S7). Also note that neurons at the preferred stimulus location were more active in the UVF than in the LVF (compare the top two panels), consistent with Figs. 1, 4A-C, 5. **(B)** Potential implication of saccade-related firing rate and RF area asymmetries on historically contentious debates about the SC's role in saccade generation. We performed a similar reconstruction of population activity to that performed in **(A)**. However, this time, we reconstructed saccade-related activity (instead of visually-evoked activity) for two example saccades (from the delayed visually-guided saccade task, Experimental Procedures): one to the UVF (left column) and one to the LVF (right column). The solid vertical lines show the times of peak saccade-related discharge in each panel. Besides the fact that the more central neurons (compare the bottom two panels, noting the difference in scale bars) were more active in the LVF condition than in the UVF condition (confirming **A**), we also found an additional asymmetry in the motor responses. Specifically, in the LVF condition (right column), more central neurons show a later peak discharge than more peripheral neurons encoding the actual saccade endpoint (compare vertical saturated and faint red lines). This effect means that central neurons become activated later than peripheral neurons (akin to a spread of activity during the saccade) [S2]. This effect was absent for a similarly sized saccade in the UVF (left column). We also replicated the effect for other large saccade amplitudes (>10 deg). We should emphasize here that we did not explicitly sample "buildup" SC neurons, for which the spread has been most robustly reported in the literature [S2]. Nonetheless, we still see evidence of an effect even in our more superficial visual-motor neurons, and, more importantly, we also see evidence that this phenomenon might critically depend on UVF/LVF asymmetries. This makes sense in retrospect, because such spreading of activity is expected to depend on lateral interactions [S3], which our results suggest might be very different in the UVF and LVF. Also, note that the effect in the right column is small, which is consistent with evidence that saccade-related spreading occurs most robustly for saccades >20-30 deg [S4], which are larger than those we investigated here. Error bars in all panels denote s.e.m.

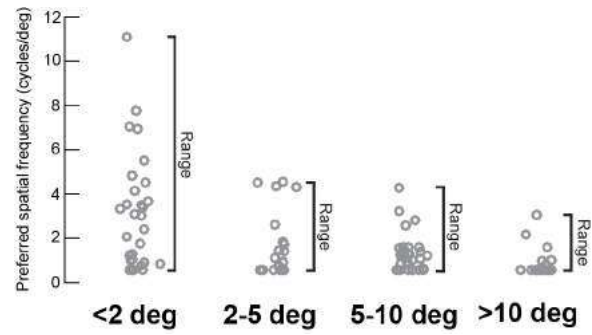


**Figure S5, Related to Figure 3.** Preferred spatial frequencies of individual SC neurons at different retinotopic eccentricities. Each circle represents a neuron (note that we jittered the horizontal position of the circles within a column in order to avoid multiple neurons from masking each other). Consistent with cortical visual areas, neurons at a given eccentricity exhibited a range of preferred spatial frequencies (square brackets highlight the ranges of spatial-frequency channels observed in each eccentricity range). Thus, multiple spatial-frequency channels are represented within a given eccentricity in the SC. Moreover, and again consistent with cortical visual areas, spatial-frequency preferences consistently decreased with increasing retinotopic eccentricity ( $p < 0.05$ , 1-way ANOVA with eccentricity as the main factor). Thus, the SC becomes increasingly low-pass in the periphery. The main text shows that in addition to the properties shown in this figure, there are also UVF/LVF asymmetries in spatial-frequency channels in the SC (Fig. 3A, B).



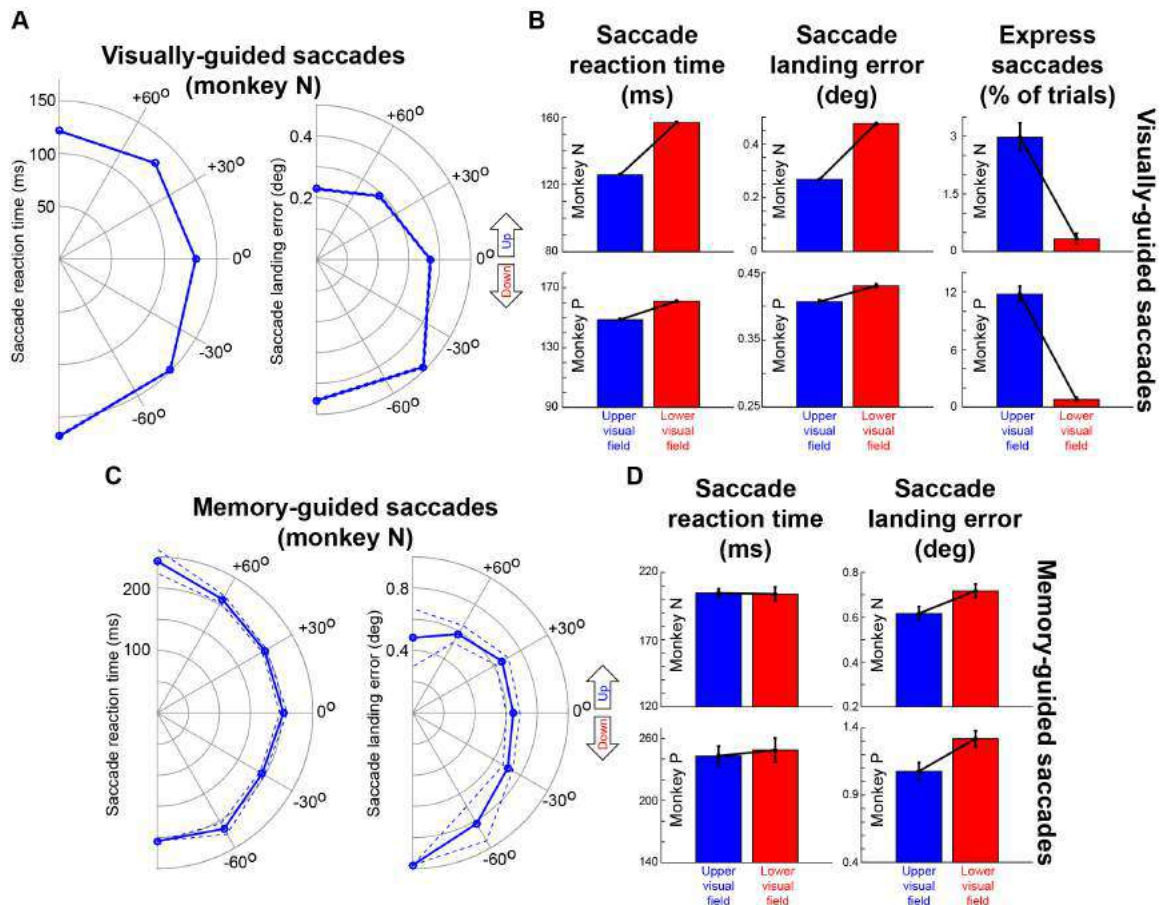


**Figure S6, Related to Figures 2, 4, 5.** Lower-latency, more accurate UVF saccades. **(A)** Saccadic RT (left) and landing error (right) as a function of target location during immediate, visually-guided saccades from one monkey. Right/left target locations were collapsed onto one side to facilitate viewing of UVF/LVF effects. Both RT and landing error decreased in the UVF ( $p < 0.05$ , two-tailed t-test between UVF and LVF locations for each of RT and landing error). The RT effect likely reflects stronger and lower-latency UVF SC visual bursts, and the landing error effect likely reflects smaller UVF visual and motor RF areas. **(B)** The leftmost two columns summarize the results in **(A)** for each of the two monkeys. In both monkeys, RT and landing error were smaller in the UVF ( $p < 0.05$ , two-tailed t-test). In the rightmost column, we plotted the likelihood of express saccades in the same data. There was a 9-fold to 14-fold increase in express saccade probability in the UVF (error bars in this column show 95% confidence intervals and demonstrate the statistical significance of the result). This is a strong effect given that express saccades are expected to be rare or completely absent in this kind of immediate, visually-guided saccade task. **(C)** For memory-guided saccades, RT's were not affected by visual field location (left panel;  $p > 0.05$ , two-tailed t-test between UVF and LVF locations), but landing error decreased in the UVF (right panel;  $p < 0.05$ , two-tailed t-test). The lack of RT effect is expected because of the prior knowledge about target location provided in this memory-guided saccade task (Experimental Procedures), but there was still a landing error effect likely reflecting smaller UVF motor RF areas. **(D)** This effect was consistent across the two monkeys: RT was not shorter in the UVF ( $p > 0.05$ , two-tailed t-test) but landing error was still smaller ( $p < 0.05$ , two-tailed t-test). Note that for memory-guided saccade data, we restricted analyses to eye movements  $< 8$  deg in amplitude, to be in line with **(A, B)**. Error bars, when visible, denote s.e.m., except for express saccade proportions (in which case they denote 95% confidence intervals as stated above).

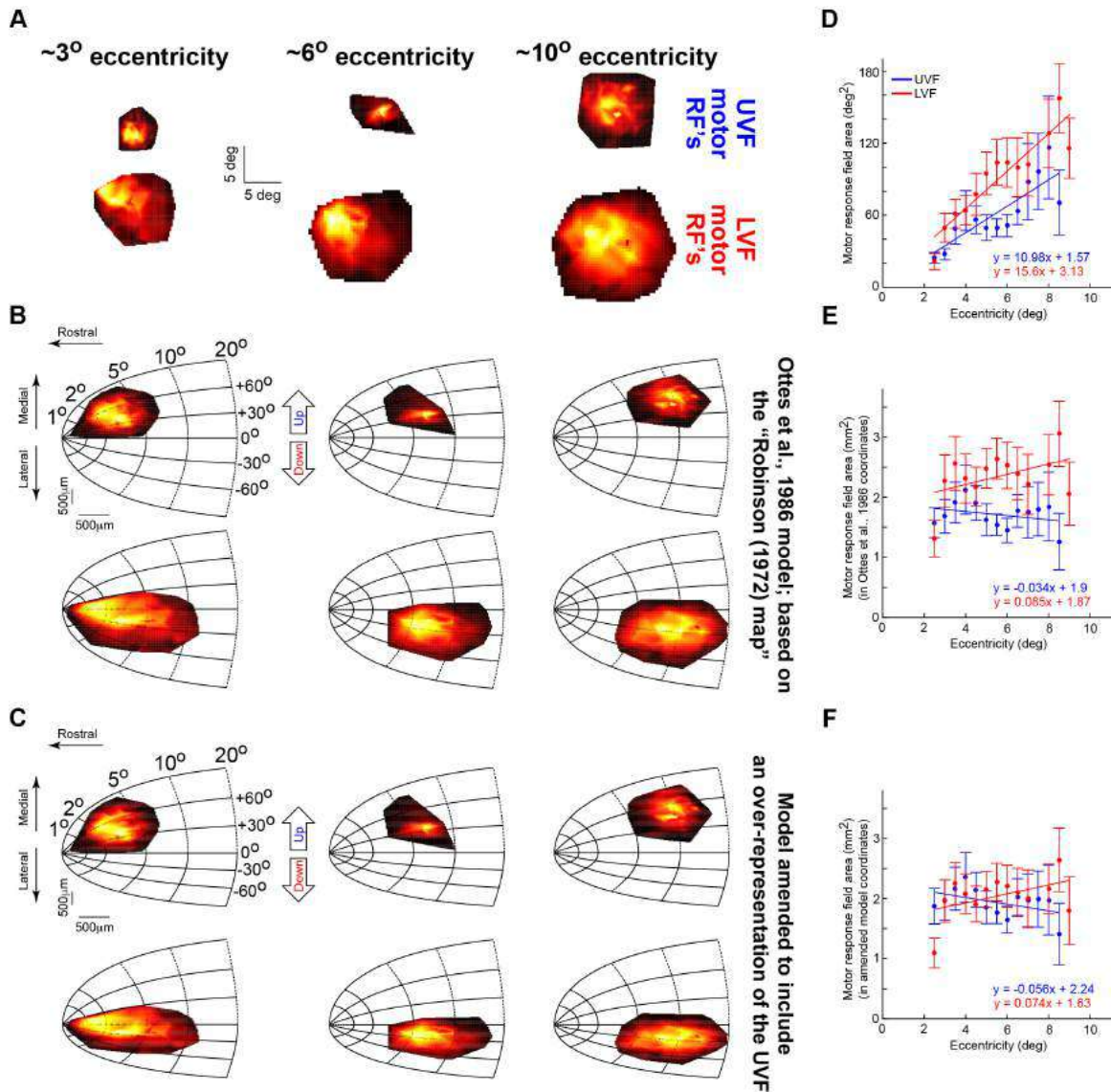


**Figure S7, Related to Figure 7.** Implications of an over-representation of the UVF on the size of the active SC population for a given saccade endpoint. This figure is identical in format to that in Fig. 7. However, in the current analysis, we plotted motor RF's as opposed to visual RF's. Similar conclusions to those made in Fig. 7 were reached. Specifically, in retinotopic coordinates, motor RF's increased in area with increasing eccentricity, and the UVF RF's were smaller than the LVF RF's (A, D). This is consistent with Fig. 2D, E and Fig. S3. When converted to SC coordinates using the Ottes et al. model [S5] of the Robinson (1972) SC topographic map [S6], RF area was equalized in eccentricity (consistent with [S2, S5]), but the UVF/LVF asymmetry persisted (B, E). However, this UVF/LVF asymmetry was reduced using our amended model of Fig. 6D (C, F). Thus, as with visual RF's (Fig. 7), our amended model suggests that the size of the active population in the SC for a given saccade vector may be equalized in neural tissue despite changes in RF area (in retinotopic coordinates) as a function of eccentricity and UVF/LVF location. Error bars denote s.e.m.

## Supplemental Experimental Procedures

### LFP analyses

We sampled data at 40 KHz. The signal was first filtered in hardware (0.7-6 KHz bandwidth). We further filtered in software: we removed 50, 100, and 150 Hz line noise using an IIR notch filter and then applied a zero-phase-lag low-pass filter (300 Hz cutoff). We finally down-sampled to 1 KHz.

We analyzed filtered LFP traces like firing rates. To investigate stimulus-induced response strength, we measured peak LFP deflection 30-100 ms after stimulus onset, and we plotted it versus RF location (e.g. Fig. 5). LFP RF locations were estimated from those of nearby isolated neurons [S7]. For Fig. 5E, we binned RF locations by eccentricity (2 deg bins, with 2 deg steps) and direction (10 deg bins, with 10 deg steps). Within each bin, we plotted average stimulus-induced LFP response, after normalizing measurements within a given eccentricity bin (i.e. across all directions) by the maximum absolute value within this eccentricity bin.

### Population reconstruction

We picked a stimulus location and asked how different neurons, regardless of their RF locations, responded when this stimulus was presented. This provided an estimate (in visual coordinates) of how large an SC population would be activated simultaneously for the stimulus. Naturally, neurons with RF hotspots at stimulus location were more active than other neurons. However, the breadth of the active population would depend on UVF or LVF RF areas (Fig. S4A). To include as many neurons as possible in analysis, we considered all stimuli within <3 deg from the analyzed location (e.g. from each of the locations in Fig. S4A).

For saccade-related activity (Fig. S4B), population reconstruction also allowed assessing times of peak discharge. For example, if peak saccade-related discharge for rostral neurons (i.e. neurons more foveal than the saccade endpoint) is later than peak discharge for caudal neurons (i.e. neurons representing the saccade endpoint), then this is evidence of a rostrally-directed activity spread [S2]. We should emphasize, however, that we did not explicitly record from “buildup” neurons, which show spreading most reliably [S2]. Thus, our goal was simply to demonstrate that even without explicitly searching for these neurons, our results have implications on such spreading as a function of visual field location (Fig. S4B).

### SC surface topography estimates

We measured our electrode location (laterally within a recording chamber) and related it to the preferred eccentricity and direction encountered at SC surface (i.e. when the electrode tip first encountered the SC). The maximum resolution for lateral movement within a chamber was 100  $\mu\text{m}$ . In depth, the electrode was movable to within 1  $\mu\text{m}$  resolution as we detail below. Our recording chambers were oriented to allow orthogonal electrode penetrations of the SC for the regions that we recorded from in this structure [S8], and we confirmed this using structural MRI's. We also used guide tubes to maintain electrode straightness.

We identified SC surface using several criteria. First, we collected structural MRI's prior to implanting the monkeys, and we therefore had detailed knowledge of anatomical landmarks along the SC tracks, as well as the depth of the SC from skull surface. We used physiological correlates of anatomical landmarks, as well as electrode depth from the skull surface, to develop an estimate of where the SC should be encountered. Second, we defined SC surface as the point at which clear multi-unit activity was available, and the multi-unit activity additionally had to fit the criteria of spatially-specific visual and eye-movement related modulations. These were generally easy to see even with monkeys spontaneously scanning their environment without a specific task. Third, we had to isolate individual neurons in the same session for the session to be acceptable, and these isolated neurons had to meet all the well-known characteristics of superficial SC neurons. The average depth of the first isolated visual neuron after SC surface was 496  $\mu\text{m}$  +/- 66  $\mu\text{m}$  s.e.m. for monkey P and 634  $\mu\text{m}$  +/- 72  $\mu\text{m}$  s.e.m. for monkey N, consistent with known SC anatomy. Fourth, we confirmed (e.g. Fig. 6A), that medial electrode tracks represented upper visual field locations, lateral tracks represented lower visual field locations, rostral tracks represented central locations, and caudal tracks represented peripheral locations [S6, S9]. Finally, we confirmed that there was a known depth ordering of visual, visual-motor, and motor neurons across our penetrations. The average depth of

pure visual neurons from SC surface was  $813.7 \mu\text{m} \pm 47.8 \mu\text{m}$  s.e.m., and the average depth of visual-motor neurons was  $1290.1 \mu\text{m} \pm 37.5 \mu\text{m}$  s.e.m. For motor-only neurons, the average depth was  $1626.1 \mu\text{m} \pm 227.5 \mu\text{m}$  s.e.m. These values (as well as their distributions) were remarkably similar to those reported in the literature (e.g. [S10]).

We ensured that our depth estimates reported above were accurate and repeatable by using an electrode micro-manipulator having  $1 \mu\text{m}$  resolution, and we moved the electrode slowly at a speed of  $1 \mu\text{m/s}$  using a computer-controlled stepper motor. We also minimized variance in our estimates of SC surface across experiments by using the following measures:

- 1) We fixed the electrode and manipulator to the skull of the monkey, such that the reference frame was controllable and repeatable across days.
- 2) We “zeroed” our electrode position in depth before every experiment (by aligning it to our skull-based reference). We did so not by hand, but by slowly moving it with  $1 \mu\text{m}$  resolution using our computer-controlled micro-manipulator. The variance of our electrode “zero” position across sessions was  $336 \mu\text{m}$  std. dev. for one monkey (P) and  $211 \mu\text{m}$  std. dev. for the second monkey (N). As s.e.m. values, the variance values were  $39.6 \mu\text{m}$  for monkey P and  $30.8 \mu\text{m}$  for monkey N.
- 3) We regularly calibrated our micro-manipulator system, and we maintained the reference frame relative to the skull (even for guide tubes, which were mounted together with the electrodes using the same holder). This gave us consistent results in finding the SC at the depth that we expected to find it at.
- 4) We used structural MRI’s and physiological characteristics during each penetration to predict when the SC surface should be reached relative to the skull surface. This gave us highly reliable points at which we were confident that we had hit the SC surface. To quantify this, we took all SC locations in which we visited the same SC location for two consecutive days. We had a total of 24 such unique SC locations. The mean difference in the depth of SC surface between the second and first attempts was  $239.9 \mu\text{m}$  with a std. dev. of  $172.4 \mu\text{m}$ .

After establishing SC surface, we instructed the monkeys to perform one of our mapping tasks described in Experimental Procedures (*delayed visually-guided saccade task* or *fixation visual RF mapping task*), and we searched for the RF hotspot. We used online (i.e. real-time) measurement and display of multi-unit activity, along with audio feedback of this activity, to find RF hotspot, and we later confirmed offline that this hotspot was similar to that obtained from the first isolated single neuron. As stated above, we sometimes visited the same electrode track location more than once. Thus, we averaged the obtained RF hotspot eccentricity and direction across the multiple visits in analyses (e.g. Fig. 6A).

### Modeling

In [S5], a mapping function converts polar visual coordinates of eccentricity ( $R$ ) and direction ( $\theta$ ) onto Cartesian coordinates ( $X$ ,  $Y$ ) of SC neural tissue (in mm). Neurons at  $X$ ,  $Y$  are “tuned” for visual angles of  $R$ ,  $\theta$  according to:

$$X = B_x \log_e \left( \frac{\sqrt{R^2 + 2AR \cos(\theta) + A^2}}{A} \right) \quad (\text{Equation S1})$$

$$Y = B_y \arctan \left( \frac{R \sin(\theta)}{R \cos(\theta) + A} \right) \quad (\text{Equation S2})$$

Parameter values of  $A = 3 \text{ deg}$ ,  $B_x = 1.4 \text{ mm}$ , and  $B_y = 1.8 \text{ mm}$  provide good fits to Robinson’s electrical stimulation data [S5, S6].

However, the SC contains a functional discontinuity (e.g. Figs. 2, 4, 5) across the horizontal meridian. This necessitates an over-representation of the UVF, which we confirmed (Fig. 6A, B). We thus revised the model to include a functional discontinuity:

$$X = B_x \log_e \left( \frac{\sqrt{R^2 + 2AR \cos(\theta) + A^2}}{A} \right) \quad (\text{Equation S3})$$

$$Y = \begin{cases} \sqrt{AF} \cdot B_y \arctan \left( \frac{R \sin(\theta)}{R \cos(\theta) + A} \right) & \theta > 0 \\ \frac{1}{\sqrt{AF}} \cdot B_y \arctan \left( \frac{R \sin(\theta)}{R \cos(\theta) + A} \right) & \theta \leq 0 \end{cases} \quad (\text{Equation S4})$$

where the parameter  $AF$  (area factor) dictates how much the UVF representation is bigger compared to the LVF. We selected  $AF = 1.6$ , which seems to be in line with our experimental observations (Figs. 2, 6). This value is sufficient to roughly “equalize” the size of the active population in the SC regardless of eccentricity or UVF/LVF location (Figs. 7, S7).

## Supplemental References

- S1. Previc, F.H. (1990). Functional specialization in the lower and upper visual-fields in humans - its ecological origins and neurophysiological implications. *Behav Brain Sci* 13, 519-575.
- S2. Munoz, D.P., and Wurtz, R.H. (1995). Saccade-related activity in monkey superior colliculus. II. Spread of activity during saccades. *J Neurophysiol* 73, 2334-2348.
- S3. Nakahara, H., Morita, K., Wurtz, R.H., and Optican, L.M. (2006). Saccade-related spread of activity across superior colliculus may arise from asymmetry of internal connections. *J Neurophysiol* 96, 765-774.
- S4. Choi, W.Y., and Guitton, D. (2009). Firing patterns in superior colliculus of head-unrestrained monkey during normal and perturbed gaze saccades reveal short-latency feedback and a sluggish rostral shift in activity. *J Neurosci* 29, 7166-7180.
- S5. Ottes, F.P., Van Gisbergen, J.A., and Eggermont, J.J. (1986). Visuomotor fields of the superior colliculus: a quantitative model. *Vision Res* 26, 857-873.
- S6. Robinson, D.A. (1972). Eye movements evoked by collicular stimulation in the alert monkey. *Vision Res* 12, 1795-1808.
- S7. Ikeda, T., Boehnke, S.E., Marino, R.A., White, B.J., Wang, C.A., Levy, R., and Munoz, D.P. (2015). Spatio-temporal response properties of local field potentials in the primate superior colliculus. *Eur J Neurosci* 41, 856-865.
- S8. Chen, C.Y., Ignashchenkova, A., Thier, P., and Hafed, Z.M. (2015). Neuronal response gain enhancement prior to microsaccades. *Curr Biol* 25, 2065-2074.
- S9. Cynader, M., and Berman, N. (1972). Receptive-field organization of monkey superior colliculus. *J Neurophysiol* 35, 187-201.
- S10. Munoz, D.P., and Wurtz, R.H. (1995). Saccade-related activity in monkey superior colliculus. I. Characteristics of burst and buildup cells. *J Neurophysiol* 73, 2313-2333.

**4. A neural locus for spatial-frequency specific saccadic suppression in visual-motor neurons of the primate superior colliculus**

RESEARCH ARTICLE | *Higher Neural Functions and Behavior*

## A neural locus for spatial-frequency specific saccadic suppression in visual-motor neurons of the primate superior colliculus

Chih-Yang Chen<sup>1,2,3</sup> and Ziad M. Hafed<sup>1,3</sup>

<sup>1</sup>Werner Reichardt Centre for Integrative Neuroscience, Tuebingen University, Tuebingen, Germany; <sup>2</sup>Graduate School of Neural and Behavioural Sciences, International Max Planck Research School, Tuebingen University, Tuebingen, Germany; and <sup>3</sup>Hertie Institute for Clinical Brain Research, Tuebingen, Germany

Submitted 28 November 2016; accepted in final form 17 January 2017

**Chen CY, Hafed ZM.** A neural locus for spatial-frequency specific saccadic suppression in visual-motor neurons of the primate superior colliculus. *J Neurophysiol* 117: 1657–1673, 2017. First published January 18, 2017; doi:10.1152/jn.00911.2016.—Saccades cause rapid retinal-image shifts that go perceptually unnoticed several times per second. The mechanisms for saccadic suppression have been controversial, in part because of sparse understanding of neural substrates. In this study we uncovered an unexpectedly specific neural locus for spatial frequency-specific saccadic suppression in the superior colliculus (SC). We first developed a sensitive behavioral measure of suppression in two macaque monkeys, demonstrating selectivity to low spatial frequencies similar to that observed in earlier behavioral studies. We then investigated visual responses in either purely visual SC neurons or anatomically deeper visual motor neurons, which are also involved in saccade generation commands. Surprisingly, visual motor neurons showed the strongest visual suppression, and the suppression was dependent on spatial frequency, as in behavior. Most importantly, suppression selectivity for spatial frequency in visual motor neurons was highly predictive of behavioral suppression effects in each individual animal, with our recorded population explaining up to ~74% of behavioral variance even on completely different experimental sessions. Visual SC neurons had mild suppression, which was unselective for spatial frequency and thus only explained up to ~48% of behavioral variance. In terms of spatial frequency-specific saccadic suppression, our results run contrary to predictions that may be associated with a hypothesized SC saccadic suppression mechanism, in which a motor command in the visual motor and motor neurons is first relayed to the more superficial purely visual neurons, to suppress them and to then potentially be fed back to cortex. Instead, an extraretinal modulatory signal mediating spatial-frequency-specific suppression may already be established in visual motor neurons.

**NEW & NOTEWORTHY** Saccades, which repeatedly realign the line of sight, introduce spurious signals in retinal images that normally go unnoticed. In part, this happens because of perisaccadic suppression of visual sensitivity, which is known to depend on spatial frequency. We discovered that a specific subtype of superior colliculus (SC) neurons demonstrates spatial-frequency-dependent suppression. Curiously, it is the neurons that help mediate the saccadic command itself that exhibit such suppression, and not the purely visual ones.

saccades; microsaccades; superior colliculus; saccadic suppression; perceptual stability

A LONG-STANDING QUESTION in visual neuroscience has been about how we normally experience a sense of perceptual stability despite incessant eye movements (Wurtz 2008). Saccadic eye movements, in particular, dramatically alter retinal images several times per second. During each saccade, retinal images undergo rapid motion, which can be beyond the range of motion sensitivity of many neurons. Such motion ought, at least in principle, to cause a brief period of “gray out” every time a saccade occurs (Campbell and Wurtz 1978; Matin 1974; Wurtz 2008; Wurtz et al. 2011), much like the gray out experienced by persons while standing near train tracks as high-speed trains sweep by.

Several theories about why we do not experience saccade-related visual disruptions have been debated in the literature. On the one hand, purely visual mechanisms, such as masking (Matin et al. 1972), can be sufficient to suppress perception of saccade-induced gray out and/or motion (Wurtz 2008). Consistent with this, people are not entirely “blind” during saccades, as long as spatiotemporal properties of perisaccadic stimuli remain within sensitivity ranges of visual neurons (Burr and Ross 1982; Castet et al. 2001; Castet and Masson 2000; García-Pérez and Peli 2011; Ilg and Hoffmann 1993; Matin et al. 1972; Ross et al. 1996). On the other hand, extraretinal mechanisms (Sperry 1950; von Holst and Mittelstaedt 1950) for suppression are supported by the lack of suppression during simulated image displacements (Diamond et al. 2000), the dependence of suppression on spatial frequency (Burr et al. 1982, 1994; Hass and Horwitz 2011; Volkman et al. 1978), and the observation of saccade-related modulation of neural excitability in the absence of visual stimulation (Rajkai et al. 2008).

Although it is likely that a combination of visual and extraretinal mechanisms coexist (Wurtz 2008), further understanding of neural mechanisms is needed to resolve some of the debates surrounding saccadic suppression. We were particularly interested in potential mechanisms for extraretinal suppression, whose sources remain elusive. For example, it was suggested from behavioral studies that selective suppression of low spatial frequencies is evidence for selective magnocellular (achromatic) pathway suppression (Burr et al. 1994). However, in lateral geniculate nucleus (LGN) and primary visual cortex (V1), two early visual areas possessing clear magno- and parvocellular segregations, selective magnocellular suppres-

Address for reprint requests and other correspondence: Z. M. Hafed, Werner Reichardt Centre for Integrative Neuroscience, Otfried-Mueller Str. 25, Tuebingen, BW 72076, Germany (e-mail: ziad.m.hafed@cin.uni-tuebingen.de).



sion is not established (Hass and Horwitz 2011; Kleiser et al. 2004; Ramcharan et al. 2001; Reppas et al. 2002; Royal et al. 2006). In addition, a hypothesis about a source of saccadic suppression is that a “corollary” of saccade commands in visual motor and motor neurons of the superior colliculus (SC) is fed back to superficial purely visual neurons to suppress their sensitivity and to jumpstart a putative feedback pathway for cortical suppression through pulvinar (Berman and Wurtz 2008; Berman and Wurtz 2010; Berman and Wurtz 2011; Isa and Hall 2009; Lee et al. 2007; Phongphanphane et al. 2011; Wurtz 2008; Wurtz et al. 2011). However, evidence for an SC saccadic suppression pathway from visual motor/motor neurons to visual neurons comes primarily from rodent SC slices (Isa and Hall 2009; Lee et al. 2007; Phongphanphane et al. 2011). In the awake, behaving primate, findings of stronger suppression in visual motor rather than visual neurons (Chen et al. 2015; Hafed et al. 2015; Hafed and Krauzlis 2010) suggest a more nuanced set of mechanisms. Moreover, spatial-frequency-specific suppression of visual sensitivity in either visual or visual motor SC neurons has not yet been investigated.

In this study, we visited the question of neural loci for saccadic suppression in the SC by looking for spatial frequency specificity of visual suppression. We have previously shown that SC neurons exhibit time courses of saccadic suppression remarkably similar to those of perceptual effects in humans (Hafed and Krauzlis 2010). However, our previous experiments did not investigate any potential spatial frequency dependence in saccadic suppression, as might be expected from earlier human experiments (Burr et al. 1994). Our earlier experiments only presented a white bar stimulus within a neuron’s visual response field (RF). Thus, in this study, we adapted our behavioral paradigm from (Hafed and Krauzlis 2010) to first establish selectivity in saccadic suppression during this paradigm, and we then asked whether visual neural modulations in either purely visual or visual motor SC neurons would reflect such selectivity. Contrary to what we might have predicted on the basis of a suppressive pathway from deep to superficial layers (Isa and Hall 2009; Lee et al. 2007; Phongphanphane et al. 2011), we observed spatial-frequency-specific saccadic suppression only in the deeper visual motor neurons. Visual neurons showed mild suppression, but this suppression was not modulated as a function of spatial frequency. Moreover, we recorded local field potentials (LFPs) as a proxy for population and synaptic activity around our isolated neurons (Hafed and Chen 2016; Ikeda et al. 2015), and we found evidence that the visual suppression of firing rates that we observed in isolated neurons may have been mediated by the presence of modulatory signals in the SC associated with the motor generation of saccades, and particularly in the visual motor layers. Our results suggest that the SC may indeed be relevant for spatial-frequency-specific saccadic suppression, which has been reported previously in humans (Burr et al. 1994), but that the putatively extraretinal modulatory signal mediating suppression may already be established in the visual motor neurons.

From a technical standpoint, we exploited microsaccades to study saccadic suppression in this study because microsaccades offer important experimental advantages while at the same time being mechanistically similar to larger saccades (Hafed 2011; Hafed et al. 2009; Hafed et al. 2015; Zuber et al. 1965). First, microsaccades are small (median amplitude in our data:

~7.5 min arc). Thus pre- and postmovement visual RFs are not displaced by much, minimizing the problem of dramatic spatial image shifts caused by saccades (Wurtz 2008; Wurtz et al. 2011). Experimentally, this meant presenting the same stimulus at the same screen location with and without microsaccades to isolate suppression effects. Second, microsaccades have velocities significantly <100 deg/s (median peak velocity in our data: ~17.7 deg/s). Thus image motion caused by microsaccades is well within the range of motion sensitivity, even for small features (Thiele et al. 2002), allowing us to study suppression even when no motion-induced gray out is expected to occur. Third, we have previously shown, with simple white bars, that SC visual sensitivity exhibits pre-, peri-, and post-microsaccadic suppression that is similar in time course and amplitude to perceptual saccadic suppression in humans with larger saccades, and we also have demonstrated a sensitive behavioral paradigm for the same phenomenon (Hafed and Krauzlis 2010). Fourth, and more importantly, we avoided potential masking effects by only presenting stimuli immediately after microsaccades. This allowed us to study suppression after saccades, which is known to still occur (Chen et al. 2015; Hafed and Krauzlis 2010; Zuber et al. 1966), and to ensure comparison of “no-microsaccade” to “microsaccade” conditions without the latter involving saccade-induced retinal image motion. Finally, it was established long ago that at the behavioral level, microsaccades are associated with similar suppression to larger saccades (Zuber et al. 1966) and that saccadic suppression is also expected to occur far away from the movement end point (Knöll et al. 2011); this meant that using microsaccades as a model system for saccadic suppression was reasonable. Thus the logic of all of our experiments was to present high-contrast gratings (80% contrast), which were highly visible and well within the saturation regime of SC contrast sensitivity curves (Chen et al. 2015; Hafed and Chen 2016; Li and Basso 2008), and to ask whether either behavioral or visual neural responses to these gratings were altered if the gratings appeared immediately after a microsaccade.

## MATERIALS AND METHODS

### *Animal Preparation*

Ethics committees at regional governmental offices in Tuebingen approved experiments. *Monkeys N and P* (male, *Macaca mulatta*, age 7 yr) were prepared as detailed earlier (Chen and Hafed 2013; Chen et al. 2015; Hafed and Chen 2016; Hafed and Ignashchenkova 2013). Briefly, under isoflurane anesthesia and aseptic conditions, we first attached a head holder to the skull. The head holder consisted of a titanium implant that was embedded under the skin and attached to the skull using titanium screws. In a subsequent surgery, we made a small skin incision on top of the head and attached a metal connector to the previously implanted head holder. This connector acted as the interface for fixing the head to a standard position in the laboratory during data collection. In the same surgery, a scleral search coil was implanted in one eye to allow measurement of eye movements with high temporal and spatial precision using the magnetic induction technique (Fuchs and Robinson 1966; Judge et al. 1980). After the animals completed the behavioral training and experimental sessions, we implanted recording chambers to access the SC. The chambers were placed on the midline, aimed at 1 mm posterior to and 15 mm above the interaural line. Chambers were tilted posterior to vertical (by 35° and 38° for *monkeys N and P*, respectively).

### Behavioral Tasks

In all tasks, the monkeys initially fixated a small, white spot presented over a gray background (Chen and Hafed 2013; Chen et al. 2015; Hafed and Ignashchenkova 2013). Spot and background luminance values were 72 and 21 cd/m<sup>2</sup>, respectively.

**Behavioral tests.** Trials started with an initial fixation interval of random duration (between 600 and 1,500 ms). After this interval, we initiated a real-time process to detect microsaccades (Chen and Hafed 2013). Briefly, this process evaluated instantaneous radial eye velocity on the basis of recently sampled eye positions, and it flagged the presence of a microsaccade when this velocity exceeded a user-defined threshold. If a microsaccade was detected within 500 ms, a stationary vertical Gabor grating (having 80% contrast relative to background luminance) appeared at 3.5° to the right or left of fixation, and the fixation spot was removed simultaneously. Monkeys oriented to the grating using a saccadic eye movement, and saccadic reaction time (RT) served as a sensitive behavioral measure of SC visual response strength (Boehnke and Munoz 2008; Hafed and Chen 2016; Hafed and Krauzlis 2010; Hafed et al. 2015; Tian et al. 2016; also see DISCUSSION). Because of their extensive training on visually guided saccades, our monkeys were likely making speeded reactions to the gratings, further justifying the use of RT. Grating onset occurred ~25, 50, 75, 100, 150, or 200 ms after online microsaccade detection, and we later measured precise times of microsaccade onset during data analysis for all results presented in this article (see *Data Analysis*). Our choice of times to sample (listed above) was based on earlier observations that saccadic suppression effects in the SC subside by ~100 ms after the movements (Chen et al. 2015; Hafed and Krauzlis 2010). If no microsaccade was detected during our 500-ms online detection window, a grating was presented anyway, and the data contributed to “baseline” measurements (i.e., ones with the stimulus appearing without any nearby microsaccades). The grating was 2° in diameter. Spatial frequency in cycles per degree (cpd) was one of five values: 0.56, 1.11, 2.22, 4.44, or 11.11 (Hafed and Chen 2016), and phase was randomized. Our monitor resolution allowed display at the highest spatial frequency without aliasing and distortion. We collected 8,153 and 7,117 trials from *monkeys N* and *P*, respectively. We removed trials with an intervening microsaccade between fixation spot removal and the orienting saccade.

**Neural recordings.** We isolated single neurons online, and we identified their RF locations and sizes using standard saccade tasks (Chen et al. 2015; Hafed and Chen 2016). We then ran our main experimental paradigm. In each trial, monkeys fixated while we presented a vertical grating similar to the one we used in the behavioral tests described above (i.e., with similar contrast and spatial frequency ranges), but the grating was now inside the recorded neuron’s RF. Grating size was optimized for the recorded neuron and was specifically chosen to fill as much of the RF as possible (and showing >1 cycle of the lowest spatial frequency). Task timing was identical to that in Chen et al. (2015); briefly, a grating was presented for 250 ms while monkeys fixated, and the monkeys never generated any saccadic or manual responses to the grating (they simply maintained fixation, during which they generated microsaccades, and they were rewarded at the end of the 250-ms stimulus presentation phase for maintaining fixation). We collected data from 90 neurons ( $n = 39$  from *monkey N* and  $n = 51$  from *monkey P*), covering 1°–24° eccentricities. We classified neurons as purely visual neurons or visual motor neurons by using previous criteria from visually guided and memory-guided saccade tasks (Chen et al. 2015; Hafed and Chen 2016). To ensure sufficient microsaccades for statistical analyses (i.e., with sufficient trials having stimulus onset within the critical post-movement intervals that we analyzed), we collected >800 trials per neuron. We then separated trials as ones having no microsaccades within ±100 ms from grating onset (>100 trials per neuron; mean: 289 trials per neuron; median: 191 trials per neuron) or ones with grating onset within 50 ms after microsaccades (>25 trials per

neuron; mean: 79 trials per neuron; median: 79 trials per neuron). The former trials provided an estimate of “baseline” responses without the influence of saccadic suppression, and the latter trials provided an estimate of the suppressed responses due to saccadic suppression. Moreover, the times chosen were justified on the basis of previous descriptions of the time courses of saccadic suppression (e.g., Hafed and Krauzlis 2010; Zuber et al. 1966). Some of our analyses also included grating onsets up to 100 ms after microsaccades.

It is important to note that for all neurons reported in this article, we never observed a microsaccade-related movement burst (Hafed et al. 2009; Hafed and Krauzlis 2012). Thus, even for stimuli appearing immediately after a microsaccade, the neural responses that we analyzed were visual bursts in response to stimulus onset, and not movement-related saccade or microsaccade bursts. The only difference between purely visual and visual motor neurons in this study was that visual motor neurons would, in principle, exhibit a saccade-related burst if the monkeys were to hypothetically generate saccades toward the RF location (but not if they generated smaller microsaccades during fixation). Thus any neural modulations that we report in this study are not direct microsaccade-related motor bursts.

It also is important to note that our monkeys did not generate any targeting saccades to the gratings during recordings. We were simply studying visual sensitivity if a stimulus appeared near an eye movement. Our approach was thus very similar to classic ways of studying neural correlates of saccadic suppression (i.e., monkeys make saccades while neurons are visually stimulated; e.g., Bremmer et al. 2009; Hafed and Krauzlis 2010; Zanos et al. 2016).

### Data Analysis

In all figures, we plotted mean values (along with suitable measures of variance, such as SE) for the parameters that we were visualizing; we used the mean in the figures because this is a standard way of presenting data. However, in quantitative descriptions in the text, we sometimes report median values in addition to mean values, and for statistical analyses, we always performed nonparametric statistical tests because our neural and behavioral data were not always normally distributed.

In all neural data analyses, we combined results from both monkeys. This was justified because the two monkeys showed consistent results with each other, and also consistent results with the prior literature (e.g., Chen et al. 2015; Hafed and Krauzlis 2010). However, for relating neural activity to behavior, it was unfair to compare the behavior of an individual monkey with neural data combined from both animals. Thus, only when relating neural activity to behavior, we separated the neural data into individual monkey data. This had the added advantage of demonstrating the consistency of neural results across individual monkeys, justifying our pooling of the animals for the summary figures of neural data analyses.

**Behavioral analyses.** For behavior, we measured reaction time (RT) as a function of spatial frequency and time of grating onset relative to microsaccades. We also counted “express saccade” RT trials, which we defined as trials with RT <100 ms (Fischer and Boch 1983).

During offline analysis, we re-detected microsaccades using previously described methods (Hafed et al. 2009), because we could now use noncausal filters for better estimates of eye velocity and because we could also refine the time of movement onset/end on the basis of eye acceleration. We used such detection to identify grating onset time relative to microsaccade onset or offset. We defined no-microsaccade trials as trials with no microsaccades <250 ms from grating onset. RT on these trials constituted our baseline.

**Firing rate analyses.** For neural data, we measured stimulus-evoked firing rate after the onset of a given spatial frequency grating under two scenarios: 1) when the grating appeared without any nearby microsaccades within ±100 ms and 2) when the grating appeared immediately after a microsaccade. Baseline, no-microsaccade spatial

frequency tuning curves (i.e., responses for each given spatial frequency) were described recently (Hafed and Chen 2016), but in this study we analyzed microsaccadic influences on these curves. We did not analyze trials with grating onset immediately before or during microsaccades, to avoid pre-movement modulations (Chen et al. 2015; Hafed 2013) and retinal image shift effects caused by movement of the eyes, but previous studies have demonstrated suppression also during these intervals (Hafed and Krauzlis 2010).

To analyze stimulus-evoked firing rate, we measured peak visual response 20–150 ms after grating onset. To compare visual sensitivity on microsaccade and no-microsaccade trials, we created a “normalized firing rate” modulation index for each individual spatial frequency. We measured firing rate on microsaccade trials (i.e., trials with grating onset within 50 ms after microsaccades) and divided it by rate on no-microsaccade trials (i.e., trials with no microsaccades within <100 ms from grating onset). A value <1 indicates suppression. Note that we only considered neurons with a >5 spikes/s stimulus-evoked response (even on 11.11 cpd trials, which frequently had the lowest firing rates), thus avoiding “divide by zero” problems. Also, note that this modulation index isolates changes in visual sensitivity associated with saccadic suppression, regardless of how visual sensitivity itself might depend on spatial frequency without microsaccades. For example, visual responses in general are expected to be weaker for high spatial frequencies (Hafed and Chen 2016); however, our modulation index would normalize activity within a given spatial frequency to isolate any further suppression of visual sensitivity due to saccadic suppression.

In our analyses (including behavioral analyses), we combined microsaccades toward or away from the grating because suppression is not direction dependent in the postmovement interval that we focused on (Chen et al. 2015). However, we also confirmed this when analyzing the present data set (e.g., see Fig. 5). Our population analyses also combined neurons representing different eccentricities. We did so because we found that suppression is independent of eccentricity during the postmovement interval that we focused on (Chen et al. 2015).

To investigate the relationship between neural modulations and behavioral effects, we correlated behavioral patterns of saccadic suppression from the behavioral tests to neural modulations obtained from the recordings. For example, we related visual response firing rate strength to mean RT as a function of time of grating onset after microsaccades. The mean RT was obtained from all collected behavioral trials (i.e., including the minority of express RT trials; see RESULTS) because visual responses are expected to affect overall behavior, without being specifically “labeled” in the brain as belonging to either a potential express RT trial or a regular trial.

For all analyses with time courses, we used bin steps of 10 ms and bin widths of 50 ms (except for Fig. 2, G, H, J, and K with both bin steps and bin widths of 25 ms).

**Local field potential analyses.** To analyze LFPs, we sampled neurophysiological activity at 40 KHz. The signal was first filtered in hardware (0.7–6 kHz). We then removed 50-, 100-, and 150-Hz line noise using an IIR notch filter and then applied a zero-phase lag low-pass filter (300-Hz cutoff). We finally downsampled to 1 kHz. We analyzed filtered LFP traces like firing rates (Hafed and Chen 2016; Ikeda et al. 2015), and we classified electrode track locations as visual or visual motor according to the neurons isolated from these tracks in the same sessions (Hafed and Chen 2016).

To obtain a measure of intrinsic perimicrosaccadic modulation of LFPs independent of visual stimulation, we took all microsaccades occurring in a prestimulus interval (20–100 ms before grating onset). We then aligned LFP traces on either microsaccade onset or end, to uncover any systematic LFP modulation time-locked to the movement execution. To compare these data to baseline, we took analysis intervals of identical length, again from prestimulus periods, but with no microsaccades occurring anywhere within these intervals.

To correlate LFP responses to behavioral dynamics of saccadic suppression (similar to what we did with firing rates), we measured peak transient LFP deflection as the minimum in the stimulus-evoked LFP trace 20–150 ms after grating onset. We created a “field potential index” by dividing this measurement on microsaccade trials by that on no-microsaccade trials. An index >1 indicates enhancement. For a control analysis, we computed the index after correcting for a micro-saccade-related LFP level shift that may have happened due to intrinsic perimicrosaccadic modulation of the LFP independent of visual stimulation. We did this according to the following procedure. On microsaccade trials, we measured the average LFP value –25 to 25 ms from grating onset. We then subtracted the peak stimulus-evoked LFP deflection from this baseline measurement before dividing by the no-microsaccade trials. If an intrinsic perimicrosaccadic LFP modulation explained our results of LFP enhancement with increasing spatial frequency (see RESULTS), then the baseline-shifted index should show no enhancement.

We also analyzed transient stimulus-evoked LFP deflection latency. We found the first time at which the LFP was >2 SD away from baseline LFP (calculated as the mean LFP value –25 to 25 ms from grating onset), and there also had to be >5 ms of continuous >2 SD deviation from baseline. We did this separately for microsaccade and no-microsaccade trials, and we subtracted the measurements to obtain the influences of saccadic suppression on stimulus-evoked LFP deflection latency. If the LFP transient deflection occurs faster on microsaccade trials, then the subtraction gives a negative value.

## RESULTS

### *Selective Microsaccadic Suppression of Low Spatial Frequencies in Behavior*

Isolation of spatial-frequency-specific saccadic suppression requires demonstrating a selective form of suppression in behavior and subsequently asking which neurons reflect such selectivity. Thus we first developed a behavioral measure demonstrating selective suppression, which was based on our earlier results (Hafed and Krauzlis 2010). We did so for microsaccades because they are mechanistically similar to larger saccades while at the same time providing important experimental advantages (see Introduction). Monkeys fixated, and we initiated a computer process for real-time microsaccade detection (Chen and Hafed 2013). After such detection by a programmable delay, we presented a stationary vertical Gabor grating (80% contrast). The monkeys oriented toward the grating as fast as possible. Because SC visual bursts are strongly correlated with RT (Boehnke and Munoz 2008; Chen et al. 2015; Hafed and Chen 2016; Hafed and Krauzlis 2010; Hafed et al. 2015; Tian et al. 2016), we used RT changes in this task as a sensitive measure of microsaccadic influences on visual sensitivity (Hafed and Krauzlis 2010; Tian et al. 2016; also see DISCUSSION).

Similar to previously reported perceptual effects with large saccades (Burr et al. 1994) and also microsaccades (Hass and Horwitz 2011), grating onset after microsaccades had a strong, yet selective impact on behavior in our monkeys. Figure 1A shows example eye position (*left*) and velocity traces (*right*) recorded from one monkey while we presented a 1.11 cpd grating. The black traces show trials without microsaccades <250 ms from grating onset, and the gray traces show trials with grating onset ~20–100 ms after microsaccades. There was a marked increase in RT during microsaccade trials (Fig. 1A). However, when we presented 4.44 (Fig. 1B) or 11.11 cpd gratings (Fig. 1C), RTs on microsaccade and no-microsaccade

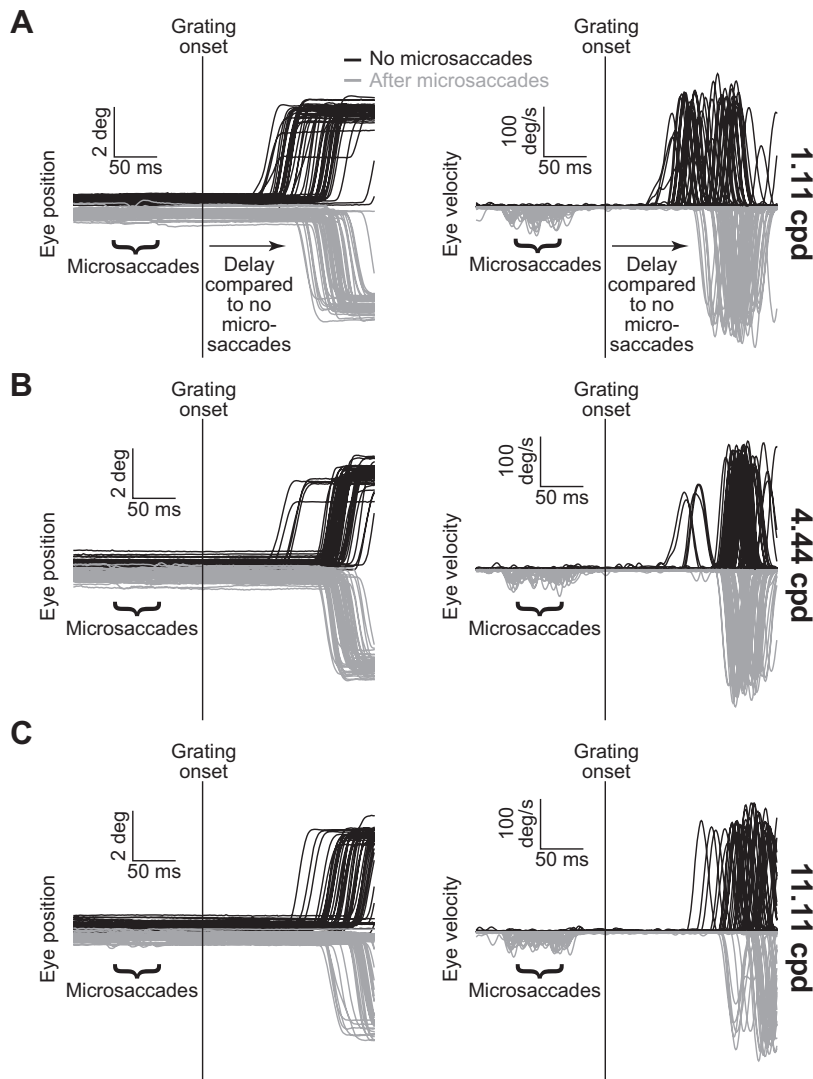


Fig. 1. Behavioral measure of microsaccadic suppression across spatial frequencies. *A*: eye position (*left*) and radial eye velocity (*right*) traces from 100 sample trials from *monkey N* during a stimulus detection task. A 1.11 cpd grating appeared during fixation either with no nearby microsaccades (black;  $n = 50$  randomly selected trials) or  $\sim 20$ – $100$  ms after microsaccades (gray;  $n = 50$  randomly selected trials), and the monkey had to orient as fast as possible to the grating. Reaction time (RT) on the microsaccade trials was slower than on the no-microsaccade trials. Note that we flipped the gray position and velocity traces around the horizontal axis to facilitate comparison to the black traces, and we also displaced the initial fixation position in the position traces. The microsaccades are more visible in the velocity traces because they constitute spikes of eye velocity. *B*: same analysis as in *A*, but from 100 randomly selected trials having a higher spatial frequency grating (4.44 cpd). RTs in this case were more similar between the microsaccade and no-microsaccade trials, suggesting that the effect in *A* disappears with increasing spatial frequency. *C*: observations similar to those in *B* were also made for 11.11 cpd gratings. Note that RTs in this case were longer than in *A* and *B*, meaning that some traces were truncated either before saccade onset or midway through saccades. Also, note that results of statistical tests for this and other figures are detailed in the text.

trials were more similar to each other (compare the gray and black distributions in each panel). Thus the microsaccadic suppressive effect (causing slower RTs relative to no-microsaccade baselines) was diminished for higher frequency gratings. These sample trial results demonstrate a correlate in our monkeys of selective perceptual suppression of low spatial frequencies by large saccades and also microsaccades (Burr et al. 1982, 1994; Hass and Horwitz 2011; Volkmann et al. 1978), even though we used a different behavioral measure.

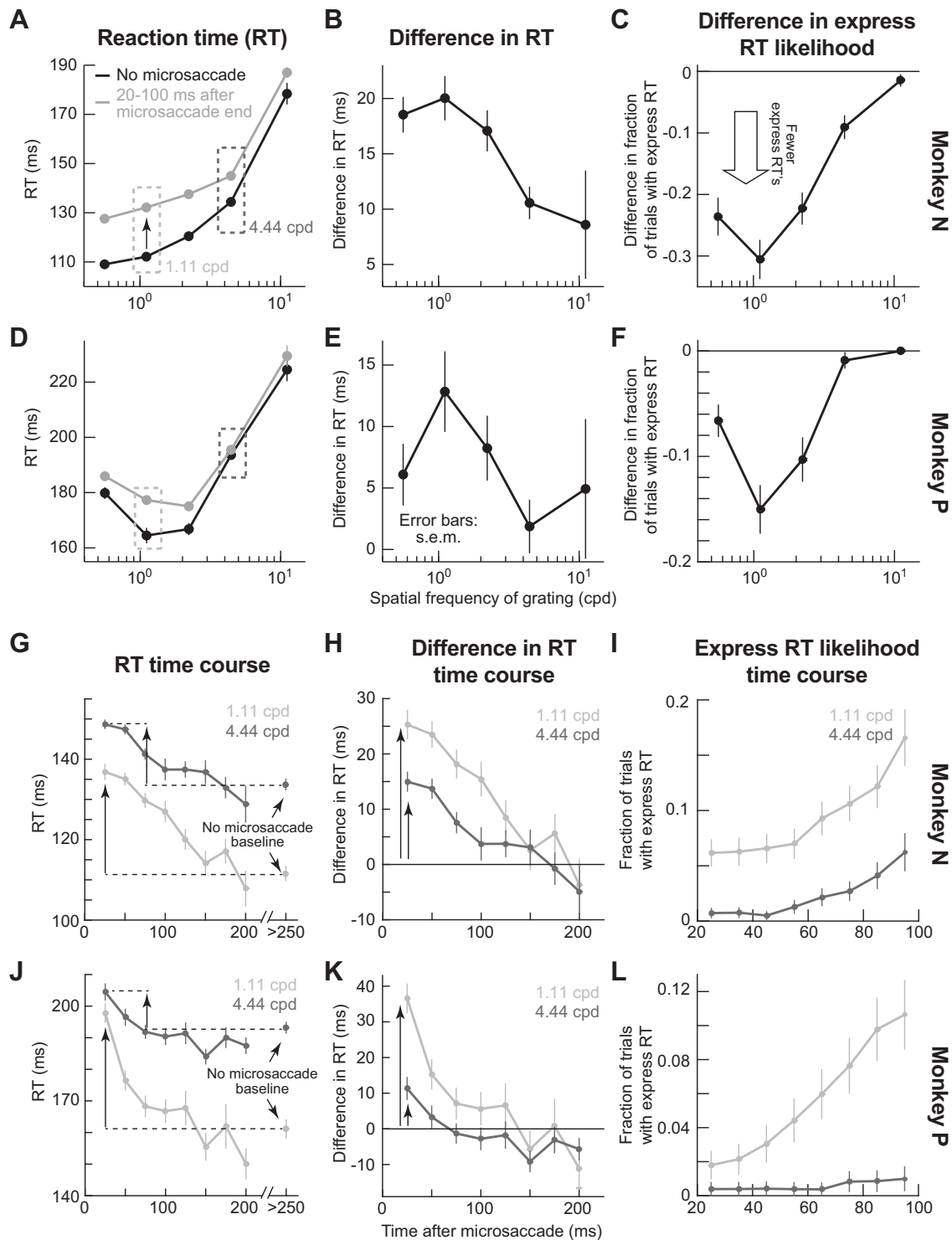
Across behavioral sessions, both monkeys showed selective RT increases for low spatial frequencies (Fig. 2, *A* and *D*). On no-microsaccade trials (black curves), mean RT increased with increasing spatial frequency, as expected from dynamics of the early visual system (Breitmeyer 1975) and SC (unpublished observations). For example, mean RT for 0.56 cpd gratings was  $109.1 \pm 1.37$  ms (mean  $\pm$  SE) in *monkey N* and  $179.8 \pm 2.12$  ms in *monkey P*, whereas it was  $178.4 \pm 4.37$  ms in *monkey N* and  $224.5 \pm 4.2$  ms in *monkey P* for 11.11 cpd. This effect was statistically significant ( $P < 0.01$  for *monkey N* and  $P < 0.01$  for *monkey P*, Kruskal-Wallis test with spatial frequency as the main factor). However, with gratings appearing  $\sim 20$ – $100$  ms after microsaccades, the RT cost relative to

no-microsaccade trials (i.e., the difference in RT between microsaccade and no-microsaccade trials) was strongest for the lowest spatial frequencies (Fig. 2, *B* and *E*;  $P < 0.01$  for *monkey N* and  $P < 0.01$  for *monkey P*, Kruskal-Wallis test with spatial frequency as the main factor). This effect was not a ceiling effect on RT, because it was still possible for RT to increase even more at higher spatial frequencies. For example, at 4.44 cpd, RT on microsaccade and no-microsaccade trials was similar (Fig. 2, *A* and *D*; dark gray dashed boxes), but it got even slower for 11.11 cpd regardless of eye movements. This effect is also shown in the raw black traces of Fig. 1*C*, exhibiting longer RT values than the black traces of Fig. 1*B*. Importantly, even at 11.11 cpd, RT on microsaccade trials was modestly longer than on no-microsaccade trials in both animals (Fig. 2, *A* and *D*), suggesting that the impact of microsaccades could still be visible even when RT itself was very long because of high spatial frequencies. Thus the reduction in RT differences between microsaccade and no-microsaccade trials for high spatial frequencies (Fig. 2, *B* and *E*) was suggestive of a selective suppression of low spatial frequencies, and not necessarily a ceiling effect on RT.

On a small subset of the trials in Fig. 2, *A* and *D*, our monkeys' RT values fell within a so-called "express" range

(which we defined as trials having RT < 100 ms). Overall, 11.05% and 6.34% of all trials in *monkeys N* and *P*, respectively, were express. These trials formed a small but distinct peak in RT distributions typical of express saccades (although this small peak appeared to merge with regular RT distributions for the lowest spatial frequency in *monkey N* because of this monkey's low overall RT values). We thus additionally analyzed how these specific express responses were affected by microsaccades occurring near grating onset. In both monkeys

(Fig. 2, *C* and *F*), there was a reduction in express RT trials (i.e., the small low-latency peak in RT distributions was further reduced); moreover, the change in express RT trial likelihood between microsaccade and no-microsaccade trials was largest for low spatial frequencies, consistent with the spatial frequency-specific lengthening of RTs in Fig. 2, *A*, *B*, *D*, and *E*. Thus the spatial frequency-specific microsaccadic influence that we describe in this study affected our monkeys' behavior even during express RT trials.



Our behavioral paradigm also provided rich information about saccadic suppression dynamics, which we could later use to relate to SC neural modulations. For example, we evaluated microsaccadic suppression time courses across different spatial frequencies. Figure 2, *G*, *H*, *J*, and *K*, illustrates this by plotting mean RT from Fig. 2, *A* and *D* as a function of when a 1.11 or 4.44 cpd grating appeared after microsaccades. Microsaccadic occurrence had a clear time course of RT costs for each spatial frequency, with both monkeys showing lower RT costs for the higher spatial frequency immediately after microsaccades and then a gradual return toward the baseline no-microsaccade performance for a given frequency. Similarly, when we only focused on the subset of express RT trials, we found that the likelihood of express RTs was decreased immediately after microsaccades and gradually recovered (i.e., increased), and the magnitude of the recovery was again spatial frequency specific (Fig. 2, *I* and *L*).

Therefore, using a behavioral measure sensitive to SC visual response strength (Boehnke and Munoz 2008; Hafed and Chen 2016; Hafed and Krauzlis 2010; Hafed et al. 2015), we found a robust and selective pattern of microsaccadic suppression, which we think is analogous to perceptual suppression in humans with large saccades (Burr et al. 1982; Burr et al. 1994; Volkman et al. 1978). Note that our results are also consistent with spatial frequency-specific suppression of contrast detection performance in monkeys around the time of microsaccades (Hass and Horwitz 2011), which confirms that microsaccades have similar effects to larger saccades and that our RT measures in the present study were indeed sufficient to establish a behavioral effect in our animals. We were now in a position to evaluate neural correlates of this behavioral effect and to specifically test whether spatial-frequency-specific suppression would emerge in purely visual SC neurons, as we might predict from a previously published hypothesis about an SC circuit model for saccadic suppression (Berman and Wurtz 2008, Berman and Wurtz 2010; Berman and Wurtz 2011; Isa and Hall 2009; Lee et al. 2007; Phongphananee et al. 2011; Wurtz 2008; Wurtz et al. 2011).

#### *Selective Suppression of Low Spatial Frequencies in Visual Motor but not Visual SC Neurons*

Using the same animals but in completely different experimental sessions not requiring any saccadic responses at all (see MATERIALS AND METHODS), we recorded the activity of purely visual SC neurons (24 neurons; located  $680 \pm 95 \mu\text{m}$  below

SC surface) or visual motor neurons (66 neurons;  $1,159 \pm 66 \mu\text{m}$  below SC surface). Both types of neurons exhibit robust visual responses, but the question remains as to which would show spatial-frequency-specific suppression. We presented gratings similar to those used in Figs. 1 and 2 inside each neuron's RF (see MATERIALS AND METHODS). However, the task was now a fixation task with no saccadic eye movements toward the gratings; we only analyzed either no-microsaccade trials or trials in which the gratings appeared immediately after microsaccades (see MATERIALS AND METHODS).

Ensuring fixation during the recordings was especially important to demonstrate behavioral relevance of our neural modulations. Specifically, one of our goals was to directly correlate neural dynamics to behavior in each animal (as will be presented later). Showing that a specific SC cell class is highly correlated with behavior compared with another cell class, even when the correlations are made across completely independent sessions and tasks, would demonstrate the behavioral relevance of the cell class. Moreover, demonstrating that neural suppression dynamics appear on visual responses, even in the complete absence of an overt response, shows that it is sensory responses that matter during saccadic suppression. Finally, ensuring fixation avoided influences on visual sensitivity that take place during tasks requiring monkeys to generate a subsequent saccade to the presented stimulus (Li and Basso 2008).

Visual motor SC neurons showed the strongest saccadic suppression, and in a spatial-frequency-selective manner. Figure 3*A* shows the activity of two sample pure visual neurons (one per row) during presentations of different spatial frequencies (across columns), and Fig. 3*B* shows the activity of two sample visual motor neurons (in the same format). In each graph, black traces show activity with no microsaccades <100 ms from grating onset, and gray traces show activity when the same grating was presented within 50 ms after microsaccades. In no-microsaccade trials, all neurons showed expected visual bursts, but burst strength varied with spatial frequency (Fig. 3, black). This is suggestive of spatial frequency tuning (Hafed and Chen 2016), but our purpose was to investigate suppression relative to no-microsaccade responses; thus we scaled the y-axis in each panel such that, across panels, no-microsaccade curves visually appeared to be roughly equal in height. With the use of such scaling, visual burst suppression (Fig. 3, gray) was rendered clearer (quantitatively, we always measured suppression relative to the no-microsaccade responses within

Fig. 2. Spatial-frequency-selective microsaccadic suppression in behavior. *A*: mean RT as a function of spatial frequency. On no-microsaccade trials (black), RT increased with spatial frequency, consistent with dependence of visual response dynamics on spatial frequency (Breitmeyer 1975). If the same gratings appeared ~20–100 ms after microsaccades (gray), RT increased relative to no-microsaccade trials (a behavioral correlate of suppressed visual sensitivity), but more dramatically for low rather than high spatial frequencies (compare gray and black curves at different spatial frequencies). *B*: difference in RT between microsaccade and no-microsaccade trials (i.e., difference between gray and black curves in *A*), demonstrating the diminishing effects of microsaccades on RT behavioral costs with increasing spatial frequency. *C*: difference in the likelihood of express RT trials between microsaccade and no-microsaccade trials, demonstrating diminishing effects of microsaccades on reducing the likelihood of express RTs. *D–F*: same analyses as in *A–C* but for a second monkey. *G* and *H*: time courses of mean RT (*G*; as in *A*) or difference in RT (*H*; as in *B*) as a function of the time of grating onset after microsaccade end. The time courses are from 2 sample spatial frequencies (complete time courses from all spatial frequencies, and for each animal individually, are also shown in Fig. 6). For the difference in RT time course, RTs on trials with no microsaccades within <250 ms from grating onset were taken as the baseline. The initial RT cost caused by microsaccades was weaker for higher spatial frequency gratings (compare vertical arrows, consistent with *A*). *I*: likelihood of express RT trials as a function of time after microsaccade end, for the same spatial frequencies as in *G* and *H*. Immediately after microsaccades, there was an express RT cost (i.e., fewer express RTs), with gradual recovery in time. Moreover, the recovery dynamics were different for different spatial frequencies, as with overall RT (*G* and *H*). Also, note that the baseline fraction of express RTs (i.e., long after microsaccades) was different for different spatial frequencies so that the recovery for different spatial frequencies is toward different absolute values (as in *G*). *J–L*: same analyses as in *G–I* but for a second monkey. Error bars, when visible, denote SE;  $n = 8,153$  trials for monkey *N*, and  $n = 7,117$  for monkey *P*.

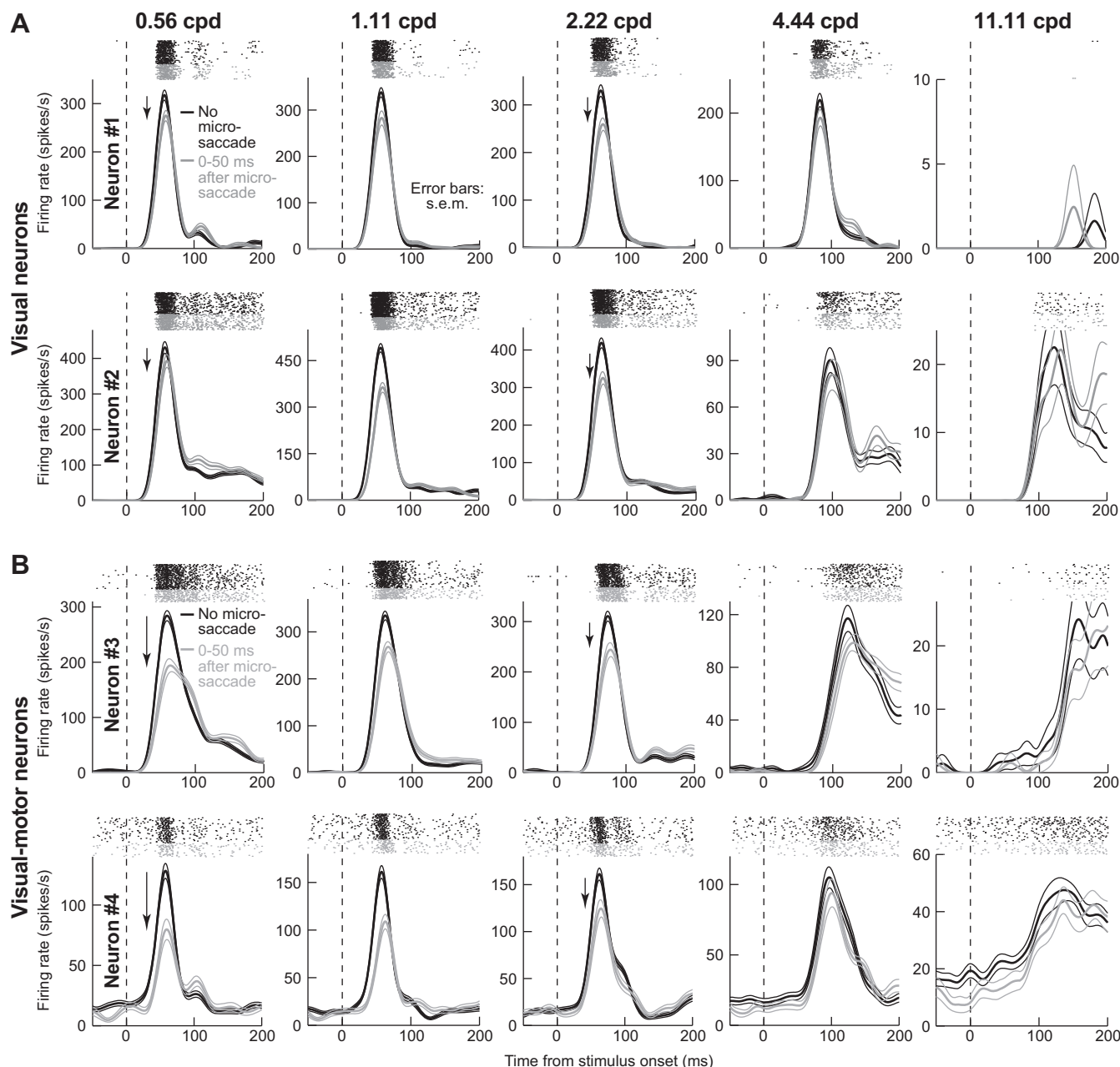


Fig. 3. Spatial-frequency-selective microsaccadic suppression of visual motor SC neurons. *A*: neural activity as a function of time after grating onset for 2 sample purely visual SC neurons (1 per row). Each graph in a row shows activity after presentation of a specific spatial frequency (indicated above each graph). Rasters above each firing rate curve show individual action potentials emitted by the neuron across individual trials. We divided trials into ones in which there was no microsaccade within  $<100$  ms from grating onset (black;  $n \geq 38$  trials per spatial frequency in these sample neurons) and ones in which the grating appeared immediately after microsaccades (gray;  $n \geq 30$  trials per spatial frequency). The y-axis was scaled in each panel such that the no-microsaccade firing rates visually appear to have approximately similar heights across panels, allowing easier comparison of suppression effects. Both neurons showed moderate microsaccadic suppression, with no clear pattern across spatial frequencies. *B*: same format as *A*, but for 2 sample visual motor neurons. The neurons showed stronger suppression at the lowest spatial frequency, and the suppression gradually decreased in strength with increasing spatial frequency (as in behavior); by 4.44 and 11.11 cpd, there was no suppression left. For these neurons,  $n \geq 28$  trials per spatial frequency for no microsaccade trials (black), and  $n \geq 22$  trials per spatial frequency trials for microsaccade trials (gray).

each given spatial frequency independently, and not across spatial frequencies; see MATERIALS AND METHODS). Importantly, there were differences in suppression patterns between visual and visual motor neurons. For the visual neurons (Fig. 3*A*), suppression was mild and relatively inconsistent across spatial frequencies; for the visual motor neurons (Fig. 3*B*), there was strong suppression for the lowest spatial frequency (*neuron 3*:  $\sim 32\%$ ; *neuron 4*:  $\sim 38\%$ ;  $P < 0.01$  for each neuron, Wilcoxon

rank sum test), and there was also a systematic reduction in suppression strength with increasing frequency (by 4.44 and 11.11 cpd, there was no suppression left;  $P = 0.49$  for 4.44 cpd and  $P = 0.41$  for 11.11 cpd in *neuron 3*, and  $P = 0.15$  for 4.44 cpd and  $P = 0.99$  for 11.11 cpd in *neuron 4*, Wilcoxon rank sum test). Importantly, the eye movement associated with suppression in all panels had ended before grating onset. Thus the suppression cannot be attributed to blurring of the gratings by eye movements.

Across neurons, there was selective suppression of visual sensitivity as a function of spatial frequency, but only in visual motor neurons. Figure 4A summarizes these findings by plotting a suppression index (see MATERIALS AND METHODS) as a function of spatial frequency. Peak visual response was suppressed in both visual and visual motor neurons (suppression index  $< 1$ ). However, the suppression was not spatial frequency selective and was weaker in visual neurons; in visual motor neurons, there was strong suppression for the lowest spatial frequencies, and the effect gradually dissipated away with increasing frequency. Quantitatively, the average suppression value in visual neurons was 11% across spatial frequencies, and it was 22% in visual motor neurons. When the data are separated for low and high spatial frequencies, the average suppression value in visual neurons for the lowest two spatial frequencies or the highest two spatial frequencies was 11%, meaning that the suppression value was similar for the two groups of frequencies ( $P = 0.77$ , Wilcoxon rank sum test). On the other hand, visual motor neurons were suppressed by 23% for the lowest two spatial frequencies and 17% for the highest two spatial frequencies, and the difference between the groups of spatial frequencies was significant ( $P < 0.01$ , Wilcoxon rank sum test).

A difference between visual and visual motor neurons also appeared in suppression temporal dynamics, again showing weaker suppression in the visual neurons (Fig. 4B). Thus there are differences in saccadic suppression strength between visual and visual motor SC neurons, and visual motor neuron suppression selectivity appears more similar to behavioral effects, both in our own experiments (Figs. 1 and 2) and in the literature of human perceptual effects (Burr et al. 1982; Burr et al. 1994; Volkman et al. 1978) and monkey contrast detection thresholds (Hass and Horwitz 2011).

Even though our previously published results revealed no differences in postmicrosaccadic suppression in the SC as a function of microsaccade direction (Chen et al. 2015), we

nonetheless analyzed movement directions in the present study, as well. Across our population, the direction of a microsaccade relative to the location of a neuron's RF hotspot was fairly uniformly distributed (Fig. 5A; similar to Chen et al. 2015). This means that our results in Figs. 3 and 4 described above are not an artifact of biased sampling of microsaccade directions. Moreover, for each spatial frequency, and for each of either visual or visual motor neurons, we computed the suppression index of Fig. 4, but now separately for microsaccades either toward or opposite the RF location (with "toward" and "opposite" being defined as in Chen et al. 2015). Figure 5B shows the results of this analysis for an example spatial frequency. As shown, for either visual or visual motor neurons, the suppression values observed were statistically similar whether the microsaccade occurring before stimulus onset was directed toward or away from the grating location ( $P = 0.64$  for visual neurons and  $P = 0.42$  for visual motor neurons, Wilcoxon rank sum test). This result also held for all other spatial frequencies ( $P > 0.07$  for either visual or visual motor neurons, Wilcoxon rank sum test). Because of this, we combined microsaccade directions in all subsequent analyses.

#### Better Correlation Between Visual Motor Neuron Dynamics and Behavior than Between Visual Neuron Dynamics and Behavior

To further explore the apparent similarity between visual motor neuron suppression patterns (Fig. 4) and behavior (Fig. 2), we used the dynamics of our recorded population as a proxy for how the SC might be engaged in our behavioral task of Figs. 1 and 2. We plotted the time course of behavioral suppression (similar to Fig. 2, *H* and *K*) for each spatial frequency and each monkey individually (Fig. 6, *A* and *E*), and we also plotted the neural time course of visual motor neuron suppression, again for each monkey individually (Fig. 6, *B* and *F*; an example time course for purely visual neurons is also

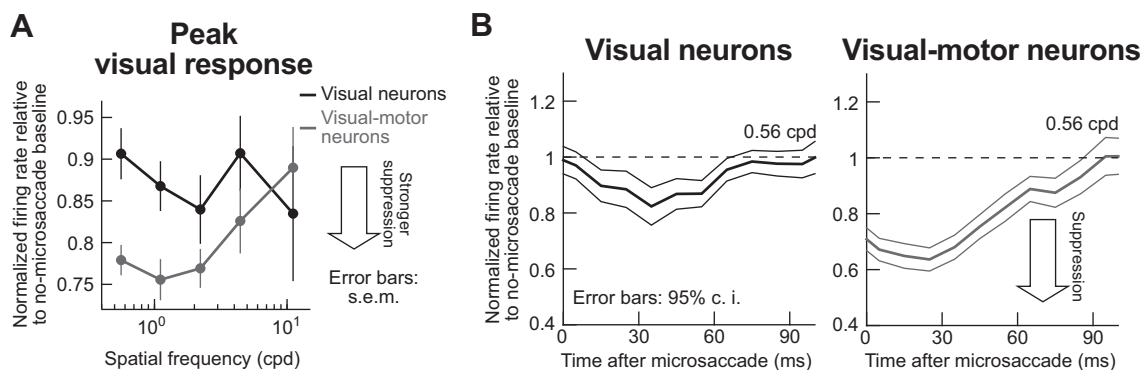


Fig. 4. Spatial-frequency-dependent microsaccadic suppression of visual bursts in visual motor but not visual SC neurons. *A*: we measured peak stimulus-evoked visual burst after grating onset (e.g., from traces like those in Fig. 3) and plotted it as a function of grating spatial frequency. We grouped neurons as purely visual (dark gray) or visual motor (light gray). Visual neurons showed only ~10% suppression, and there was no consistent spatial frequency dependence of this suppression. Visual motor neurons showed ~25% suppression in the low spatial frequencies, and this effect gradually decreased with increasing spatial frequency (as in behavior). Error bars denote SE. Note that the error bars for the highest spatial frequency are larger than for other frequencies because some neurons completely stopped responding at 11.11 cpd, which reduced population size in this spatial frequency (see MATERIALS AND METHODS). *B*: time courses of microsaccadic suppression in visual (*left*) and visual motor neurons (*right*) for a sample spatial frequency. We performed an analysis similar to that described in Chen et al. (2015) but aligning on microsaccade end. For each time window after microsaccade end in which a grating appeared (*x*-axis; 50-ms bins in 10-ms steps), we measured peak firing rate evoked by grating onset (see MATERIALS AND METHODS), and we normalized it by peak firing rate on no-microsaccade trials. Visual motor neurons showed stronger suppression than visual neurons (compare *y*-axis in both graphs), and both neuron types experienced recovery with increasing time after microsaccades (consistent with behavioral effects). Note that the time course of visual motor neuron suppression is similar to the time course of behavioral effects (e.g., Fig. 2, *H* and *K*) and is also similar to the time course of saccadic suppression in the earlier literature (e.g., Diamond et al. 2000; Hafed and Krauzlis 2010; Ibbotson and Krekelberg 2011). Figure 6 shows individual monkey time courses, other spatial frequencies, and relationships between neural time courses and the respective monkey's behavioral performance dynamics.  $n = 66$  visual motor neurons, and  $n = 24$  visual neurons.



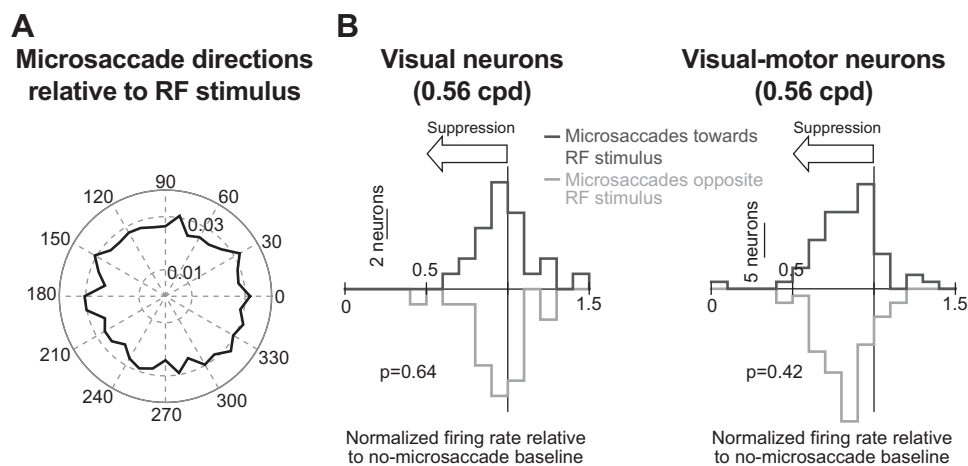


Fig. 5. Lack of dependence of microsaccadic suppression on movement direction. *A*: normalized histogram of microsaccade directions relative to stimulus location (i.e., with all neuronal hotspot locations rotated to be aligned with 0 as in Chen et al. 2015). Across our population, microsaccade directions were evenly distributed relative to the location of the RF stimulus, similar to the results of Chen et al. (2015). Thus our results from Fig. 4 are not due to biased sampling of microsaccade directions. *B*: for each visual (*left*) or visual motor neuron (*right*), we calculated a suppression index (as in Fig. 4), but only for trials in which a microsaccade was directed either toward (dark gray) or opposite (light gray) the location of the stimulus (“toward” and “opposite” microsaccades were defined as in Chen et al. 2015). Across the population of either visual or visual motor neurons, the suppression index was similar for toward and opposite microsaccades, suggesting that suppression was not dependent on movement direction. Similar observations were made with large saccades in (Knöll et al. 2011). Each graph in *B* shows the *P* value obtained from a rank sum test comparing neural suppression indexes for toward and opposite trials. Note that we also repeated the analysis shown in *B* for all other spatial frequencies (and for either visual or visual motor neurons), and we always obtained similar suppression values for toward and opposite microsaccades ( $P > 0.07$  for each performed test).

shown in Fig. 4*B*). For this comparative analysis, we used the same binning windows in both behavioral and neural data (50-ms bin widths in steps of 10 ms starting at 0 ms after microsaccade end), and we next correlated the two time courses: we plotted all samples of the behavioral time course against all samples of the neural time course irrespective of spatial frequency or time after microsaccades (Fig. 6, *C* and *G*). There was high correlation between visual burst strength in SC visual motor neurons and the behavioral effect of microsaccadic suppression: whenever visual bursts were weaker, RT costs increased, and vice versa, regardless of spatial frequency or time after microsaccades. This high correlation is particularly remarkable given that the behavioral and neural data were collected in completely different sessions and with different behavioral tasks, and even with imperfect matching of neuron locations relative to the grating location used in the behavioral study.

The highest correlation between neural patterns and behavior was observed only when we used peak visual response of visual motor SC neurons as the behavioral predictor (Fig. 6, *C* and *G*). When we correlated behavioral time courses with peak visual response of purely visual neurons, the correlations were significantly weaker (Fig. 6, *D* and *H*;  $P = 0.02$  for *monkey N* and  $P = 0.02$  for *monkey P*, Steiger’s *Z*-test; actual correlation values are shown in Fig. 6). Thus a most simple linear readout of visual motor neurons would fare better at predicting behavior than a similarly simple readout of purely visual neurons.

The results of Fig. 6 suggest that saccadic suppression in visual motor neurons is more in line with our behavioral effects than in purely visual neurons. However, one possible confound could be in the distribution of preferred spatial frequencies in visual motor neurons. For example, if only the preferred spatial frequency of a neuron experiences the strongest suppression, and if visual motor neurons only had low preferred spatial frequencies, then the selective suppression of Fig. 4*A* would emerge, because there would be more visual motor neurons

preferring low spatial frequencies than visual neurons. However, we found no clear differences in patterns of preferred spatial frequencies between visual and visual motor neurons. Specifically, across our population, both visual and visual motor neurons spanned a wide range of preferred spatial frequencies (from 0.56 to 4.54 cpd in visual neurons and from 0.56 to 4.82 cpd in visual motor neurons), with large overlap between the two neuron types; this meant that there was no statistically significant difference in preferred spatial frequencies between our visual and visual motor neurons ( $P = 0.996$ , Wilcoxon rank sum test).

To further investigate the above potential confound, we also explicitly analyzed suppression profiles of visual motor neurons as a function of the neurons’ preferred spatial frequencies. For each spatial frequency, we took only neurons preferring this spatial frequency, and we checked how these neurons were suppressed. Figure 7, *A–D*, shows the results of this analysis. There was indeed a tendency for the preferred spatial frequency of a neuron to experience the strongest suppression relative to other frequencies (e.g., black arrows). However, this strongest suppression still became progressively weaker and weaker with increasing spatial frequency (e.g., compare Fig. 7, *A* and *B* with Fig. 7, *C* and *D*). This is further demonstrated by Fig. 7*E*, in which we took the maximal suppression frequency from each of the panels in Fig. 7, *A–D*, and plotted them with an indication of the behavioral microsaccadic suppression profile (obtained as the graphical inverse of RT modulation profiles from Fig. 2, *B* and *E*, with arbitrary y-axis scaling). Importantly, we again made sure that the neural suppression data in Fig. 7 were analyzed in an identical manner to behavioral analyses (i.e., we considered the same interval of stimulus onsets happening 20–100 ms after microsaccade end as in the behavioral analyses). As shown in Fig. 7*E*, there was a clear match between neural and behavioral effects in both animals (the correlation between neural suppression and behavioral suppression was 0.99 for *monkey N* and 0.89 for *monkey P*).

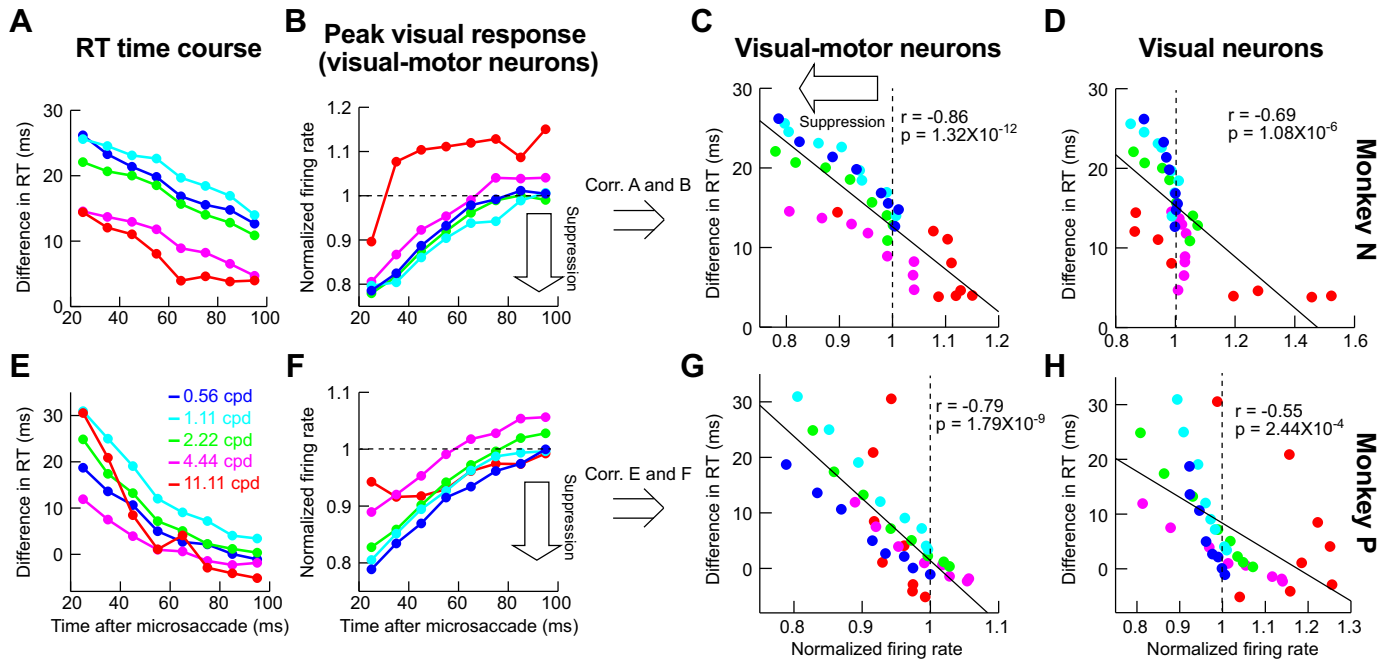


Fig. 6. Correlating behavioral microsaccadic suppression with neural microsaccadic suppression on completely different experimental sessions. *A*: time course of difference in RT from baseline (e.g., Fig. 2, *H* and *K*; see MATERIALS AND METHODS) as a function of time of grating onset after microsaccade end in our behavioral experiments (*monkey N*). Different color curves show different spatial frequencies. Immediately after microsaccades, there was a strong cost in RT for low spatial frequencies and a more moderate cost for high spatial frequencies. In all spatial frequencies, the RT cost associated with microsaccadic suppression slowly dissipated in time. *B*: analysis similar to that in *A* but for the peak visual response in our neural experiments, on completely different sessions from the behavioral data, and only for visual motor neurons. *C*: correlation (Corr.) between the data points in *A* and those in *B*, regardless of time or spatial frequency. There was strong correlation between visual burst strength and RT cost, even on completely different experimental sessions, suggesting that visual motor neurons are modulated during microsaccadic suppression in a manner that could be relevant for the phenomenon reported by Burr et al. (1994). *D*: we correlated the behavioral points in *A* with similar points, but for visual neuron time courses (e.g., Fig. 4*B*). The correlation with behavior was worse than in visual motor neurons. *E–H*: observations similar to those in *A–D* for a second monkey (*monkey P*).  $n = 24$  visual motor neurons for *monkey N*, and  $n = 42$  visual motor neurons for *monkey P*;  $n = 15$  visual neurons for *monkey N*, and  $n = 9$  visual neurons for *monkey P*.

Thus the selective suppression of Figs. 3–6 was not an artifact of potential biased spatial frequency tuning properties of only visual motor neurons.

Taken together, our results so far suggest that spatial-frequency-specific SC saccadic suppression is localized in the visual motor neurons, with visual neurons only showing modest and nonselective suppression.

#### Influence of a Putative Microsaccadic Source Signal on Local SC Population Activity During Suppression

To demonstrate that there may indeed be a saccadic source signal associated with suppressed SC visual bursts (i.e., putative corollary discharge associated with the movement command), we analyzed local field potentials (LFPs) around our

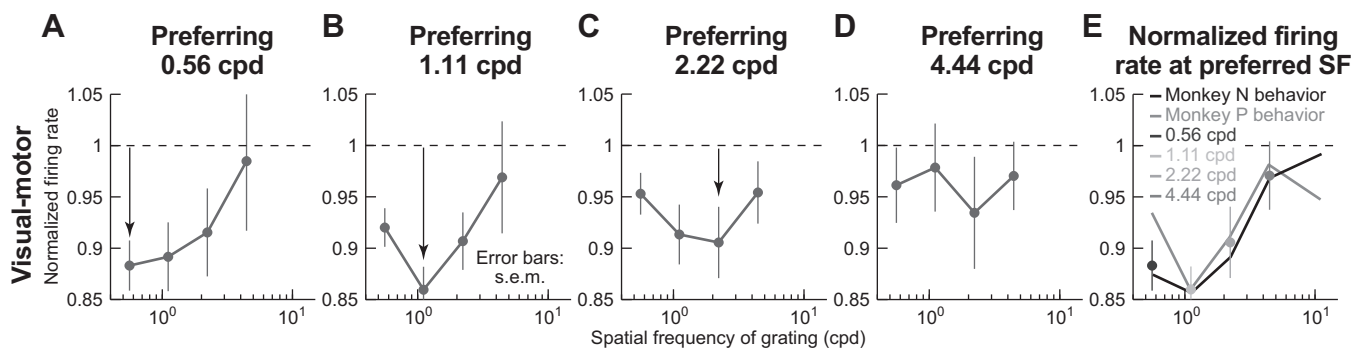


Fig. 7. Selective low-frequency suppression in visual motor neurons independent of preferred spatial frequency. *A–D*: in each panel, we selected only neurons preferring a single spatial frequency on no-microsaccade trials (see MATERIALS AND METHODS). We then repeated the analysis of Fig. 4*A*. The preferred spatial frequency tended to experience the strongest suppression compared with other spatial frequencies (black arrows). However, the strength of the suppression even for the preferred spatial frequency consistently decreased with increasing spatial frequency (compare arrows in individual panels). Note that we did not have neurons preferring 11.11 cpd in this analysis, and thus we do not show this spatial frequency in this figure. *E*: we collected the maximally suppressed spatial frequency from each panel *A–D* (see key), and we plotted them together. The *monkey N* and *monkey P* behavior lines are a copy of the behavioral RT microsaccadic suppression curves of Fig. 2, *B* and *E*, but are inverted (and with arbitrary y-axis scaling) to match the neural suppression curves. As can be seen, even if the preferred spatial frequency of neurons always experienced maximal suppression, this maximal suppression was still decreased with increasing spatial frequency. Thus the spatial frequency selectivity of visual motor neural suppression was still correlated with behavior. Error bars denote SE;  $n = 26, 19, 8,$  and  $5$  neurons in *A, B, C,* and *D*, respectively.

electrodes (see MATERIALS AND METHODS). Stimulus onset in no-microsaccade trials caused a negative-going “stimulus-evoked” LFP deflection for both visual and visual motor electrode tracks (Hafed and Chen 2016; Ikeda et al. 2015). For example, Fig. 8 shows LFP traces (in a format similar to Fig. 3) as a function of spatial frequency for an example superficial track (i.e., among visual neurons; Fig. 8A) and an example deeper track (among visual motor neurons; Fig. 8B). Remarkably, on microsaccade trials, stimulus-evoked LFP response was not suppressed for any of the spatial frequencies. In fact, for the visual motor electrode track (Fig. 8B), LFP response was enhanced, and more so with increasing spatial frequency (Fig. 9A;  $P < 0.01$ , Kruskal-Wallis test on the modulation index with spatial frequency as the main factor). Given that LFPs reflect not only local population spiking activity but also putative synaptic inputs, these results suggest the existence of a possible microsaccade-related input modulating visual bursts. This effect, an enhanced LFP response with increasing spatial frequency, was again stronger in visual motor than visual electrode tracks, as summarized in Fig. 9A. However, it is important to emphasize that this signal was not a direct microsaccade command, because none of our neurons at all electrode locations in this study exhibited microsaccade-related movement bursts (see MATERIALS AND METHODS).

Our interpretation of an increased LFP negativity as reflecting a possible movement-related input mediating firing rate suppression effects is consistent with the enhanced LFP response shown in Figs. 8 and 9A for high spatial frequencies. These frequencies evoke the weakest visual activity (Figs. 3 and 8, black). Thus, if the LFP signal reflects both visual inputs associated with the stimulus onset as well as movement-related modulatory inputs to the population associated with movement execution (which do not depend on visual response strength), then the influence of the modulatory input (i.e., the putative saccadic source signal for suppression) should become increas-

ingly more obvious in the LFP with increasing spatial frequency (Fig. 9A). However, we cannot tell from these data whether the two signals integrated in the LFP reflect pure superposition of visual and modulatory inputs, or whether a more complex integration takes place. In any case, combined with earlier firing rate results, our LFP analyses reveal that visual motor SC neurons may be closely associated with a movement-related source for spatial-frequency-specific saccadic suppression.

One possible confound with the above result is that microsaccades (even though they ended before stimulus onset) might cause long-lasting LFP modulations, which would be superimposed on a stimulus-evoked LFP deflection in Fig. 8. In other words, the evoked response could potentially still be suppressed, but it could be level-shifted because it rides on a microsaccade-induced LFP modulation. We thus tested for intrinsic microsaccade-induced LFP modulation. During simple fixation without any other visual stimuli, both visual and visual motor SC electrode locations exhibited prolonged microsaccade-related LFP modulations, involving a subtle negativity after microsaccade end, as shown in Fig. 10 (additional evidence of such negativity can also be seen in the prestimulus interval of Fig. 8, but it is washed out because of alignment to stimulus onset rather than to microsaccades). We wondered whether this modulation is sufficient to explain the lack of LFP suppression in stimulus-evoked LFPs (Fig. 8). We corrected for a baseline shift at grating onset (see MATERIALS AND METHODS), and we still found no suppression in the strength of the stimulus-evoked LFP response (Fig. 9A). Thus, as represented in Figs. 8–10, we believe that we have uncovered evidence for a putative microsaccade-related modulatory input at the time of visual burst suppression in both SC visual and visual motor neurons. This input does not itself necessarily trigger microsaccades (see DISCUSSION); it may instead mediate visual burst suppression in firing rates, although

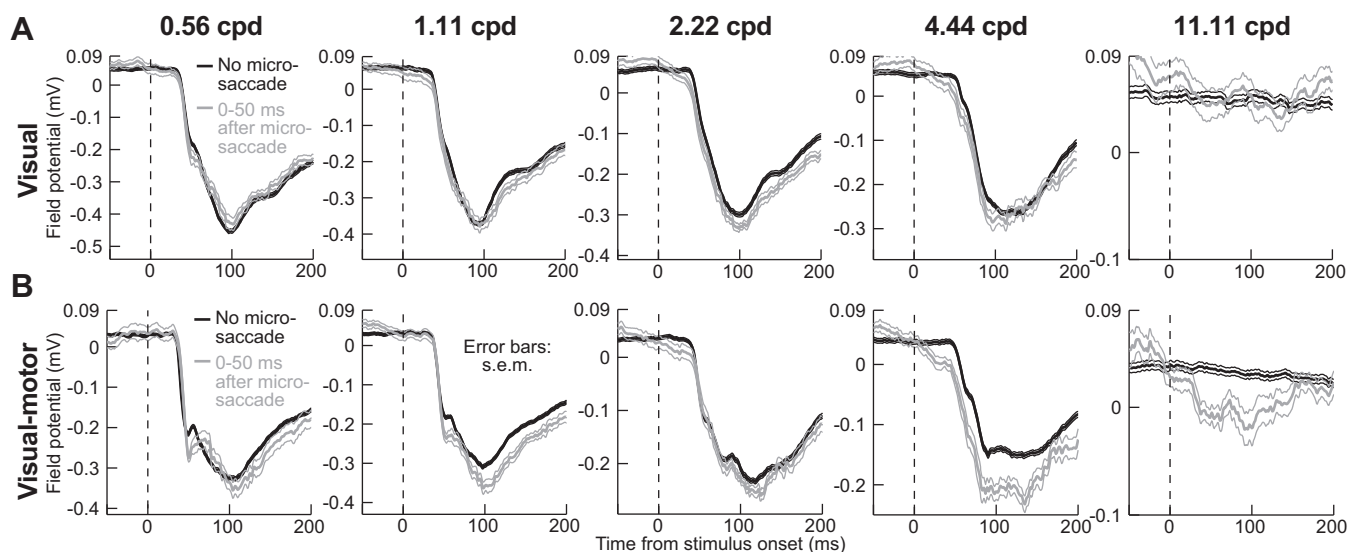


Fig. 8. LFP modulations during microsaccadic suppression. *A* and *B* are formatted similarly to Fig. 3, except that LFP modulations are plotted around a sample electrode track near visual (*A*) or visual motor neurons (*B*). There was no evidence of a reduced LFP-evoked response for trials with grating onset after microsaccades (faint colors). If anything, the peak evoked response and the latency to evoked response were stronger and shorter, respectively (see Fig. 9). This effect was not explained by an intrinsic perimicrosaccadic modulation of LFP (see Figs. 9A and 10), but it is consistent with an additional movement-related modulatory signal associated with saccade execution that influences stimulus-evoked spiking activity. Error bars denote SE. For the visual track (*A*),  $n \geq 113$  trials per spatial frequency on no-microsaccade trials (black), and  $n \geq 25$  trials per spatial frequency on microsaccade trials (gray). For the visual motor track (*B*),  $n \geq 140$  trials per spatial frequency on no-microsaccade trials (black), and  $n \geq 12$  trials on microsaccade trials (gray).

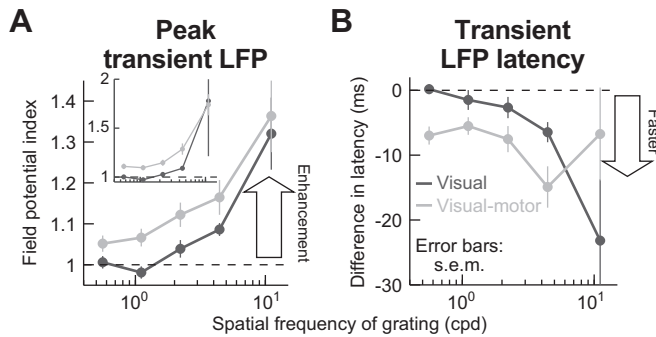


Fig. 9. Lack of microsaccadic suppression in LFP stimulus-evoked responses. *A*: we performed an analysis similar to that shown in Fig. 4*A*, but on LFPs. We measured peak LFP response with and without microsaccades and then obtained a modulation index (see MATERIALS AND METHODS). The *inset* shows the modulation index from raw measurements, whereas the main panel shows the same analysis but after a baseline shift was subtracted from the microsaccade trials. Specifically, data shown in Fig. 10 suggest that there is a negativity in LFPs after microsaccades that and stimulus onset in the microsaccade trials came after a previous microsaccade. Thus we measured the peak LFP stimulus-evoked response on microsaccade trials as the difference between the raw LFP stimulus-evoked negativity minus the baseline LFP value that was present at the time of grating onset (see MATERIALS AND METHODS). In both the *inset* and the main panel, there was no suppression in the stimulus-evoked LFP response, contrary to firing rate results (Fig. 4*A*). Rather, there was response enhancement, which progressively increased with increasing spatial frequency, and this happened for both visual and visual motor electrode track locations ( $P < 0.01$  for either baseline-corrected or raw measurements and for each of visual-only or visual motor electrode tracks; Kruskal-Wallis test with spatial frequency as the main factor). *B*: analyses similar to those in *A* but measuring the latency to LFP stimulus-evoked response, which decreased on microsaccade trials ( $y$ -axis values  $< 0$  ms;  $P < 0.02$  for visual electrode tracks and  $P = 0.07$  for visual motor electrode tracks; Kruskal-Wallis test with spatial frequency as the main factor). Thus, when a stimulus appeared immediately after a microsaccade, the stimulus-evoked LFP response started earlier than without a microsaccade. Error bars denote SE.

the exact mechanisms remain to be explored. Moreover, the modulatory input shows differential modulation between superficial and intermediate electrode tracks (Fig. 9*A*), consistent with our firing rate results.

Enhanced stimulus-evoked LFP response amplitudes (Fig. 9*A*) were also accompanied by slightly faster LFP responses (Fig. 9*B*), again consistent with a movement-related source modulating neural firing rates at the time visual burst occurrence (because the movement happened before stimulus onset). It is also interesting to note that, like firing rate time courses, time courses of stimulus-evoked LFP modulations for stimuli appearing after microsaccades were also correlated with behavioral microsaccadic suppression dynamics (as in Fig. 6). In the LFPs, the best behavioral predictor was the latency of stimulus-evoked LFP deflection (Fig. 11, formatted similarly to Fig. 6), and visual motor electrode tracks again showed higher correlation values with behavior (Fig. 11, *C* and *G*) than visual electrode tracks (Fig. 11, *D* and *H*). For *monkey N*, this effect was significant ( $P < 0.01$ , Steiger's *Z*-test), but it did not reach significance in *monkey P* ( $P = 0.38$ ).

Our results combined demonstrate that visual motor neurons are more in line with selective effects of saccadic suppression, in both humans (Burr et al. 1982, 1994; Volkman et al. 1978) and monkeys (Fig. 2; also see Hass and Horwitz 2011), than purely visual neurons. This suggests that the mechanisms for saccadic suppression in the SC are more complicated than those suggested by a hypothesized pathway of a simple inhib-

itory relay to superficial SC layers from deeper centers of the saccade motor command.

## DISCUSSION

We found spatial-frequency-selective saccadic suppression in SC visual motor neurons, and the neural dynamics of visual motor neuron suppression were well correlated with behavior. Visual neurons showed weaker suppression overall, which also was not dependent on spatial frequency. These results suggest that SC visual motor neurons are among the neural loci for spatial-frequency-specific saccadic suppression. Because spatial frequency specificity is a robust characteristic of saccadic suppression (Burr et al. 1994; Hass and Horwitz 2011), identifying neural loci for this phenomenon is important. In what follows, we discuss our methodological choices, the implications of our results, and how these results fit within our current understanding of saccades, active vision, and the SC.

Our results are in line with interpretations of saccadic suppression as a reduction in response gain (Chen et al. 2015;

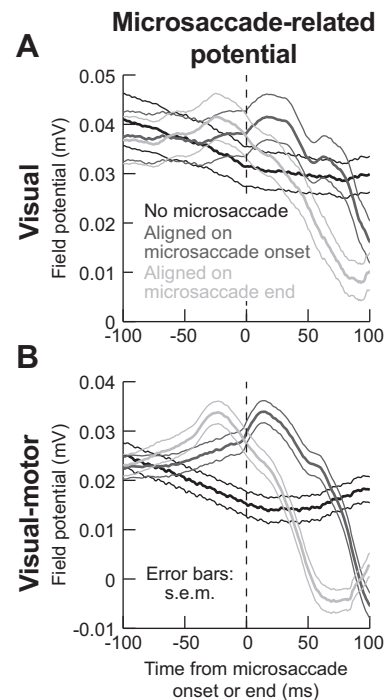


Fig. 10. Microsaccade-related LFP modulations in the absence of an RF stimulus. We aligned LFP activity to either microsaccade onset (dark gray) or microsaccade end (light gray) during a baseline fixation interval with no RF stimulus at all (see MATERIALS AND METHODS). The black curves show LFP activity during equally long control intervals, again with no RF stimulus, but also with no microsaccade occurrence. Even though there was no microsaccade-related spiking at all the sites investigated in this study, microsaccades caused systematic modulations in both visual (*A*) and visual motor (*B*) electrode locations in the SC, even though our electrodes were primarily placed in extrafoveal SC representations far from the movement end points. Thus these LFP modulations, similar to previously reported saccade-related LFP modulations (Liu et al. 2009), reflect a potential microsaccade-related modulatory signal that can mediate microsaccadic suppression of firing rates in extrafoveal SC neurons. Also, note how the effect on visual motor layers (*B*) is more systematic and robust than in visual layers (*A*). This is further evidence of a putative extraretinal signal in the SC visual motor layers that might mediate saccadic suppression (and explain the data in Fig. 6), and it also makes it unlikely that the LFP modulations in this figure are due to ocular muscle artifacts. Error bars denote SE;  $n = 66$  electrode tracks visual motor layers (*B*), and  $n = 24$  electrode tracks for visual layers (*A*).

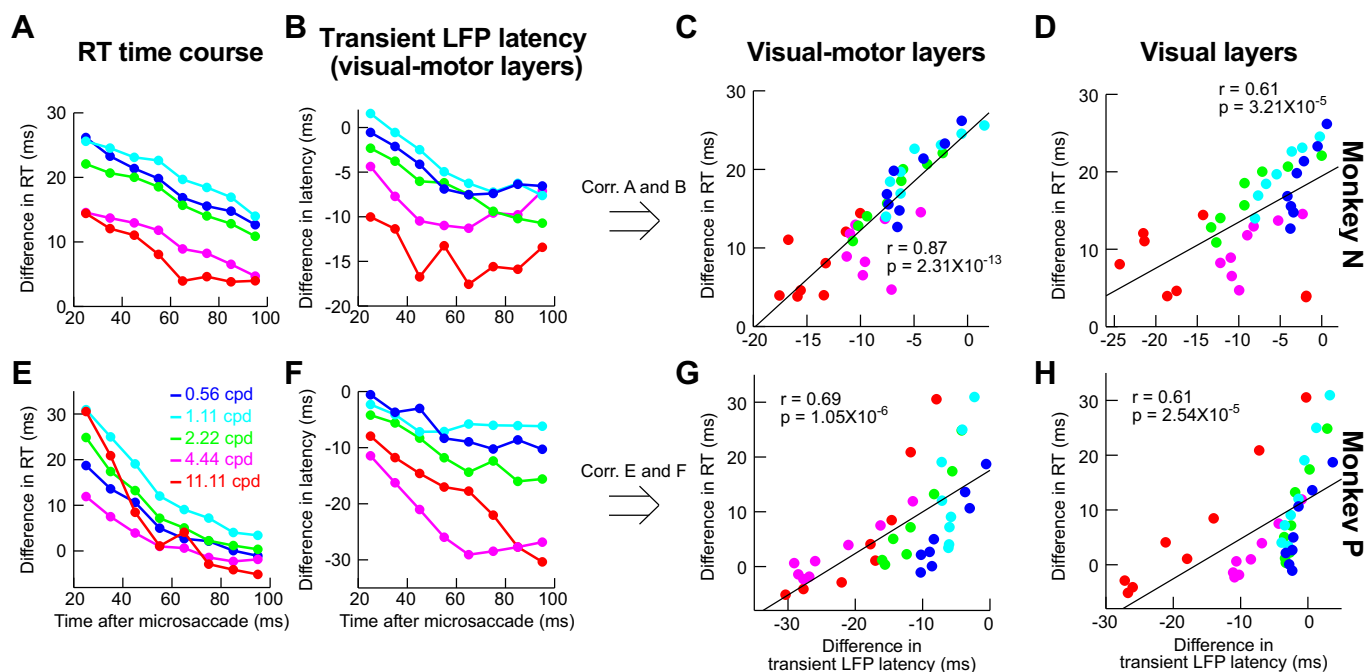


Fig. 11. Correlation between LFP modulation parameters and behavioral effects of suppression. This figure is formatted similarly to Fig. 6, except that we have plotted LFP time courses instead of firing rate time courses. Specifically, in *B* and *F*, we plotted the time course of LFP stimulus-evoked response latency (e.g., Fig. 9*B*) as a function of spatial frequency and time after microsaccades. The correlation between this latency in visual motor layers and behavior was better (*C* and *G*) than in visual layers (*D* and *H*). Thus it is again the visual motor layers that are better predictors of behavior, as in Fig. 6, although firing rates (Fig. 6) showed higher correlations to behavior in general. Note that we also measured correlations between behavior and LFP stimulus-evoked response strength rather latency (data not shown), but the LFP response latency always showed the better correlations with behavior.

Guez et al. 2013; Hafed and Krauzlis 2010). Consistent with this, we have recently found that SC neural contrast thresholds are increased after microsaccades (Chen et al. 2015). We also have found that for SC neurons possessing some baseline activity in the absence of a stimulus, there was very modest perimicrosaccadic modulation of activity (see Fig. S2 of Chen et al. 2015) compared with the modulations in stimulus-evoked visual bursts that we observed in the present study and earlier (Chen et al. 2015; Hafed and Krauzlis 2010). We believe that observations like these place constraints on the potential sources and mechanisms of extraretinal modulation often invoked in theories of saccadic suppression.

There have been few successful demonstrations of spatial-frequency-specific patterns of saccadic suppression in neural activity. In early visual areas, selective magnocellular pathway suppression is not clear (Hass and Horwitz 2011; Kleiser et al. 2004; Ramcharan et al. 2001; Reppas et al. 2002; Royal et al. 2006), even though behavioral effects strongly predicted them (Burr et al. 1982, 1994; Hass and Horwitz 2011; Volkman et al. 1978). Rather, there is mild suppression, regardless of magno- or parvocellular pathway. Higher areas, primarily in the dorsal stream, do show saccadic suppression dynamics (Bremmer et al. 2009; Han et al. 2009; Ibbotson et al. 2007, 2008; Krock and Moore 2016; Thiele et al. 2002; Zanos et al. 2016), but the origins of such suppression remain elusive. In fact, it has been suggested that suppression in motion-related areas MT and MST (Bremmer et al. 2009; Ibbotson et al. 2007, 2008; Thiele et al. 2002) may be inherited from earlier visual areas (Ibbotson et al. 2007, 2008), which themselves have weak and unselective suppression. Thus there is a pressing need for better understanding of saccadic suppression mechanisms.

The fact that primarily motion areas have been shown to exhibit the most convincing suppression additionally does not help account for the fact that saccadic suppression may be useful for perception even if the “motion problem” (Wurtz 2008) caused by saccades, which we described in the Introduction, is solved. For example, suppression could help regularize processing of stimuli after saccades, regardless of the image shift itself. Consistent with this, we saw SC suppression for microsaccades, even though both the retinal-image motion and displacement caused by these eye movements are quite mild. Moreover, we saw suppression even with purely stationary gratings.

Related to the above, the fact that we saw any effects with microsaccades at all is interesting in its own regard, because it adds to the microsaccade literature, but the real advantage to studying microsaccades was that they allowed better experimental control. Microsaccades are mechanically similar to larger saccades (Hafed 2011; Hafed et al. 2009, 2015; Zuber et al. 1965), making them an extremely viable tool to understand saccadic suppression. However, these movements simplify several challenges associated with large saccades. For example, studies with large saccades have to contend with large image shifts caused by eye movements. As a result, full field stimuli often become necessary (Ibbotson et al. 2007, 2008). In our case, we could use stimuli identical to how normal experiments might stimulate RFs. More importantly, microsaccades allowed us to dissociate the location of saccadic suppression from the movement end-point location, as is known to happen with large saccades (Knöll et al. 2011). This has allowed us to make the intriguing observation of movement-related LFP modulations (Fig. 10) even in extrafoveal SC (i.e., with no microsaccade-related bursting neurons). These modulations,

similarly to saccade-related LFP modulations in human SC (Liu et al. 2009), can potentially explain recently observed perimicrosaccadic alterations in neural activity and behavior at eccentricities much farther than microsaccade amplitudes (Chen et al. 2015; Hafed 2013; Hafed et al. 2015; Tian et al. 2016).

Another experimental advantage was the fact that SC shows suppression after saccades in our type of paradigm (Chen et al. 2015; Hafed and Krauzlis 2010). This allowed us to avoid probing neurons during the eye movements themselves. Of course, saccadic suppression would be even stronger during the microsaccades themselves, as we have recently shown (Chen et al. 2015; Hafed and Krauzlis 2010), which is further evidence of a consistency between our visual motor neural modulations and classic perceptual effects of saccadic suppression in humans (e.g., Zuber et al. 1966). Thus our choice to focus on postmovement modulations was one of exploiting the experimental advantages of doing so as opposed to one of a conceptual difference between our visual motor neural modulations and the phenomenon itself.

Concerning superficial visual neurons, one can speculate about their source of mild and unselective suppression. This suppression could reflect retinal effects, because the superficial SC receives retinal projections (Pollack and Hickey 1979). Indeed, retinal outputs do show transient perturbations in response to saccade-like image displacements (Roska and Werblin 2003). Additionally, the effect could be inherited from V1, which does not show selectivity (Hass and Horwitz 2011). Regardless of the source, suppression in visual neurons is not selective for spatial frequency as is known in perception (e.g., Burr et al. 1994). Of course, such suppression could still be functional. For example, a collicular-thalamic-cortical pathway from superficial SC may selectively target motion-related areas (Berman and Wurtz 2008, 2010, 2011; Wurtz et al. 2011). As a result, superficial SC may still contribute to saccadic suppression of motion (Bridgeman et al. 1975; Burr et al. 1982); in this case, selectively suppressing motion by superficial SC neurons would arise not necessarily because the neurons themselves are selective in their suppression profiles, but instead because of selectivity in their connections to cortical targets. Although this idea is consistent with similarities of neural saccadic suppression dynamics between superficial SC neurons and MT neurons (Berman et al., in press), it receives substantially less support from SC inactivation experiments in the same study (Berman et al., in press). In these experiments, inactivating the superficial SC did not reduce MT suppression effects, whereas inactivating the deeper SC layers did. In this regard, we believe that the pathway from intermediate SC layers to frontal eye field (FEF) via thalamus (Sommer and Wurtz 2004) is the more likely source of cortical saccadic suppression in general, not only in MT but also in other cortical areas such as FEF (Krock and Moore 2016) and V4 (Han et al. 2009; Zanos et al. 2016). This is consistent with our present results showing that saccadic suppression may already be established in the intermediate SC layers themselves without the need for an internal inhibitory relay to superficial layers. This inhibitory relay (Isa and Hall 2009; Lee et al. 2007; Phongphanphanee et al. 2011) could be used for other functions, perhaps in coordination with an excitatory relay in parallel, which has also been identified (Ghitani et al. 2014).

Our observation of a lack of suppression selectivity in purely visual neurons also helps address an important question regarding the nature of our selective visual motor neuron modulations. Specifically, it may be argued that (peripheral) SC neurons may preferentially over-sample low spatial frequencies in their tuning curves (Hafed and Chen 2016), meaning that they exhibit higher sensitivity for low spatial frequencies even without microsaccades. This, in turn, could mean that we only saw stronger suppression at low spatial frequencies (in the visual motor neurons) simply because the baseline visual responses were stronger. However, our visual neurons preferred similar ranges of spatial frequencies as our visual motor neurons. If our effects are explained by the dependence of suppression on baseline visual sensitivity in the absence of microsaccades, then our visual neurons should have shown the same patterns of selective suppression as the visual motor neurons, but they did not (Figs. 3 and 4). Second, we specifically examined suppression within each spatial frequency relative to the no-microsaccade baseline of the same frequency, to isolate the suppression effect independent of baseline response strength. This avoided questions of absolute firing sensitivity across spatial frequencies. Third, in Fig. 7, we explicitly examined suppression as a function of preferred spatial frequency and still found diminishing returns in suppression strength with increasing spatial frequency even when each spatial frequency bin only included the neurons preferring that frequency. Finally, because the visual system is inherently generally low pass anyway (especially in the periphery), even a mechanism in which suppression simply scales with visual sensitivity of a given spatial frequency would still explain the well-known perceptual phenomenon of selective suppression of low spatial frequencies in humans.

There also may be an additional potential counter-interpretation of our results. Specifically, it may be argued that we uncovered a highly specific effect only modulating saccadic RTs and that SC modulations are irrelevant for other forms of behavior (e.g., not requiring saccadic responses). However, this is unlikely. First, the SC contributes to behavior even with nonsaccadic outputs. For example, during attentional tasks with button presses, SC lesions impair performance (Sapir et al. 1999), suggesting that it is sensory and/or cognitive modulations that are relevant. Consistent with this, the SC contributes to attentional paradigms with a variety of response modalities (Lovejoy and Krauzlis 2010; Zénon and Krauzlis 2012). Second, we only looked at the earliest visual responses and uncovered strong correlations to behavior observed in separate experiments. This indicates that it was the sensory response that mattered. Consistent with this, we have recently found that the occurrence of a microsaccade near the time of stimulus onset affected both manual and saccadic RTs in a similar fashion despite the different motor response modalities (Tian et al. 2016). Third, our behavioral effects on RT are themselves remarkably similar to perceptual effects of saccadic suppression in humans, but with different perceptual measures and response modalities (Burr et al. 1982, 1994; Volkman et al. 1978). Fourth, we found that *monkey P* had a stronger suppression effect in behavior than *monkey N* at the low spatial frequencies (compare the light gray curves in Fig. 2, *H* and *K*) even though *monkey P* had significantly longer saccadic RTs to begin with (compare the black no-microsaccade curves in Fig. 2, *A* and *D*). If our behavioral and neural effects were restricted

to limits on saccadic RT, perhaps due to potential saccadic refractory periods between successive saccades and microsaccades, then *monkey P* should have shown weaker behavioral suppression than *monkey N* because this monkey's saccadic system had plenty of time to recover from the previous generation of a microsaccade before having to generate the next saccadic RT. Given all of the above, as well as further arguments in Hafed and Krauzlis (2010), we find it unlikely that our modulations are only specific to modulating saccadic RTs.

If that is the case, then why might the SC be among the neural substrates for spatial-frequency-specific saccadic suppression? We think that the SC has several appealing features to place it well within a hypothetical saccadic suppression system. For example, the SC contributes to triggering the saccade command. Thus a source of corollary discharge is already present in the visual motor layers, as demonstrated by our differential firing rate (Figs. 3–7) and LFP effects (Figs. 8–10). Second, proximity of the SC to motor outputs confers an additional advantage: SC suppression, besides having potential perceptual effects, could help to regularize how often subsequent saccades are made to sample the visual world. That is, in reality, suppression could serve to control the temporal structure of saccades, which can be very important both behaviorally (Tian et al. 2016) and cortically (Lowet et al. 2016). This becomes even more interesting in light of the strong prevalence of low spatial frequencies in natural scene statistics (Field 1987), suggesting that selective suppression of low spatial frequencies is indeed functional. Moreover, controlling the temporal structure of saccades might explain refractory periods between successive movements, which we briefly alluded to above. Specifically, it is known that signal delays from the retina to the eye muscles can be much shorter than typically observed intersaccadic intervals. For example, SC neurons receive visual responses within ~50 ms after stimulus onset, and SC stimulation can trigger saccades within ~20 ms (i.e., a total of ~70 ms); on the other hand, typical RT values or intersaccadic intervals are at least twice as long (Boch et al. 1984; Robinson 1972; Schiller and Stryker 1972; Wurtz and Mohler 1976). This has led to talk of saccadic refractory periods (e.g., Becker and Jürgens 1979), but the mechanisms for such refractory periods are not known. If the SC is desensitized after every saccade, then this can delay subsequent saccades, introducing refractoriness and also more generally controlling the temporal structure of eye movement generation.

## GRANTS

This work was funded by the Werner Reichardt Centre for Integrative Neuroscience (CIN) at the Eberhard Karls University of Tübingen. The CIN is an Excellence Cluster funded by the Deutsche Forschungsgemeinschaft (DFG) within the framework of the Excellence Initiative (EXC 307).

## DISCLOSURES

No conflicts of interest, financial or otherwise, are declared by the authors.

## AUTHOR CONTRIBUTIONS

C.-Y.C. and Z.M.H. conceived and designed research; C.-Y.C. and Z.M.H. performed experiments; C.-Y.C. and Z.M.H. analyzed data; C.-Y.C. and Z.M.H. interpreted results of experiments; C.-Y.C. and Z.M.H. prepared figures; C.-Y.C. and Z.M.H. drafted manuscript; C.-Y.C. and Z.M.H. edited and revised manuscript; C.-Y.C. and Z.M.H. approved final version of manuscript.

## REFERENCES

- Becker W, Jürgens R. An analysis of the saccadic system by means of double step stimuli. *Vision Res* 19: 967–983, 1979. doi:10.1016/0042-6989(79)90222-0.
- Berman RA, Cavanaugh J, McAlonan K, Wurtz RH. A circuit for saccadic suppression in the primate brain. *J Neurophysiol*. In press. doi:10.1152/jn.00679.2016.
- Berman RA, Wurtz RH. Exploring the pulvinar path to visual cortex. *Prog Brain Res* 171: 467–473, 2008. doi:10.1016/S0079-6123(08)00668-7.
- Berman RA, Wurtz RH. Functional identification of a pulvinar path from superior colliculus to cortical area MT. *J Neurosci* 30: 6342–6354, 2010. doi:10.1523/JNEUROSCI.6176-09.2010.
- Berman RA, Wurtz RH. Signals conveyed in the pulvinar pathway from superior colliculus to cortical area MT. *J Neurosci* 31: 373–384, 2011. doi:10.1523/JNEUROSCI.4738-10.2011.
- Boch R, Fischer B, Ramsperger E. Express-saccades of the monkey: reaction times versus intensity, size, duration, and eccentricity of their targets. *Exp Brain Res* 55: 223–231, 1984. doi:10.1007/BF00237273.
- Boehnke SE, Munoz DP. On the importance of the transient visual response in the superior colliculus. *Curr Opin Neurobiol* 18: 544–551, 2008. doi:10.1016/j.conb.2008.11.004.
- Breitmeyer BG. Simple reaction time as a measure of the temporal response properties of transient and sustained channels. *Vision Res* 15: 1411–1412, 1975. doi:10.1016/0042-6989(75)90200-X.
- Bremmer F, Kubischik M, Hoffmann KP, Krekelberg B. Neural dynamics of saccadic suppression. *J Neurosci* 29: 12374–12383, 2009. doi:10.1523/JNEUROSCI.2908-09.2009.
- Bridgeman B, Hendry D, Stark L. Failure to detect displacement of the visual world during saccadic eye movements. *Vision Res* 15: 719–722, 1975. doi:10.1016/0042-6989(75)90290-4.
- Burr DC, Holt J, Johnstone JR, Ross J. Selective depression of motion sensitivity during saccades. *J Physiol* 333: 1–15, 1982. doi:10.1113/jphysiol.1982.sp014434.
- Burr DC, Morrone MC, Ross J. Selective suppression of the magnocellular visual pathway during saccadic eye movements. *Nature* 371: 511–513, 1994. doi:10.1038/371511a0.
- Burr DC, Ross J. Contrast sensitivity at high velocities. *Vision Res* 22: 479–484, 1982. doi:10.1016/0042-6989(82)90196-1.
- Campbell FW, Wurtz RH. Saccadic omission: why we do not see a grey-out during a saccadic eye movement. *Vision Res* 18: 1297–1303, 1978. doi:10.1016/0042-6989(78)90219-5.
- Castet E, Jeanjean S, Masson GS. ‘Saccadic suppression’- no need for an active extra-retinal mechanism. *Trends Neurosci* 24: 316–318, 2001. doi:10.1016/S0166-2236(00)01828-2.
- Castet E, Masson GS. Motion perception during saccadic eye movements. *Nat Neurosci* 3: 177–183, 2000. doi:10.1038/72124.
- Chen CY, Hafed ZM. Postmicrosaccadic enhancement of slow eye movements. *J Neurosci* 33: 5375–5386, 2013. doi:10.1523/JNEUROSCI.3703-12.2013.
- Chen CY, Ignashchenkova A, Thier P, Hafed ZM. Neuronal response gain enhancement prior to microsaccades. *Curr Biol* 25: 2065–2074, 2015. doi:10.1016/j.cub.2015.06.022.
- Diamond MR, Ross J, Morrone MC. Extraretinal control of saccadic suppression. *J Neurosci* 20: 3449–3455, 2000.
- Field DJ. Relations between the statistics of natural images and the response properties of cortical cells. *J Opt Soc Am A* 4: 2379–2394, 1987. doi:10.1364/JOSAA.4.002379.
- Fischer B, Boch R. Saccadic eye movements after extremely short reaction times in the monkey. *Brain Res* 260: 21–26, 1983. doi:10.1016/0006-8993(83)90760-6.
- Fuchs AF, Robinson DA. A method for measuring horizontal and vertical eye movement chronically in the monkey. *J Appl Physiol* 21: 1068–1070, 1966.
- García-Pérez MA, Peli E. Visual contrast processing is largely unaltered during saccades. *Front Psychol* 2: 247, 2011. doi:10.3389/fpsyg.2011.00247.
- Ghitani N, Bayguinov PO, Vokoun CR, McMahon S, Jackson MB, Basso MA. Excitatory synaptic feedback from the motor layer to the sensory layers of the superior colliculus. *J Neurosci* 34: 6822–6833, 2014. doi:10.1523/JNEUROSCI.3137-13.2014.
- Guez J, Morris AP, Krekelberg B. Intrасaccadic suppression is dominated by reduced detector gain. *J Vis* 13: 4, 2013. doi:10.1167/13.8.4.

- Hafed ZM.** Mechanisms for generating and compensating for the smallest possible saccades. *Eur J Neurosci* 33: 2101–2113, 2011. doi:10.1111/j.1460-9568.2011.07694.x.
- Hafed ZM.** Alteration of visual perception prior to microsaccades. *Neuron* 77: 775–786, 2013. doi:10.1016/j.neuron.2012.12.014.
- Hafed ZM, Chen C-Y.** Sharper, stronger, faster upper visual field representation in primate superior colliculus. *Curr Biol* 26: 1647–1658, 2016. doi:10.1016/j.cub.2016.04.059.
- Hafed ZM, Chen C-Y, Tian X.** Vision, perception, and attention through the lens of microsaccades: mechanisms and implications. *Front Syst Neurosci* 9: 167, 2015. doi:10.3389/fnsys.2015.00167.
- Hafed ZM, Goffart L, Krauzlis RJ.** A neural mechanism for microsaccade generation in the primate superior colliculus. *Science* 323: 940–943, 2009. doi:10.1126/science.1166112.
- Hafed ZM, Ignashchenkova A.** On the dissociation between microsaccade rate and direction after peripheral cues: microsaccadic inhibition revisited. *J Neurosci* 33: 16220–16235, 2013. doi:10.1523/JNEUROSCI.2240-13.2013.
- Hafed ZM, Krauzlis RJ.** Microsaccadic suppression of visual bursts in the primate superior colliculus. *J Neurosci* 30: 9542–9547, 2010. doi:10.1523/JNEUROSCI.1137-10.2010.
- Hafed ZM, Krauzlis RJ.** Similarity of superior colliculus involvement in microsaccade and saccade generation. *J Neurophysiol* 107: 1904–1916, 2012. doi:10.1152/jn.01125.2011.
- Han X, Xian SX, Moore T.** Dynamic sensitivity of area V4 neurons during saccade preparation. *Proc Natl Acad Sci USA* 106: 13046–13051, 2009. doi:10.1073/pnas.0902412106.
- Hass CA, Horwitz GD.** Effects of microsaccades on contrast detection and V1 responses in macaques. *J Vis* 11: 1–17, 2011. doi:10.1167/11.3.3.
- Ibbotson M, Krekelberg B.** Visual perception and saccadic eye movements. *Curr Opin Neurobiol* 21: 553–558, 2011. doi:10.1016/j.conb.2011.05.012.
- Ibbotson MR, Crowder NA, Cloberty SL, Price NS, Mustari MJ.** Saccadic modulation of neural responses: possible roles in saccadic suppression, enhancement, and time compression. *J Neurosci* 28: 10952–10960, 2008. doi:10.1523/JNEUROSCI.3950-08.2008.
- Ibbotson MR, Price NS, Crowder NA, Ono S, Mustari MJ.** Enhanced motion sensitivity follows saccadic suppression in the superior temporal sulcus of the macaque cortex. *Cereb Cortex* 17: 1129–1138, 2007. doi:10.1093/cercor/bhl022.
- Ikeda T, Boehnke SE, Marino RA, White BJ, Wang CA, Levy R, Munoz DP.** Spatio-temporal response properties of local field potentials in the primate superior colliculus. *Eur J Neurosci* 41: 856–865, 2015. doi:10.1111/ejn.12842.
- Ilg UJ, Hoffmann KP.** Motion perception during saccades. *Vision Res* 33: 211–220, 1993. doi:10.1016/0042-6989(93)90159-T.
- Isa T, Hall WC.** Exploring the superior colliculus in vitro. *J Neurophysiol* 102: 2581–2593, 2009. doi:10.1152/jn.00498.2009.
- Judge SJ, Richmond BJ, Chu FC.** Implantation of magnetic search coils for measurement of eye position: an improved method. *Vision Res* 20: 535–538, 1980. doi:10.1016/0042-6989(80)90128-5.
- Kleiser R, Seitz RJ, Krekelberg B.** Neural correlates of saccadic suppression in humans. *Curr Biol* 14: 386–390, 2004. doi:10.1016/j.cub.2004.02.036.
- Knöll J, Binda P, Morrone MC, Bremmer F.** Spatiotemporal profile of peri-saccadic contrast sensitivity. *J Vis* 11: 386–15, 2011. doi:10.1167/11.14.15.
- Krock RM, Moore T.** Visual sensitivity of frontal eye field neurons during the preparation of saccadic eye movements. *J Neurophysiol* 116: 2882–2891, 2016. doi:10.1152/jn.01140.2015.
- Lee PH, Sooksawat T, Yanagawa Y, Isa K, Isa T, Hall WC.** Identity of a pathway for saccadic suppression. *Proc Natl Acad Sci USA* 104: 6824–6827, 2007. doi:10.1073/pnas.0701934104.
- Li X, Basso MA.** Preparing to move increases the sensitivity of superior colliculus neurons. *J Neurosci* 28: 4561–4577, 2008. doi:10.1523/JNEUROSCI.5683-07.2008.
- Liu X, Nachev P, Wang S, Green A, Kennard C, Aziz T.** The saccade-related local field potentials of the superior colliculus: a functional marker for localizing the periventricular and periaqueductal gray. *J Clin Neurophysiol* 26: 280–287, 2009. doi:10.1097/WNP.0b013e3181b2f2c1.
- Lovejoy LP, Krauzlis RJ.** Inactivation of primate superior colliculus impairs covert selection of signals for perceptual judgments. *Nat Neurosci* 13: 261–266, 2010. doi:10.1038/nn.2470.
- Lowet E, Roberts MJ, Bosman CA, Fries P, De Weerd P.** Areas V1 and V2 show microsaccade-related 3–4-Hz covariation in gamma power and frequency. *Eur J Neurosci* 43: 1286–1296, 2016. doi:10.1111/ejn.13126.
- Matin E.** Saccadic suppression: a review and an analysis. *Psychol Bull* 81: 899–917, 1974. doi:10.1037/h0037368.
- Matin E, Clymer AB, Matin L.** Metaccontrast and saccadic suppression. *Science* 178: 179–182, 1972. doi:10.1126/science.178.4057.179.
- Phongphanphane P, Mizuno F, Lee PH, Yanagawa Y, Isa T, Hall WC.** A circuit model for saccadic suppression in the superior colliculus. *J Neurosci* 31: 1949–1954, 2011. doi:10.1523/JNEUROSCI.2305-10.2011.
- Pollack JG, Hickey TL.** The distribution of retino-collicular axon terminals in rhesus monkey. *J Comp Neurol* 185: 587–602, 1979. doi:10.1002/cne.901850402.
- Rajkai C, Lakatos P, Chen CM, Pincze Z, Karmos G, Schroeder CE.** Transient cortical excitation at the onset of visual fixation. *Cereb Cortex* 18: 200–209, 2008. doi:10.1093/cercor/bhm046.
- Ramcharan EJ, Gnadt JW, Sherman SM.** The effects of saccadic eye movements on the activity of geniculate relay neurons in the monkey. *Vis Neurosci* 18: 253–258, 2001. doi:10.1017/S0952523801182106.
- Reppas JB, Usrey WM, Reid RC.** Saccadic eye movements modulate visual responses in the lateral geniculate nucleus. *Neuron* 35: 961–974, 2002. doi:10.1016/S0896-6273(02)00823-1.
- Robinson DA.** Eye movements evoked by collicular stimulation in the alert monkey. *Vision Res* 12: 1795–1808, 1972. doi:10.1016/0042-6989(72)90070-3.
- Roska B, Werblin F.** Rapid global shifts in natural scenes block spiking in specific ganglion cell types. *Nat Neurosci* 6: 600–608, 2003. doi:10.1038/nm1061.
- Ross J, Burr D, Morrone C.** Suppression of the magnocellular pathway during saccades. *Behav Brain Res* 80: 1–8, 1996. doi:10.1016/0166-4328(96)00012-5.
- Royal DW, Sáry G, Schall JD, Casagrande VA.** Correlates of motor planning and postsaccadic fixation in the macaque monkey lateral geniculate nucleus. *Exp Brain Res* 168: 62–75, 2006. doi:10.1007/s00221-005-0093-z.
- Sapir A, Soroker N, Berger A, Henik A.** Inhibition of return in spatial attention: direct evidence for collicular generation. *Nat Neurosci* 2: 1053–1054, 1999. doi:10.1038/15977.
- Schiller PH, Stryker M.** Single-unit recording and stimulation in superior colliculus of the alert rhesus monkey. *J Neurophysiol* 35: 915–924, 1972.
- Sommer MA, Wurtz RH.** What the brain stem tells the frontal cortex. I. Oculomotor signals sent from superior colliculus to frontal eye field via mediodorsal thalamus. *J Neurophysiol* 91: 1381–1402, 2004. doi:10.1152/jn.00738.2003.
- Sperry RW.** Neural basis of the spontaneous optokinetic response produced by visual inversion. *J Comp Physiol Psychol* 43: 482–489, 1950. doi:10.1037/h0055479.
- Thiele A, Henning P, Kubischik M, Hoffmann KP.** Neural mechanisms of saccadic suppression. *Science* 295: 2460–2462, 2002. doi:10.1126/science.1068788.
- Tian X, Yoshida M, Hafed ZM.** A microsaccadic account of attentional capture and inhibition of return in Posner cueing. *Front Syst Neurosci* 10: 23, 2016. doi:10.3389/fnsys.2016.00023.
- Volkman FC, Riggs LA, White KD, Moore RK.** Contrast sensitivity during saccadic eye movements. *Vision Res* 18: 1193–1199, 1978. doi:10.1016/0042-6989(78)90104-9.
- von Holst E, Mittelstaedt H.** Das Reafferenzprinzip: Wechselwirkungen zwischen Zentralnervensystem und Peripherie. *Naturwissenschaften* 37: 464–476, 1950. doi:10.1007/BF00622503.
- Wurtz RH.** Neuronal mechanisms of visual stability. *Vision Res* 48: 2070–2089, 2008. doi:10.1016/j.visres.2008.03.021.
- Wurtz RH, Joiner WM, Berman RA.** Neuronal mechanisms for visual stability: progress and problems. *Philos Trans R Soc Lond B Biol Sci* 366: 492–503, 2011. doi:10.1098/rstb.2010.0186.
- Wurtz RH, Mohler CW.** Organization of monkey superior colliculus: enhanced visual response of superficial layer cells. *J Neurophysiol* 39: 745–765, 1976.
- Zanos TP, Mineault PJ, Guitton D, Pack CC.** Mechanisms of saccadic suppression in primate cortical area V4. *J Neurosci* 36: 9227–9239, 2016. doi:10.1523/JNEUROSCI.1015-16.2016.
- Zénon A, Krauzlis RJ.** Attention deficits without cortical neuronal deficits. *Nature* 489: 434–437, 2012. doi:10.1038/nature11497.
- Zuber BL, Stark L, Cook G.** Microsaccades and the velocity-amplitude relationship for saccadic eye movements. *Science* 150: 1459–1460, 1965. doi:10.1126/science.150.3702.1459.
- Zuber BL, Stark L, Lorber M.** Saccadic suppression of the pupillary light reflex. *Exp Neurol* 14: 351–370, 1966. doi:10.1016/0014-4886(66)90120-8.



## **5. Spatial vision by macaque midbrain**

## **Spatial vision by macaque midbrain**

Chih-Yang Chen<sup>1,2,3</sup>, Lukas Sonnenberg<sup>4</sup>, Simone Weller<sup>4</sup>, Thede Witschel<sup>4</sup>, and Ziad M. Hafed<sup>1,3</sup>

1. Werner Reichardt Centre for Integrative Neuroscience, Tuebingen University, Tuebingen, BW, 72076, Germany
2. Graduate School of Neural and Behavioural Sciences, International Max Planck Research School, Tuebingen University, Tuebingen, BW, 72074, Germany
3. Hertie Institute for Clinical Brain Research, Tuebingen University, Tuebingen, BW, 72076, Germany
4. Master's Program for Neurobiology, Tuebingen University, Tuebingen, BW, 72076, Germany

### **Corresponding Author/Lead Contact:**

Ziad M. Hafed  
Werner Reichardt Centre for Integrative Neuroscience  
Otfried-Mueller Str. 25  
Tuebingen, 72076, Germany  
Tel: +49 7071 29-88819  
E-mail: [ziad.m.hafed@cin.uni-tuebingen.de](mailto:ziad.m.hafed@cin.uni-tuebingen.de)

# Spatial vision by macaque midbrain

Chih-Yang Chen<sup>1,2,3</sup>, Lukas Sonnenberg<sup>4</sup>, Simone Weller<sup>4</sup>, Thede Witschel<sup>4</sup>, and Ziad M. Hafed<sup>1,3</sup>

1. Werner Reichardt Centre for Integrative Neuroscience, Tuebingen University, Tuebingen, BW, 72076, Germany
2. Graduate School of Neural and Behavioural Sciences, International Max Planck Research School, Tuebingen University, Tuebingen, BW, 72074, Germany
3. Hertie Institute for Clinical Brain Research, Tuebingen University, Tuebingen, BW, 72074, Germany
4. Master's Program for Neurobiology, Tuebingen University, Tuebingen, BW, 72076, Germany

## Summary

Visual brain areas exhibit tuning characteristics that are well suited for image statistics present in our natural environment. However, visual sensation is an active process, and if there are any brain areas that ought to be particularly “in tune” with natural scene statistics, it would be sensory-motor areas critical for guiding behavior. Here we found that the primate superior colliculus, a structure instrumental for rapid visual exploration with saccades, detects low spatial frequencies, which are the most prevalent in natural scenes, much more rapidly than high spatial frequencies. Importantly, this accelerated detection happens independently of a neuron's spatial frequency preference. At the population level, the superior colliculus additionally over-represents low spatial frequencies in neural response sensitivity, even at foveal eccentricities, thus providing potentially both temporal and response gain mechanisms for efficient gaze realignment in natural environments.

## Highlights

- Superior colliculus neurons respond fastest to low image spatial frequencies
- Neural responses for low frequencies are fastest regardless of response sensitivity
- Visual response latency and sensitivity predict saccade behavior remarkably well
- We proposed a spatial vision pathway that facilitates exploring natural scenes

## Results and Discussion

Visual and motor responses in the superior colliculus (SC) have traditionally been studied using highly impoverished stimuli, like small spots of light. However, ecological constraints (Hafed and Chen, 2016; Previc, 1990) on both visual perception and eye movements imply that the SC, like other brain regions, should best function if its neurons' properties were well matched with the properties of the environment. Among such properties is the preponderance of low spatial frequencies in natural scene statistics (Ruderman and Bialek, 1994; Tolhurst et al., 1992). In early visual areas, such preponderance is well matched with a variety of observations, including coarse-to-fine neural image analysis (Bredfeldt and Ringach, 2002; Mazer et al., 2002; Purushothaman et al., 2014) and neural image filtering kernels that are suitable for natural scene statistics (Olshausen and Field, 1996; Simoncelli and Olshausen, 2001; van Hateren and van der Schaaf, 1998). Curiously, such observations are often also used to account for motor rather than perceptual effects, for example on manual and saccadic reaction times (Breitmeyer, 1975; Ludwig et al., 2004; White et al., 2008), even though these early visual areas are more relevant for perception than action. Here we hypothesized that the SC, being action centered (Gandhi and Katnani, 2011; Veale et al., 2017), can be equally well matched to spatial properties present in natural scenes as early visual areas, if not more so, and in a manner that is highly conducive of behavioral motor effects.

We recorded visual responses in macaque monkeys that were passively fixating a small spot of light (Chen and Hafed, 2013; Chen et al., 2015). During such passive fixation, we

presented a high contrast sine wave grating filling the visual response field (RF) of a recorded neuron (Materials and Methods). We varied the spatial frequency of the presented grating from trial to trial and noticed a systematic rank ordering of neural response latencies as a function of spatial frequency. For example, in the neuron of Fig. 1A, visually-evoked action potentials arrived earliest for gratings of 0.56 or 1.11 cycles/degree (cpd), and their latency progressively increased for higher spatial frequencies. This observation is reminiscent of coarse-to-fine image coding properties of early cortical visual areas (Bredfeldt and Ringach, 2002; Mazer et al., 2002; Purushothaman et al., 2014), but it still violated an expected inverse relationship between response latency and response sensitivity (i.e. response strength) that has been reported in both the SC (Marino et al., 2012) and early cortical visual areas (Maunsell and Gibson, 1992). Instead, visual sensitivity in this neuron was highest for 4.44 cpd (Fig. 1B), but visual response latency at this spatial frequency was longer than at lower frequencies. This meant that plotting tuning curves of either visual sensitivity (Fig. 1C, top; Materials and Methods) or visual latency (Fig. 1C, bottom) against spatial frequency revealed a dissociation between the two neural response properties: the preferred spatial frequency in terms of sensitivity was ~4 cpd, whereas the preferred spatial frequency in terms of response latency was much lower.

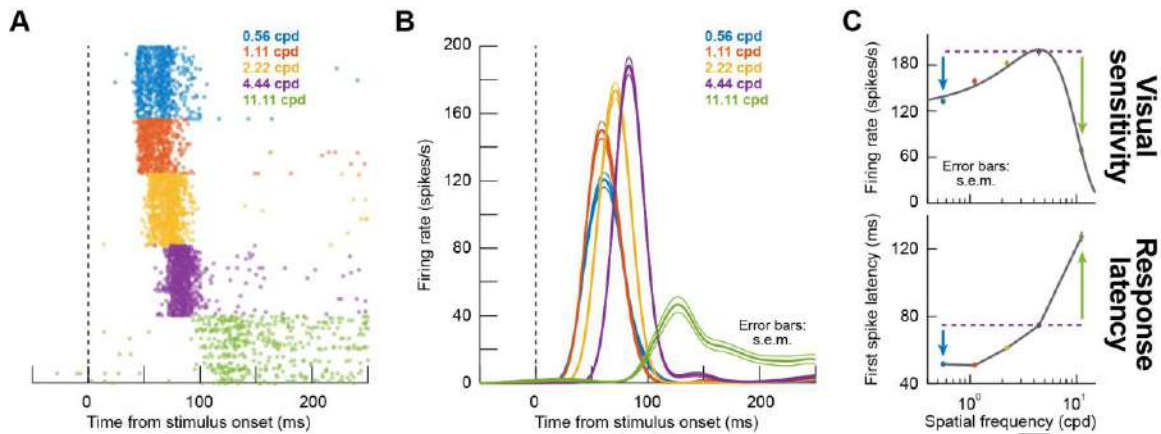


**Figure 1 Rapid detection of low spatial frequencies by macaque superior colliculus (SC).** (A) Visual responses of an example SC neuron to gratings of different spatial frequencies (color-coded according to the legend) presented within the neuron’s visual RF. The raster plots show times of individual action potentials with different trials stacked in rows, and the trials were grouped by color only for easier presentation in the figure; in the experiment, different spatial frequencies were presented randomly. There was a rank ordering of response latency, with the lowest spatial frequencies (e.g. 0.56 and 1.11 cpd) evoking the shortest-latency neural responses. (B) This effect happened even though higher spatial frequencies (e.g. 2.22 and 4.44 cpd) uncovered stronger response gain by this neuron (i.e. the neuron had higher sensitivity for the higher spatial frequencies). In this panel, this is illustrated by plotting firing rates for the same neuron, because it is easier to infer response amplitude from firing rates. As can be seen, the neuron emitted the strongest visual responses for 4.44 cpd gratings even though the responses came later than for lower spatial frequencies. Thus, there was a dissociation between response latency and response sensitivity. (C) This dissociation can also be seen by inspecting tuning curves. The top panel plots the tuning curve of the neuron according to response sensitivity (i.e. response amplitude as a function of spatial frequency; Materials and Methods). Visual responses were highest for 4.44 cpd gratings with both lower and higher spatial frequencies (e.g. the colored arrows) evoking significantly weaker responses. On the other hand, in the lower panel, the latency to first visually-evoked spike (Materials and Methods) at 4.44 cpd was longer than for lower spatial frequencies but shorter than for higher spatial frequencies (e.g. the colored arrows). Error bars in B, C, when visible, denote s.e.m.

We confirmed the dissociation between visual sensitivity and visual latency across our recorded population. For example, for neurons preferring 4.44 cpd in terms of visual sensitivity (Fig. 2A, B), we plotted either such sensitivity (Fig. 2A) or instead response latency (Fig. 2B) for different spatial frequencies. In terms of visual sensitivity (Fig. 2A), all spatial frequencies other than 4.44 cpd expectedly elicited weaker neural responses

than 4.44 cpd, since all the neurons selected in this analysis preferred 4.44 cpd by definition. However, despite such preference, visual response latency (Fig. 2B) in the same neurons was either shorter or longer than the latency observed for 4.44 cpd, and following a very simple rule: for 0.56, 1.11, and 2.22 cpd spatial frequencies, response latencies were shorter than for 4.44 cpd, whereas response latencies were longer for 11.11 cpd. Again, for all these spatial frequencies, response sensitivity was weaker than for 4.44 cpd. Thus, faster SC detection of low spatial frequencies occurs independently of neuronal sensitivity to spatial frequency.

This observation also persisted when we considered neurons preferring other spatial frequencies. For example, in Fig. 2C, we plotted visually-evoked responses for different spatial frequencies across neurons, but after separating their preferred spatial frequency in terms of response sensitivity in each panel. In the leftmost panel, neurons responded the strongest for 0.56 cpd, and in the rightmost panel, neurons responded the strongest for 4.44 cpd, and so on for the other panels. Yet, and as can be seen from the arrows indicating the times of peak visual responses for each spatial frequency, the lowest two spatial frequencies always evoked the fastest responses followed by a systematic increase in response latency with increasing spatial frequency; again, this happened regardless of neural preference for a given frequency in terms of sensitivity.

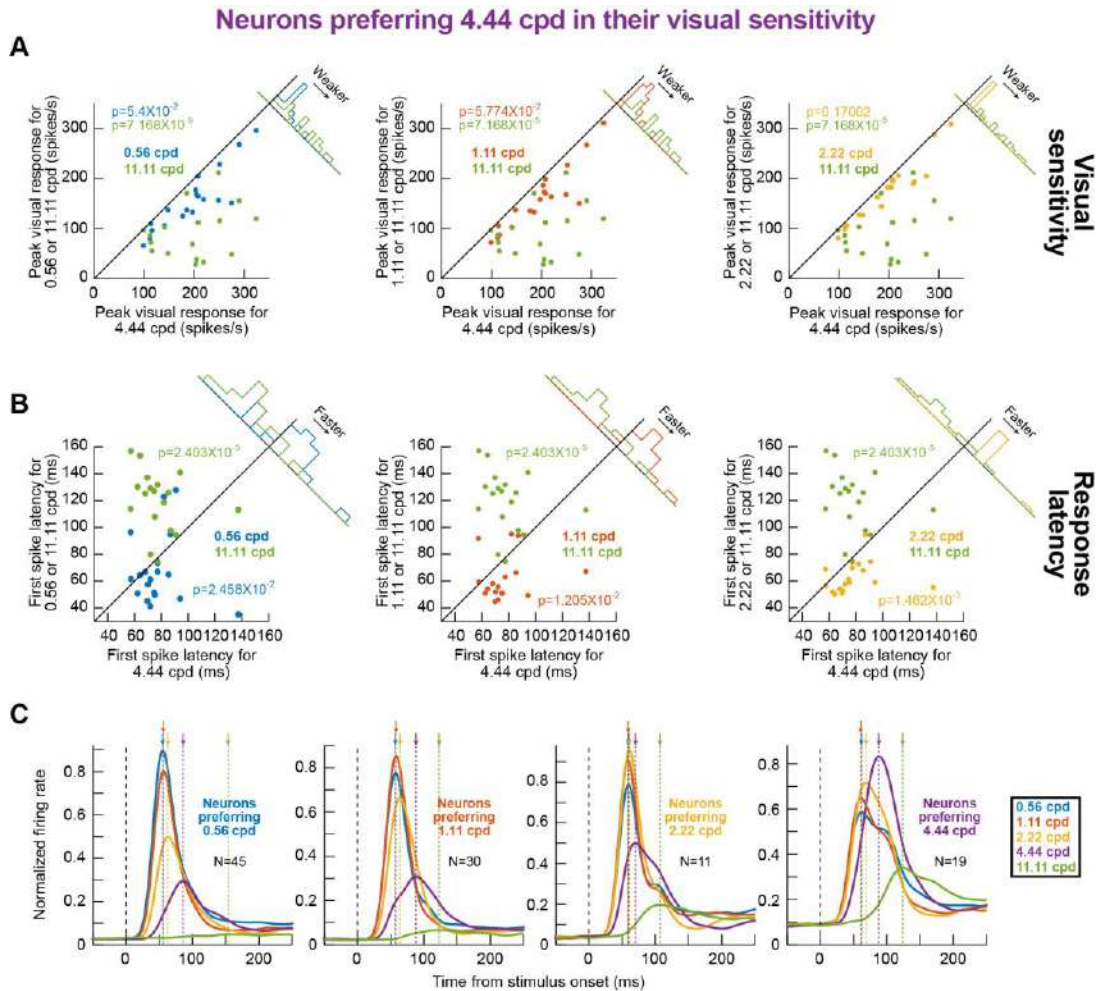


**Figure 2 Prioritization of low spatial frequencies in the macaque SC independent of neural sensitivity.** (A) For neurons showing the highest visual responses to 4.44 cpd gratings, we plotted in each panel the visual response strength for either higher or lower spatial frequencies (y-axis) against the response strength for 4.44 cpd. As expected, response strength was always highest for 4.44 cpd. P-values are indicated in each panel, reflecting a comparison between either the higher or lower spatial frequency (color-coded according to the legend) to 4.44 cpd using a Ranksum test. (B) We measured first-spike latency for 4.44 cpd gratings (x-axis) and related it to first-spike latency for either lower or higher spatial frequencies (y-axis), and we did this again only for neurons preferring 4.44 cpd. Even though 4.44 cpd gratings always evoked the strongest visual response (A), the first-spike latency for 4.44 cpd gratings was either longer or shorter than the latency for other gratings. Moreover, whether first-spike latency for the preferred spatial frequency (4.44 cpd) was shorter or longer than in other spatial frequencies simply depended on the rank-ordering of spike timing observed in Fig. 1. Thus, coarse-to-fine visual sensation by the SC is independent of response strength. (C) This effect persisted for neurons preferring other spatial frequencies. In each panel, we took only neurons preferring one spatial frequency in terms of their visual sensitivity. As expected, gratings of non-preferred spatial frequencies emitted weaker visual responses than the preferred spatial frequency in each panel. However, regardless of visual sensitivity to a given spatial frequency, the relative timing of the visual bursts as a function of spatial frequency was similar across all panels (indicated by the downward arrows highlighting the time of peak visual response for each spatial frequency). For example, the response to 4.44 cpd gratings always came later than the response to 1.11 cpd gratings regardless of which spatial frequency the neurons preferred. Note that we did not have enough neurons preferring 11.11 cpd to include in this analysis (see Figs. 4-5). The numbers of neurons contributing to each panel are indicated in the figure.



We next analyzed the properties of SC visual response latencies. Across the population, the lowest two spatial frequencies (0.56 and 1.11 cpd) consistently evoked the shortest visual response latencies followed by a monotonic increase with increasing spatial frequency (Fig. 3A, B). Moreover, this increase was accompanied by increased latency variability (Fig. 3C), and it persisted for either purely visual or visual-motor SC neurons (Fig. S1). This effect was also independent of differences in response latency between upper and lower visual field SC representations (Hafed and Chen, 2016), because the impact of spatial frequency on response latency still occurred even after we separated neurons as either representing upper or lower visual fields (Fig. S2).

Interestingly, we found that SC visual response latency was as early as in the earliest visual areas reported in the literature, if not slightly faster than early cortical areas. For example, Schmolesky and others (Schmolesky et al., 1998) have characterized visual response latencies in lateral geniculate nucleus (LGN) and a variety of cortical areas. These authors used large spots or bars filling each neuron's RF, meaning that their stimuli activated a broad spectrum of low and high spatial frequency channels. When we plotted our observed SC visual response latencies along with these authors' results (Fig. 3D), we found that the SC consistently exhibited earlier responses than primary visual cortex (V1) at spatial frequencies of up to 2.22 cpd (compare the colored traces to the solid black line in Fig. 3D). Moreover, even when we measured SC visual response latencies using small bright spots, that is, still activating a broad spectrum of spatial frequencies as in (Schmolesky et al., 1998), the SC still exhibited earlier latencies than V1 (compare the dashed and dotted black lines). Even though the Schmolesky data were

collected using anesthetized animals, in which response latencies can be delayed relative to the awake condition (Vaiceliunaite et al., 2013), these results at the very least indicate that SC visual responses are indeed among the most rapidly evolving responses in the entire visual system (Fig. 3D). This is consistent with the SC receiving direct retinal projections (Pollack and Hickey, 1979) and with the fact that eye movements, including microsaccades, can be reflexively altered by visual stimuli with latencies much earlier than the latencies of most cortical visual areas (Buonocore et al., 2017; Edelman and Keller, 1996; Hafed et al., 2015; Hafed and Ignashchenkova, 2013).

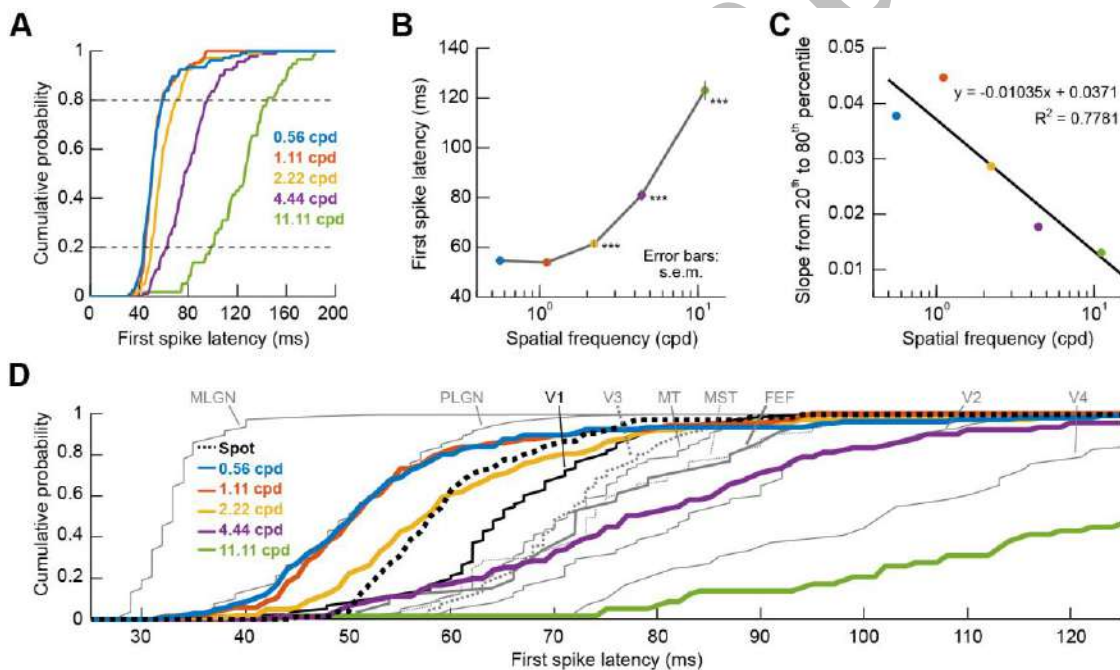


**Figure 3 Early visual sensation by the macaque SC.** (A) Cumulative histograms of first-spike latency (Materials and Methods) in our recorded neurons, separated by the spatial frequency of the presented stimulus. For each neuron, we measured the average first-spike latency of the evoked visual response after a given spatial frequency grating was presented on multiple trials. We then repeated the measurement for other spatial frequencies. The evoked response consistently came earlier for low spatial frequencies than for high spatial frequencies. (B) The rank-ordering of spatial frequencies in A is also seen when plotting the mean first-spike latency from all neurons as a function of spatial frequency. Low spatial frequencies evoked a visual response earlier than high spatial frequencies. Error bars denote s.e.m., and the asterisks indicate  $p < 0.001$  comparing first spike latency of 0.56 cpd to other spatial frequencies. (C) Variability of first-spike latency was higher for higher spatial frequencies. We plotted the slope of the cumulative histograms in A between the 20<sup>th</sup> and 80<sup>th</sup> data percentiles as a function of spatial frequency. This slope

progressively decreased, suggesting progressive increase in first-spike latency variability. **(D)** Our data from **A** plotted along with data from multiple visual areas in gray from (Schmolesky et al., 1998). SC visual responses for low spatial frequencies were among the earliest responses in the visual system, but it has to be noted that the Schmolesky et al. data was from anesthetized animals that would be expected to exhibit slightly delayed visual responses when compared to awake ones. Note that the thick dashed curve shows the distribution of first-spike latencies in our neurons when a small spot of light was presented instead of a grating (i.e. a stimulus with broad-band spatial frequency stimulus). The spot latency was expectedly longer than the latencies for low spatial frequencies, because the spot is a broad-spectrum stimulus.

Besides rapidly detecting low spatial frequencies, being able to efficiently guide behavior implies that the SC's pattern analysis machinery might also be more sensitive to such low spatial frequencies and not just be faster in responding to them. Indeed, when we plotted all tuning curves as done in Fig. 1C (top), we found primarily low pass characteristics in the population even at foveal eccentricities. Specifically, Fig. 4A shows sensitivity tuning curves of 3 example neurons from different retinotopic eccentricities, and Fig. 4B, C summarizes the population results. The variety of preferred spatial frequencies was expectedly higher at foveal eccentricities than at extra-foveal ones (Fig. 4C), but the overall population curves (Fig. 4B) were primarily low-pass, reminiscent of LGN spatial frequency tuning curves (Kaplan and Shapley, 1982) rather than V1 ones, which tend to be band-pass (De Valois et al., 1982). This suggests that the SC over-represents low spatial frequencies in terms of visual response sensitivity in addition to its boosting of such spatial frequencies in terms of response latency.

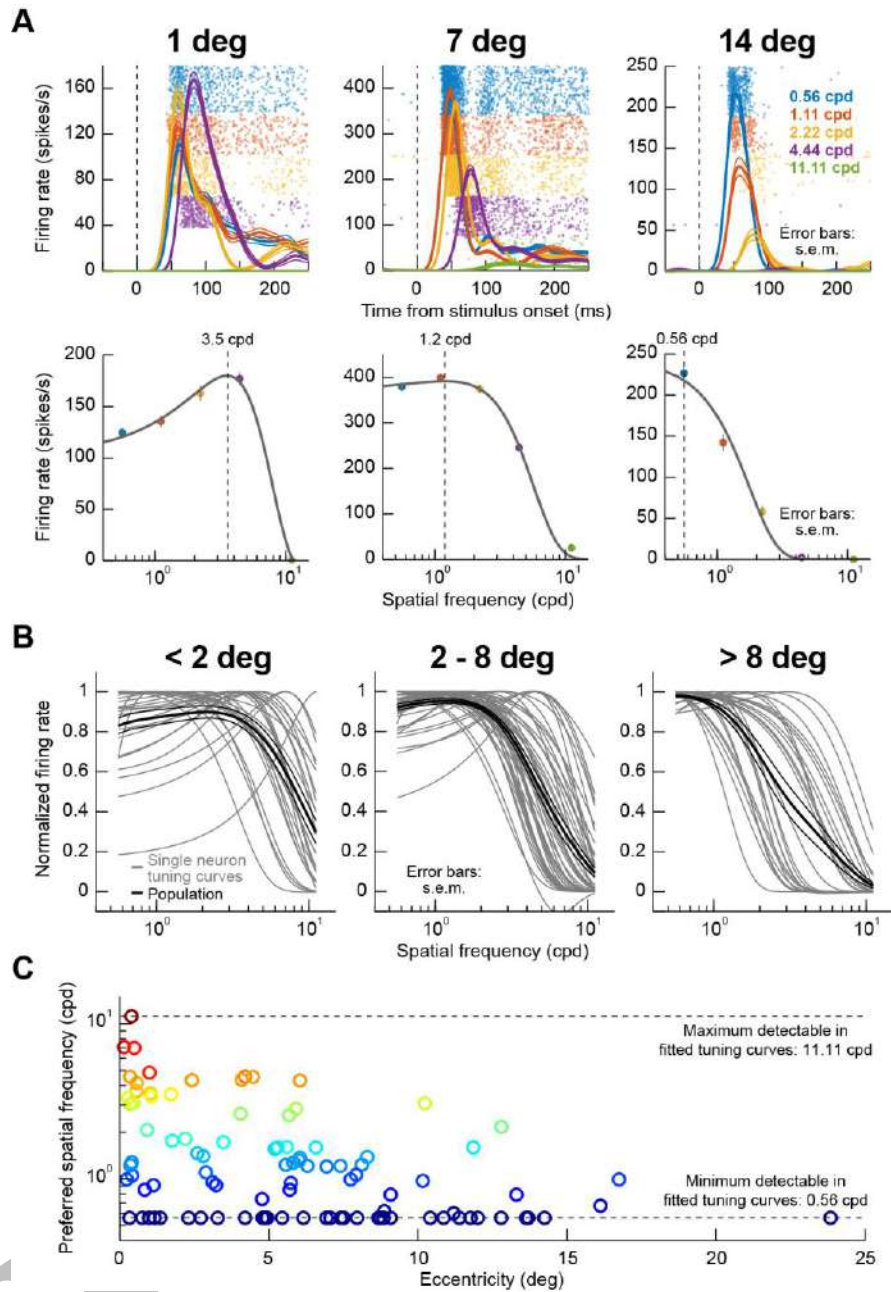


**Figure 4 Dependence of spatial frequency preference on eccentricity.** Example visual responses of 3 SC neurons preferring different retinotopic eccentricities (1, 7, or 14 deg). Each panel in the top row plots firing rate as a function of time from stimulus onset for gratings presented within each neuron’s visual RF; color codes indicate the spatial frequency of the presented stimulus. Raster plots in the background show times of individual action potentials with different trials stacked in rows. Firing rate curves show mean and s.e.m. as thick and thin lines, respectively. The foveal neuron (1 deg) preferred higher spatial frequencies than the more eccentric neurons, as evidenced by the higher responses for 4.44 cpd gratings than for lower spatial frequencies in this neuron. The bottom panels show spatial frequency tuning curves for the same neurons. The dashed vertical line in each panel indicates the preferred spatial frequency of each neuron based on the tuning curves. **(B)** Tuning curves from all neurons in our population, grouped into 3 different eccentricity bins in the 3 panels. Thin curves show individual neuron tuning curves, and thick black curves show the mean tuning curve within a given panel, along with s.e.m. error bars as thin black lines. Regardless of eccentricity, population tuning curves showed primarily low-pass characteristics (thick black

curves), and this effect got stronger and stronger the more eccentric the neurons were (compare panels). (C) Preferred spatial frequency as a function of neuronal preferred eccentricity. Foveal neurons had a broad range of preferred spatial frequencies, but this range gradually decreased as more eccentric SC neurons were sampled. Preferred spatial frequency was selected in this figure as the peak in fitted tuning curves, like those shown in A. Thus, for extremely low- or high-pass neurons, the preferred spatial frequency indicated in this analysis was only an estimate that was cut-off by the end of the fitted curves constrained by our sampled spatial frequencies (dashed horizontal lines).

We explored the over-representation further by first counting the number of neurons responding the most for 0.56 cpd spatial frequencies as opposed to other spatial frequencies. These neurons accounted for >40% of our population, and no other single spatial frequency recruited as many neurons (Fig. 5A). Interestingly, this over-representation of low spatial frequencies became more obvious when assessing local population activity reflected in field potentials (LFP's) recorded simultaneously around our electrode tips along with the isolated neurons (Materials and Methods). We measured either the evoked (Fig. 5B) or sustained (Fig. 5C) local population activity after grating onset (Materials and Methods), and the great majority of our electrode locations, whether in foveal or extra-foveal locations, picked up the strongest responses for the lowest spatial frequency that we presented (Fig. 5B, C). This effect can also be clearly seen when inspecting raw LFP traces from 3 sample electrode penetrations shown in Fig. 5D. We specifically plotted the raw evoked LFP deflections from the same electrode penetrations as those shown for the sample neurons of Fig. 4A. As can be seen, even though the foveal neuron in Fig. 4A (leftmost) responded the most for the 4.44 cpd grating, the local population picked up by the LFP signal in the same experiment still showed the strongest stimulus-evoked deflection (as well as sustained response) for 0.56 and 1.11 cpd gratings (Fig. 5D, leftmost). In other words, at the population level, even foveal SC eccentricities over-represent low spatial frequencies with LFP. Similar effects

were also observed for the other two example eccentricities in Fig. 5D. Therefore, the SC over-represents low spatial frequencies both in terms of neural sensitivity (Figs. 4-5) as well as neural response latency (Figs. 1-3).

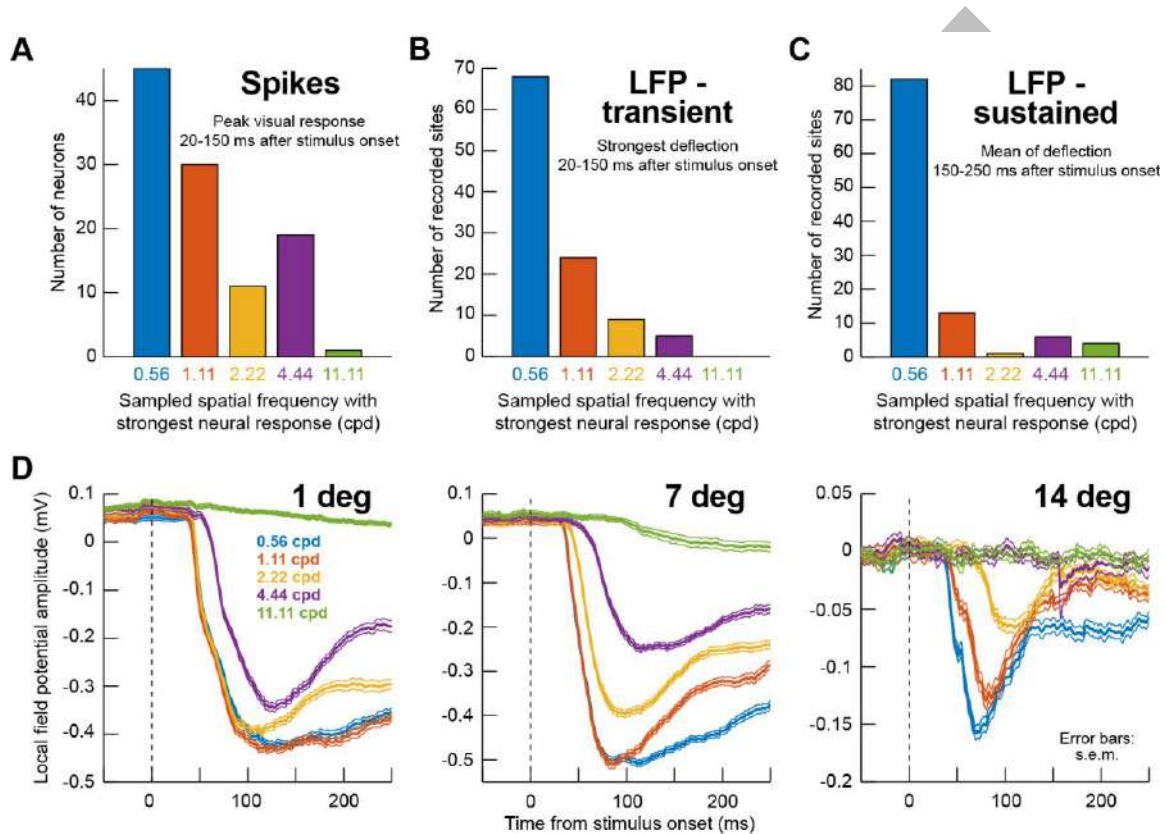


**Figure 5 Low-pass spatial frequency filtering characteristics of the macaque SC.** (A) Distribution of preferred spatial frequencies in our population of recorded SC neurons. In this analysis, we binned neurons according to the presented spatial frequency grating that elicited maximal neuronal response. More neurons were driven the strongest by the lowest spatial frequency (0.56 cpd) than by any other higher spatial frequency. (B) We performed a similar analysis but on the transient evoked local field potential (LFP) response (Materials and Methods; also see D for example evoked LFP responses, which are negative going). The number of electrode penetrations that showed maximal response for 0.56 cpd was even higher than for the isolated neurons in A. (C) This effect was even stronger in the sustained LFP response starting after 150 ms from stimulus onset. Thus, at the population level, the SC is primarily tuned to low spatial frequencies. (D) Stimulus-evoked LFP responses from the same electrode penetrations in which the example neurons of Fig. 4A were isolated and recorded. In the LFP, all 3 electrode tracks, regardless of eccentricity, showed a preference for low spatial frequencies, even in the foveal SC region where the neuron preferring 3.5 cpd in Fig. 4A was isolated. This means that the SC over-represents low spatial frequencies. Error bars are defined in the figure.

Finally, we related SC visual response latency and sensitivity to behavior. In completely separate behavioral sessions, we asked our monkeys to generate visually guided saccades to gratings of different spatial frequencies, as in (Chen and Hafed, 2017). We confirmed that each monkey exhibited saccadic reaction time modulations as a function of spatial frequency (Fig. 6C, I) (Chen and Hafed, 2017; Ludwig et al., 2004), but we also found that these modulations correlated strongly with visual neural modulations in the SC even though the visual neural modulations were obtained in different sessions and with a purely passive fixation task (Materials and Methods). For example, in Fig. 6A, B, we plotted visual response sensitivity and latency, respectively, as a function of spatial frequency, but only for neurons collected from monkey N (Materials and Methods). A simple linear combination of the two neural properties allowed predicting this monkey's behavior (Fig. 6C, green curve) quite well ( $r^2$ : 0.9996). Moreover, a similar idea applied when relating the variance in this monkey's neural (Fig. 6D, E) and behavioral (Fig. 6F) performance by a simple linear equation, and also when repeating the same exercise for monkey P and its behavior (Fig. 6G-L).

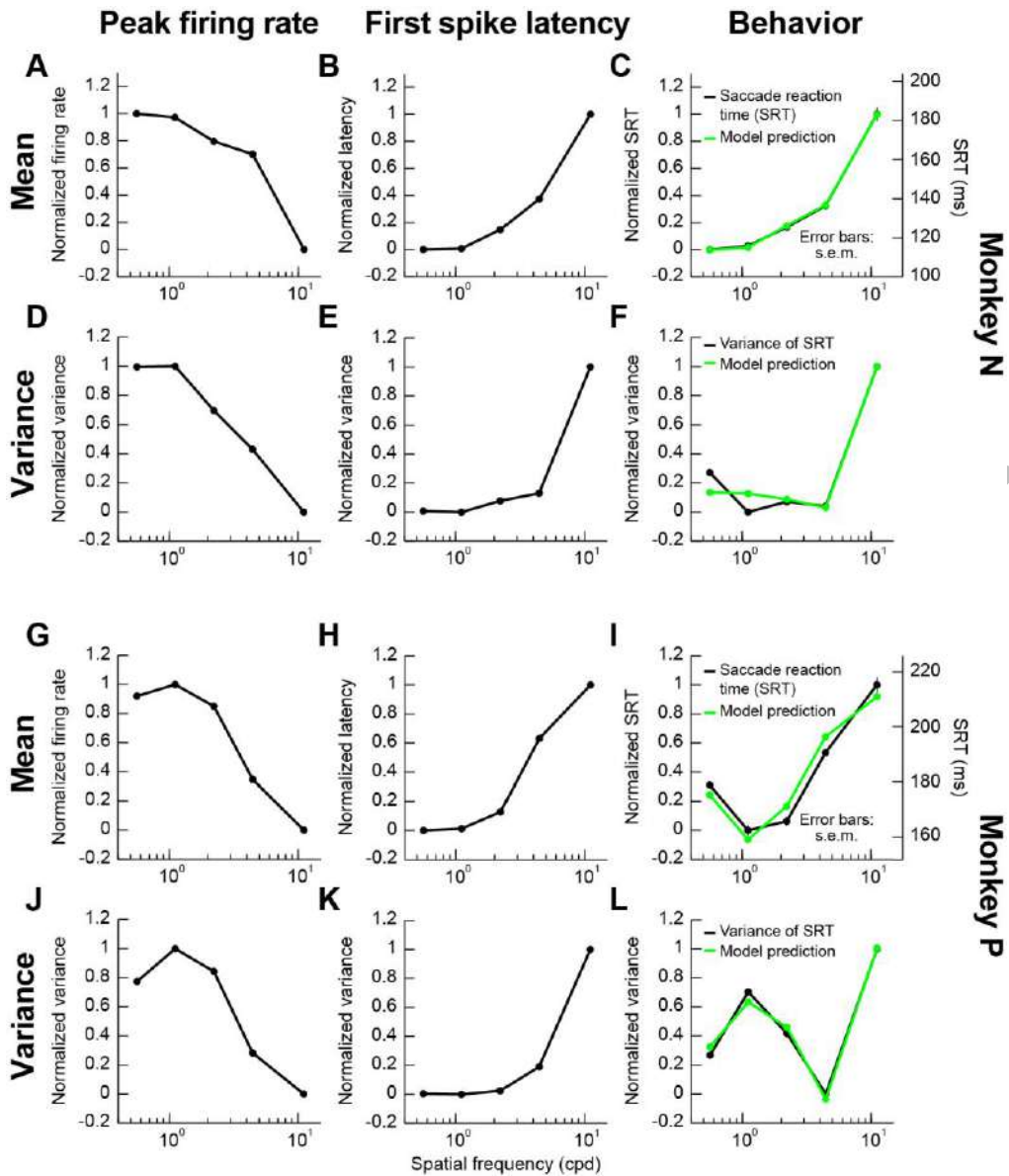


**Figure 6 Linking visual response latency and sensitivity to saccade behavior.** (A) For monkey N, we plotted the average response as a function of spatial frequency for neurons covering an eccentricity similar to an eccentricity used in separate behavioral sessions requiring a saccade to the gratings (Materials and Methods). Low spatial frequencies were associated with higher responses, as shown in Fig. 5. (B) We performed a similar analysis for neural response latency from the same neurons; this time, low spatial frequencies were associated with more rapid neural responses, as shown in Figs. 1-3. (C) The black curve shows the monkey's saccade reaction time from completely different behavioral sessions, and the green curve shows a linear combination of the neural curves in A, B. As can be seen, behavioral performance matches neural performance remarkably well. (D-F) Similar analyses but this time relating variance in neural activity to variance in behavioral performance. Once again, performance was highly correlated with SC visual neural response parameters. (G-L) Similar analyses for monkey P. Error bars are defined in the figure where appropriate.



We also performed human behavioral experiments testing the predictions of our SC results. We ran a visual search task exercising different spatial frequencies in active gaze behavior. Subjects had to search for a grating with an oddball orientation from among many other ones having the same spatial frequency but a slightly different orientation (Fig. 7A; Materials and Methods). The task was demanding enough that subjects had to generate many saccades to search for the oddball target, and example scan paths of these saccades are shown in green in Fig. 7A. We found that inter-saccadic intervals increased in duration when the search array consisted of high spatial frequencies as opposed to low spatial frequencies (Fig. 7B), consistent with our neural and behavioral results above. Importantly, this effect was not due to a speed-accuracy tradeoff, in which it may be the case that fast inter-saccadic intervals were associated with worse task performance. Instead, Fig. 7C demonstrates that target detection performance was fairly constant for the spatial frequencies in which inter-saccadic intervals showed the biggest changes. Therefore, even in searching gaze behavior, the effects of spatial frequencies on inter-movement intervals are consistent with a role of the SC in facilitating and over-representing low spatial frequencies.

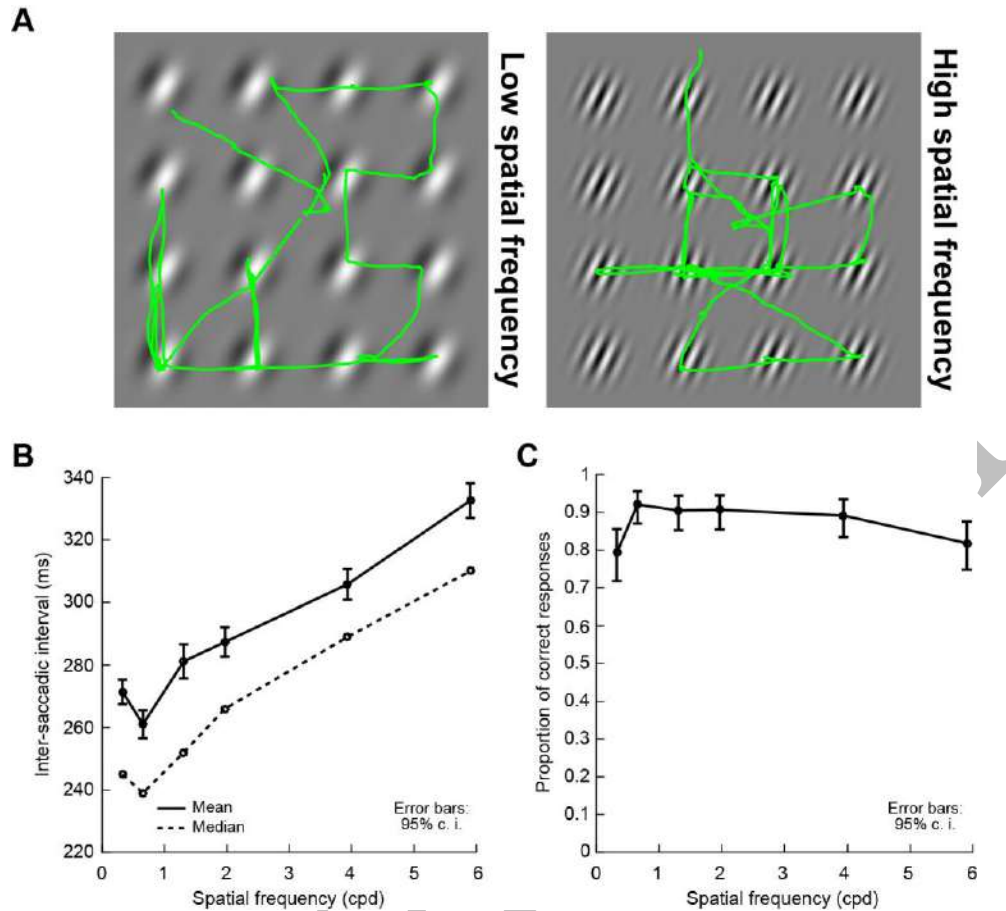


**Figure 7 Saccade times during visual search are affected by spatial frequency in a manner consistent with SC neural properties.** (A) Example visual search arrays and eye movement scan paths (green) superimposed on them. The left panel shows a search array of targets with a low spatial frequency, and the right panel shows a search array of targets with a higher spatial frequency. Subjects searched for an oddball orientation in the array, and the task was made difficult enough to require many scanning saccades of the array. (B) Mean (solid) and median (dashed) inter-saccadic intervals during target search as a function of the spatial frequency of the targets in the search array. Error bars denote 95% confidence intervals. As can be seen, inter-saccadic intervals progressively increased with higher spatial frequencies, as in our earlier neural and behavioral results. (C) Proportion of correct oddball identifications (Materials and Methods) as a function of spatial frequency in the target search array. Subjects faithfully searched the array until they could correctly identify the target on the great majority of trials, meaning that the changes in inter-saccadic intervals in B were not due to potential speed-accuracy tradeoffs during search. Error bars denote 95% confidence intervals.

In all, our results demonstrate that the visual properties of the SC are organized to facilitate exploring natural scenes with rapid gaze shifts. It has also not escaped us that these properties may allow the SC to preferentially process face-like stimuli (Nguyen et

al., 2014) and to also support an alternative visual pathway during blindsight (Weiskrantz et al., 1974), in which patients with V1 loss exhibit spatial frequency capabilities that are remarkably similar to those we have found here (Sahraie et al., 2010; Sahraie et al., 2002; Trevethan and Sahraie, 2003).

Confidential

## **Materials and Methods**

Monkey experiments were approved by regional governmental offices in Tuebingen. For the human experiments, ethics committees at Tuebingen University reviewed and approved our protocols. All human subjects provided written informed consent in accordance with the Declaration of Helsinki.

### **Animal preparation**

Monkeys P and N (male, *Macaca mulatta*, aged 7 years) were prepared for behavior and superior colliculus (SC) recordings earlier (Chen and Hafed, 2013; Chen et al., 2015).

Briefly, we placed a recording chamber centered on the midline and aimed at a stereotaxically defined point 1 mm posterior of and 15 mm above the inter-aural line. The chamber was tilted posterior of vertical (by 38 and 35 deg for monkeys P and N, respectively).

### **Monkey recording task**

The monkeys performed a pure fixation task while we recorded the activity of visually-responsive SC neurons. In each trial, a white fixation spot (8.5x8.5 min arc) appeared over a gray background. Fixation spot and background luminance were described earlier (Chen and Hafed, 2013). After an initial fixation interval (400-550 ms), the fixation spot transiently dimmed for ~50 ms, which reset microsaccadic rhythms (Hafed and Ignashchenkova, 2013; Tian et al., 2016) and also attracted attention to the spot rather than to the response field (RF) stimulus. After an additional 110-320 ms, a stationary, vertical Gabor patch with 80% relative contrast (defined as  $L_{max}$ -

Lmin/Lmax+Lmin) appeared for 300 ms within the neuron's RF. The RF was estimated earlier in the session using standard saccade tasks (Chen et al., 2015; Hafed and Chen, 2016), and the Gabor patch size was chosen to fill as much of the RF as possible. The spatial frequency of the patch, in cycles/degree (cpd), was varied randomly across trials (from among 0.56, 1.11, 2.22, 4.44, and 11.11 cpd). Grating phase was randomized from trial to trial, and the monkey was rewarded only for maintaining fixation; no orienting to the grating or any other behavioral response was required. We used only vertical gratings, but we confirmed that they elicit robust responses in the SC. In pilot data, we also confirmed that any potential orientation tuning in the SC was very broad and included robust responses to vertical gratings (Chen et al., 2015).

We recorded from 115 neurons. We excluded trials with microsaccades occurring within +/-100 ms from stimulus onset because such occurrence can alter neural activity. In fact, the trials with microsaccades near stimulus onset were analyzed recently, from the same set of neurons, to explore spatial-frequency dependence of saccadic suppression in the SC (Chen and Hafed, 2017). Our focus here was to only analyze baseline neural activity and not activity modulated due to the presentation of peri-movement stimuli. We excluded 9 neurons from further analyses because they did not have >25 repetitions per tested spatial frequency after excluding the microsaccade trials. This number was our chosen threshold for the minimum number of observations in order to have sufficient confidence in our interpretations of the results. For the remaining neurons that were included in the analyses, we collected >295 trials per neuron (average: 935 +/- 271 s.d.).

### **Monkey saccade reaction time task**

In completely different purely behavioral sessions, we ran our monkeys on a simple saccade reaction time task, which we recently described in detail (Chen and Hafed, 2017). Briefly, the monkeys fixated, and a Gabor patch of 2 deg diameter could appear at 3.5 deg eccentricity either to the right or left of fixation. The patch was otherwise identical to that used in the recording task described above, and the fixation spot disappeared simultaneously with patch appearance in order to cue the monkeys to generate a targeting saccade towards the patch. We measured reaction time (RT) and correlated it with SC visual responses collected from completely different sessions and critically not involving a saccadic response at all (i.e. the recording task above). We analyzed 2,522 trials from Monkey N and 3,392 trials from Monkey P. As with the neural data above, we only analyzed trials without any microsaccades within 100 ms before or after Gabor patch onset, to avoid peri-movement effects on RT that were described in detail elsewhere (Chen and Hafed, 2017).

### **Human visual scanning task**

Subjects sat in a dark room facing a computer display (41 pixels per deg; 85 Hz), and head fixation was achieved through a custom-made chin/forehead rest (Hafed, 2013). We collected data from 8 subjects (3 females; 5 authors).

Each trial started with an initial fixation spot presented at display center. After ~1030 ms of steady fixation, a search array consisting of 4x4 Gabor patches appeared. Each patch was 6.1 deg in diameter, and all 16 patches were distributed evenly in a grid layout across the display. Grating contrast was set to maximum (100%), and all patches had the same spatial frequency within a given trial. Spatial frequency was altered randomly across trials from among 6 possible values (0.33, 0.66, 1.31, 1.97, 3.93, and 5.9 cpd). Moreover, all but one patch had the same orientation within a given trial (picked randomly across trials from all possible orientations with a resolution of 1 deg). The odd patch was tilted by 7 deg either to the right or left from the orientation of all other patches, and the subjects' task was to search for the oddly oriented patch and indicate whether it was tilted to the right or left from all other patches. The task was very difficult to perform during fixation, and therefore required prolonged scanning of the entire grid array of patches with many saccades until the odd patch was found and correctly discriminated. This allowed us to obtain sufficient search performance data, with many inter-saccadic intervals that were the focus of our analysis (i.e. our goal was to investigate how inter-saccadic intervals were affected by spatial frequency). We collected 180 trials per subject (i.e. 30 trials per spatial frequency), but each trial had many more inter-saccadic intervals that could be analyzed (as detailed below).

### **Neuron classification**

We used similar neuron classification criteria to those used in our recent studies (Chen et al., 2015; Hafed and Chen, 2016). Briefly, a neuron was labeled as visual if its activity 0-200 ms after target onset in a delayed saccade task (Hafed and Chen, 2016; Hafed and

Krauzlis, 2008) was higher than activity 0-200 ms before target onset ( $p < 0.05$ , paired t-test). The neuron was labeled as visual-motor if its pre-saccadic activity (-50-0 ms from saccade onset) was also elevated in the delayed saccade task relative to an earlier fixation interval (100-175 ms before saccade onset) (Li and Basso, 2008). In most cases, our results were similar for either visual or visual-motor neurons, so we combined neuron types in analyses unless otherwise explicitly stated.

### **Eye movement analyses**

We measured eye movements in monkeys using scleral search coils (Fuchs and Robinson, 1966; Judge et al., 1980), and we used a video-based eye tracker for humans (Hafed, 2013). We detected saccades and microsaccades using velocity and acceleration criteria detailed elsewhere (Buonocore et al., 2017; Chen and Hafed, 2013; Hafed et al., 2009; Hafed and Ignashchenkova, 2013).

For the monkey recordings, we detected microsaccades in order to exclude trials with such movements occurring near stimulus onset (see above). For the monkey saccade reaction time task, we detected the targetting saccade after grating onset and measured its RT. We only considered trials in which there were no microsaccades within 100 ms from target onset, because microsaccades near target onset alter RT (Chen and Hafed, 2017; Hafed and Krauzlis, 2010), and because these trials with peri-microsaccadic stimuli were analyzed separately elsewhere (Chen and Hafed, 2017).



For the human scanning task, we measured inter-saccadic intervals during search. The inter-saccadic interval was defined as the time period between the offset of one saccade and the onset of the next. We only considered saccades occurring between search array onset and trial end (i.e. button press) when computing inter-saccadic intervals. Moreover, we only analyzed trials in which there were no blinks during the entire period from which we were collecting inter-saccadic intervals. Because trials were long until subjects found the odd patch, meaning that we had many inter-saccadic intervals within any trial, removal of blink trials did not reduce our data set dramatically; in the end, we had a total of 3,325-4,743 accepted inter-saccadic intervals per spatial frequency in our analyses (from a total of 145-182 accepted trials per spatial frequency).

### **Firing rate analyses**

We analyzed SC visual bursts by measuring peak firing rate 20-150 ms after stimulus onset (Chen and Hafed, 2017). We then obtained spatial frequency tuning curves by plotting peak visual response as a function of grating spatial frequency. We performed a least squares fit of the measurements to the following difference-of-Gaussians function:

$$f(x) = a_1 * e^{-\left(\frac{x-b_1}{c_1}\right)^2} - a_2 * e^{-\left(\frac{x-b_2}{c_2}\right)^2} + B \quad (\text{equation 1})$$

where  $f$  is firing rate,  $x$  is spatial frequency,  $a_1$  and  $a_2$  represent the amplitude of each Gaussian function,  $b_1$  and  $b_2$  represent the mean of each Gaussian function,  $c_1$  and  $c_2$  are the bandwidth of each Gaussian function, and  $B$  is the baseline firing rate (obtained from all trials as the mean firing rate in the interval 0-50 ms before Gabor patch onset). The

goodness of fit was validated computing the percentage of the variance across stimuli for which the model accounted (Carandini et al., 1997). Only neurons that had >80% explained variance by the fit were included in summaries of tuning curve fits in Results (97 out of 106 neurons).

We estimated the preferred spatial frequency of each neuron as the spatial frequency within the sampled range of 0.56-11.11 cpd for which the fitted tuning curve from the above equation peaked. To combine different neurons' tuning curves (e.g. Fig. 4), we first normalized the peak of the tuning curve of each neuron to 1. We then combined neurons and obtained a mean curve across neurons along with s.e.m. estimates.

We estimated first spike latency using Poisson spike train analysis (Legendy and Salzman, 1985). Most of our neurons had very little or no baseline activity, meaning that our estimate of first spike latency using this method was very robust, and it gave us a sense of how quickly our neurons responded to the onset of a given stimulus.

### **Local field potential analyses**

We obtained local field potentials from wide-band neural signals using methods that we described recently (Chen and Hafeed, 2017; Hafeed and Chen, 2016). We then aligned LFP traces on Gabor patch onset, and we measured evoked responses in two ways. First, we measured the strongest deflection occurring in the interval 20-150 ms after stimulus onset, to obtain a measure that we called the transient LFP response. Second, we measured the mean deflection in the period 150-250 ms after stimulus onset, to obtain what we referred

to as the sustained LFP response. Since the LFP evoked response is negative going, when we refer to a “peak” LFP response, we mean the most negative value of the measured signal.

### **Predicting saccade reaction times from visual responses recorded on completely different sessions**

Our approach was to ask the simple question of whether RT from behavioral sessions can be related in a simple manner to visual response strength and first spike latency from completely separate neural recording sessions in which no saccade to the patch was ever made. We used linear models of the form:

$$RT(PV, FSL, x) = a * PV(x) + b * FSL(x) + c \quad (\text{equation 2})$$

where  $x$  is spatial frequency,  $PV(x)$  is the average peak visual response of all included neurons for spatial frequency  $x$ ;  $FSL(x)$  is first spike latency of all included neurons for spatial frequency  $x$ ; and  $a, b, c$  are model parameters. Since the behavioral RT's were experimentally obtained from horizontal targets at 3.5 deg eccentricity, we only included neurons with preferred RF locations centered within the range of 2-10 deg in eccentricity and +/-45 deg in direction from horizontal (i.e. 46 neurons). Moreover, we separated each monkey's neurons so that its own neural activity was used to predict its behavioral variability.

For modeling mean RT, we normalized the range of RT values to the range from 0 to 1, with 0 corresponding to the shortest RT (e.g. that obtained from the lowest spatial frequency in monkey N). We similarly normalized the range of peak visual response and first spike latency. We then fit the best parameters to equation 2 above that matched the data. To test whether including either first spike latency or peak visual response alone gave similar model fits to the case where both quantities were part of the model, we also ran the fitting with either parameter a or b in equation 2 pegged at 0.

We also took a similar approach in estimating RT variance and relating it to the variance of peak visual responses and/or first spike latencies. We essentially ran equation 2 again, but using variances of all parameters instead of means.

Confidential

### **Author Contributions**

C.-Y. C. and Z. M. H. performed the neural experiments and analyzed the data. L. S., S. W., T. W., and Z. M. H. performed the human experiments. Z. M. H. wrote the paper.

### **Acknowledgments**

We were funded by the Werner Reichardt Centre for Integrative Neuroscience (CIN), an Excellence Cluster (EXC307) funded by the Deutsche Forschungsgemeinschaft (DFG). We were also supported by the Hertie Institute for Clinical Brain Research.

Confidential

## References

Bredfeldt, C.E., and Ringach, D.L. (2002). Dynamics of spatial frequency tuning in macaque V1. *J Neurosci* 22, 1976-1984.

Breitmeyer, B.G. (1975). Simple reaction time as a measure of the temporal response properties of transient and sustained channels. *Vision Res* 15, 1411-1412.

Buonocore, A., Chen, C.Y., Tian, X., Idrees, S., Muench, T., and Hafed, Z.M. (2017). Alteration of the microsaccadic velocity-amplitude main sequence relationship after visual transients: implications for models of saccade control. *J Neurophysiol*, jn 00811 02016.

Carandini, M., Heeger, D.J., and Movshon, J.A. (1997). Linearity and normalization in simple cells of the macaque primary visual cortex. *J Neurosci* 17, 8621-8644.

Chen, C.Y., and Hafed, Z.M. (2013). Postmicrosaccadic enhancement of slow eye movements. *The Journal of neuroscience : the official journal of the Society for Neuroscience* 33, 5375-5386.

Chen, C.Y., and Hafed, Z.M. (2017). A Neural Locus for Spatial-Frequency Specific Saccadic Suppression in Visual-Motor Neurons of the Primate Superior Colliculus. *J Neurophysiol*, jn 00911 02016.

Chen, C.Y., Ignashchenkova, A., Thier, P., and Hafed, Z.M. (2015). Neuronal Response Gain Enhancement prior to Microsaccades. *Curr Biol* 25, 2065-2074.

De Valois, R.L., Albrecht, D.G., and Thorell, L.G. (1982). Spatial frequency selectivity of cells in macaque visual cortex. *Vision Res* 22, 545-559.

Edelman, J.A., and Keller, E.L. (1996). Activity of visuomotor burst neurons in the superior colliculus accompanying express saccades. *Journal of neurophysiology* 76, 908-926.

Fuchs, A.F., and Robinson, D.A. (1966). A method for measuring horizontal and vertical eye movement chronically in the monkey. *J Appl Physiol* 21, 1068-1070.

Gandhi, N.J., and Katnani, H.A. (2011). Motor functions of the superior colliculus. *Annual review of neuroscience* 34, 205-231.

Hafed, Z.M. (2013). Alteration of visual perception prior to microsaccades. *Neuron* 77, 775-786.

Hafed, Z.M., and Chen, C.-Y. (2016). Sharper, stronger, faster upper visual field representation in primate superior colliculus. *Current Biology*  
<http://dx.doi.org/10.1016/j.cub.2016.04.059>.

Hafed, Z.M., Chen, C.-Y., and Tian, X. (2015). Vision, perception, and attention through the lens of microsaccades: mechanisms and implications. *Frontiers in systems neuroscience* 9, 167.

Hafed, Z.M., Goffart, L., and Krauzlis, R.J. (2009). A neural mechanism for microsaccade generation in the primate superior colliculus. *Science* 323, 940-943.

Hafed, Z.M., and Ignashchenkova, A. (2013). On the dissociation between microsaccade rate and direction after peripheral cues: microsaccadic inhibition revisited. *J Neurosci* 33, 16220-16235.

Hafed, Z.M., and Krauzlis, R.J. (2008). Goal representations dominate superior colliculus activity during extrafoveal tracking. *J Neurosci* 28, 9426-9439.

Hafed, Z.M., and Krauzlis, R.J. (2010). Microsaccadic suppression of visual bursts in the primate superior colliculus. *J Neurosci* 30, 9542-9547.

Judge, S.J., Richmond, B.J., and Chu, F.C. (1980). Implantation of magnetic search coils for measurement of eye position: an improved method. *Vision Res* 20, 535-538.

Kaplan, E., and Shapley, R.M. (1982). X and Y cells in the lateral geniculate nucleus of macaque monkeys. *J Physiol* 330, 125-143.

Legendy, C.R., and Salzman, M. (1985). Bursts and recurrences of bursts in the spike trains of spontaneously active striate cortex neurons. *J Neurophysiol* 53, 926-939.

Li, X., and Basso, M.A. (2008). Preparing to move increases the sensitivity of superior colliculus neurons. *The Journal of neuroscience : the official journal of the Society for Neuroscience* 28, 4561-4577.

Ludwig, C.J., Gilchrist, I.D., and McSorley, E. (2004). The influence of spatial frequency and contrast on saccade latencies. *Vision Res* 44, 2597-2604.

Marino, R.A., Levy, R., Boehnke, S., White, B.J., Itti, L., and Munoz, D.P. (2012). Linking visual response properties in the superior colliculus to saccade behavior. *Eur J Neurosci* 35, 1738-1752.

Maunsell, J.H., and Gibson, J.R. (1992). Visual response latencies in striate cortex of the macaque monkey. *J Neurophysiol* 68, 1332-1344.

Mazer, J.A., Vinje, W.E., McDermott, J., Schiller, P.H., and Gallant, J.L. (2002). Spatial frequency and orientation tuning dynamics in area V1. *Proc Natl Acad Sci U S A* 99, 1645-1650.

Nguyen, M.N., Matsumoto, J., Hori, E., Maior, R.S., Tomaz, C., Tran, A.H., Ono, T., and Nishijo, H. (2014). Neuronal responses to face-like and facial stimuli in the monkey superior colliculus. *Front Behav Neurosci* 8, 85.

Olshausen, B.A., and Field, D.J. (1996). Emergence of simple-cell receptive field properties by learning a sparse code for natural images. *Nature* 381, 607-609.

Pollack, J.G., and Hickey, T.L. (1979). The distribution of retino-collicular axon terminals in rhesus monkey. *J Comp Neurol* 185, 587-602.

Previc, F.H. (1990). Functional Specialization in the Lower and Upper Visual-Fields in Humans - Its Ecological Origins and Neurophysiological Implications. *Behavioral and Brain Sciences* 13, 519-575.

Purushothaman, G., Chen, X., Yampolsky, D., and Casagrande, V.A. (2014). Neural mechanisms of coarse-to-fine discrimination in the visual cortex. *J Neurophysiol* 112, 2822-2833.

Ruderman, D.L., and Bialek, W. (1994). Statistics of natural images: Scaling in the woods. *Phys Rev Lett* 73, 814-817.

Sahraie, A., Hibbard, P.B., Trevethan, C.T., Ritchie, K.L., and Weiskrantz, L. (2010). Consciousness of the first order in blindsight. *Proc Natl Acad Sci U S A* 107, 21217-21222.

Sahraie, A., Weiskrantz, L., Trevethan, C.T., Cruce, R., and Murray, A.D. (2002). Psychophysical and pupillometric study of spatial channels of visual processing in blindsight. *Exp Brain Res* 143, 249-256.

Schmolesky, M.T., Wang, Y., Hanes, D.P., Thompson, K.G., Leutgeb, S., Schall, J.D., and Leventhal, A.G. (1998). Signal timing across the macaque visual system. *J Neurophysiol* 79, 3272-3278.

Simoncelli, E.P., and Olshausen, B.A. (2001). Natural image statistics and neural representation. *Annu Rev Neurosci* 24, 1193-1216.



Tian, X., Yoshida, M., and Hafed, Z.M. (2016). A Microsaccadic Account of Attentional Capture and Inhibition of Return in Posner Cueing. *Frontiers in systems neuroscience* 10, 23.

Tolhurst, D.J., Tadmor, Y., and Chao, T. (1992). Amplitude spectra of natural images. *Ophthalmic Physiol Opt* 12, 229-232.

Trevelyan, C.T., and Sahraie, A. (2003). Spatial and temporal processing in a subject with cortical blindness following occipital surgery. *Neuropsychologia* 41, 1296-1306.

Vaiceliunaite, A., Eriskien, S., Franzen, F., Katzner, S., and Busse, L. (2013). Spatial integration in mouse primary visual cortex. *J Neurophysiol* 110, 964-972.

van Hateren, J.H., and van der Schaaf, A. (1998). Independent component filters of natural images compared with simple cells in primary visual cortex. *Proc Biol Sci* 265, 359-366.

Veale, R., Hafed, Z.M., and Yoshida, M. (2017). How is visual salience computed in the brain? Insights from behaviour, neurobiology and modelling. *Philos Trans R Soc Lond B Biol Sci* 372.

Weiskrantz, L., Warrington, E.K., Sanders, M.D., and Marshall, J. (1974). Visual capacity in the hemianopic field following a restricted occipital ablation. *Brain* 97, 709-728.

White, B.J., Stritzke, M., and Gegenfurtner, K.R. (2008). Saccadic facilitation in natural backgrounds. *Curr Biol* 18, 124-128.

## Supplementary Figures

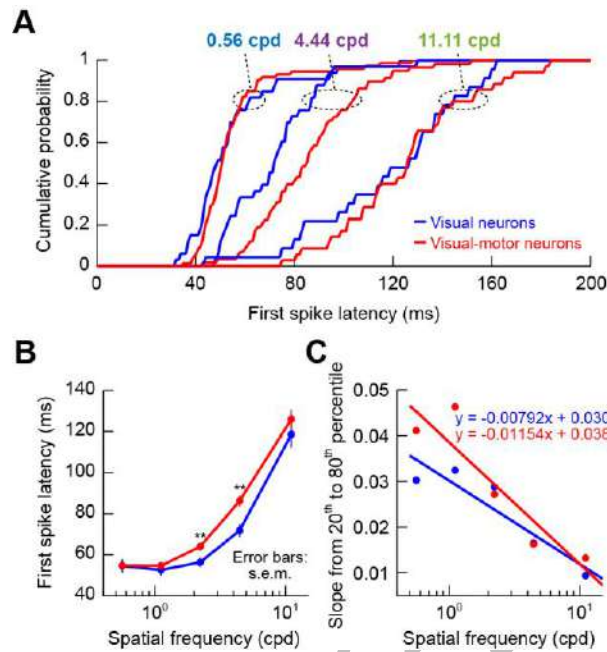


**Figure S1 Response latencies of visual and visual-motor SC neurons.** (A) Cumulative histograms of first spike latency as in Fig. 3, but after separating neurons as either being purely visual (blue) or visual-motor (red). To reduce clutter, only 3 spatial frequencies are shown. As can be seen, the dependence of response latency on spatial frequency was similar whether neurons were purely visual or visual-motor, but visual neurons tended to exhibit slightly shorter latencies, especially at 4.44 cpd. (B) Mean response latencies across neurons as a function of spatial frequency, again as in Fig. 3, but separating visual and visual-motor neurons. Consistent with A, response latency increased with increasing spatial frequency for both types of neurons. Also, again consistent with A, visual neurons showed earlier responses than visual-motor neurons, especially during intermediate frequencies. Asterisks mean  $p < 0.01$  for the comparison between visual and visual-motor neurons at a given spatial frequency (Ranksum test). (C) Estimate of variance in response latency as a function of spatial frequency, as in Fig. 3. Both visual and visual-motor neurons behaved similarly as a function of spatial frequency.

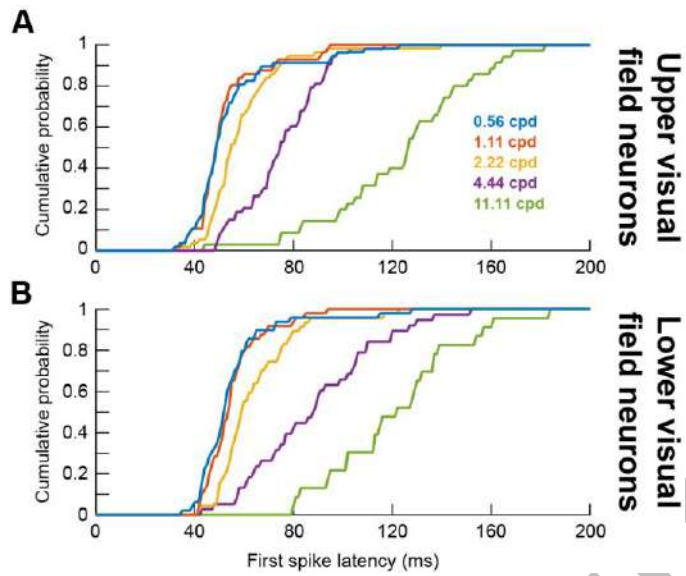


**Figure S2 Response latencies for upper and lower visual field neurons.** (A) Same as Fig. 3A but for neurons in the upper visual field representation of the SC. (B) Same as Fig. 3A but for neurons in the lower visual field representation of the SC. In both cases, the rank ordering of response latencies as a function of spatial frequency is evident, with an additional observation of upper visual field neurons responding faster in general than lower visual field neurons, consistent with (Hafed and Chen, 2016).

**6. Orientation and contrast tuning properties and temporal flicker fusion characteristics of primate superior colliculus neurons**

# **Orientation and contrast tuning properties and temporal flicker fusion characteristics of primate superior colliculus neurons**

Chih-Yang Chen<sup>1,2,3</sup> and Ziad M. Hafed<sup>1,3</sup>

1. Werner Reichardt Centre for Integrative Neuroscience, Tuebingen University, Tuebingen, BW, 72076, Germany
2. Graduate School of Neural and Behavioural Sciences, International Max Planck Research School, Tuebingen University, Tuebingen, BW, 72074, Germany
3. Hertie Institute for Clinical Brain Research, Tuebingen University, Tuebingen, BW, 72076, Germany

## **Corresponding Author/Lead Contact:**

Ziad M. Hafed  
Werner Reichardt Centre for Integrative Neuroscience  
Otfried-Mueller Str. 25  
Tuebingen, 72076, Germany  
Tel: +49 7071 29-88819  
E-mail: [ziad.m.hafed@cin.uni-tuebingen.de](mailto:ziad.m.hafed@cin.uni-tuebingen.de)

# **Orientation and contrast tuning properties and temporal flicker fusion characteristics of primate superior colliculus neurons**

Chih-Yang Chen<sup>1,2,3</sup> and Ziad M. Hafed<sup>1,3</sup>

1. Werner Reichardt Centre for Integrative Neuroscience, Tuebingen University, Tuebingen, BW, 72076, Germany
2. Graduate School of Neural and Behavioural Sciences, International Max Planck Research School, Tuebingen University, Tuebingen, BW, 72074, Germany
3. Hertie Institute for Clinical Brain Research, Tuebingen University, Tuebingen, BW, 72074, Germany

## **Summary**

The primate superior colliculus is traditionally studied from the perspectives of gaze control, target selection, and visual attention. However, this structure is ultimately a visual structure, and it is the primary visual structure in lower animals. Thus, understanding the visual tuning properties of primate superior colliculus neurons is important, especially given that this structure is part of an alternative visual pathway running in parallel to the predominant geniculo-cortical pathway. In recent previous studies, we have characterized receptive field organization and spatial frequency tuning properties of the superior colliculus. Here, we continue our characterization by exploring additional aspects like orientation tuning, putative center-surround interactions, and temporal frequency tuning characteristics of visually-responsive collicular neurons. We found that orientation tuning is at best weak in superior colliculus, contrary to some recent reports in rodents. We also used stimuli of different sizes to explore contrast sensitivity and potential center-surround interactions. We found that stimulus size affects the slope of contrast sensitivity curves without altering maximal firing rate or semi-saturation contrast. Additionally, sustained firing rates, long after stimulus onset, strongly depend on stimulus size, and this is also reflected in local field potentials. This suggests the presence of inhibitory interactions within and around classical receptive fields. Finally, superior colliculus neurons exhibit temporal frequency tuning for frequencies lower than 30 Hz, with critical flicker fusion frequencies of less than 20 Hz. These results support hypotheses that the superior colliculus might dominate the visual performance capabilities of blindsight subjects who lose portions of their primary visual cortex.

## **Highlights**

- Superior colliculus neurons show weak orientation tuning
- Stimulus size affects contrast sensitivity of superior colliculus neurons
- Sustained visual responses reflect potential post-excitation inhibition
- Superior colliculus neurons show temporal frequency tuning characteristics

## Introduction

It has been shown since more than 70 years ago that superior colliculus (SC) neurons have visual responses. Almost in parallel with these findings, researchers have recognized that the SC is also a crucial midbrain structure for orienting behavior, especially for saccadic eye movements (Wurtz and Optican, 1994). As a result, there was an explosion of studies aimed at understanding subcortical connections for movement control, as well as cortical neural substrates for eye movements (Gandhi and Katnani, 2011). More recently, studies on the role of the SC in active vision have focused much more heavily on cognitive tasks like target selection and visual attention (Krauzlis et al., 2013). The visual properties of SC neurons, however, have been largely left out after some simple characterizations using light dots and bars.

In separate lines of research, it became recognized that saccadic patterns, orienting efficiency, and target selection can drastically differ under a variety of visual conditions and in natural scene scenarios (Veale et al., 2017). This means that low level image statistics can strongly influence eye movements (Ludwig et al., 2004). Motivated by this, we have recently begun to characterize SC visual properties from an ecological perspective (Hafed and Chen, 2016). Our starting point was that the SC can be an important neural substrate for implementing visual salience maps that can guide behavior (Veale et al., 2017), and this is consistent with how visual topography in the SC is already co-registered with the deeper saccade map topography in the same structure. We have shown that visual topography is asymmetric between upper and lower visual fields

(Hafed and Chen, 2016), and also that spatial frequency tuning properties of SC allow it to facilitate gaze behavior under natural scene scenarios in which low spatial frequencies are predominant (unpublished observations). Here, we continued our investigations of the SC's visual properties. We focused on orientation tuning, especially given that recent rodent work has yielded some controversy (Ahmadlou and Heimel, 2015; Feinberg and Meister, 2015; Inayat et al., 2015). We also explored potential center-surround RF interactions as well as temporal frequency tuning properties. In all, we believe that our results, coupled with our recent findings on spatial frequency tuning (unpublished observations), support hypotheses that the SC can play an important role in determining the visual capabilities of blindsight patients who lose conscious visual perception through loss of their primary visual cortex (V1) (Cowey, 2010; Leopold, 2012).

## **Results and Discussion**

*Highly orientation selective neurons were rare in the SC and first spike latency was similar for the most and least preferred orientations*

We recorded visual responses in macaque monkeys that were fixating a small spot, while we presented an oriented grating of 2.22 cycles/deg (cpd) within a neuron's visual response field (RF). The grating was stationary and was presented for ~200 ms. Figure 1a shows the responses of an example neuron exhibiting substantial orientation selectivity. Each colored curve shows raw firing rates from the neuron when a specific orientation



was presented, and the orientations are arranged graphically according to the graphic placement of a firing rate plot (e.g. the magenta trace reflects responses to a grating that was tilted slightly rightward of purely vertical). The central part of the figure shows a plot of peak firing rate after stimulus onset as a function of grating orientation. As can be seen, this neuron responded the most for a grating oriented to the bottom right (the cyan trace). We computed an orientation selectivity index (OSI) according to the literature from early cortical visual areas, and we found that this neuron had an OSI of 0.186. However, this neuron did not represent the majority of SC neurons that we recorded. Instead, we were more likely to encounter neurons like that shown in Fig. 1b. In this case, orientation tuning was much broader, as also reflected by the lower OSI value than in Fig. 1a. Across the population, only approximately one third of our neurons had strong OSI values  $>0.15$  and only approximately one half had mild OSI values  $>0.1$  (Fig. 1c).

We also checked the efficiency with which neurons responded to different orientations, by measuring first spike latency as we have done earlier (Hafed and Chen, 2016). Regardless of whether a grating was vertical, the least preferred orientation of a given neuron, or the most preferred orientation of a given neuron, first spike latency was similar (Fig. 1d). This means that broad orientation tuning was also accompanied by a lack of preference for orientations in terms of how fast neural responses were evoked.

Since in our previous studies, we used vertical gratings to study SC modulations around the time of microsaccades (Chen and Hafed, 2017; Chen et al., 2015), we also confirmed that this was a reasonable strategy for SC neurons. For neurons not preferring vertical

orientations, we plotted visual responses to either the most preferred, the least preferred, or a vertical orientation and compared them (Fig. 1e). We found modest changes in responses across all these conditions, suggesting that vertical gratings were still able to evoke responses in SC neurons. This is consistent with the results of Fig. 1a-d.

For a subset of neurons, we also checked whether placing a grating orthogonal or parallel to the line connecting the fovea to the grating location matters. We found that parallel gratings (Fig. 1f) were least effective in driving SC neurons, but this effect was relatively modest, again consistent with broad orientation tuning properties of SC neurons.

Confidential

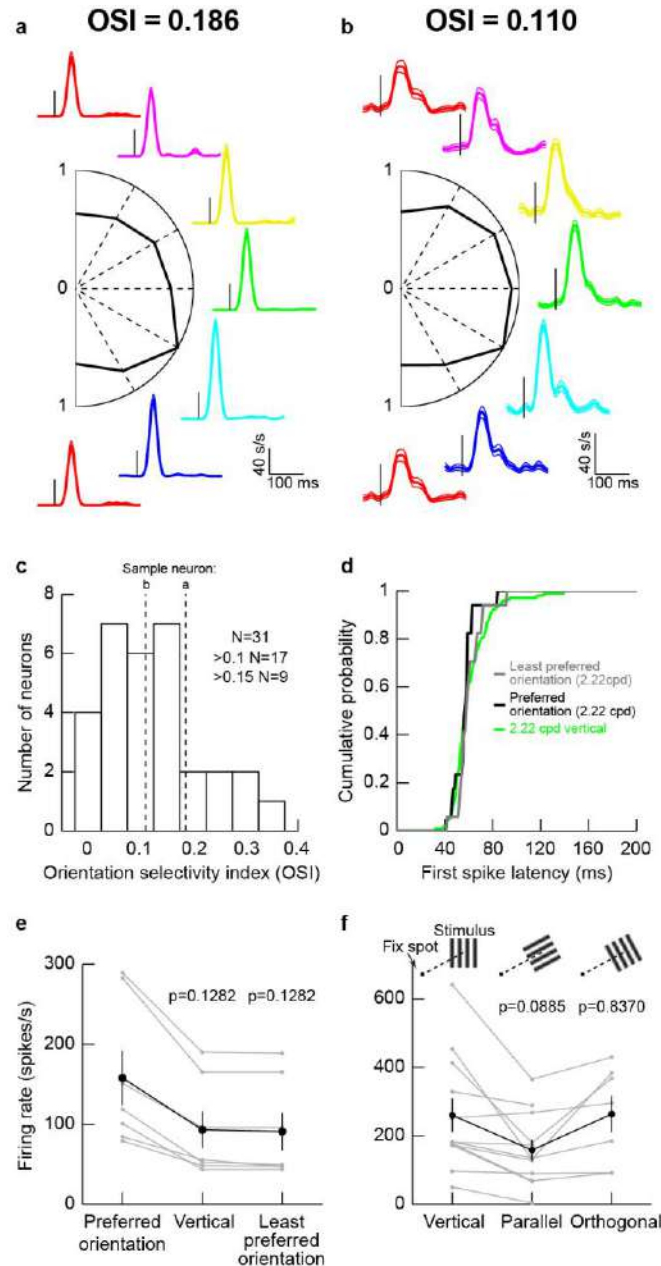


**Figure 1 Mild orientation tuning in the macaque superior colliculus (SC).** (a) Visual responses of an example SC neuron to gratings of different orientations (color-coded) presented within the neuron's visual response field (RF). The firing rate curves are graphically arranged according to the grating orientation. For example, the red curves are for vertical gratings, and the green curve is for horizontal gratings. In the center, we plot the peak visual response (normalized to the maximum at one of the orientations) as a function of grating orientation. As can be seen, this neuron preferred an orientation of 30 deg below horizontal (cyan firing rate curve). The OSI (Materials and Methods) of this neuron is indicated. (b) A second neuron with weaker orientation selectivity. The neuron responded almost equally well to all orientations. (c) Distribution of OSI values across our population. The majority of neurons had mild or weak orientation selectivity. (d) Consistent with this, first spike latency did not depend on stimulus orientation, regardless of neural orientation preference. (e) Also, for neurons not preferring vertical orientations, the differences between the preferred, the least preferred, and the vertical orientations were mild. The black curve shows the summary across neurons, and the gray curves show responses for individual neurons. (f) A similar

observation was made when testing parallel versus orthogonal orientations relative to the line connecting the fovea to the RF stimulus location. Parallel gratings had mildly weaker responses than orthogonal ones. Error bars denote s.e.m.

### *Small RF stimuli resulted in sharper contrast sensitivity curves*

We next explored potential local RF interactions by changing stimulus size at a given location. We ran conditions using a vertical grating as in (Chen et al., 2015), but this time, we compared responses when the grating was either filling as much of the RF as possible or when the stimulus was significantly smaller. We varied the contrast of the grating from trial to trial in order to obtain contrast sensitivity curves. In the sample neuron of Fig. 2a, b, we obtained an expected dependence of visual response strength on stimulus contrast; the higher the contrast, the higher and earlier the visual response was, and this happened for both a large and a small grating in the RF. However, closer inspection of the contrast sensitivity curves revealed an additional property: there was a sharpening of these curves for the smaller stimulus (Fig. 2c). In this sample neuron, semi-saturation contrast ( $c_{50}$ ) appeared to be also affected, but this effect was not significant across the population (Fig. 2d). Instead, across the population, the only significant effect was on the slope ( $n$ ) of the contrast sensitivity curve. We confirmed this by plotting in Figs. 2e-g the different parameters of the contrast sensitivity curve equation (displayed in the inset of Fig. 2c) for each neuron. Across the population, only the slope parameter of contrast sensitivity curves was significantly different between small and large stimuli. This effect is also evident in Fig. 2h, in which we plotted the peak firing rate for each stimulus contrast for either small or large stimuli. Firing rates between small and large stimuli were similar for

high contrasts regardless of stimulus size. However, for lower contrasts (5% and 10%), responses were weaker in the smaller stimuli, again consistent with a sharpening of contrast sensitivity curves.

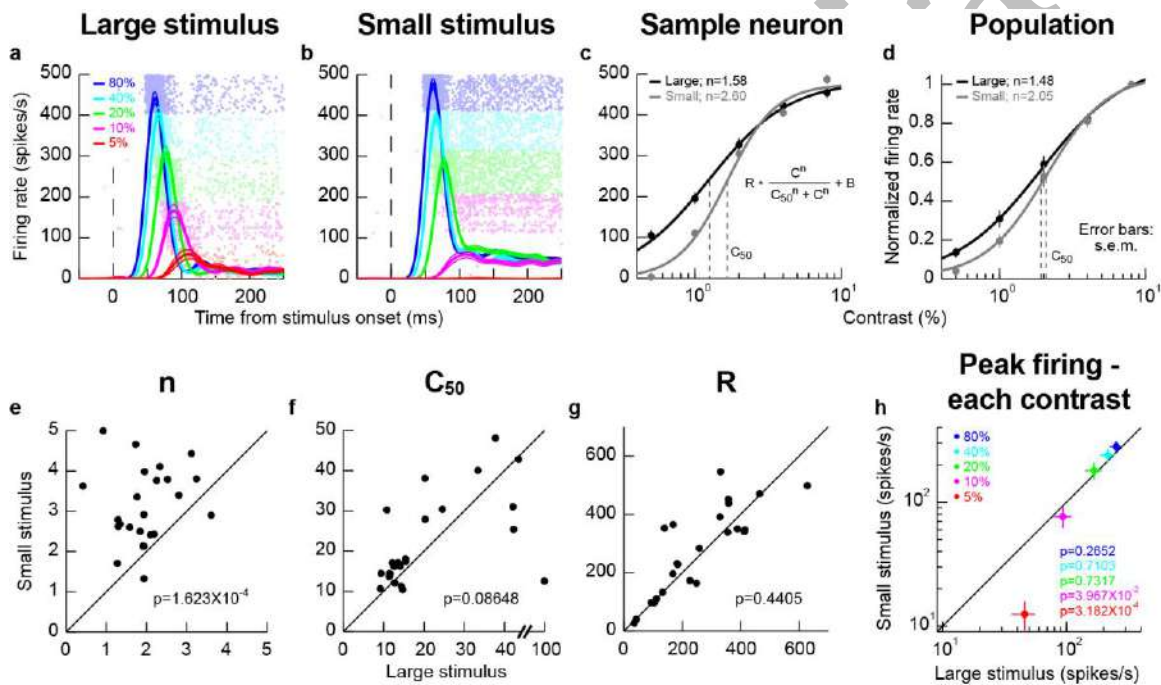


**Figure 2 Stimulus size effects on contrast sensitivity.** (a, b) Responses of a sample neuron to different stimulus contrasts (color-coded according to the legend). On the left, the stimulus filled the RF; on the right, the stimulus was much smaller. The responses of the neuron were similar except that the evoked response at low contrasts (5% and 10%) was much weaker for the small stimuli. This suggests that there is excitatory drive by the big stimulus, and that the contrast sensitivity curve of the neuron is sharper for small stimuli. (c) We confirmed this last point. We plotted the responses as a function of contrast, and fitted the data with the shown equation. In this neuron, the slope parameter ( $n$ ) was different for large and small stimuli. The semi-saturation contrast ( $c_{50}$ ) was also apparently altered. (d) However, across the population, the only significant effect was on  $n$ , meaning that contrast sensitivity curves were sharper for small stimuli. (e-g) The parameters of the contrast sensitivity curve equation across neurons for small versus large stimuli. Across the population, only  $n$  showed a significant effect of stimulus size. (h) Consistent with this, when we plotted peak firing rate as a function of contrast, we found that the rate was significantly lower for small versus big stimuli (p-values in the colored-text) only for low contrasts. For high contrasts, neural sensitivity was similar for different stimulus sizes.

*Small RF stimuli resulted in higher sustained activity*

The results above with small stimuli might suggest differences in local lateral interactions caused by an extended stimulus. This idea was rendered clearer when inspecting sustained firing rates after the initial onset transient. In the sample neuron of Fig. 2a, b, it can be seen that sustained activity was elevated for small stimuli. For example, for 10% stimulus contrast, even though the initial evoked response was much weaker in the small stimulus configuration than in the large stimulus configuration, the sustained activity was significantly higher in the small stimulus configuration. This suggests that with the large stimulus, an inhibitory effect kicks in after the initial excitatory stimulus transient.

We also observed evidence for such an inhibitory effect in local field potentials (LFP's), reflecting local population activity around our recording electrodes. For example, in Fig. 3a, b, we plotted LFP evoked responses for different contrasts and different stimulus sizes from the same electrode penetration in which the sample neuron of Fig. 2a, b was isolated. As can be seen, the sharpening of contrast sensitivity curves can be clearly seen in the LFP evoked responses. For example, for the small stimulus, the initial evoked LFP transient for 10% contrast was much weaker than with a large stimulus (compare the magenta curves of Fig. 3a, b). On the other hand, initial evoked responses for high contrast stimuli were very similar whether the stimuli were large or small. Interestingly, after the initial evoked transient had subsided, there was a bigger change in LFP amplitude between the transient and sustained response (labeled  $\Delta$  in Fig. 3a, b) for large

stimuli than for small stimuli, suggesting a potential inhibitory effect kicking in after the initial excitation. Across the population of experiments, this effect of a bigger  $\Delta$  with big stimuli persisted (Fig. 3c), and it was mirrored by higher sustained firing rates for small stimuli in the isolated neurons (Fig. 3d). Naturally, these effects were weakest for the lowest stimulus contrast (5%), because this contrast evoked the weakest responses anyway.

Therefore, our experiments with small and large stimuli have revealed potential local lateral interactions in and around classical SC RF's. These interactions are not identical to inhibitory surround interactions in V1 (Vaičiūnaitė et al., 2013). For example, in our case, the bigger stimulus did not reduce the SC response for high contrast stimuli as might be expected from surround suppression in V1 (Vaičiūnaitė et al., 2013), suggesting that this stimulus was still within the classical RF boundaries. Nonetheless, subsequent inhibition in neural responses during the sustained stimulus interval still occurred in our neurons.

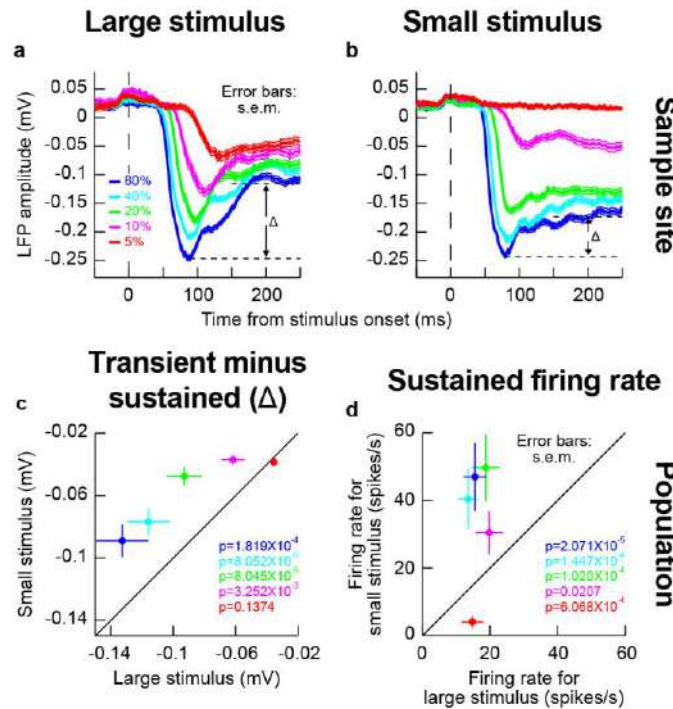


**Figure 3 Local population activity for different stimulus sizes.** (a) LFP responses for the same electrode track as the one for which the example neuron of Fig. 2 was isolated. For the large stimulus, evoked LFP response resembled the expectations based on firing rate analyses. (b) When the stimulus was small, the evoked response at 10% and 5% contrast was much smaller. However, note that the transient response component remained elevated. In other words, the difference between the peak evoked response and the transient response ( $\Delta$ ) was smaller for the small stimulus than for the big stimulus (a). This means that in the big stimulus, after the evoked excitatory response, a potential inhibitory signal started to kick in. This explains the higher sustained firing rates for small stimuli that are evident in the sample neuron of Fig. 2a, b even at low stimulus contrasts (10%). (c) Across electrode sites, we confirmed that the value of  $\Delta$  was bigger for the big stimulus than for the small stimulus across contrasts (except for the lowest contrast which already evoked very weak responses). (d) Consistent with this, across neurons, sustained firing rates for small stimuli were consistently higher than sustained firing rates for big stimuli, even for low 10% contrasts for which the initial evoked response was much weaker (Fig. 2). Again, for the lowest contrast, the effect is not present but this contrast evoked very weak or non-existent responses to begin with. Thus, stimulus onset in the SC is dominated by an early excitatory drive followed by subsequent inhibition.

*First spike latency reflected changes in contrast sensitivity curves for small stimuli*

The above results suggest that for small stimuli, low contrast stimuli evoke weaker responses. This should also result in later evoked responses, since visual response latency tends to be correlated with visual response amplitude in the SC (Marino et al., 2012). We



confirmed this to be the case. We plotted first spike latency as we have done earlier (Hafed and Chen, 2016), and related it to stimulus contrast (Fig. 4). As contrast increased, first spike latency decreased, which is a concomitant effect with increasing response gain (Fig. 2). For the small stimulus, first spike latency at 10% contrast was longer than for the big stimulus, consistent with the sharper decrease in response gain for this contrast with small stimuli. For the lowest contrast (5%), the effect was not clear, but this was because this contrast already evokes very weak SC responses. Note that Fig. 4 also shows first spike latency for other spatial frequencies (colored dots), confirming our earlier observations (unpublished observations).

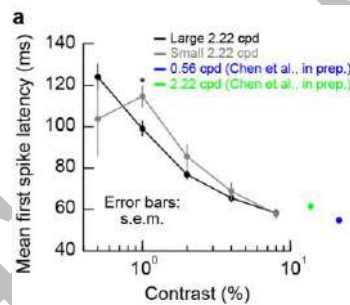


**Figure 4 Visual response latency for different stimulus parameters.** A plot of first spike latency as a function of stimulus contrast. Higher contrasts evoke stronger responses, and therefore also earlier responses. For small stimuli, earlier analyses revealed that the low contrast responses were weakened (resulting in sharpened contrast sensitivity curves). This was also reflected in first spike latency, which was elevated at 10% contrast for small stimuli. For 5% contrast, this effect was not evident because a lot of the neurons were completely silent at this contrast anyway. The blue and green dots show responses from other studies and with different spatial frequencies (but with high contrast), and demonstrate the robustness of our estimates of first spike latency.

*SC temporal frequency tuning preferred primarily 10-20 Hz*

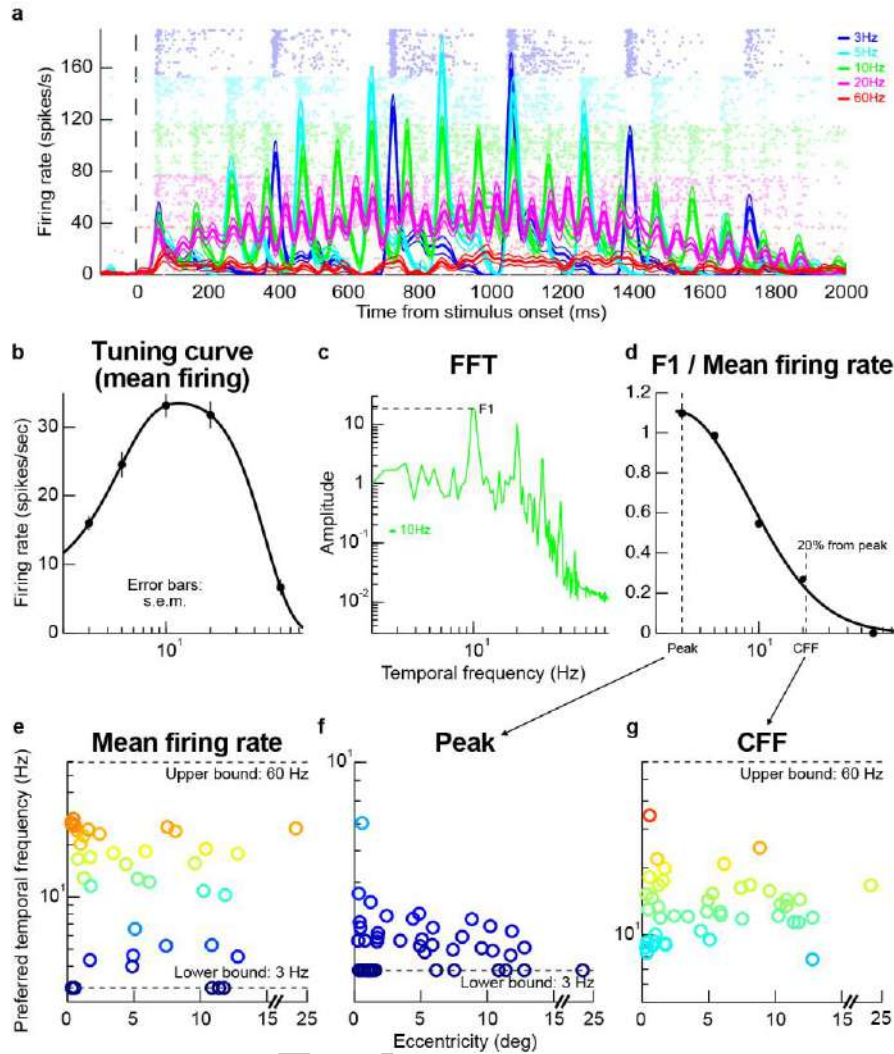
We next explored the temporal properties of SC neurons. We presented flickering gratings and varied the flicker frequency from trial to trial (Materials and Methods).

Figure 5a shows example results that we obtained from a sample neuron. At low flicker frequencies (e.g. 3 Hz), the neuron responded in a phasic manner to each stimulus onset event, and the phasic response reflected the gradual increases and decreases in stimulus contrast near the beginning and end, respectively, of a given trial (Materials and Methods). At higher frequencies (e.g. 20 Hz), the phasic events were less obvious than for low frequencies (e.g. 3 Hz), and they were replaced with a more sustained response. This means that 20 Hz was close to the critical flicker fusion frequency (Wells et al., 2001) of this neuron. Interestingly, increasing the frequency more to 60 Hz, resulted in a much weaker neural response even though the stimulus was practically constantly on the monitor for the entire duration. This means that the neuron exhibited tuning for temporal frequencies, and that 60 Hz was outside the neuron's preferred frequency range.

We assessed the neuron's frequency tuning curve, as done in the previous literature for cortical visual neurons, by measuring the average firing rate during trials and plotting it as a function of stimulus flicker frequency. Figure 5b shows the tuning curve obtained for the same sample neuron as in Fig. 5a, and the curve was obtained by fitting the data to a difference-of-gaussians equation (Materials and Methods). As can be seen, the neuron was most sensitive to temporal frequencies of 10-20 Hz. We also assessed the amplitude of the neuron's sensitivity to a given frequency. As others have done for cortical visual neurons, we computed a so-called F1/F0 ratio. Briefly, we performed a Fourier transformation of firing rate at a given frequency (e.g. 10 Hz in Fig. 5c). As expected, we obtained a primary harmonic at the stimulus frequency (F1). The amplitude of the harmonic was then divided by the mean firing rate (or the 0 Hz response of the neuron),

and we repeated this for different stimulus frequencies. For the neuron in Fig. 5a, this procedure resulted in the F1/F0 curve shown in Fig. 5d. This curve means that the phasic response at 3 Hz was much stronger relative to the mean firing rate than, say, the phasic response at 10 Hz, which is also evident from inspecting Fig. 5a. Additionally, this curve was used to define the flicker fusion frequency, or the frequency at which the phasic response at the stimulus frequency was much reduced (to 20% of the peak). In the neuron of Fig. 5d, this frequency was just above 20 Hz, again consistent with the raw data in Fig. 5a. In other words, above ~20 Hz, the neuron just emitted a more-or-less constant response as opposed to a phasic response to each stimulus cycle.

Across the population, our neurons' tuning curves were relatively broad (Fig. 5e), with a range of neurons preferring a range of flicker frequencies, but none of the neurons preferred >30 Hz. Similarly, most neurons had a critical flicker fusion frequency of ~20 Hz (Fig. f, g). These temporal SC properties are very similar to those observed in the visual capabilities of blindsight patients who lose portions of their primary visual cortex.



**Figure 5 Temporal frequency tuning by macaque SC.** (a) Example firing rates and raster plots from a neuron exposed to flicker of different frequencies. At low frequencies, the neuron emitted phasic responses to individual stimulus events. At higher frequencies, the individual phasic events started to merge or fuse (e.g. at 20Hz). At even higher frequencies (e.g. 60 Hz), the neuron stopped responding completely even though the stimulus was practically almost permanently on. Thus, the neuron exhibited temporal frequency tuning. (b) The tuning curve of the neuron obtained by plotting mean firing rate as a function of temporal frequency. The neuron responded best for 10-20 Hz frequencies. (c) Fourier transform of firing rate for the same neuron with 10 Hz flicker. The neuron had a dominant harmonic at 10 Hz (F1) along with power at different frequencies (including DC, indicating a non-zero average response). (d) We plotted the power at F1 divided by the mean response (or the DC response), to estimate how big the phasic response to individual stimulus events is relative to the overall average. For this same neuron, the phasic response at 3 Hz was very strong (also evident in a). At near 20 Hz, the individual phasic response was much weaker compared to the overall average firing rate, suggesting “flicker fusion”. We defined the critical flicker fusion frequency as the frequency for which F1/F0 was 20% of the peak. (e) Preferred temporal flicker frequencies of all neurons based on tuning curves like in b, and plotted as a function of each neuron’s preferred retinotopic eccentricity. There was no apparent eccentricity dependence of temporal tuning. (f, g) the parameters of the curve in d across all our neurons. Most neurons had a critical flicker fusion frequency near 20 Hz.

### *Discussion remarks*

In all, our results clarify additional visual properties of the SC. We clarified orientation tuning in the macaque SC, which has been a contentious issue after rodent work suggested the presence of orientation columns in this structure (Feinberg and Meister, 2015). We also explored potential lateral interactions in and around RF's, and we explored temporal tuning properties. Combined with our earlier work, like (Hafed and Chen, 2016) and (unpublished observations), our aggregate results demonstrate that the visual properties of the SC are organized to facilitate exploring natural scenes with rapid gaze shifts. It may even be the case that the visual properties of the SC can allow it to preferentially treat certain important stimuli. For example, faces (Nguyen et al., 2014) might benefit from the pattern analysis machinery of the SC. Similarly, the SC may preferentially detect predatory images (e.g. of snakes) in order to initiate a rapid avoidance response by the same structure.

We find our results intriguing because of how they may link to the role of the SC as an alternative visual pathway. Blindsight is a phenomenon that after lesion of primary visual cortex, with very little or sometimes no awareness of a stimulus presented in the blind field, patients can still perform discrimination tasks if they are forced to and be way above chance level, especially if the stimulus is salient (Cowey, 2010; Cowey and Stoerig,

1991; Leopold, 2012; Ptito and Leh, 2007; Weiskrantz et al., 1974). The visual stimuli that are optimal for these patients are critical. They perform the best with first-order low spatial frequency patches, with a cut off of around 3 cpd (Sahraie et al., 2010; Sahraie et al., 2002; Trevethan and Sahraie, 2003). Transient stimuli are usually better, with a range around 10 to 33 Hz, peaking at around 20 Hz. These tuning properties are very similar to what we found in the SC neurons, both in this study and in earlier work (unpublished observations). Patients can also perform color discrimination tasks (Boyer et al., 2005; Silvanto et al., 2008). It is also known that the pupillary reflex can be a reliable predictor of performance (Sahraie et al., 2002). Because the LGN and pulvinar project directly to extrastriate cortex, and because both of them also receive superficial SC and retinal input, it could be that blindsight reflects residual vision from this alternative visual pathway through LGN, SC, or pulvinar, or all of them to the extrastriate cortex (Cowey and Stoerig, 1991; Isa and Yoshida, 2009; Leopold, 2012). The remarkable observation based on our results is that the SC visual properties are highly similar to those of blindsight patients, which could add to the discussion on whether a collicular pathway is more or less important during blindsight than the other potential pathways.

## **Materials and Methods**

Monkey experiments were approved by regional governmental offices in Tuebingen.

### **Animal preparation**

Monkeys P and N (male, *Macaca mulatta*, aged 7 years) were prepared for behavior and superior colliculus (SC) recordings earlier (Chen and Hafed, 2013; Chen et al., 2015).

Briefly, we placed a recording chamber centered on the midline and aimed at a stereotaxically defined point 1 mm posterior of and 15 mm above the inter-aural line. The chamber was tilted posterior of vertical (by 38 and 35 deg for monkeys P and N, respectively).

### **Orientation tuning task**

The monkeys performed a pure fixation task while we recorded the activity of visually-responsive SC neurons. In each trial, a white fixation spot (8.5x8.5 min arc) appeared over a gray background. Fixation spot and background luminance were described earlier (Chen and Hafed, 2013). After an initial fixation interval (400-550 ms), the fixation spot transiently dimmed for ~50 ms, which reset microsaccadic rhythms (Hafed and Ignashchenkova, 2013; Tian et al., 2016) and also attracted attention to the spot rather than to the response field (RF) stimulus. After an additional 110-320 ms, a stationary Gabor patch with 80% relative contrast (defined as  $L_{max}-L_{min}/L_{max}+L_{min}$ )

appeared for 300 ms within the neuron's RF. The RF was estimated earlier in the session using standard saccade tasks (Chen et al., 2015; Hafed and Chen, 2016), and the Gabor patch size was chosen to fill as much of the RF as possible. The spatial frequency of the grating was 2.2 cycles/deg (cpd) because this spatial frequency drove our neurons well (Chen et al., 2015). Moreover, the orientation of the grating was varied randomly across trials. In monkey N, the orientations were 0, 30, 60, 90, 120, or 150 deg clockwise from vertical; in monkey P, the orientations were 0, 45, 90, or 135 deg clockwise from vertical. Grating phase was randomized from trial to trial, and the monkey was rewarded only for maintaining fixation; no orienting to the grating or any other behavioral response was required.

We recorded from 43 neurons. We excluded trials with microsaccades occurring within +/-100 ms from stimulus onset because such occurrence can alter neural activity. Because of this, we further excluded 12 neurons since they did not have >20 repetitions for all the tested orientations. For the neurons we included here, we had sufficient trials for analysis (we collected >255 trials per neuron; average: 389 +/- 175 s.d.).

### **Contrast sensitivity task with different stimulus sizes**

We used the same contrast sensitivity task of (Chen et al., 2015). However, in some trials, the stimulus was filling as much of the RF as possible, as in (Chen et al., 2015), and in other trials, the stimulus was small (0.5 to 1deg). This size was chosen to still allow at least 1 cycle of the 2.2 cpd grating to appear within the stimulus. We compared contrast sensitivity curves for the big and small stimuli.



We recorded from 27 neurons. We also excluded trials with microsaccades occurring within +/-100 ms from stimulus onset as discussed above. We further excluded 2 neurons since they did not have >25 repetitions for all the tested stimuli. Across neurons, we collected >181 trials per neuron (average: 253 +/- 50 s.d.).

### **Temporal flicker task**

In this task, a vertical grating of 2.2 cpd spatial frequency was flickered within the RF of a neuron for 2000 ms. Flicker frequency could be 3, 5, 10, 20, or 60 Hz. To avoid onset and offset transients, we gradually increased stimulus contrast at trial onset in the first 1000 ms of a trial, and we similarly gradually decreased stimulus contrast at trial end for the final 1000 ms of a trial. This was similar to the approach used to study flicker perception capabilities in blindsight human patients (Trevelyan and Sahraie, 2003). The monkey was required to maintain fixation throughout the entire stimulus presentation sequence.

We recorded from 55 neurons. 10 neurons were excluded because they did not have >25 repetitions for all the tested stimuli. Across neurons, we collected >137 trials per neuron (average: 166 +/- 29 s.d.).

### **Neuron classification**

We used similar neuron classification criteria to those used in our recent studies (Chen et al., 2015; Hafed and Chen, 2016). Briefly, a neuron was labeled as visual if its activity 0-200 ms after target onset in a delayed saccade task (Hafed and Chen, 2016; Hafed and Krauzlis, 2008) was higher than activity 0-200 ms before target onset ( $p < 0.05$ , paired t-test). The neuron was labeled as visual-motor if its pre-saccadic activity (-50-0 ms from saccade onset) was also elevated in the delayed saccade task relative to an earlier fixation interval (100-175 ms before saccade onset) (Li and Basso, 2008). Our results were similar for either visual or visual-motor neurons, so we combined neuron types in analyses.

### **Firing rate analyses**

We analyzed SC visual bursts by measuring peak firing rate 20-150 ms after stimulus onset (Chen and Hafed, 2017). We then obtained contrast sensitivity curves as in (Chen et al., 2015). We estimated semi-saturation contrast, baseline activity, and maximal firing rate in these curves between small and large stimuli.

For orientation tuning, we computed an orientation selectivity index similar to that used in cortical visual areas [refs]. This allowed us to directly compare orientation tuning properties in the SC to other cortical visual areas.

For temporal flicker, in addition to raw plots of firing rates, we measured mean firing rate throughout a trial. We then measured all means across trials and plotted the average of these measurements as a function of temporal frequency of the stimulus. We fitted these measurements using a difference-of-gaussians [refs] function to obtain a “tuning curve”

for temporal frequency. We also performed fourier transforms on the average firing rates obtained from a given flicker frequency. This allowed us to identify the primary oscillation frequency of firing rate (F1), which should match the flicker frequency of the stimulus. We then computed the ratio of the amplitude of the oscillation at F1 to the amplitude at 0 Hz (i.e. the mean DC value of the firing rate) to obtain a sensitivity to the flicker at F1. The stimulus flicker frequency for which the ratio of F1 amplitude to mean firing rate was below 20% of the peak ratio (obtained by comparing all the other stimulus flicker frequencies) was taken as the critical flicker fusion frequency of a given neuron [refs].

### **Local field potential analyses**

For the stimulus size manipulation, we also analyzed local field potentials (LFP's). We obtained LFP's from wide-band neural signals using methods that we described recently (Chen and Hafeed, 2017; Hafeed and Chen, 2016). We then aligned LFP traces on Gabor patch onset, and we measured evoked and sustained responses. First, we measured the strongest deflection occurring in the interval 20-150 ms after stimulus onset, to obtain a measure that we called the transient LFP response. Second, we measured the mean deflection in the period 150-250 ms after stimulus onset, to obtain what we referred to as the sustained LFP response. Since the LFP evoked response is negative going, when we refer to a "peak" LFP response, we mean the most negative value of the measured signal.

### **Author Contributions**

C.-Y. C. and Z. M. H. performed the neural experiments and analyzed the data. Z. M. H. wrote the paper.

### **Acknowledgments**

We were funded by the Werner Reichardt Centre for Integrative Neuroscience (CIN), an Excellence Cluster (EXC307) funded by the Deutsche Forschungsgemeinschaft (DFG).

We were also supported by the Hertie Institute for Clinical Brain Research.

Confidential

## References

- Ahmadlou, M., and Heimel, J.A. (2015). Preference for concentric orientations in the mouse superior colliculus. *Nat Commun* 6, 6773.
- Boyer, J.L., Harrison, S., and Ro, T. (2005). Unconscious processing of orientation and color without primary visual cortex. *Proc Natl Acad Sci U S A* 102, 16875-16879.
- Chen, C.Y., and Hafed, Z.M. (2013). Postmicrosaccadic enhancement of slow eye movements. *The Journal of neuroscience : the official journal of the Society for Neuroscience* 33, 5375-5386.
- Chen, C.Y., and Hafed, Z.M. (2017). A Neural Locus for Spatial-Frequency Specific Saccadic Suppression in Visual-Motor Neurons of the Primate Superior Colliculus. *J Neurophysiol*, jn 00911 02016.
- Chen, C.Y., Ignashchenkova, A., Thier, P., and Hafed, Z.M. (2015). Neuronal Response Gain Enhancement prior to Microsaccades. *Curr Biol* 25, 2065-2074.
- Cowey, A. (2010). The blindsight saga. *Exp Brain Res* 200, 3-24.
- Cowey, A., and Stoerig, P. (1991). The neurobiology of blindsight. *Trends Neurosci* 14, 140-145.
- Feinberg, E.H., and Meister, M. (2015). Orientation columns in the mouse superior colliculus. *Nature* 519, 229-232.
- Gandhi, N.J., and Katnani, H.A. (2011). Motor functions of the superior colliculus. *Annual review of neuroscience* 34, 205-231.
- Hafed, Z.M., and Chen, C.-Y. (2016). Sharper, stronger, faster upper visual field representation in primate superior colliculus. *Current Biology*  
<http://dx.doi.org/10.1016/j.cub.2016.04.059>.
- Hafed, Z.M., and Ignashchenkova, A. (2013). On the dissociation between microsaccade rate and direction after peripheral cues: microsaccadic inhibition revisited. *J Neurosci* 33, 16220-16235.
- Hafed, Z.M., and Krauzlis, R.J. (2008). Goal representations dominate superior colliculus activity during extrafoveal tracking. *J Neurosci* 28, 9426-9439.

Inayat, S., Barchini, J., Chen, H., Feng, L., Liu, X., and Cang, J. (2015). Neurons in the most superficial lamina of the mouse superior colliculus are highly selective for stimulus direction. *J Neurosci* 35, 7992-8003.

Isa, T., and Yoshida, M. (2009). Saccade control after V1 lesion revisited. *Curr Opin Neurobiol* 19, 608-614.

Krauzlis, R.J., Lovejoy, L.P., and Zenon, A. (2013). Superior colliculus and visual spatial attention. *Annu Rev Neurosci* 36, 165-182.

Leopold, D.A. (2012). Primary visual cortex: awareness and blindsight. *Annu Rev Neurosci* 35, 91-109.

Li, X., and Basso, M.A. (2008). Preparing to move increases the sensitivity of superior colliculus neurons. *The Journal of neuroscience : the official journal of the Society for Neuroscience* 28, 4561-4577.

Ludwig, C.J., Gilchrist, I.D., and McSorley, E. (2004). The influence of spatial frequency and contrast on saccade latencies. *Vision Res* 44, 2597-2604.

Marino, R.A., Levy, R., Boehnke, S., White, B.J., Itti, L., and Munoz, D.P. (2012). Linking visual response properties in the superior colliculus to saccade behavior. *Eur J Neurosci* 35, 1738-1752.

Nguyen, M.N., Matsumoto, J., Hori, E., Maior, R.S., Tomaz, C., Tran, A.H., Ono, T., and Nishijo, H. (2014). Neuronal responses to face-like and facial stimuli in the monkey superior colliculus. *Front Behav Neurosci* 8, 85.

Ptito, A., and Leh, S.E. (2007). Neural substrates of blindsight after hemispherectomy. *Neuroscientist* 13, 506-518.

Sahraie, A., Hibbard, P.B., Trevethan, C.T., Ritchie, K.L., and Weiskrantz, L. (2010). Consciousness of the first order in blindsight. *Proc Natl Acad Sci U S A* 107, 21217-21222.

Sahraie, A., Weiskrantz, L., Trevethan, C.T., Cruce, R., and Murray, A.D. (2002). Psychophysical and pupillometric study of spatial channels of visual processing in blindsight. *Exp Brain Res* 143, 249-256.

Silvanto, J., Cowey, A., and Walsh, V. (2008). Inducing conscious perception of colour in blindsight. *Curr Biol* 18, R950-951.

Tian, X., Yoshida, M., and Hafed, Z.M. (2016). A Microsaccadic Account of Attentional Capture and Inhibition of Return in Posner Cueing. *Frontiers in systems neuroscience* 10, 23.

Trevelyan, C.T., and Sahraie, A. (2003). Spatial and temporal processing in a subject with cortical blindness following occipital surgery. *Neuropsychologia* 41, 1296-1306.

Vaiceleunaite, A., Eriskien, S., Franzen, F., Katzner, S., and Busse, L. (2013). Spatial integration in mouse primary visual cortex. *J Neurophysiol* 110, 964-972.

Veale, R., Hafed, Z.M., and Yoshida, M. (2017). How is visual salience computed in the brain? Insights from behaviour, neurobiology and modelling. *Philos Trans R Soc Lond B Biol Sci* 372.

Weiskrantz, L., Warrington, E.K., Sanders, M.D., and Marshall, J. (1974). Visual capacity in the hemianopic field following a restricted occipital ablation. *Brain* 97, 709-728.

Wells, E.F., Bernstein, G.M., Scott, B.W., Bennett, P.J., and Mendelson, J.R. (2001). Critical flicker frequency responses in visual cortex. *Exp Brain Res* 139, 106-110.

Wurtz, R.H., and Optican, L.M. (1994). Superior colliculus cell types and models of saccade generation. *Curr Opin Neurobiol* 4, 857-861.